

**SOIL RESPIRATION AND NUTRIENT DYNAMICS AT A
MATURE TEMPERATE WOODLAND –
THE BIFoR FACE EXPERIMENT**

By

ANGELIKI KOURMOULI

A Thesis Submitted to the University of Birmingham for the degree of
DOCTOR OF PHILOSOPHY

School of Geography, Earth and Environmental Sciences

College of Life and Environmental Sciences

University of Birmingham

March 2021

UNIVERSITY OF
BIRMINGHAM

University of Birmingham Research Archive

e-theses repository

This unpublished thesis/dissertation is copyright of the author and/or third parties. The intellectual property rights of the author or third parties in respect of this work are as defined by The Copyright Designs and Patents Act 1988 or as modified by any successor legislation.

Any use made of information contained in this thesis/dissertation must be in accordance with that legislation and must be properly acknowledged. Further distribution or reproduction in any format is prohibited without the permission of the copyright holder.

This work is dedicated to all the victims of patriarchy and white supremacy.

To all those whose body parts, skin colour, gender performance, and expression, femininity or “lack” of masculinity, socio-economic status, and heritage were used as a justification of an act of violence.

“The most violent element in society is ignorance.”

Emma Goldman

Abstract

The atmospheric carbon dioxide (CO₂) concentrations have increased approximately 50% since the beginning of the industrial era (1750), breaking the record of 415 ppm, annually. CO₂ is considered one of the most important contributing gases to climate change and future predictions support a continuous increase. The rate of anthropogenic emissions increases and the ecosystemic capacity to take up and store carbon (C) govern the predicted atmospheric CO₂ increase. The terrestrial biosphere is the principal aspect of the C cycle and climate change. Interestingly, the terrestrial biosphere is also associated with the highest uncertainties in its response to environmental change.

Forests are of global significance in the C cycle, storing approximately 860 ± 60 Pg C, with Northern temperate forests being dominant regulators, sequestering one-third of the total C uptake. The general line of thinking was that young forests could sequester C more effectively than mature forests; however recent scientific outcomes suggest that mature forests can continue sequestering C. Nonetheless, disturbances, such as increasing atmospheric CO₂, can alter the C storage capacity of the mature forests ecosystem. Although forest ecosystems serve as a CO₂ sink currently, the future projections of forest ecosystems' C storage capacity are highly uncertain.

This work aims to address the short-term belowground responses of mature temperate woodland, utilising Birmingham's Institute of Forest Research Free Air CO₂ Enrichment (BIFoR FACE) facility. BIFoR FACE is the only large-scale climatic experiment in the Northern Hemisphere, studying a mature forest ecosystem's responses under the atmospheric CO₂ scenario of 2050. Subsequently, this work aims to provide an insight into the belowground interactions of three biogeochemical

cycles (C, N, and P) and the potential shifts under elevated CO₂ using high-resolution frequency measurements for the first time in the history of forest FACE experiments.

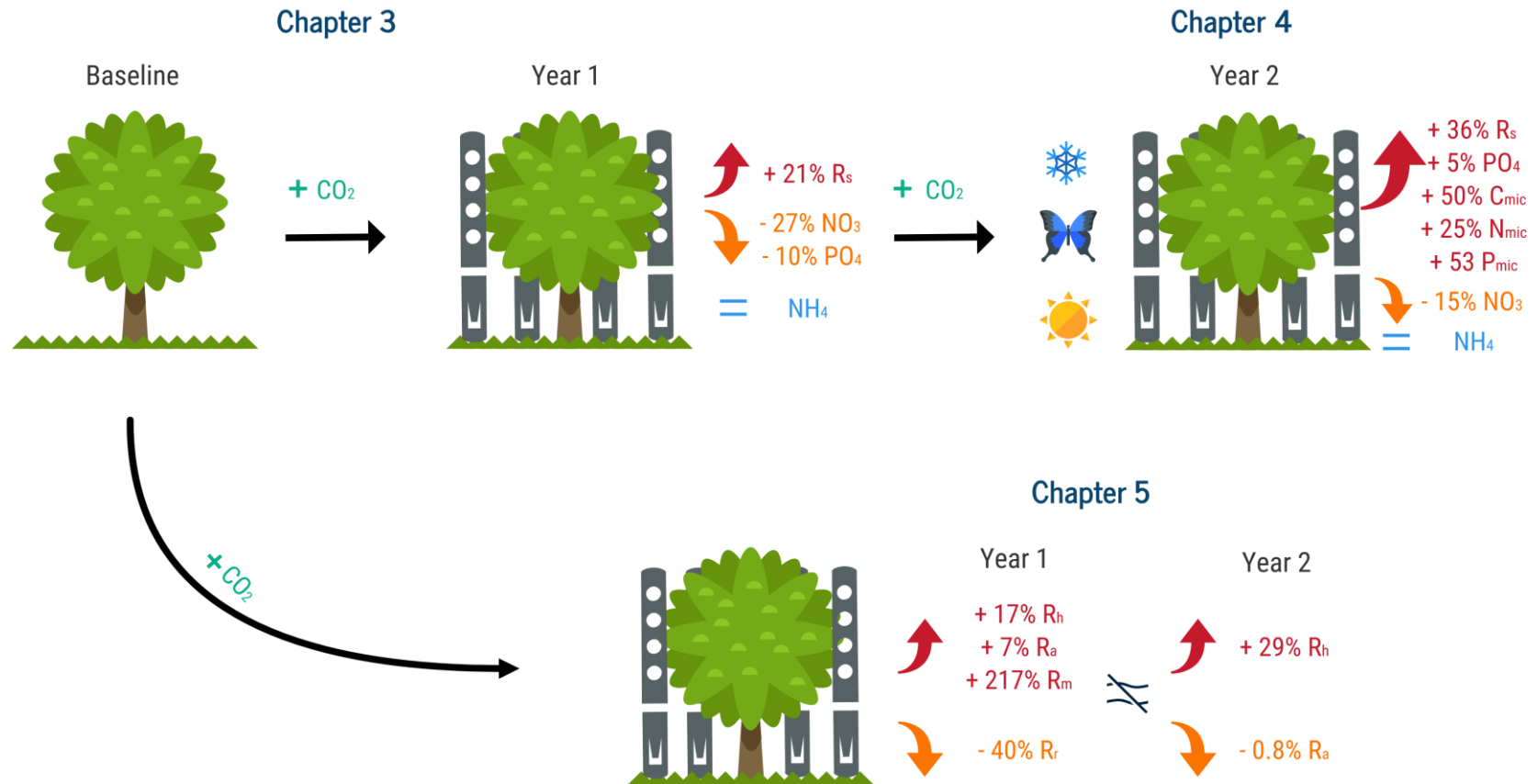
During the first year of eCO₂ enrichment, a 21% increase was observed in soil respiration, on an annual average, releasing approximately 283 g C m⁻² y⁻¹ more than in ambient CO₂. Moreover, NO₃⁻-N availability showed a prompt and sustained decrease, up to 37% in monthly averages, in eCO₂ arrays, whereas eCO₂ did not affect NH₄⁺-N and PO₄³⁻-P availability in the soil.

During the second year of eCO₂ enrichment, we also had the opportunity to monitor a series of extreme events (Beast from the East, winter moth outbreak, and 6-week summer heatwave), alongside the belowground responses to eCO₂. The drought caused by the heatwave had a severe effect on soil respiration, suppressing soil respiration by 47 and 40% in ambient and eCO₂ arrays, respectively, compared with the previous year. eCO₂ dampened the extreme event's impact by increasing soil respiration by ~36% in eCO₂ arrays, releasing approximately 259 g C m⁻² y⁻¹ more to the atmosphere. A winter moth outbreak led to a short-lived manifold increase in soil nutrient availability during autumn for all three nutrients, with the effect being more prominent under eCO₂.

Moreover, we attempted to partition soil respiration to its respiratory sources (autotrophic, heterotrophic, root, and hyphal respiration), *in situ*, during the first two years of eCO₂ enrichment. eCO₂ stimulated all respiratory components, except for root respiration, during the experiment's first year. This contribution was persistent during the second year through the series of extreme events. The heterotrophic component was the main contributor to soil respiration in both years. However, the respiratory

components' sensitivities to abiotic factors (soil temperature and moisture) were altered under the combined effects of eCO₂ and extreme events.

Content & Structure of the Ph.D. thesis



Acknowledgements

One does not simply walk to Mordor on their own.

I would like to thank my partner, Marc Marquez, without whose continuous support, encouragement, love, and understanding, I could not have come this far. For constantly reminding me that life is an unceasing fight and our right to exist in spaces, social or academic, is not granted; rather it is gained. Thus, I am forever thankful for being by my side throughout this act of revolution that survival is, this rollercoaster of a Ph.D., for giving me my space for personal and professional growth, and for handing numerous glasses of gin without even being asked!

I would also like to thank my entire family, my parents, Manolis and Irini and my brother and sister, Giannis and Maria. Without your belief, support, and nurturing love, I would not have attempted to reach this far. Although leaving the country for pursuing a Ph.D. was one of the most hurtful decisions I have taken, you have never stopped showing me how proud you are of the woman I have become. My mom's response the night I called them in tears wanted to quit the Ph.D. "My little birdie, if that is your decision, I will go now and make the bed for you, but don't you ever disrespect your effort and your hard work. Our dream would be for you to come back but don't you dare quitting something that you have put your heart in.", gave me the motivation and self-belief to come through with this mammoth task. Moreover, I would like to thank my friends of over fifteen years, Katerina Diamanti, Vicky Karagiorgi, Iro Mamalaki, and Giorgos Tzortzinakis, for making sure I followed my mum's threat, supporting my decisions every step of the way and for being the most extraordinary chosen family ever!

A very special thank you to Dr. Liz Hamilton, my supervisor, my mentor, my teacher, my role model, my inspiration, my cheerleader, my fag-partner, my dearest friend! I

am forever grateful for everything you have done for me, personally and professionally, the past four years, and this piece of work wouldn't have existed without you. I am also grateful to my entire supervisory, official and unofficial, team Dr. Rebecca Bartlett, Professor Rob Mackenzie, Dr. Sami Ullah, and Professor Iain Hartley, for their practical guidance and knowledgeable insight over the past four years.

I would also like to thank the entire BIFoR Tech team, Nick Harper, Peter Miles, Gael Denny, and Robert Grzesik for always providing their absolute greatest on-site and off-site, numerous lifts to and from BIFoR FACE and are more than happy to share their top quality coffee and cakes! I am also eternally grateful to the BIFoR Manager, THE ABSOLUTE LEGEND OF A MANAGER, Dr. Kris Hart who is the epitome of "count on me, I've got your back", going above and beyond every single time to support both my Ph.D. and me.

I would like to thank Aileen Baird, Anna Gardner, and Michaela Reay for the multiple lifts to BIFoR, early morning rants and comfort snacks! You have all supported me greatly and inspired me with how excellent scientist you are. Josep Barba, the mixed-model-whisperer, Deanne Brettell, the BIFoR Wonder woman and volunteer-shepherd, the numerous BIFoR volunteers, the G325 office residents, and the Lab 106 residents, a huge thank you for the invaluable help and support you have provided through the course of my Ph.D.

Lastly, I would like to thank the JABBS Trust, the John Horseman Trust, the British Society of Soil Science, the Royal Society of Chemistry, and the School of Geography, Earth and Environmental Sciences, University of Birmingham, for funding various aspects of this work.

Table of Contents

Abstract.....	i
Acknowledgements.....	v
List of Figures and Tables	xi
List of Abbreviations	xvi
Chapter 1: Introduction	1
1.1 Importance of Forest Ecosystems.....	1
1.1.1 Temperate Forests	3
1.1.2 Tropical Forests.....	4
1.1.3 Boreal Forests	5
1.2 Forest Carbon Cycle	7
1.3 Soil Respiration	9
1.3.1 Controlling factors on soil respiration	11
1.3.1.1 Soil Moisture	11
1.3.1.2 Soil Temperature.....	12
1.3.1.3 Soil Organic Matter Content	13
1.4 Soil Nutrients.....	14
1.4.1 Nitrogen Cycle.....	18
1.4.2 Phosphorus Cycle	22
1.5 Future of Forests under a Changing Atmosphere.....	24
1.5.1 Atmospheric CO ₂	24
1.5.2 Impacts of elevated CO ₂ on soil respiration.....	25
1.5.3 Impacts of elevated CO ₂ on soil nutrients	26
1.5.4 Models uncertainty.....	28
1.6 FACE experiments	28
1.7 BIFoR FACE experiment.....	31
1.8 Thesis layout	32
1.9 References	34
Chapter 2: Methodology.....	43
2.1 Site Description	43
2.1.1 Birmingham's Institute of Forest Research (BIFoR)	43
2.1.2 BIFoR Free Air CO ₂ Enrichment (FACE) facility	45
2.2 Field Methods	47
2.2.1 Soil respiration	47
2.2.1.1 Experimental design.....	47
2.2.1.2 Soil respiration measurements	50

2.2.2. Environmental factors.....	52
2.2.3 Soil Bioavailable nutrients.....	53
2.2.4 Soil sampling	54
2.2.4.1 Experimental design.....	54
2.2.4.2 Soil core extraction	56
2.3 Laboratory Methods	57
2.3.1 Soil Bioavailable nutrients.....	57
2.3.2 Daily IEM Loading Capacity Assessment	59
2.3.3 Extraction time assessment	62
2.3.4 Soil analysis	65
2.3.4.1 Soil moisture and bulk density.....	66
2.3.4.2 Microbial biomass	66
2.3.4.3 Total organic C and N	67
2.3.4.4 Inorganic N	68
2.3.4.5 Microbial P	68
2.4 Statistical Methods	68
2.4.1 Chapter 3 – Additional methodology.....	70
2.4.1.1 Environmental drivers and R_s	70
2.4.1.2 Annual R_s estimates.....	71
2.4.1.3 Bioavailable nutrients	71
2.4.2 Chapter 4 – Additional methodology.....	72
2.4.2.1 Environmental drivers and R_s	72
2.4.2.2 Annual R_s estimates.....	73
2.4.2.3 Soil bioavailable nutrients.....	73
2.4.2.4 Microbial biomass and inorganic N.....	74
2.4.3 Chapter 5 – Additional methodology.....	74
2.5 References	74
Chapter 3: Short-term carbon cycling and nutrient availability responses of a mature oak woodland under elevated CO_2	77
3.1 Abstract.....	77
3.2 Introduction	78
3.3 Methodology.....	82
3.3.1 Experimental site	82
3.3.2 BIFoR FACE facility.....	82
3.3.3 Measurements	84
3.3.3.1 Soil respiration, R_s	84

3.3.3.2 <i>Environmental drivers</i>	85
3.3.3.3 <i>Biota available (bioavailable) inorganic N and P</i>	86
3.3.4 Statistical analysis	87
3.3.4.1 <i>Environmental drivers and R_s</i>	87
3.3.4.2 <i>Bioavailable nutrients</i>	89
3.3.5 <i>Estimate of annual R_s</i>	89
3.4 Results	90
3.4.1 R_s response to environmental drivers and eCO_2	90
3.4.2 Estimates of annual R_s	97
3.4.3 Biota available (bioavailable) inorganic N and P	100
3.5 Discussion	103
3.5.3 Interactions of carbon and nutrient cycling to eCO_2	115
3.5.4 Future implications	116
3.6 Conclusions	117
3.7 References	120
3.8 Supplementary material	130
Chapter 4: Dominance of extreme events over elevated CO_2 : the responses of forest belowground processes in a Free Air CO_2 Enrichment experiment	135
4.1 Abstract	135
4.2 Introduction	135
4.3 Methodology	138
4.3.1 Site and extreme events description	138
4.3.2 Measurements	143
4.3.2.1 R_s	143
4.3.2.2 Environmental drivers	145
4.3.2.3 Bioavailable inorganic N and P	145
4.3.2.4 Microbial biomass and inorganic N	146
4.3.3 Statistical analysis	148
4.3.3.1 Environmental drivers and R_s	148
4.3.3.2 Estimate of annual R_s	149
4.3.3.3 Soil bioavailable nutrients	150
4.3.3.4 Microbial biomass and inorganic N	150
4.4 Results	151
4.4.1 R_s response to environmental drivers and eCO_2	151
4.4.2 Annual R_s estimates	157
4.4.3 Bioavailable nutrients	158

4.4.4 Microbial biomass and inorganic N.....	163
4.4.5 Year 1 vs. Year 2	168
4.5 Discussion.....	170
4.5.1 Soil respiration and environmental drivers	171
4.5.2 Bioavailable inorganic N and P.....	176
4.5.3 Microbial biomass and inorganic N.....	177
4.5.4 Year 1 vs. Year 2	178
4.5.5 Interactions of carbon and nutrient cycling.....	180
4.5.6 Future implications	181
4.6 Conclusions	182
4.7 References	183
4.8 Supplementary material	191
Chapter 5: A double entendre challenge - Partitioning the components of soil respiration in a mature temperate woodland under eCO ₂	196
5.1 Abstract	196
5.2 Introduction	197
5.3 Methodology.....	199
5.3.1 Measurements - Soil respiration and its partition components.....	200
5.3.2 Statistical analysis	204
5.4 Results	204
5.5 Discussion.....	212
5.6 Conclusions	218
5.7 References	219
5.8 Supplementary material	224
Chapter 6: Conclusions	232
Chapter 7: Future Outlook	234

List of Figures and Tables

Figure 1- 1: Simplified schematic diagram of the terrestrial C cycle in a forest ecosystem ...	6
Figure 1- 2: Simplified schematic diagram of soil respiration sources in a forest ecosystem	10
Figure 1- 3: Simplified schematic diagram of the three most important terrestrial biogeochemical cycles (C, N, and P) in a forest ecosystem	16
Figure 1- 4: Simplified schematic diagram of the terrestrial N cycle in a forest ecosystem .	21
Figure 1- 5: Simplified conceptual model of the terrestrial P cycle in a forest ecosystem ...	23
Table 1- 1: Forest Free Air CO ₂ enrichment (FACE) experiments in a descending chronological order	30
Figure 1- 6: Previous forest FACE experiments and the atmospheric CO ₂ concentration during their first year of eCO ₂ enrichment. With light blue colour are the FACE experiments conducted in young forests of plantations, while with dark red colour are the FACE experiments conducted in mature forests. Note that only EucFACE and BIFoR FACE are still in operation (graph adapted by David Ellsworth presentation, atmospheric CO ₂ concentration data from Tiseo, 2021).....	32
.....	44
Figure 2- 1: Schematic map of the BIFoR FACE facility with Mill Haft wood. The green coloured area highlights the total experimental area controlled by the University of Birmingham, while the thick black line area represents the greater forest area. The circles coloured in orange, blue, and brown represent the eCO ₂ , ambient, and ghost arrays, respectively. The red line represents the main access road, while the blue line represents the Mill Brook stream flowing through the northern side of the woodland from NNE to WSW. The blue triangle represents a 40 m flux tower (adapted from Hart et al., 2019).....	44
Figure 2- 2: Schematic representation of a BIFoR FACE infrastructure array. (a) Plan view of a 30 m diameter experimental patch with the structures at its circumference. The dotted line represents the center's radius to the outer plenum edge (R ~ 20 m). In contrast, the dashed line represents the radius from the centre to the research array's inner edge (R ~ 15 m). (b) The front view depicts the screw pile system penetrating the bedrock, providing secure anchoring and bypassing the need for supporting the towers with guy cables (Hart et al., 2019).	46
Figure 2- 3: Daily atmospheric CO ₂ averages in ambient (red dots) and eCO ₂ (blue dots) arrays at BIFoR FACE during Season 1 (4 th April – 27 th October 2017) (adapted from Hart et al., 2019).....	47
Figure 2- 4: Schematic representation of the soil respiration experimental blocks used at BIFoR FACE (adapted from Heinemeyer et al., 2007). Surface collars were only 5 cm deep inserted in the soil allowing roots, hyphal, and microbial growth. Medium and fine collars were inserted 30 cm deep in the soil, excluding fine roots from entering the collar. The fine collars were allowing only microbial growth.	48
Figure 2- 5: Maps of all six FACE arrays (n = 3 ambient and n = 3 eCO ₂) shown as the initially assigned pairs (ambient-eCO ₂). The purple squares denote the soil sampling plots (n = 3 per array, except array 2 and 5 where n = 4), the purple circles denote the soil respiration experimental blocks (n = 3 per array), and the purple crosses denote the ion-exchange soil resin membrane locations (n = 8 per array).....	55
Table 2- 1: Summary of the number of samples taken, analysis, and methods used for all four soil campaigns at BIFoR FACE.	56
Table 2- 2: Summary of detection limits and wavelengths used during the soil bioavailable nutrient analysis, inorganic N, and microbial P analyses provided by the manufacturer (for NH ₄ ⁺ and NO ₃ ⁻) and as calculated (for PO ₄ ³⁻). The units reported are mg NH ₄ ⁺ -N, NO ₃ ⁻ -N, and PO ₄ ³⁻ -P/L. Detection limits for all three analyses were calculated using 0.5M HCl as the matrix.	59
Figure 2- 6: Daily IEM loading capacity assessment for NH ₄ ⁺ (A), NO ₃ ⁻ (B), and PO ₄ ³⁻ (C). The light blue circles represent the extracted from IEMS concentrations, the dark blue circles	

represent the stock solution concentrations, and the green circles represent the residuals concentrations. The concentrations are in mg/L, and the error bars represent the standard deviation.	61
Figure 2- 7: Extraction time assessment for NH_4^+ (A), NO_3^- (B) and PO_4^{3-} (C). The green bars represent the lower concentrations, the yellow bars represent the medium concentrations, and the red bards represent the high concentrations for all three bioelements. The error bars represent the standard deviation.	64
Figure 2- 8: Tree diagram depicting an example of the cores extracted in one array and the subsequent subsampling for the different analyses.	65
Table 2- 3: Summary of the different horizons' masses used for the CHCl_3 fumigation analysis.	67
Figure 3- 1: Canopy “greenness index” at BIFoR FACE measured from PhenoCam showing the 90 th percentile of the daily green chromatic coordinate (GCC) of the canopy phenology nine months before the eCO_2 switch-on until the end of the first year of eCO_2 enrichment. Data are shown from May 2016 (9 months before the eCO_2 enrichment) until December 2017 (end of the first year of eCO_2 enrichment). The grey lines indicate gaps in the dataset due to technical failures of the PhenoCam, while the red lines enclose the period of eCO_2 enrichment (https://phenocam.sr.unh.edu/webcam/sites/millhaft/)	83
Figure 3- 2: Seasonal variation of R_s (a), VWC and precipitation (b), and T_s (c) at BIFoR FACE during the Pre-treatment and first year of eCO_2 enrichment (October 2016 – October 2017). The blue coloured lines/solid points denote the eCO_2 arrays, while the orange lines/solid points denote the ambient arrays. The lighter coloured ribbons around the lines and the error bars indicate the SE for R_s , VWC, and T_s . All data describe daily averages, except the solid points in (a), which reflect the R_s monthly averages. The vertical dashed lines enclose the period when the eCO_2 enrichment was switched on (Year 1, 3 rd April – 27 th October 2017), whereas the period before reflects the Pre-treatment period (19 th October 2016 – 2 nd April 2017).....	91
Figure 3- 3: (a) Example responses of R_s to precipitation events during Year 1 of eCO_2 enrichment at BIFoR FACE. Warm colours reflect ambient arrays, while cold colours reflect eCO_2 arrays. Note that not all arrays were measured for R_s simultaneously; instead, an ambient and an eCO_2 array were measured for a two-weekly period. (b) VWC (lines) and precipitation (bars), and (c) T_s during the same period. All data presented in hourly averages.	93
Table 3- 1: Mean, number of observations ('n'), minimum and maximum VWC, T_s , and R_s for Pre-treatment and Year 1 in ambient and eCO_2 arrays based on daily averages (mean \pm sd), as well as Q_{10} values and p-values from simple mixed-effects models. Significance values are based on the mixed-effects model approach with eCO_2 as the main effect and array, location within an array, and the number of days since the beginning of the measurement as random effects.	94
Figure 3- 5: a) Observed and predicted R_s measurements under ambient conditions, b) Observed and predicted R_s measurements under eCO_2 conditions. The black solid points denote the daily-average (mean \pm sd) observed R_s measurements, while the pink solid points denote the predicted R_s values. The dashed lines enclose the Year 1 of eCO_2 enrichment. c) Predicted and observed R_s correlation for eCO_2 (blue line) and ambient (orange line) arrays. The blue solid points denote the eCO_2 arrays, while the orange solid points denote the ambient arrays. d) Mean annual R_s in $\text{g C m}^{-2} \text{ y}^{-1}$ in ambient (orange) and eCO_2 (blue) arrays during the first year at BIFoR FACE. The error bars denote the standard error. ...	99
Table 3- 4: Summary of mixed-effects models of the environmental variables and their interactions with eCO_2 on bioavailable soil nutrients. Fixed factors are VWC, T_s , and their interactions with eCO_2 . The degrees of freedom for each explanatory variable is 1. P-value < 0.1 is shown in bold.	103
Figure S3- 1: R_s response (LOESS) on VWC (a) and T_s (b) in both eCO_2 and ambient conditions during Year 1. The blue solid points represent the eCO_2 arrays, while the orange solid points represent the ambient arrays.....	131
Figure S3- 2: Model validation for estimating soil respiration during Pre-treatment for homoscedasticity, normality of residuals, and outliers and random effects.	132

Figure S3- 3: Model validation for estimating soil respiration during Year 1 for homoscedasticity, normality of residuals, and outliers and random effects.....	132
Table S3- 1: Fixed effects parameter estimates (coefficients) for the best-fitted model for Pre-treatment and Year 1.	133
Figure S3- 4: (a) NO_3^- -N, (b) NH_4^+ -N, (c) PO_4^{3-} -P availability, and (d) N:P ratios in correlation with VWC, T_s , and P at BIFoR FACE during Year 1 of eCO_2 enrichment. The triangles reflect the eCO_2 conditions while the circles reflect the ambient conditions. The colour luminance reflects the monthly cumulative precipitation in *10 mm, which increases as the precipitation increases. The size of the shapes reflects the availability of soil nutrients and N:P ratios, which increase as the availability increases.	134
Figure 4- 1: Schematic diagram of the study period timeline (October 2016 – October 2018) and important extreme events.	141
Figure 4- 2: Weather parameters (air temperature, rainfall, snowfall and snow days, and sun hours) from a weather station 3.2 miles from BIFoR FACE from 2009 until 2018 (Gnosall, Staffordshire, United Kingdom Weather Averages Monthly Average High and Low Temperature Average Precipitation and Rainfall days World Weather Online, no date).	142
Figure 4- 3: Canopy "greenness index" at BIFoR FACE measured from PhenoCam showing the 90 th percentile of the daily green chromatic coordinate (GCC) of the canopy phenology nine months before the eCO_2 switch-on until the end of the second year of eCO_2 enrichment. Data inside the red lines show the first and second years of the eCO_2 enrichment. The dashed line indicated the difference in the GCC between Year 1 and Year 2 of eCO_2 enrichment due to the extreme events. The grey lines indicate gaps in the dataset due to technical failures of the PhenoCam, while the red lines enclose the period of eCO_2 enrichment (https://phenocam.sr.unh.edu/webcam/sites/millhaft/).....	143
Table 4- 1: Mean, minimum and maximum VWC, T_s , and R_s for Dormant and Year 2 in ambient and eCO_2 arrays based on daily averages (mean \pm sd), as well as Q_{10} values and p-values from simple mixed-effects models. Significance values are based on the mixed-effects model approach with eCO_2 as the main effect and array, location within an array, and the number of days since the beginning of the measurement as random effects. p-value <0.1 is shown in bold.....	154
Figure 4- 5: R_s response (LOESS) on VWC (a) and T_s (b) in both eCO_2 and ambient conditions during Year 2. The blue solid points represent the eCO_2 arrays, while the orange solid points represent the ambient arrays.	155
Table 4- 2: Analysis of R_s and its drivers' variance during Dormant and Year 2 at BIFoR FACE. The degrees of freedom for each explanatory variable is 1, p-value < 0.1 is shown in bold.	157
Figure 4- 6: a) Observed and predicted R_s measurements under ambient conditions, b) Observed and predicted R_s measurements under eCO_2 conditions. The black solid points denote the daily-average (mean \pm sd) observed R_s measurements, while the pink solid points denote the predicted R_s values. The dashed lines enclose Year 1 of eCO_2 enrichment. c) Predicted and observed R_s correlation for eCO_2 (blue line) and ambient (orange line) arrays. The blue solid points denote the eCO_2 arrays, while the orange solid points denote the ambient arrays. d) Mean annual R_s in $\text{g C m}^{-2} \text{ y}^{-1}$ in ambient (orange) and eCO_2 (blue) arrays during the second year at BIFoR FACE. The error bars denote the standard error.	160
Table 4- 3: Soil nutrients availability and N:P ratios during the Dormant and Year 2 at ambient and eCO_2 arrays (mean \pm sd), and summary of mixed-effects models of the eCO_2 effect on nutrient availability. All nutrients units are per unit area of membrane in $\mu\text{g cm}^{-2} \text{ d}^{-1}$ (refer to section 4.3.3.3 Bioavailable nutrients for method). p-value < 0.1 is shown in bold.....	161
Figure 4- 7: Temporal changes in ion exchange resin membranes (a) NO_3^- -N, (b) NH_4^+ -N and (c) PO_4^{3-} -P concentrations, (d) log(N:P ratios), (mean \pm se, n = 3). The orange solid points reflect the nutrient availability in the ambient arrays, whereas the blue solid points reflect the nutrient availability in the eCO_2 arrays. The shaded area denotes eCO_2 treatment (Year 1 and Year 2), whereas the white areas reflect the Pre-treatment and Dormant period (no eCO_2 enrichment).....	162

Figure 4- 8: Mean annual R_s in $\text{g C m}^{-2} \text{y}^{-1}$ in ambient (orange) and eCO_2 (blue) arrays during the first two years at BIFoR FACE. The error bars denote the standard error.	170
Figure 4- 9: Percentage change of R_s , soil nutrient availability (bioavailable and inorganic N), microbial biomass C, N, and P (per soil horizon) between ambient and eCO_2 conditions at BIFoR FACE the first two years of eCO_2 enrichment. The error bars denote standard error. Note that data for inorganic N and microbial biomass C, N, and P are available only for Year 2	180
Figure S4- 1: Model validation for estimating soil respiration during Dormant for homoscedasticity, normality of residuals, and outliers and random effects.....	191
Figure S4- 2: Model validation for estimating soil respiration during Year 2 for homoscedasticity, normality of residuals, and outliers and random effects.....	192
Figure S4- 3: (a) NO_3^- -N, (b) NH_4^+ -N, (c) PO_4^{3-} -P availability and (d) N:P ratios in correlation with VWC, T_s and P at BIFoR FACE during Year 2 of eCO_2 enrichment. The triangles reflect the eCO_2 conditions while the circles reflect the ambient conditions. The colour luminance reflects the availability of soil nutrients and N:P ratios, which turns darker as the nutrient availability increases. The size of the shapes reflect the monthly cumulative precipitation in $\times 10 \text{ mm}$, which increases as the precipitation increases.....	193
Table S4- 2: Analysis of variance results for VWC and T_s during Year 2 at BIFoR FACE. p-value < 0.1 is shown in bold.	195
Figure 5- 1: Schematic representation of the soil respiration experimental blocks used at BIFoR FACE (adapted from Heinemeyer et al., 2007). Surface collars were only 5 cm deep inserted in the soil allowing roots, hyphal, and microbial growth. Medium and fine collars were inserted 30 cm deep in the soil, excluding fine roots from entering inside the collar. The fine collars were allowing only microbial growth.....	201
Figure 5- 2: Seasonal course of heterotrophic respiration, R_h ; autotrophic respiration R_a ; root respiration, R_r , and hyphal respiration, R_m during the Pre-treatment and first two years of eCO_2 enrichment (October 2016 – October 2018). The blue coloured bars denote the eCO_2 arrays, while the orange bars denote the ambient arrays. All data describe monthly averages, while the error bars denote standard error.	205
Figure 5- 3: Percentage contribution of soil respiratory components (R_h , R_a , R_r , and R_m), on an annual basis, to total soil respiration in ambient and eCO_2 arrays during the first two years of eCO_2 enrichment at BIFoR FACE. Note that partitioning R_a to R_r and R_m during Year 2 was not possible.....	206
Figure 5- 4: Mean annual R_h , R_a , R_r , and R_m in ambient (orange) and eCO_2 (blue) arrays during the first two years of eCO_2 enrichment at BIFoR FACE. The error bars denote the se.	208
Figure 5- 5: R_h , R_a , R_r , and R_m responses on VWC in both ambient and eCO_2 arrays during the first two years of eCO_2 enrichment at BIFoR FACE. The blue solid points represent the eCO_2 arrays, while the orange solid points represent the ambient arrays.....	210
Figure S5- 1: Investigation of experimental design failures for all three experimental blocks in Array 1 (eCO_2 array) in daily averages during the first two years of eCO_2 enrichment at BIFoR FACE. Surface collars are denoted with dark green solid lines, medium collars are denoted with green dotted lines, while fine collars are denoted with light green dashed lines.	224
.....	225
Figure S5- 2: Investigation of experimental design failures for all three experimental blocks in Array 2 (ambient array) in daily averages during the first two years of eCO_2 enrichment at BIFoR FACE. Surface collars are denoted with dark green solid lines, medium collars are denoted with green dotted lines, while fine collars are denoted with light green dashed lines.	225
.....	226
Figure S5- 3: Investigation of experimental design failures for all three experimental blocks in Array 3 (ambient array) in daily averages during the first two years of eCO_2 enrichment at BIFoR FACE. Surface collars are denoted with dark green solid lines, medium collars are denoted with green dotted lines, while fine collars are denoted with light green dashed lines.	227

Figure S5- 4: Investigation of experimental design failures for all three experimental blocks in Array 4 (eCO ₂ array) in daily averages during the first two years of eCO ₂ enrichment at BIFoR FACE. Surface collars are denoted with dark green solid lines, medium collars are denoted with green dotted lines, while fine collars are denoted with light green dashed lines.	227
Figure S5- 5: Investigation of experimental design failures for all three experimental blocks in Array 5 (ambient array) in daily averages during the first two years of eCO ₂ enrichment at BIFoR FACE. Surface collars are denoted with dark green solid lines, medium collars are denoted with green dotted lines, while fine collars are denoted with light green dashed lines.	228
Figure S5- 6: Investigation of experimental design failures for all three experimental blocks in Array 6 (eCO ₂ array) in daily averages during the first two years of eCO ₂ enrichment at BIFoR FACE. Surface collars are denoted with dark green solid lines, medium collars are denoted with green dotted lines, while fine collars are denoted with light green dashed lines.	229
Table S5- 1: Linear equations retrieved from VWC and T correlations with R _h , R _a , R _r and R _m (daily averages) during Year 1 and 2 at BIFoR FACE.	230
Figure S5- 7: Experimental design failures in the root exclusion collars. Roots were penetrating the exclusion collars via the open bottom of the collar or through the meshed windows.	231

List of Abbreviations

BIFoR – Birmingham’s Institute of Forest Research

°C – degrees of Celsius

C – Carbon

cm - centimetre

CO₂ – Carbon dioxide

Ca₃(PO₄)₂ – Calcium phosphate

eCO₂ – Elevated CO₂

EE – Extreme events

EM – Ectomycorrhizal fungi

FACE – Free Air CO₂ Enrichment

F_c - soil CO₂ efflux rate

FePO₄ – Iron phosphate

GPP – Gross primary productivity

H – Hydrogen

IEM – Ion-exchange membrane

km – Kilo metres

Mg₃(PO₄)₂ – Magnesium phosphate

Mha – Mega hectares

mm - Millimetre

mol - Mole

N – Nitrogen

N₂ – Dinitrogen

N₂O – Nitrous oxide

NH₄⁺ – Ammonium

NO₂⁻ - Nitrite

NO₃⁻ – Nitrate

NO – Nitrogen oxide

NEP – Net ecosystem productivity

NPP – Net primary productivity

O – Oxygen

P – Phosphorus

P_0 - Pressure

Pg – Pentagrams

PO_4^{3-} - Phosphate

ppm – parts per million

Q_{10} – Temperature sensitivity

R - Gas constant

R_a – Autotrophic respiration

R_e – Ecosystem respiration

R_h – Heterotrophic respiration

R_m – Hyphal respiration

R_r – Root respiration

R_s – Soil respiration

S - Soil surface area

T_0 - Air temperature

T_s – Soil temperature

V - volume

VWC – Soil moisture

W_0 - Water vapour mole fraction

$(\partial C')/\partial t$ - Rate of change in water-corrected CO_2 mole fraction

μ - micro

Chapter 1: Introduction

This Chapter introduces fundamental knowledge of the importance of forested ecosystems and the forests' carbon cycle. An introduction to soil respiration and its controlling factors are included and the nitrogen and phosphorus biochemical cycles. Following this, an introduction to climate change and, more specifically, on elevated atmospheric carbon dioxide and a brief literature review on elevated carbon dioxide impacts on soil respiration and nutrient dynamics. Finally, previous FACE experiments, the BIFoR FACE experiment, and the thesis' layout are discussed.

1.1 Importance of Forest Ecosystems

The term forest ecosystem includes the living organisms of the forest (plants, animals, microbes, fungi) and their interaction with their environment's chemical and physical components. It extends vertically upward to the atmospheric layer encasing forest canopies (can be up to 120 m height; Tao *et al.*, 2016) and downward to the lowest soil layers affected by roots and biotic processes (up to 68 m; Canadell *et al.*, 1996).

Forest ecosystems are of high importance to natural systems and society through the services they provide. The services are classified in the following categories: *provisioning services*, such as food, medicinal, and forest products; *regulating services* that affect floods and climate, through energy, water, carbon dioxide, and other chemical species with the atmosphere; *supporting services*, such as nutrient cycling, soil formation and refuges for biodiversity; and *cultural services* that include aesthetic, spiritual, educational and recreational uses (Hassan, Scholes and Ash, 2005). Another vital ecosystem service that is often overlooked is that for millennia, forests have

provided a home for millions of people worldwide, and their survival is highly dependent on the forest (Soussan, Shrestha and Uprety, 1995).

Forests currently cover ~42 million km², accounting for almost one-third of the land surface, storing ~45% of terrestrial carbon (C), and contributing ~50% of terrestrial net primary production (Field and Raupach, 2004). In the 1990s, the terrestrial C sink was estimated around 2.6 Pg C year⁻¹ (Nabuurs *et al.*, 2007), while more recent analyses estimate the net terrestrial C sink in the range of 2 to 3.4 Pg C year⁻¹ (Khatriwala, Primeau and Hall, 2009; Le Quéré *et al.*, 2009). Forests can veil the high albedo of snow due to their low surface albedo (Jin *et al.*, 2002), which exacerbates the planet's warming through increased land solar heating. They can also cool the climate since they regulate the hydrologic cycle through evapotranspiration (Baldocchi and Xu, 2007). Thus, forests are of high significance in the global C cycle by absorbing carbon dioxide (CO₂) and storing it within the ecosystem.

Among different terrestrial ecosystems, forest soil contains more than two-thirds of the global soil organic C, being the highest C-rich ecosystem among the different land used-based ecosystems (Ahmed, 2018). The current global C stock in the world's forests is estimated to be 861 ± 66 Pg C, with 383 ± 30 Pg C in the soil, 363 ± 28 Pg C in live biomass (above and below ground), 73 ± 6 Pg C in deadwood and 43 ± 3 Pg C in the litter. Geographically, 55% of the global C stock is stored in tropical forests, 32% in boreal, and 14% in temperate forests (Pan *et al.*, 2011).

Humans can affect forest ecosystems through their activities by influencing the composition, cover, age, and density of the vegetation, by altering the kinds of stands present and their spatial arrangement, influencing the movement of wind, water, animals, and soils, by introducing by-products into the atmosphere that may fertilize

or harm the forests. Moreover, the continuous consumption of fossil fuels has led to an increase in the atmospheric CO₂ concentration, altering the biogeochemical cycles inducing climate change. The higher demand for forest products is exhilarating the transfer of products from one country to another, introducing non-native species and associated pests, threatening native forests and fauna.

1.1.1 Temperate Forests

Temperate forests are located in the mid-latitudes and form a patchwork of discontinuous forests on five continents surrounded by prairies, steppes, or deserts. They are characterized by species diversity, warm-temperate mixed broadleaved species, cold-temperate coniferous, evergreens, deciduous broadleaved, and mixed broadleaved/coniferous species. All temperate forests have been directly impacted by human beings, except those in major mountain areas, since extensive forest areas were cleared for agriculture since the 12th century (Wisniewski and Sampson, 1993). It is uncommon for temperate forests to cover more than 40% of the land area since they tend to be surrounded by agricultural land and urban areas. The temperate forest biome area has been increasing since the beginning of the 20th century, both due to the ecosystem's natural recovery after agriculture abandonment and increased newly planted forests (Fang *et al.*, 2001; Birdsey and Lucier, 2006; Kauppi *et al.*, 2006).

Temperate forests cover 767 Mha of the global land surface and are currently storing 119 ± 6 Pg C (Pan *et al.*, 2011). They have 42% of C stored in biomass and 48% in soil. For the past two decades, they have been an increasing carbon sink, absorbing $\sim 0.72 \pm 0.1$ Pg C year⁻¹, primarily due to an increase in forest area and biomass density (Birdsey, Pregitzer and Lucier, 2006; Kauppi *et al.*, 2006). Notably, China's and U.S.

C sink showed 33 and 34% increase, respectively, due to increased forest area, growth of immature forests, and increased area of newly planted forests (Fang *et al.*, 2001; Birdsey, Pregitzer and Lucier, 2006), CO₂ fertilization and N deposition (Pan *et al.*, 2009). However, the European C sink was stable for the past decades (Ciais *et al.*, 2008).

1.1.2 Tropical Forests

Tropical forests are located around the equator, in three continents, and are the most complex biome in terms of vegetation structure and species richness. Climatically, these regions are characterized by high moisture and temperature all year round, creating an ideal environment for broadleaved evergreen types. Due to the high precipitation rates and the fact that these forests are grown on bedrock, most nutrients are leached away. These forests have undergone many land-use changes over the centuries, with many mature forests converted to logged forests, permanent agriculture, and pasture or shifting cultivation. The rates of land-use change depend on social, economic, and political factors.

Tropical forests cover 1949 Mha, accounting for the largest global forest biomes and currently storing 471 ± 93 Pg C. Tropical forests have 56% of C stored in biomass and 32% in soil. For the past two decades, tropical forests have been a decreasing C sink, absorbing $\sim 2.8 \pm 0.7$ Pg C year⁻¹ (Pan *et al.*, 2011), equivalent to more than half of the total C sink in established forests. The sink reduction observed was due to deforestation of the intact forest area (Houghton, 2007) and severe Amazon drought (Phillips *et al.*, 2009).

1.1.3 Boreal Forests

Boreal forests form a circumpolar belt through northern Eurasia and North America. Its northern boundary is formed with subarctic woodlands containing treeless patches and stunted forest stands that form the boundary between the boreal forests and the tundra zones. The southern boundary is dominated by temperate deciduous forests where oceanic influences moderate climate and arid steppe or prairie. There is no defined boundary between the boreal and the temperate forests; instead, there is a transitional zone with mixed-species stands or a patchwork of temperate deciduous forests and boreal conifers. These ecosystems are characterized by short growing seasons and low mean temperatures resulting in a forest cover dominated by coniferous vegetation.

Boreal forests cover 1135 Mha of the Northern Hemisphere and currently store 272 ± 23 Pg C. Boreal forests have 20% of C stored in biomass and 60% in soil. The past two decades have been a consistent carbon sink, absorbing $\sim 0.5 \pm 0.1$ Pg C year⁻¹ (Pan *et al.*, 2011). Mainly, Asian Russia, which is the most significant boreal sink, exhibited no overall change, regardless of the increased emissions from wildfire disturbances. Moreover, in European Russia and Northern Europe, there was a 35% sink increase due to increases in forest areas after agricultural abandonment, reduced harvesting, and forest age structure changes to more productive stages (Kauppi *et al.*, 2010; Schepaschenko *et al.*, 2015). Conversely, in Canada, the C sink was reduced by 50% due to biomass loss from intensified wildfires and insect outbreaks (Stinson *et al.*, 2011).

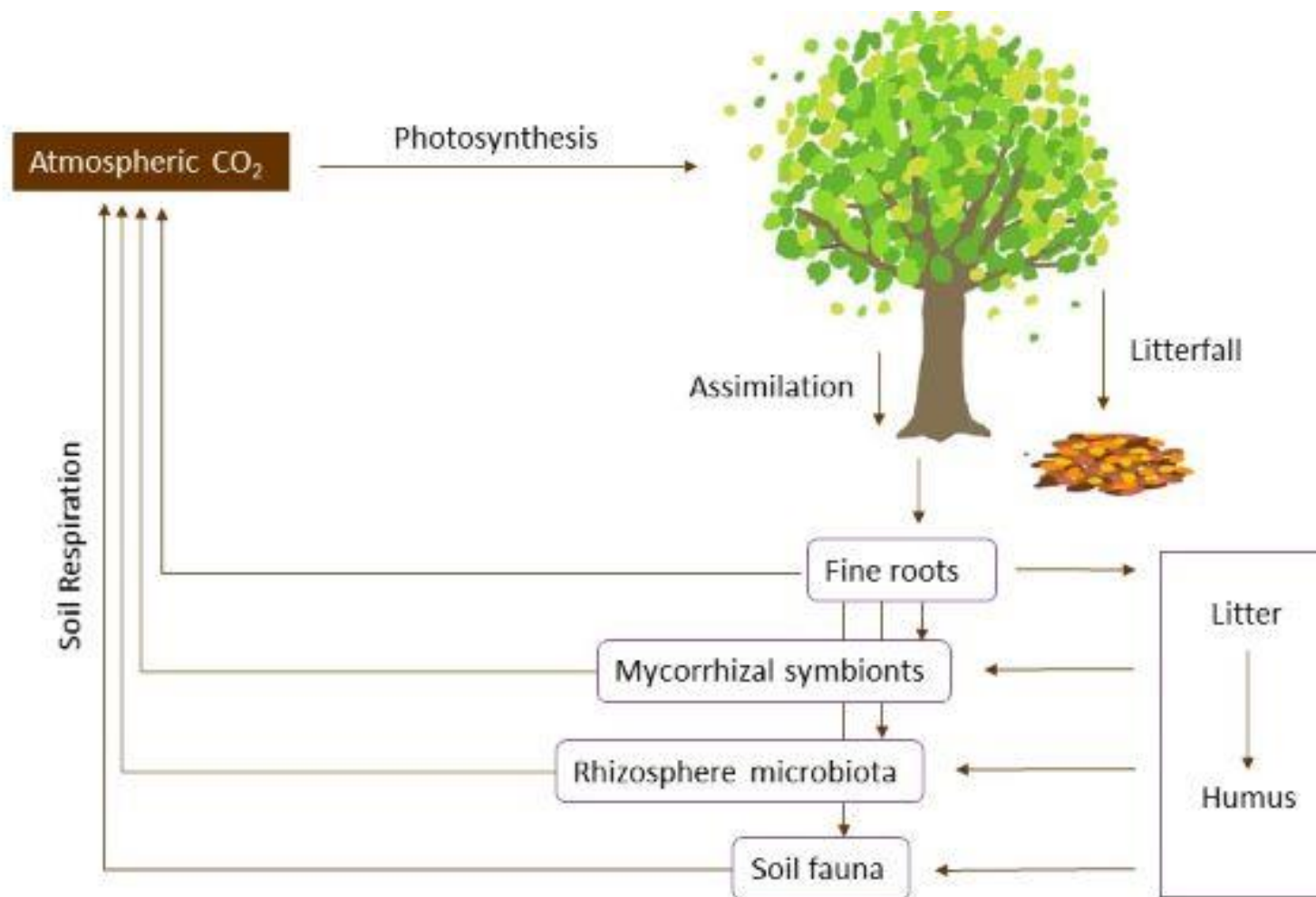
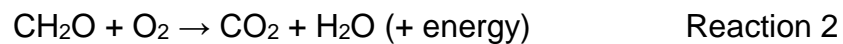
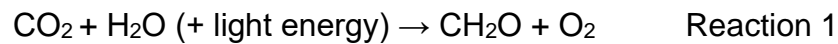


Figure 1- 1: Simplified schematic diagram of the terrestrial C cycle in a forest ecosystem

1.2 Forest Carbon Cycle

In the forest ecosystem, carbon enters the system (Fig. 1-1) when plants assimilate atmospheric CO₂ through photosynthesis into reduced sugars (Reaction 1). CO₂ enters the plants by diffusion through leaves' stomata and then is transferred to photosynthesis sites. Photosynthesis is the process by which plants convert CO₂ to carbon products and takes place within cells containing chloroplasts. This process is restricted by physical and biochemical processes and involves reactions that require both light and dark.



Approximately half of the gross photosynthetic products (GPP) are used up by plants through autotrophic respiration (R_a) for synthesis and maintenance of living cells, releasing CO₂ back to the atmosphere (Reaction 2). The remaining photosynthetic products go into foliage, branches, stems, roots, and plant reproductive organs, potentially stored on short, medium, and long term in the forest. This rate is called net primary production (NPP) and is the difference between GPP and R_a (Equation 1).

$$NPP = GPP - R_a \quad (1-1)$$

Therefore, NPP is the amount of C and energy that enters the ecosystem. NPP provides energy for all biotic processes, such as decomposer organisms' activity that recycle nutrients essential for supporting primary production and is the product of multiple interactions among elements, organisms, and the environment. Thus, small changes in these processes can significantly impact NPP and shift the forest's ability from a C sink to a C source.

Eventually, plants will shed leaves and roots; the dead organic matter forms a substrate that supports microbes, fungi, and animals, which, through their metabolic processes, release CO₂ back into the atmosphere (R_h). Some detritus decompose quickly (respired to the atmosphere, Reaction 2), and some are modified to carbon that decomposes more slowly. The rate at which the decomposition will take place depends on the dead tissues' chemical composition and environmental conditions. The turnover of detritus and microbial biomass is less than ten years, whereas modified soil organic C turnover can be up to centuries. A small amount of the modified carbon is further converted to much more resistant to decomposition compounds, creating a recalcitrant carbon pool.

The difference between NPP and R_h determines how much carbon is lost or gained by the ecosystem in the absence of disturbances. Annually, undisturbed forest ecosystems exhibit a small net gain of C, and this represents the net ecosystem production (NEP) and is the difference between the GPP and the total ecosystem respiration (R_e) (Equation 2).

$$NEP = GPP - R_e \quad (1-2)$$

In forests, the major contributors of the soil C stock are the decomposed plant tissues, above and belowground, and the root exudates; however, the fine root and mycorrhizal turnover on soil C storage are considered to be more crucial than the C in the aboveground litter (Rasse, Rumpel and Dignac, 2005). Microbial biomass, bacteria, archaea, and mycorrhizal fungi contribute to soil organic carbon stock by releasing stored C through decomposition and respiration, and biomass production.

1.3 Soil Respiration

Soil contains almost double the amount of C of the vegetation and atmosphere combined (van Groenigen *et al.*, 2015), and soil respiration (R_s) is the second-largest flux of CO_2 in the terrestrial ecosystems, linking soil and atmospheric C, through the C cycle (Ahmed, 2018). The soil C pool is approximately four times higher than the atmospheric pool; thus, minor changes in the flux of CO_2 from soil to the atmosphere may significantly impact the balance of the atmospheric CO_2 (Luo and Zhou, 2006).

R_s , the CO_2 efflux from the forest soil, is a combination of autotrophic root activity and associated rhizosphere organisms, heterotrophic bacteria and fungi, and soil fauna activity (Fig. 1-2). R_s is divided into autotrophic respiration (R_a), which is the CO_2 produced from the metabolic activity for root growth and maintenance; and heterotrophic respiration (R_h), which is the CO_2 produced from the decomposition of organic matter used as energy source for microbial communities (Savage *et al.*, 2013).

Usually, the ectomycorrhizal (EM) fungi respiration (R_m) is included in the R_a , due to the difficulty in separating the root from the EM, *in situ*, leading to overestimation of the R_a and underestimations of the R_h (Tomè *et al.*, 2016). It is essential to highlight that each soil component (roots, fungi, free-living microbes, and soil animals) has a unique dependence on substrate quality and abiotic factors and may exhibit different behaviours under a change in their environment or climate change (Wei, Weile and Shaopeng, 2010; Ma *et al.*, 2014). Thus, it is crucial to quantify the flux from each component to understand better the drivers and the processes involved and make more accurate model predictions.

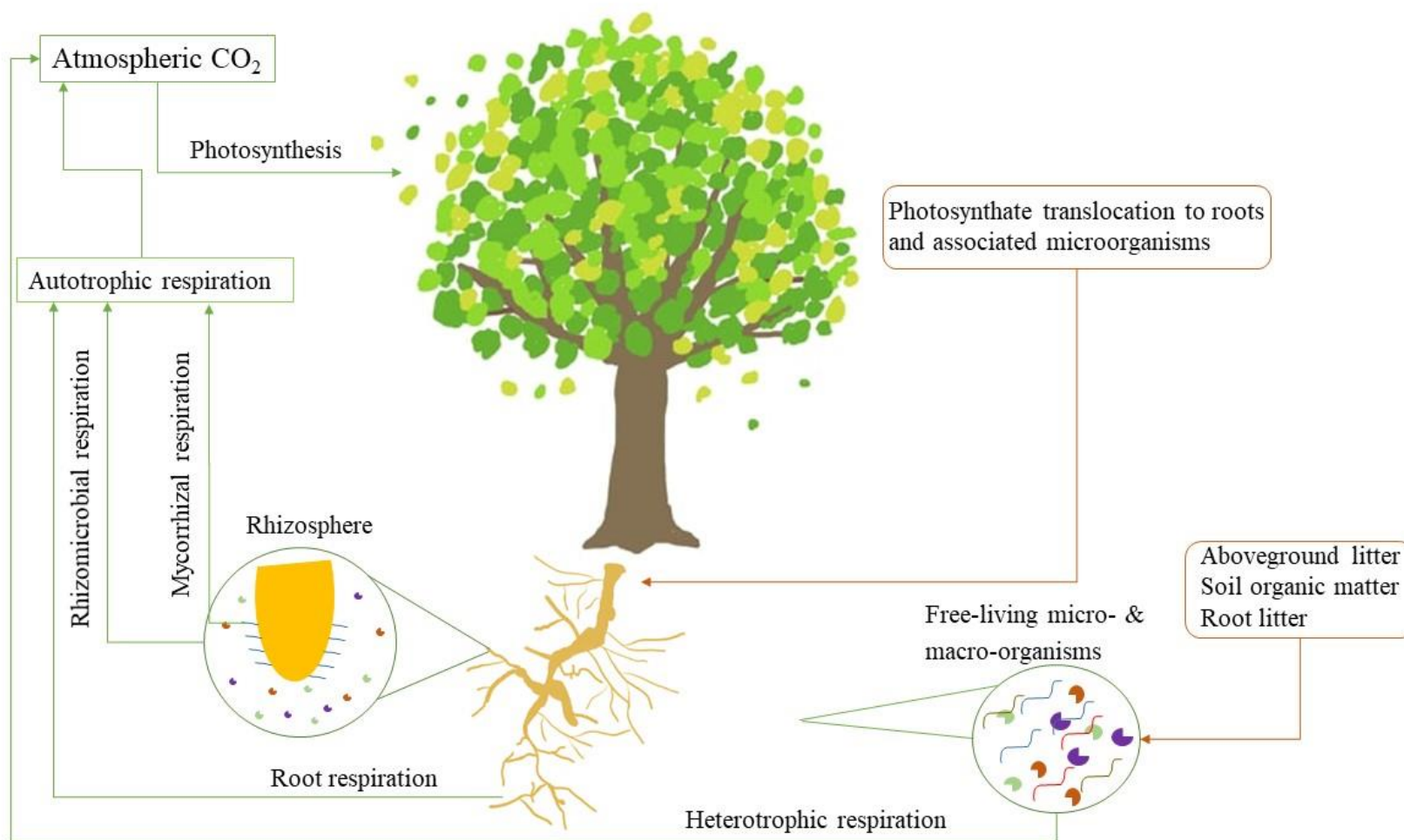


Figure 1- 2: Simplified schematic diagram of soil respiration sources in a forest ecosystem

Mycorrhizal fungi form a symbiotic relationship with the plant roots, depending on the roots for their C needs, and in exchange, the fungi provide essential nutrients to the plants. By having a smaller diameter than tree roots, fungal hyphae can access films of water on soil particles that roots cannot. Specifically, in the temperate regions, roots are in symbiosis with EM fungi, which form a sheath around the fine roots' tips, increasing the root system efficiency. Due to this mutual relationship, EM do not have to compete with other soil heterotrophs for energy sources; instead, they acquire essential sugars directly from the roots (Brady and Weil, 2017).

At the beginning of the growing season, little to no decomposable material is added to the soil via litterfall; thus, R_h rates are low. As the growing season progresses and litterfall increases, more decomposable material is added to the soil, and R_h rates increase. R_a and R_h have similar seasonal behaviour, with R_a increasing slightly during the growing season than R_h (Högberg *et al.*, 2001). Each soil component's relative contributions vary hugely, from 10% to 90%, depending on the type of ecosystem, the time of the year, and the measurement technique (Hanson *et al.*, 2000).

1.3.1 Controlling factors on soil respiration

Various factors control R_s in a complex way. The most influential factors in temperate ecosystems (Ryan and Law, 2005) are soil moisture, soil temperature, and substrate supply (Suseela *et al.*, 2012).

1.3.1.1 Soil Moisture

Soil moisture is a significant control on R_s because it can alter the soil oxygen levels, which both R_a and R_h are sensitive to. High water content inhibits both aerobic root

respiration and microbial decomposition (Brady and Weil, 2017) by filling up the soil pores and preventing oxygen (O) diffusion into the soil. It alters the CO₂ movement in the soil and acts as a barrier for diffusion (Pumpanen *et al.*, 2008). Moreover, high water content can trigger an increase in R_s in the short term, e.g., after rainfall events pulse responses (Gaumont-Guay *et al.*, 2006; Yan *et al.*, 2014). Low water content limits the substrate diffusion for R_h and causes R_a's desiccation stress (Davidson and Janssens, 2006; Van der Molen *et al.*, 2011). Nevertheless, soil fungi are better adapted to water stress than bacteria or soils' microfauna (Swift, Heal and Anderson, 1979).

It is difficult to interpret the effect of soil moisture on R_s due to other factors that vary seasonally, such as the seasonal covariance of photosynthetic rate, precipitation, litterfall, root, and microbial activity (Jassal *et al.*, 2008). However, studies have suggested that the optimal conditions for R_s are at intermediate water content levels (Davidson, Belk, and Boone, 1998) and appear to be a primary driver of R_s when the volumetric soil moisture content is less than 20% (Jassal *et al.*, 2008; Almagro *et al.*, 2009).

1.3.1.2 Soil Temperature

While temperature is a critical driver for R_s, and especially for R_h (Suseela *et al.*, 2012), as with soil moisture, there is a difficulty when interpreting the effect of temperature on R_s due to other important factors such as accessibility and supply of organic substrate to microbes that limits R_h (Davidson and Janssens, 2006), and long term substrate limitations that inhibit R_a (Schindlbacher *et al.*, 2009).

However, the R_s sensitivity to temperature is often described with the temperature coefficient Q_{10} , a factor by which respiration rates change by a temperature rise of 10 °C. Typically, it is assumed that the respiration rates double for every 10 °C in the temperate regions (Davidson and Janssens, 2006; Noh *et al.*, 2015), but seldom studies show differences in short and long term responses of R_s to changes in temperature (Larigauderie and Körner, 1995; Atkin *et al.*, 2000). Since Q_{10} is calculated via seasonal temperature variations, it is challenging to distinguish the temperature effect from other seasonal factors, such as carbon allocation to roots, solar radiation, and moisture (Jia *et al.*, 2013; Wang *et al.*, 2014; Han *et al.*, 2014). In the literature, R_a is described twice as sensitive ($Q_{10} \sim 4$) as R_h ($Q_{10} \sim 2$) (Boone *et al.*, 1998; Epron *et al.*, 2001), but has been criticized since other seasonal factors have been overlooked (Högberg *et al.*, 2001; Bhupinderpal-Singh *et al.*, 2003; Ruehr and Buchmann, 2009; Schindlbacher *et al.*, 2009). There are studies that exhibit a lack of response of R_a and/or R_h to temperature (Högberg *et al.*, 2005; Heinemeyer *et al.*, 2007).

1.3.1.3 Soil Organic Matter Content

R_s vary significantly in different biomes because vegetation dictates the soil microclimate and structure and the quality and quantity of the substrate supply (Raich and Tufekcioglu, 2000; Mitra *et al.*, 2014). Assuming that no other factors are limiting, adding soil organic matter increases the R_h since it supplies soil heterotrophs with essential elements for their metabolism. Thus, the overall R_s increases. According to Raich and Tufekcioglu (2000), R_s increases almost proportionally with readily degradable soil organic matter. Apart from colder climates, decomposition is inhibited

due to colder temperatures, resulting in accumulating large amounts of soil organic matter (Schlesinger and Andrews, 2000).

1.4 Soil Nutrients

Various mineral/elemental cycles in a forest are strongly linked with the C cycle. Changes in the C cycle might shift other mineral cycles in the soil and negatively impact plant growth or climate change. Chemical elements and minerals that are essential or beneficial for plants' life-cycle are defined as nutrients. Plants respire the carbon acquired from photosynthesis to release energy and recycle nutrients internally from older to newer tissues. Heterotrophic and organisms associated with plants via symbiotic relationship rely on roots for their C supply to cover their energy demands and provide essential nutrients for the plant in biochemical forms.

Plants require C, hydrogen (H), and O (non-mineral elements) obtained via atmosphere and water. As described in section *1.2 Forest Carbon Cycle*, C is fixed via photosynthesis and is the primary component of many biological molecules. H is obtained almost exclusively via water and plays a crucial role in photosynthesis and respiration. O is obtained via the atmosphere or water and is also pivotal for respiration.

The rest of the essential elements required for plant maintenance and growth are obtained from the soil and are separated into two categories. Nutrients such as nitrogen (N), phosphorus (P), sulfur (S), potassium (K), calcium (Ca), and magnesium (Mg) are called macronutrients because the plants acquire them in large amounts and are essential for primary plant biological functions. Nutrients such as iron (Fe), copper (Cu), zinc (Zn), molybdenum (Mo), manganese (Mn), boron (Bo), chlorine (Cl), and

nickel (Ni) are called micronutrients because the plants require smaller amounts. Each of these elements, essential not only for plant growth but also for microbial metabolic processes, has unique chemistry in the soil, its particular relationship to lithology and atmospheric inputs, and its rate of circulation through vegetation. Alterations in inputs/outputs of biochemical cycles can lead to nutrient limitations and affect the soil's sequestering carbon capacity.

Given the importance of C, N, and P in an ecosystem, the cycles of these elements are tightly coupled and interact dynamically with each other (Fig. 1-3), thus understanding the global C balance requires scrutinised monitoring of all three cycles together in order to make understand the potential shifts in those cycles and extrapolate for the future terrestrial C feedbacks to the atmosphere. C uptake and sequestration can be profoundly constrained by N and P limitations; thus, the current hypothesis of enhanced forest growth and C storage might be highly overoptimistic, depreciating the rate and extent of climate change (Houghton, 2007).

Nutrient availability is dependent on soil age. Very young soils (formed from recent volcanic eruptions) have very high total P available ($\sim 800 \text{ mg kg}^{-1}$), while total N is very low ($< 5 \text{ mg kg}^{-1}$). Total P decreases with soil age reaching 30 mg kg^{-1} in ancient weathered soils. Total N reaches a peak (8000 mg kg^{-1}) to decrease again as the soils are becoming more weathered (Lambers *et al.*, 2008). Precipitation and temperature are the critical factors for soil development since they influence root metabolic processes, microbial activity, and erosion.

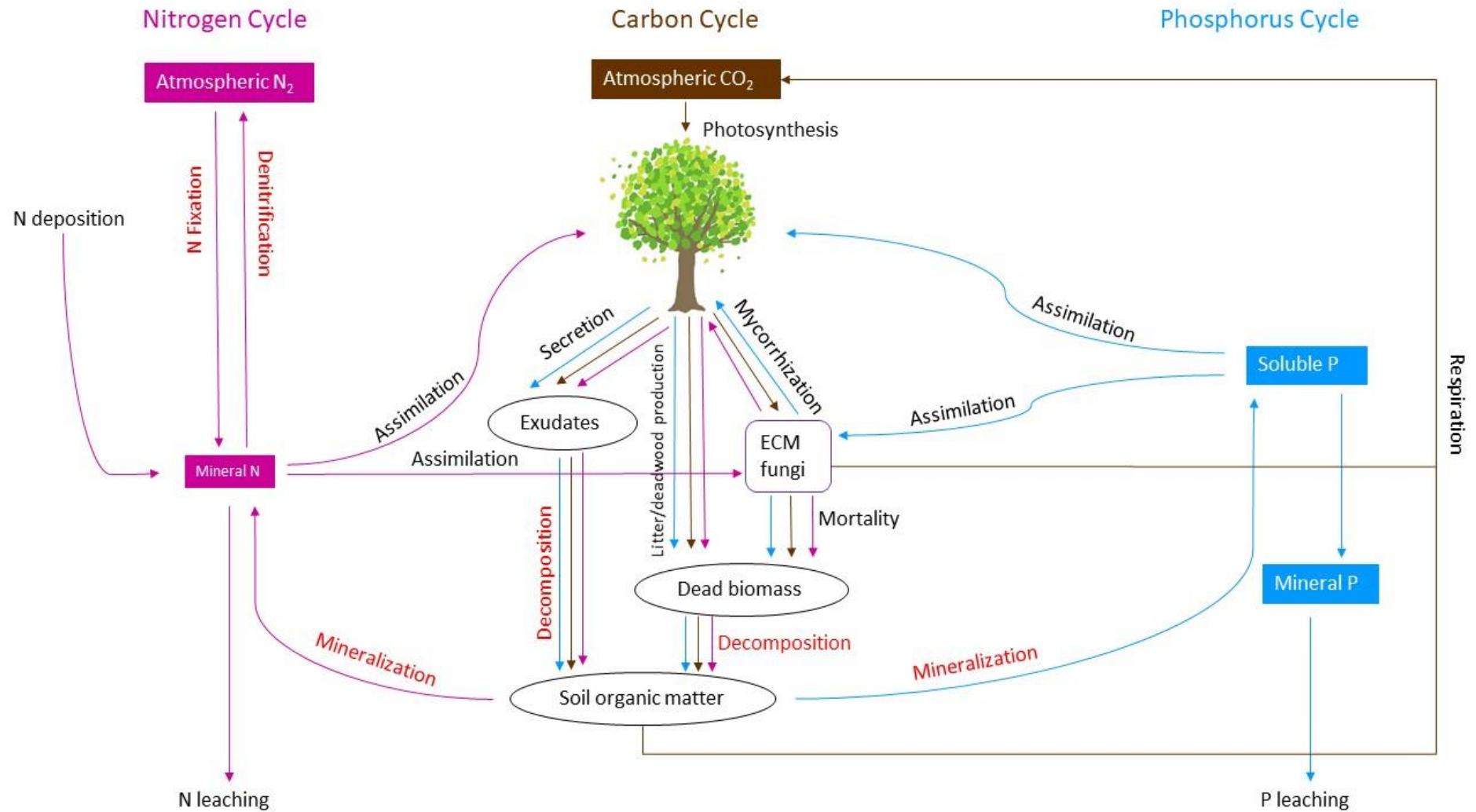


Figure 1- 3: Simplified schematic diagram of the three most important terrestrial biogeochemical cycles (C, N, and P) in a forest ecosystem

All three elements (C, N, and P) are transformed between organic and inorganic forms (Fig. 1-3). Plants uptake the inorganic forms of nutrients and convert them to organic forms, which are assimilated by the free-living soil heterotrophic microorganisms. Once the free-living heterotrophs die, saprotrophs will decompose their remains and release inorganic nutrient forms back to the soil, making them available to plants again—this way, a continuous nutrient supply is ensured across the ecosystem.

Variations in the terrestrial ecosystems' efficiency to uptake nutrients might be due to species variations among sites or even within a species due to different nutrient availability responses. In forests, an essential process that drives the nutrient availability and requirements is the annual nutrient circulation within the ecosystem through the decomposition of dead material. Hence, changes in the biogeochemical cycles can lead to significant imbalances in the system. Studies have shown that temperate deciduous forests have higher decomposition rates than coniferous forests, mainly due to lower leaf turnover rates in coniferous forests (Cole and Rapp, 1981). However, coniferous forests have lower leaching losses than deciduous (Vitousek, 1982), resulting in greater nutrient-use efficiency in coniferous forests than deciduous forests. In temperate ecosystems, nutrient availability is one of the most critical drivers for tree growth and ecosystem function (Elser *et al.*, 2007).

Three mechanisms achieve nutrient uptake by the plant roots: the diffusion of ions toward the root surface when uptake rates exceed supply; the mass flow of ions with the movement of soil water due to transpiration; the growth of roots and mycorrhizal hyphae into the soil. Often, the plant demand for N and P exceeds delivery by mass flow; thus, diffusion is the dominant mechanism that provides these macronutrients to the plants (Eissenstat and Rees, 1994). Several factors control the plants' nutrient uptake, such as the rate of photosynthesis, soil respiration, root uptake capacity,

nutrient reabsorptions during leaf senescence, differences in leaching, and inherent differences in the rate at which photosynthate is incorporated in plant growth (Schlesinger, 1991). Available nutrient concentrations at the absorbing root surface, total root surface area, and root distribution in the soil are factors that can limit nutrient uptake (Lambers *et al.*, 2008).

However, plants have developed multiple strategies to acquire more nutrients, especially in heavily weathered soils that are nutrient-impoverished. These strategies involve developing long root hair, accelerated root growth, localised accelerated root growth in nutrient-enriched zones, increased exudation of carboxylates, forming symbiotic relationships with mycorrhizal hyphae or root nodules, and specialised root structures, such as cluster roots (Lambers, Chapin and Pons, 2008). Plants do not depend only on one strategy in order to acquire the essential nutrients. Instead, they adopt a combination of strategies to optimise their nutrient uptake via scavenging and mining (Lambers *et al.*, 2003).

1.4.1 Nitrogen Cycle

Nitrogen (N) has a very complex biogeochemical cycle on the Earth. It has an essential role in the enzymes which control the biochemical reactions in which C is reduced and oxidized. A significant number of biochemical transformations of N are possible since its valence state has a range of -3 (reduced N in ammonia) to +5 (oxidised N in nitrate ions). Numerous microorganisms take advantage of that potential for transformations between these oxidation states and use the energy released by the changes in redox potential to sustain their metabolic processes (Rosswall, 1982). The most abundant and least reactive form that N can be found at the Earth's surface is the gaseous one

(N₂). Various processes convert N₂ to forms that biota can use and ultimately return it to the atmosphere as N₂.

Biological N fixation is the process where N₂, a highly unreactive gas, is converted to NH₃ via a minority of specialised microorganisms which can metabolise N₂ to NH₃ for their nutritional purposes. This process is crucial for the ecosystems since plants and organisms' plurality depends on it for NH₃, although it is indirectly available to them (Freedman, 2018). There are other pathways in which N is fixed and becomes available to the ecosystem, such as NH₄⁺ and NO₃⁻ via wet and dry atmospheric deposition and direct uptake of NO and NO₂ by plants; however, when compared to biological N fixation are considered secondary.

Most of the N in forest soils is fixed in organic compounds that cannot be directly used by plants (Fig. 1-4). Soil heterotrophic microbes decompose dead organic material on the forest floor (*decomposition*), mineralizing organic N (*mineralization*). During these processes, soil microbes respire CO₂, while nutrients are retained in microbial biomass. Through mineralization, ammonium ions (NH₄⁺) are released, and this process is called *ammonification*. Some of the NH₄⁺ produced is taken up by plant roots or immobilized by microbes (*immobilization*). As N is often a limiting nutrient for microbial growth, N immobilization is rapid and can be significant (O'Connell, 1988), dominating N processing on the soil surface, while mineralization dominates in the deeper forest floor. N is released as NH₄⁺ from dead microbial tissue (Van Veen *et al.*, 1987).

Furthermore, NH₄⁺ can be lost to sorption (fixing on clay minerals) or undergo *nitrification*. Nitrification is the process in which NH₄⁺ is oxidized to NO₃⁻ and is a two-steps process. Firstly, NH₄⁺ is converted to NO₂⁻ via *Nitrosomonas* bacteria, which is

oxidised to NO_3^- by *Nitrobacter* bacteria. The second step is much more rapid than the first step, and both bacterial types are sensitive to acidity. Thus plants growing in acidic soils must be able to utilise NH_4^+ as an N source. Some heterotrophic organisms can also convert organic N directly to NO_3^- (Waring and Running, 2007). Subsequently, NO_3^- will be uptaken by plant roots or immobilized by microbes, although soil organisms often show a distinct preference for NH_4^+ (Jackson, Schimel and Firestone, 1989). Moreover, NO_3^- can be lost from the system through leaching or undergo *denitrification*.

Denitrification is the process in which NO_3^- is converted to N_2O and N_2 , facilitated by soil aerobic heterotrophs. Contrary to nitrification, which is facilitated by specific microbial species, denitrification is facilitated by a wider bacterial variety and requires anaerobic conditions. Denitrification is accelerated under high NO_3^- amounts in soil and is considered an N fixation offset.

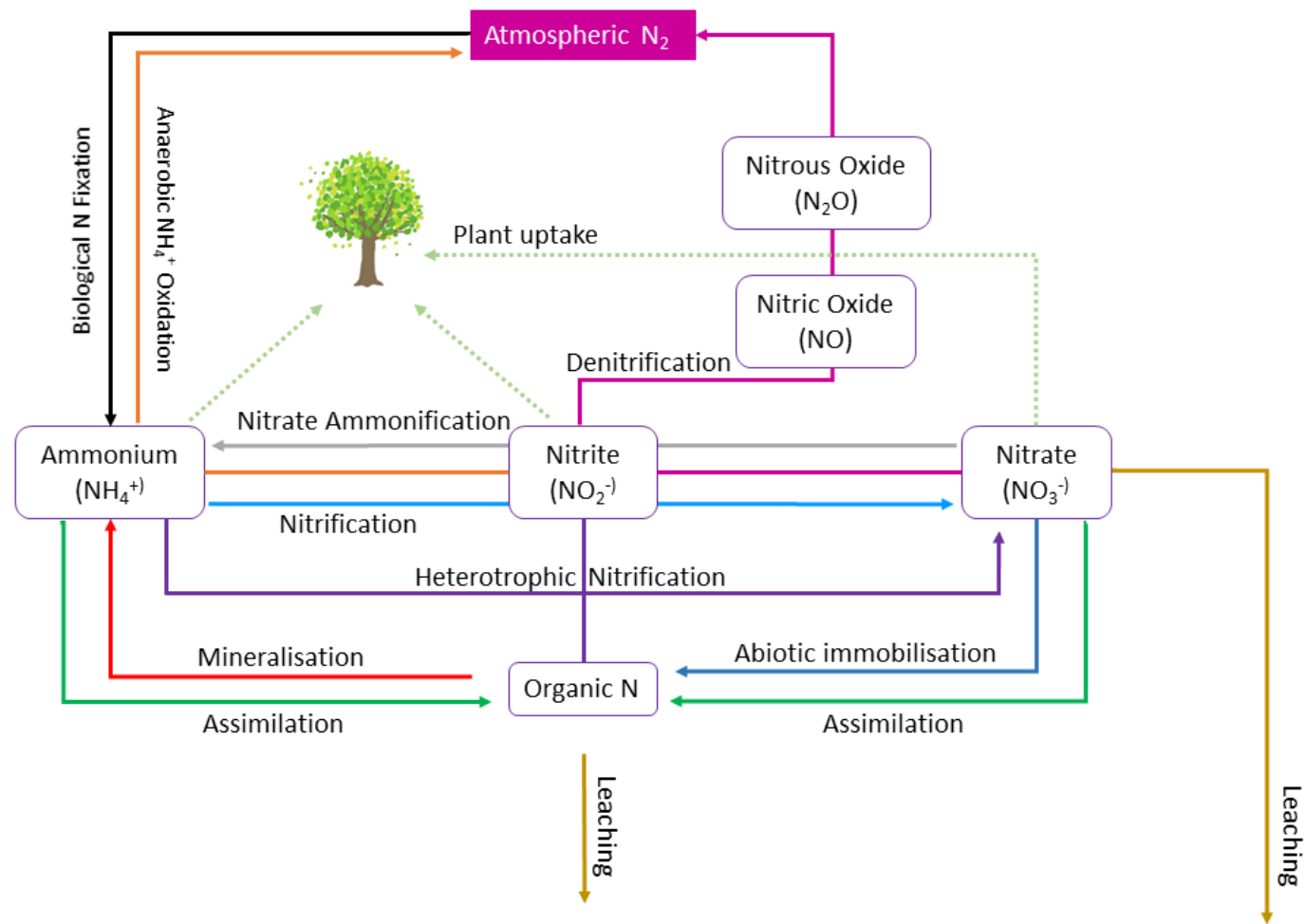


Figure 1- 4: Simplified schematic diagram of the terrestrial N cycle in a forest ecosystem

1.4.2 Phosphorus Cycle

Phosphorus (P) has a less complex cycle than N regarding the various transformations. It is unique among the significant elemental biogeochemical cycles since it does not have a significant gaseous component. Soils' redox potential is too high to allow phosphine gas production (Bartlett, 1999), except in particular localised conditions (Dévai *et al.*, 1988).

Figure 1-5 shows a simplified schematic diagram of the terrestrial P cycle in a forest ecosystem. The availability of P in forests is sustained by P cycling and is determined by the competition between biological and geochemical sinks (Attiwill and Adams, 1993). Almost all P on the land is derived from chemical weathering, in which rainwater reacts with the parental material releasing soluble P (PO_4^{3-}) and other minerals ($\text{Ca}_3(\text{PO}_4)_2$, $\text{Mg}_3(\text{PO}_4)_2$ and FePO_4). A part of the P in the soluble pool will be absorbed by the plant roots or immobilized by microbes. Through senescence or microbial population life cycle, the P returns to the soil in organic form, to be mineralized again to inorganic forms, or immobilized in the stable organic P pool in forms not available for biota.

Moreover, some of the soluble P can be geochemically transformed into secondary P minerals and enter the occluded P pool or undergo leaching. Young soils are abundant with P; however, P is very low with age, erosion, weathering, and leaching. Moreover, PO_4^{3-} has a very slow diffusion rate in the soil solution and a fast sorption rate forming secondary minerals with Fe and Al under low pH (Parfitt, 1979). The solubility of these secondary minerals is very low, thus available P in the soil solution is minimal and often is less than 10 μM (Comerford, 1998).

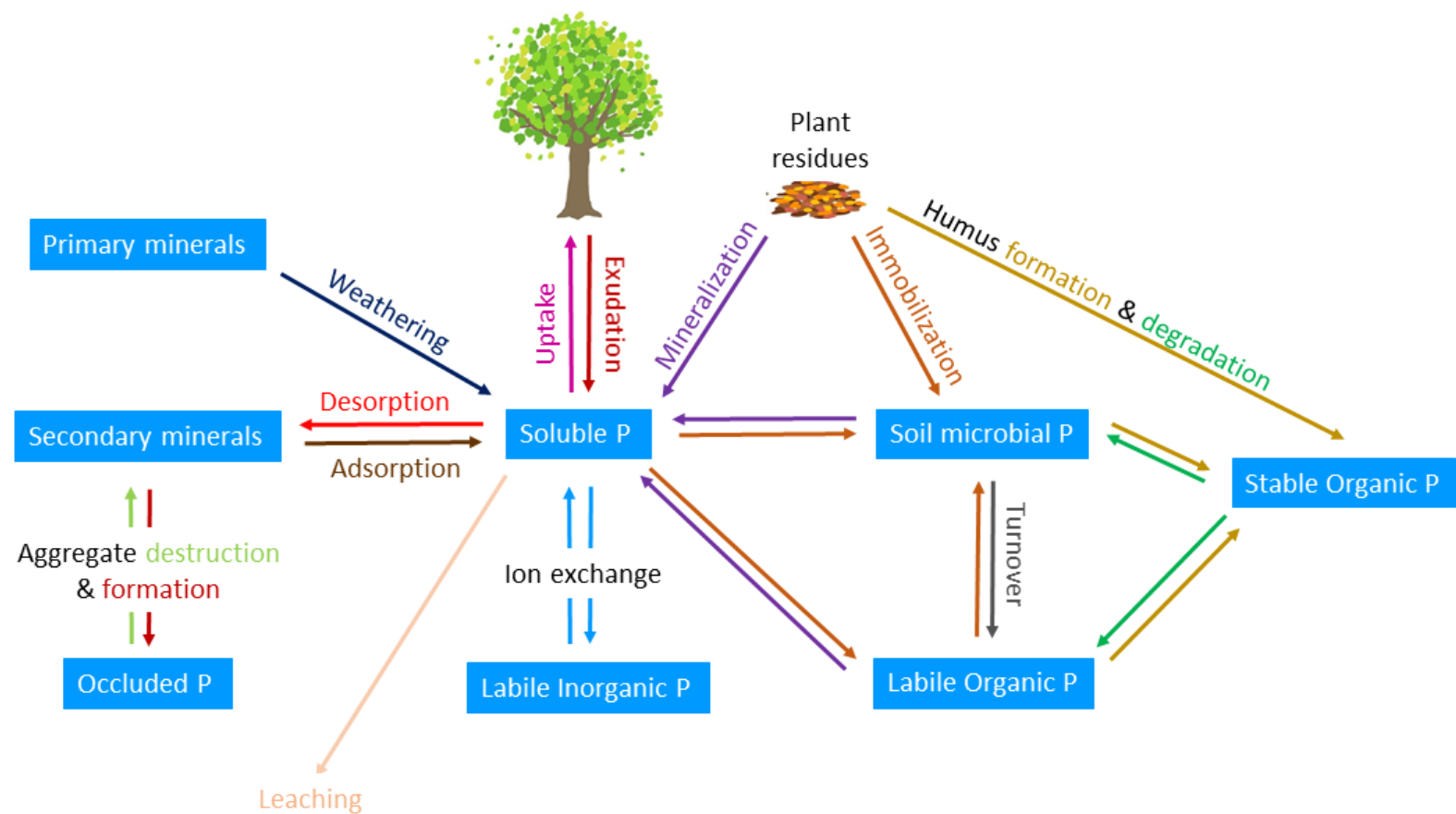


Figure 1- 5: Simplified conceptual model of the terrestrial P cycle in a forest ecosystem

1.5 Future of Forests under a Changing Atmosphere

1.5.1 Atmospheric CO₂

For the past 800,000 years and up until the preindustrial era (~1750), the concentration of CO₂ in the atmosphere was approximately 280 ± 10 ppm. Ever since, it has risen at a fast pace, following global agricultural and industrial development, to a value of 407 ppm in 2018. This year (2019), the atmospheric concentration of CO₂ broke the record by exceeding 415 ppm (www.co2.earth, 2019), and it is predicted that the concentration will exceed 500 ppm by 2050 (Prentice *et al.*, 2001).

This increase is driven by the anthropogenic burning of fossil fuels, as evidenced by decreasing atmospheric O₂, increasing proportion of biogenic ¹²C-CO₂, and higher concentrations of atmospheric CO₂ in the northern hemisphere where most fossil fuel burning occurs (Prentice *et al.*, 2001). Nevertheless, atmospheric CO₂ increases only at about half the rate of fossil fuel emissions due to the ocean and terrestrial uptake currently acting as C sink.

CO₂, alongside methane (CH₄), nitrous oxide (N₂O), chlorofluorocarbons 11 and 12 (CFC-11 and CFC-12, respectively), and a group of another 15 minor gases are called greenhouse gases because they can absorb and gradually radiate heat. Although CO₂ absorbs less heat per molecule than CH₄ and N₂O, it has a longer lifetime in the atmosphere, can be found in larger quantities than the other greenhouse gases, and absorbs thermal energy from wavelengths H₂O vapours are not able to (Lindsey, 2020).

One of the most crucial impacts of atmospheric CO₂ is the increase in Earth's temperatures, with land surface air temperature increasing faster than the global average temperature (by 1.53 and 0.87 °C, respectively), since the pre-industrial era (IPCC, 2019). Temperature increases have increased the occurrence, severity, and

extent of drought, heavy precipitation, and heat-associated events. As a result, climate change has induced growing season extension, browning of vegetation, shifts in climate zones, alterations to plant and animal species populations and life-cycles, sea-level rise and coastal erosion, permafrost thaw, threats to food security, variations in pests and diseases (IPCC, 2019). These effects are predicted to have different magnitudes globally; however, it is crucial to take mitigation actions since the fate of humans, biodiversity, and ecosystems is at risk.

It is expected that with the atmospheric CO₂ increase, plant processes and composition will be altered, thus affecting ecological communities (Hovenden and Williams, 2010). Increased atmospheric CO₂ will shift the C cycle and thus the other nutrient cycles, to which it is coupled, impacting the forest ecosystems and their function (Bonan, 2008). Subsequently, productivity and C storage will be affected, but the extent of the impacts is still not very well understood, and there is contradicting evidence in the literature. Thus it is crucial to understand how the elevated CO₂ will affect different ecosystems and gain more insight into the processes involved.

1.5.2 Impacts of elevated CO₂ on soil respiration

As described in section *1.1 Importance of forest ecosystems*, forest soils play a crucial role in uptaking atmospheric CO₂. Generally, elevated CO₂ increases the photosynthetic rate, thus the NPP (Norby *et al.*, 1999) and plant growth (Zak *et al.*, 2000). Moreover, several studies have shown increased rates of soil respiration and belowground C cycling enhancement (Janssens *et al.*, 1998; Lin *et al.*, 2001; Pataki *et al.*, 2003; Trueman and Gonzalez-Meler, 2005; Bernhardt *et al.*, 2006; Pregitzer *et al.*, 2006; Zhou, Wan and Luo, 2007; Deng *et al.*, 2010). Hence, although more C

might be sequestered in plant biomass under elevated CO₂ conditions, it might also be that a concurrent or greater amount is introduced to the atmosphere through respiration (Hungate *et al.*, 1997; Heath *et al.*, 2005; Trueman and Gonzalez-Meler, 2005), inhibiting the terrestrial ecosystems' capacity to sequester more C under increased atmospheric CO₂. Moreover, studies have shown that fine root biomass, the total number of roots and root length increased under elevated CO₂ (Rogers, Runion and Krupa, 1994; Matamala and Schlesinger, 2000; Tingey, Phillips and Johnson, 2000; Iversen, Ledford and Norby, 2008; Pritchard *et al.*, 2008), although root respiration *per se*, is not always affected (Matamala and Schlesinger, 2000), or not affected to a measurable degree (Edwards and Norby, 1999).

Furthermore, heterotrophic respiration is found to increase under elevated CO₂ due to increases in organic substrate available for decomposition from increased root production, turnover, and mortality, and litter inputs (Zak *et al.*, 2000; Deng *et al.*, 2010), or due to enhanced production and turnover of root exudates (Heath *et al.*, 2005). On the other hand, litter produced from plants grown under elevated CO₂ is found to have higher lignin and lower N concentrations, which may negatively impact heterotrophic respiration (Henry *et al.*, 2005; Knops, Naeem and Reich, 2007).

1.5.3 Impacts of elevated CO₂ on soil nutrients

Many studies have reported that elevated CO₂ is found to increase the NEP, with more substantial effects reported in higher latitudes, with temperate ecosystems being among them (Forkel *et al.*, 2016). Temperate ecosystems are also more N constrained since biological N₂ fixation is naturally low in these areas (Zaehle, 2013). The elevated CO₂ effects on soil N levels that have been reported are highly variable; they have

been shown to increase, decrease or remain stable (Gill *et al.*, 2002; Finzi and Schlesinger, 2003; Schneider *et al.*, 2004; Luo *et al.*, 2004; Reich *et al.*, 2006; Reich, Hungate and Luo, 2006; Dijkstra *et al.*, 2008; Langley *et al.*, 2009; Phillips, Bernhardt and Schlesinger, 2009; Norby *et al.*, 2010; Zak *et al.*, 2011; Mueller *et al.*, 2013; Rütting and Andresen, 2015).

The long term exposure to elevated CO₂ might result in limited N availability, thus inhibiting the CO₂ fertilization effect, and is referred to as the progressive N limitation hypothesis (Luo *et al.*, 2004; Dukes *et al.*, 2005; Hungate *et al.*, 2006; Reich, Hungate and Luo, 2006). Here, N becomes limited over time, sequestered into recalcitrant fractions of soil organic matter and long-lived plant tissues (Luo *et al.*, 2004). However, some studies suggest that progressive N limitation might not happen at all (Feng *et al.*, 2015) or maybe overcome (Lenka and Lal, 2012) since a lot of the recalcitrant biomass and soil organic matter pools have long turnover (<25 years), which is longer than most experiment's duration.

Little attention has been given to the effects of elevated CO₂ on P cycling or both the N and P dynamics. When P dynamics have been studied under field conditions, it was usually associated with N fertilization experiments. The results reported are conflicting since both increases (Khan *et al.*, 2010) or decreases (Lagomarsino *et al.*, 2008), depending on N fertilization levels. Hasegawa *et al.*, (2016) reported increased N and P availability in a P-limited mature Eucalyptus forest (EucFACE), under elevated CO₂, due to increased plant investment belowground on labile C and the associated increase of the microbial turnover of organic matter and mobilization of chemically non-available P.

1.5.4 Models uncertainty

Future changes in terrestrial carbon uptake will affect atmospheric CO₂ concentrations and, thus, the climate. Therefore the use of models for future predictions is essential. Several studies have shown that the biosphere operates as a net C sink, offsetting the climate impact of fossil fuel burning and deforestation, until positive responses from climate change, such as decreased productivity, increased soil respiration or dieback (Cox *et al.*, 2013), and land-use change emissions outpace the CO₂ effect. The extent of this feedback is critical to simulating future climate, and the results reported from observations are contradictory; the uncertainty of the land's C uptake capacity remains high (Friedlingstein *et al.*, 2006; Arora *et al.*, 2013; Jones, Stott and Christidis, 2013; Lovenduski and Bonan, 2017).

1.6 FACE experiments

The effects of elevated CO₂ in plants have been well studied in individual species grown in controlled environments or enclosures (Kimball, 1983; Ceulemans and Mousseau, 1994; Gunderson and Wullschleger, 1994; Amthor, 1995; Curtis, 1996; Drake, Gonzalez-Meler and Long, 1997; Curtis and Wang, 1998; Saxe, Ellsworth and Heath, 1998; Norby *et al.*, 1999; Wand *et al.*, 1999). However, these studies faced potential severe limitations due to the enclosed systems, such as restricted root growth or amplified photosynthetic and production rate due to 'chamber effect' (Arp, 1991; McLeod and Long, 1999; Morgan *et al.*, 2001). A solution to the confinements of controlled environment limitations was the free-air CO₂ enrichment (FACE) experiments in the 1990s (Hendrey, Lewin and Nagy, 1993; Lewin *et al.*, 1994; Miglietta *et al.*, 2001; Okada *et al.*, 2001). These experiments allowed plant exposure

to elevated CO₂ under natural conditions with no enclosed infrastructure, with temporal and spatial CO₂ concentration control throughout the canopy levels.

FACE experiments have been established in various ecosystems worldwide, studying the effects of elevated CO₂ in different species and climatic conditions (Table 1-1). FACE technology has proven to be an advantageous method providing understanding and data on the responses of the ecosystem as a whole, over spatial and temporal scales, depicting a future ecosystem image, as accurate as possible (Nowak, Ellsworth and Smith, 2004; Ainsworth and Long, 2005; Norby *et al.*, 2005; Hyvönen *et al.*, 2007; Norby and Zak, 2011).

The FACE experiments conducted from the mid-90s to mid-2000s in temperate forested ecosystems (Table 1-1) offered new insights into the forest responses under a step increase of atmospheric CO₂, C allocation, nutrient interactions, stand development (Norby and Zak, 2011), and critical improvements to models (Medlyn *et al.*, 2015). However, these experiments were conducted in young, relative homogenous stands on agricultural or disturbed soils, thus limiting the understanding of the elevated CO₂ effect to the ecosystem as an entity, the C cycle and allocation in a mature forest, and the interactions among different plant species (Norby *et al.*, 2016). Hence, FACE experiments were needed in mature ecosystems since young and mature forests sequester different amounts of C and have different C and nutrient needs. EucFACE and Web-FACE are the only two forest FACE experiments conducted in mature forests (mixed temperate and Eucalyptus forests, respectively). Web-FACE was conducted in specific stands rather than using the “ring” approach that all other FACE experiments used.

Table 1- 1: Forest Free Air CO₂ enrichment (FACE) experiments in a descending chronological order

Site	Location	Ecosystem	Ecosystem age (years)	Elevated CO ₂ (ppm)	First-year of exposure	Status
EucFACE	Richmond, Australia	Cumberland Plain forest	>75	550	2012	Ongoing
Web-FACE	Hofstetten, Switzerland	Mature temperate forest	80-120	600	2000	Closed
POPFACE	Viterbo, Italy	Poplar plantation	Planted cuttings	550	1999	Closed
ASPEN FACE – FACTS II	Rhineland, Wisconsin, USA	Aspen forest	Planted	Ambient + 200	1998	Closed
ORNL FACE	Oak Ridge, Tennessee, USA	Sweetgum plantation	Planted	Ambient+200	1998	Closed
Duke FACE – FACTS I	Duke Forest, North Carolina, USA	Loblolly pine forest	~16	Ambient + 200	1996	Closed

1.7 BIFoR FACE experiment

Although the FACE experiments that happened in the 1990s-2000s offered crucial ground for testing assumptions and responses of forested ecosystems under elevated CO₂, they were conducted in young, homogenous forested areas or recovering from disturbance ecosystems. Birmingham's Institute of Forest Research (BIFoR) FACE facility is the only FACE experiment in a mature temperate forest in the northern hemisphere, and alongside EucFACE in the southern hemisphere, are the only two 'second generation' FACE experiments in the world, testing the responses of undisturbed old-growth forests under elevated CO₂.

Mature forests are expected to respond differently to elevated CO₂ than young forests due to different developmental C needs and different internal-plant C allocations (Körner, 2006). Moreover, old-growth trees may have fully explored the belowground resource space, limiting the possibility of increased C allocation belowground to increase access to limiting nutrients (Körner, 2006). Even if mature trees can allocate more C belowground, this does not necessarily mean that the nutrient uptake will be higher if the belowground resources are already explored. Furthermore, because nutrient cycles in mature forests are more coupled than young forests, N losses might be limited in old-growth ecosystems (Zaehle *et al.*, 2014). Besides, mature trees have exhibited less flexibility in their C and nutrient use (Körner *et al.*, 2005), thus less likely to increase whole-plant nutrient use efficiency (Bader *et al.*, 2013).

BIFoR FACE facility was established in 2015 in an old-growth (>160 years) temperate forest in Staffordshire (UK) and currently is in the third year of fumigation (Fig. 1-6). Over ten years, BIFoR aims to investigate the impacts of elevated CO₂ in a mature temperate forest, C uptake and storage, nutrient dynamics and water use efficiency,

ecosystem structure and function, biodiversity, and susceptibility to abiotic and biotic stress.

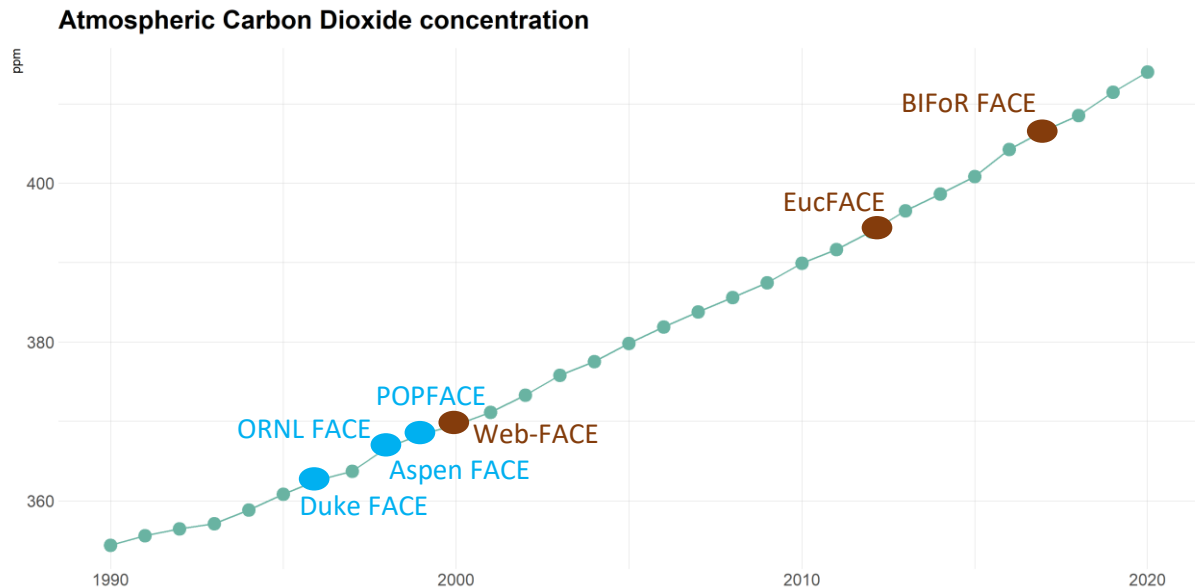


Figure 1- 6: Previous forest FACE experiments and the atmospheric CO₂ concentration during their first year of eCO₂ enrichment. With light blue colour are the FACE experiments conducted in young forests of plantations, while with dark red colour are the FACE experiments conducted in mature forests. Note that only EucFACE and BIFoR FACE are still in operation (graph adapted by David Ellsworth presentation, atmospheric CO₂ concentration data from Tiseo, 2021).

1.8 Thesis layout

This thesis aims to assess the response of forest soil biogeochemical cycles (C, N, P) to elevated CO₂; to monitor soil respiration, nutrient bioavailability, and microbial biomass under ambient and eCO₂ atmosphere at BIFoR FACE. The soil respiration is partitioned to root, hyphal and microbial respiration to quantify each soil component's contribution to soil respiration and its response to elevated CO₂. Bioavailable soil N and P dynamics are assessed using the ion-exchange resin membranes technique, while microbial biomass assessments are achieved periodically. This thesis utilises the techniques mentioned above to the highest resolution up to date in such a large-

scale climatic experiment. Hence this dataset's uniqueness makes it the first of its kind with a paramount resolution both spatially and temporally.

Chapter 2 provides a detailed outline of both the experimental designs and methodological approaches in this thesis (for *Chapters 3, 4, and 5*). It includes both field and laboratory techniques and elaborates on the statistical avenues followed for the thesis, which can be found in detail in the respective Chapters.

Chapter 3 evaluates the belowground responses before any eCO₂ enrichment at BIFoR FACE and during the first year of operation. Specifically, the short term responses of soil respiration and nutrient dynamics were monitored approximately 6 months before the eCO₂ enrichment until the end of the first year of eCO₂ enrichment.

Chapter 4 investigates the belowground responses during the second year of eCO₂ enrichment at BIFoR FACE, which coincided with a series of extreme events (Beast from the East, winter moth outbreak, heatwave). Soil respiration, nutrient dynamics and microbial biomass responses were monitored under the combined effects of eCO₂ enrichment and extreme events.

Chapter 5 quantifies the soil respiration partition to autotrophic and heterotrophic, as well as the further autotrophic partitioning to root and mycorrhizal respiratory components during the first two years of eCO₂ enrichment at BIFoR FACE.

Chapter 6 is a synthesis of the scientific outcomes of Chapters 3, 4, and 5, while Chapter 7 is a future outlook perspective on the potential further research that can improve the current understanding of belowground responses under eCO₂.

1.9 References

- Ahmed, I. U. (2018) 'Forest Soil C: Stock and Stability under Global Change', in *New Perspectives in Forest Science*. InTech. doi: 10.5772/intechopen.74690.
- Ainsworth, E. A. and Long, S. P. (2005) 'What have we learned from 15 years of free-air CO₂ enrichment (FACE)? A meta-analytic review of the responses of photosynthesis, canopy properties and plant production to rising CO₂', *New Phytologist*, 165(2), pp. 351–372. doi: 10.1111/j.1469-8137.2004.01224.x.
- Almagro, M. *et al.* (2009) 'Temperature dependence of soil CO₂ efflux is strongly modulated by seasonal patterns of moisture availability in a Mediterranean ecosystem', *Soil Biology and Biochemistry*, 41(3), pp. 594–605. doi: 10.1016/j.soilbio.2008.12.021.
- Amthor, J. S. (1995) 'Terrestrial higher-plant response to increasing atmospheric CO₂ in relation to the global carbon cycle', *Global Change Biology*, 1, pp. 243–274.
- Arora, V. K. *et al.* (2013) 'Carbon-concentration and carbon-climate feedbacks in CMIP5 earth system models', *Journal of Climate*, 26(15), pp. 5289–5314. doi: 10.1175/JCLI-D-12-00494.1.
- Arp, W. J. (1991) 'Effects of source-sink relations on photosynthetic acclimation to elevated CO₂', *Plant, Cell & Environment*, 14(8), pp. 869–875. doi: 10.1111/j.1365-3040.1991.tb01450.x.
- Atkin, O. K., Edwards, E. J. and Loveys, B. R. (2000) 'Research Review: Response of Root Respiration to Changes in Temperature and Its Relevance to Global Warming', *New Phytologist*, pp. 141–154.
- Attiwill, P. M. and Adams, M. . (1993) 'Nutrient cycling in forests', *New Phytologist*, 124, pp. 561–582. doi: 10.1533/9781845693732.1.3.
- Bader, M. K. F. *et al.* (2013) 'Central european hardwood trees in a high-CO₂ future: Synthesis of an 8-year forest canopy CO₂ enrichment project', *Journal of Ecology*, 101(6), pp. 1509–1519. doi: 10.1111/1365-2745.12149.
- Baldocchi, D. D. and Xu, L. (2007) 'What limits evaporation from Mediterranean oak woodlands – The supply of moisture in the soil, physiological control by plants or the demand by the atmosphere?', *Advances in Water Resources*, 30(10), pp. 2113–2122. doi: 10.1016/j.advwatres.2006.06.013.
- Bernhardt, E. S. *et al.* (2006) 'Long-term effects of free air CO₂ enrichment (FACE) on soil respiration', *Biogeochemistry*, 77(1), pp. 91–116. doi: 10.1007/s10533-005-1062-0.
- Bhupinderpal-Singh *et al.* (2003) *Tree root and soil heterotrophic respiration as revealed by girdling of boreal Scots pine forest: extending observations beyond the first year*, *Plant, Cell and Environment*.
- Birdsey, R., Pr, K. and Lucier, A. (2006) 'Forest Carbon Management in the United States: 1600-210.0'. doi: 10.2134/jeq2005.0162.
- Bonan, G. B. (2008) 'Forests and climate change: Forcings, feedbacks, and the climate benefits of forests', *Science*, 320(5882), pp. 1444–1449. doi: 10.1126/science.1155121.
- Boone, R. D. *et al.* (1998) 'Roots exert strong influence on the temperature sensitivity of soil respiration', *Nature*, 396.
- Brady, N. and Weil, R. (2017) *The nature and properties of soil*. 15th edn. Pearson.
- Canadell, J. *et al.* (1996) 'Maximum rooting depth of vegetation types at the global scale ', *Oecologia*, pp. 583–595.
- Ceulemans, R. and Mousseau, M. (1994) 'Effects of elevated atmospheric woody plants on', *New Phytologist*, 127, pp. 425–446.
- Ciais, P. *et al.* (2008) 'The impact of lateral carbon fluxes on the European carbon balance', *Biogeosciences*, 5, pp. 1259–1271.
- Cole, D. W. and Rapp, M. (1981) '6. Elemental cycling in forest ecosystems', in Reichle, D. E. (ed.) *Dynamic properties of forest ecosystems*. London: Cambridge University Press.

- Comerford, N. (1998) 'Soil phosphorus bioavailability', in Lynch, J. P. and Deikman, J. (eds) *Current Topics in Plant Physiology*. American Society of Plant Physiologists, pp. 136–147.
- Cox, P. M. *et al.* (2013) 'Sensitivity of tropical carbon to climate change constrained by carbon dioxide variability', *Nature*, 494(7437), pp. 341–344. doi: 10.1038/nature11882.
- Curtis, P. S. (1996) 'A meta-analysis of leaf gas exchange and nitrogen in trees grown under elevated carbon dioxide', *Plant, Cell and Environment*, 19(2), pp. 127–137. doi: 10.1111/j.1365-3040.1996.tb00234.x.
- Curtis, P. S. and Wang, X. (1998) 'A meta-analysis of elevated CO₂ effects on woody plant mass, form, and physiology', *Oecologia*, 113(3), pp. 299–313. doi: 10.1007/s004420050381.
- Daily CO₂ (2019). Available at: <https://www.co2.earth/daily-co2> (Accessed: 26 March 2020).
- Davidson, E. A., Belk, E. and Boone, R. D. (1998) 'Soil water content and temperature as independent or confounded factors controlling soil respiration in a temperate mixed hardwood forest.', *Global Change Biology*, 4, pp. 217–227.
- Davidson, E. A. and Janssens, I. A. (2006) 'Temperature sensitivity of soil carbon decomposition and feedbacks to climate change', *Nature*, 440, pp. 165–173. doi: 10.1038/nature04514.
- Deng, Q. *et al.* (2010) 'Responses of soil respiration to elevated carbon dioxide and nitrogen addition in young subtropical forest ecosystems in China', *Biogeosciences*, 7, pp. 315–328..
- Dévai, I. *et al.* (1988) 'Detection of phosphine: New aspects of the phosphorus cycle in the hydrosphere', *Nature*, 333(6171), pp. 343–345. doi: 10.1038/333343a0.
- Dijkstra, F. A. *et al.* (2008) 'Long-term enhancement of N availability and plant growth under elevated CO₂ in a semi-arid grassland', *Functional Ecology*, 22, pp. 975–982. doi: 10.1111/j.1365-2435.2008.01398.x.
- Drake, B. G., Gonzalez-Meler, M. A. and Long, S. P. (1997) 'More Efficient Plants: A Consequence of Rising Atmospheric CO₂?', *Annual review of plant physiology and plant molecular biology*, 48, pp. 609–639. doi: 10.1146/annurev.arplant.48.1.609.
- Dukes, J. S. *et al.* (2005) 'Responses of Grassland Production to Single and Multiple Global Environmental Changes', *PLoS Biol*, 3, pp. 1829–1837. doi: 10.1371/journal.pbio.0030319.
- Edwards, N. T. and Norby, R. J. (1999) 'Below-ground respiratory responses of sugar maple and red maple saplings to atmospheric CO₂ enrichment and elevated air temperature', *Plant and Soil*. Springer Netherlands, 206(1), pp. 85–97. doi: 10.1023/A:1004319109772.
- Eissenstat, D. M. and Rees, K. C. J. Van (1994) 'The Growth and Function of Pine Roots', *Ecological Bulletins*. doi: 10.2307/20113133.
- Elser, J. J. *et al.* (2007) 'Global analysis of nitrogen and phosphorus limitation of primary producers in freshwater, marine and terrestrial ecosystems', *Ecology Letters*, 10(12), pp. 1135–1142. doi: 10.1111/j.1461-0248.2007.01113.x.
- Epron, D. *et al.* (2001) 'Seasonal dynamics of soil carbon dioxide efflux and simulated rhizosphere respiration in a beech forest', *Tree Physiology*, 21, pp. 145–152.
- Fang, J. *et al.* (2001) 'Changes in Forest Biomass Carbon Storage in China Between 1949 and 1998', *Science*, 292, pp. 2320–2322.
- Feng, Z. *et al.* (2015) 'Constraints to nitrogen acquisition of terrestrial plants under elevated CO₂', *Global Change Biology*, 21, pp. 3152–3168. doi: 10.1111/gcb.12938.
- Field, C. B. and Raupach, M. R. (2004) *The global carbon cycle : integrating humans, climate, and the natural world*. Island Press.
- Finzi, A. C. and Schlesinger, W. H. (2003) 'Soil-nitrogen cycling in a pine forest exposed to 5 years of elevated carbon dioxide', *Ecosystems*, 6(5), pp. 444–456. doi: 10.1007/s10021-003-0205-1.
- Forkel, M. *et al.* (2016) 'Enhanced seasonal CO₂ exchange caused by amplified plant productivity in

northern ecosystems', *Science*.

Freedman, B. (2018) 'Chapter 5 ~ Flows and Cycles of Nutrients', in *Environmental Science*. Dalhousie University Libraries Digital Editions.

Friedlingstein, P. *et al.* (2006) 'Climate-Carbon Cycle Feedback Analysis: Results from the C 4 MIP Model Intercomparison', *Journal of Climate*, 19, pp. 3337–3353.

Gaumont-Guay, D. *et al.* (no date) 'Interpreting the dependence of soil respiration on soil temperature and water content in a boreal aspen stand'. doi: 10.1016/j.agrformet.2006.08.003.

Gill, R. A. *et al.* (2002) 'Nonlinear grassland responses to past and future atmospheric CO₂.', *Nature*, 417(6886), pp. 279–82. doi: 10.1038/417279a.

van Groenigen, K. J. *et al.* (2015) 'Application of a two-pool model to soil carbon dynamics under elevated CO₂', *Global Change Biology*, 21(12), pp. 4293–4297. doi: 10.1111/gcb.13074.

Gunderson, C. A. and Wullschleger, S. D. (1994) 'Photosynthetic acclimation in trees to rising atmospheric CO₂: A broader perspective', *Photosynthesis Research*. Kluwer Academic Publishers, 39(3), pp. 369–388. doi: 10.1007/BF00014592.

Han, G. *et al.* (2014) 'Ecosystem photosynthesis regulates soil respiration on a diurnal scale with a short-term time lag in a coastal wetland', *Soil Biology and Biochemistry*. doi: 10.1016/j.soilbio.2013.09.024.

Hanson, P. J. *et al.* (2000) 'Separating root and soil microbial contributions to soil respiration: A review of methods and observations', *Biogeochemistry*. Kluwer Academic Publishers, 48(1), pp. 115–146. doi: 10.1023/A:1006244819642.

Hasegawa, S., Macdonald, C. A. and Power, S. A. (2016) 'Elevated carbon dioxide increases soil nitrogen and phosphorus availability in a phosphorus-limited Eucalyptus woodland', *Global Change Biology*, 22(4), pp. 1628–1643. doi: 10.1111/gcb.13147.

Hassan, R., Scholes, R. and Ash, N. (2005) *Ecosystems and Human Well-being: Current State and Trends, Volume 1*. Washington: Island Press.

Heath, J. *et al.* (2005) 'Atmospheric science: Rising atmospheric CO₂ reduces sequestration of root-derived soil carbon', *Science*, 309(5741), pp. 1711–1713. doi: 10.1126/science.1110700.

Heinemeyer, A. *et al.* (2007) 'Forest soil CO₂ flux: Uncovering the contribution and environmental responses of ectomycorrhizas', *Global Change Biology*, 13(8), pp. 1786–1797. doi: 10.1111/j.1365-2486.2007.01383.x.

Hendrey, G. R., Lewin, K. F. and Nagy, J. (1993) 'Free air carbon dioxide enrichment: development, progress, results', *Vegetatio*. Kluwer Academic Publishers, 104/105, pp. 17–31. doi: 10.1007/BF00048142.

Henry, H. A. L. *et al.* (2005) 'Interactive effects of elevated CO₂, N deposition and climate change on plant litter quality in a California annual grassland', *Oecologia*, 142(3), pp. 465–473. doi: 10.1007/s00442-004-1713-1.

Högberg, P. *et al.* (2001) 'Large-scale forest girdling shows that current photosynthesis drives soil respiration', *Nature*, 411(6839), pp. 789–792. doi: 10.1038/35081058.

Houghton, R.A. (2007) 'Balancing the Global Carbon Budget', *Annual Review of Earth and Planetary Sciences*. Annual Reviews, 35(1), pp. 313–347. doi: 10.1146/annurev.earth.35.031306.140057.

Hovenden, M. J. and Williams, A. L. (2010) 'The impacts of rising CO₂ concentrations on Australian terrestrial species and ecosystems', *Austral Ecology*, 35(6), pp. 665–684. doi: 10.1111/j.1442-9993.2009.02074.x.

Hungate, B. A. *et al.* (1997) 'The fate of carbon in grasslands under carbon dioxide enrichment', *Nature*, 388(6642), pp. 576–579. doi: 10.1038/41550.

Hungate, B. A. *et al.* (2006) 'Nitrogen cycling during seven years of atmospheric CO₂ enrichment in a scrub oak woodland', *Special Feature Ecology*, 87(1), pp. 26–40.

- Hyvönen, R. *et al.* (2007) 'The likely impact of elevated CO₂, nitrogen deposition, increased temperature and management on carbon sequestration in temperate and boreal forest ecosystems: a literature review', *New Phytologist*, 163, pp. 463–480. doi: 10.1111/j.1469-8137.2007.01967.x.
- IPCC (2019) 'Summary for Policymakers', in Shukla, P. R. *et al.* (eds) *Climate Change and Land: an IPCC special report on climate change, desertification, land degradation, sustainable land management, food security, and greenhouse gas fluxes in terrestrial ecosystems*. In press.
- Iversen, C. M., Ledford, J. and Norby, R. J. (2008) 'CO₂ enrichment increases carbon and nitrogen input from fine roots in a deciduous forest', *New Phytologist*, 179, pp. 837–847. doi: 10.1111/j.1469-8137.2008.02516.x.
- Jackson, L. E., Schimel, J. P. and Firestone, M. K. (1989) 'Short-term partitioning of ammonium and nitrate between plants and microbes in an annual grassland', *Soil Biology and Biochemistry*, 21, pp. 409–415. doi: 10.1016/0038-0717(89)90152-1.
- Janssens, I. A. *et al.* (1998) 'Elevated atmospheric CO₂ increases fine root production, respiration, rhizosphere respiration and soil CO₂ efflux in Scots pine seedlings', *Global Change Biology*, 4, pp. 871–878.
- Jassal, R. S. *et al.* (2008) 'Effect of soil water stress on soil respiration and its temperature sensitivity in an 18-year-old temperate Douglas-fir stand', *Global Change Biology*, 14(6), pp. 1305–1318. doi: 10.1111/j.1365-2486.2008.01573.x.
- Jia, X. *et al.* (2013) 'Temperature Response of Soil Respiration in a Chinese Pine Plantation: Hysteresis and Seasonal vs. Diel Q₁₀', *PLoS ONE*, 8(2). doi: 10.1371/journal.pone.0057858.
- Jin, Y. B. S. *et al.* (2002) 'How does snow impact the albedo of vegetated land surfaces as analyzed with MODIS data?', *Geophysical Research Letters*, 29(10), pp. 12–15. doi: 10.1029/2001GL014132.
- Jones, G. S., Stott, P. A. and Christidis, N. (2013) 'Attribution of observed historical near-surface temperature variations to anthropogenic and natural causes using CMIP5 simulations', *Journal of Geophysical Research Atmospheres*. Blackwell Publishing Ltd, 118(10), pp. 4001–4024. doi: 10.1002/jgrd.50239.
- Kauppi, P. E. *et al.* (2006) 'Returning forests analyzed with the forest identity.', *Proceedings of the National Academy of Sciences of the United States of America*. National Academy of Sciences, 103(46), pp. 17574–9. doi: 10.1073/pnas.0608343103.
- Kauppi, P. E. *et al.* (2010) 'Changing stock of biomass carbon in a boreal forest over 93 years', *Forest Ecology and Management*, 259(7), pp. 1239–1244. doi: 10.1016/j.foreco.2009.07.044.
- Khan, F. N. *et al.* (2010) 'Tree exposure to elevated CO₂ increases availability of soil phosphorus', *Pakistan Journal of Botany*, 42(2), pp. 907–916.
- Khaliwala, S., Primeau, F. and Hall, & T. (2009) 'Reconstruction of the history of anthropogenic CO₂ concentrations in the ocean', *Nature*, 462(346). doi: 10.1038/nature08526.
- Kimball, B. A. (1983) 'Carbon Dioxide and Agricultural Yield: An Assemblage and Analysis of 430 Prior Observations', *Agronomy Journal*, 75, pp. 779–788.
- Knops, J. M. H., Naeem, S. and Reich, P. B. (2007) 'The impact of elevated CO₂, increased nitrogen availability and biodiversity on plant tissue quality and decomposition', *Global Change Biology*, 13(9), pp. 1960–1971. doi: 10.1111/j.1365-2486.2007.01405.x.
- Körner, C. *et al.* (2005) 'Carbon Flux and Growth in Mature Deciduous Forest Trees Exposed to Elevated CO₂', *Science*, 309(5739), pp. 1360–1362. doi: 10.1126/science.1113977.
- Körner, C. (2006) 'Plant CO₂ responses: an issue of definition, time and resource supply', *New Phytologist*, 172, pp. 393–411. doi: 10.1111/j.1469-8137.2006.01886.x.
- Lagomarsino, A. *et al.* (2008) 'Assessment of soil nitrogen and phosphorous availability under elevated CO₂ and N-fertilization in a short rotation poplar plantation', *Plant and Soil*, 308(1–2), pp. 131–147. doi: 10.1007/s11104-008-9614-4.
- Lambers, H. *et al.* (2003) 'Structure and functioning of cluster roots and plant responses to phosphate

- deficiency', *Plant and Soil*. Springer, 248(1–2), pp. ix–xix. doi: 10.1023/A:1025561812696.
- Lambers, H. *et al.* (2008) 'Plant nutrient-acquisition strategies change with soil age', *Trends in Ecology and Evolution*. doi: 10.1016/j.tree.2007.10.008.
- Lambers, H., Atkin, O. and Millenaar, F. (2002) 'Respiratory Patterns in Roots in Relation to Their Functioning', in Waisel, Y., Eshel, A., and Kafkafi, U. (eds) *Plant Roots: The Hidden Half*. Marcel Dekker, Inc., pp. 521–552. doi: 10.1201/9780203909423.pt6.
- Lambers, H., Chapin, F. S. and Pons, T. L. (2008) *Plant physiological ecology: Second edition, Plant Physiological Ecology: Second Edition*. Springer New York. doi: 10.1007/978-0-387-78341-3.
- Langley, J. A. *et al.* (2009) 'Priming depletes soil carbon and releases nitrogen in a scrub-oak ecosystem exposed to elevated CO₂', *Soil Biology and Biochemistry*, 41(1), pp. 54–60. doi: 10.1016/j.soilbio.2008.09.016.
- Larigauderie, A. and Körner, C. (1995) 'Acclimation of leaf dark respiration to temperature in alpine and lowland plant species', *Annals of Botany*. doi: 10.1006/anbo.1995.1093.
- Lenka, N. K. and Lal, R. (2012) 'Soil-related Constraints to the Carbon Dioxide Fertilization Effect Soil-related', *Critical Reviews in Plant Sciences*, 31, pp. 342–357. doi: 10.1080/07352689.2012.674461.
- Lewin, K. F. *et al.* (1994) 'Design and application of a free-air carbon dioxide enrichment facility', *Agricultural and Forest Meteorology*, 70(1–4), pp. 15–29. doi: 10.1016/0168-1923(94)90045-0.
- Lin, G. *et al.* (2001) 'Time-dependent responses of soil CO₂ efflux components to elevated atmospheric [CO₂] and temperature in experimental forest mesocosms', *Plant and Soil*, 229(2), pp. 259–270. doi: 10.1023/A:1004883221036.
- Lindsey, R. (2020) *Climate Change: Atmospheric Carbon Dioxide* | NOAA Climate.gov. Available at: <https://www.climate.gov/news-features/understanding-climate/climate-change-atmospheric-carbon-dioxide> (Accessed: 12 March 2021).
- Lovenduski, N. S. and Bonan, G. B. (2017) 'Reducing uncertainty in projections of terrestrial carbon uptake', *Environmental Research Letters*, 12(4). doi: 10.1088/1748-9326/aa66b8.
- Luo, Y. *et al.* (2004) 'Progressive nitrogen limitation of ecosystem responses to rising atmospheric carbon dioxide', *BioScience*, 54, pp. 731–739.
- Luo, Y. and Zhou, X. (2006) *Soil respiration and the environment*. Elsevier Academic Press.
- Ma, Y. *et al.* (2014) 'Stand ages regulate the response of soil respiration to temperature in a Larix principis-rupprechtii plantation', *Agricultural and Forest Meteorology*. doi: 10.1016/j.agrformet.2013.10.008.
- Matamala, R. and Schlesinger, W. H. (2000) 'Effects of elevated atmospheric CO₂ on fine root production and activity in an intact temperate forest ecosystem', *Global Change Biology*, 6(8), pp. 967–979. doi: 10.1046/j.1365-2486.2000.00374.x.
- McLeod, A. R. and Long, S. P. (1999) 'Free-air Carbon Dioxide Enrichment (FACE) in Global Change Research: A Review', *Advances in Ecological Research*, 28, pp. 1–56. doi: 10.1016/S0065-2504(08)60028-8.
- Medlyn, B. E. *et al.* (2015) 'Using ecosystem experiments to improve vegetation models', *Nature Climate Change*. Nature Publishing Group, 5(6), pp. 528–534. doi: 10.1038/nclimate2621.
- Miglietta, F. *et al.* (2001) 'Free-air CO₂ enrichment (FACE) of a poplar plantation: The POPFACE fumigation system', *New Phytologist*, 150(2), pp. 465–476. doi: 10.1046/j.1469-8137.2001.00115.x.
- Mitra, B. *et al.* (2014) 'Does vegetation structure regulate the spatial structure of soil respiration within a sagebrush steppe ecosystem?', *Journal of Arid Environments*, 103, pp. 1–10. doi: 10.1016/j.jaridenv.2013.12.006.
- Van der Molen, M. K. *et al.* (2011) 'Drought and ecosystem carbon cycling', *Agricultural and Forest Meteorology*. doi: 10.1016/j.agrformet.2011.01.018.

- Morgan, J. A. *et al.* (2001) 'Elevated CO₂ enhances water relations and productivity and affects gas exchange in C 3 and C 4 grasses of the Colorado shortgrass steppe', *Global Change Biology*, 7, pp. 451–466.
- Mueller, K. E. *et al.* (2013) 'Effects of plant diversity, N fertilization, and elevated carbon dioxide on grassland soil N cycling in a long-term experiment', *Global Change Biology*, 19(4), pp. 1249–1261. doi: 10.1111/gcb.12096.
- Nabuurs, G. J., Masera, O. and *et al* (2007) 'Forestry in Climate Change 2007: Mitigation', in *Contribution of working Group III to the Fourth Assessment Report of the Intergovernmental Panel on Climate Change*. Cambridge: Cambridge University Press, pp. 541–584.
- Noh, N.-J. *et al.* (2015) 'Responses of Soil, Heterotrophic, and Autotrophic Respiration to Experimental Open-Field Soil Warming in a Cool-Temperate Deciduous Forest'. doi: 10.1007/s10021-015-9948-8.
- Norby, R. J. (1996) 'Oaks in a high-CO₂ world To cite this version : Review article Oaks in', *Annales des Sciences Forestieres*, 53, pp. 413–429.
- Norby, R. J. *et al.* (1999) 'Tree responses to rising CO₂ in field experiments: Implications for the future forest', *Plant, Cell and Environment*, 22(6), pp. 683–714. doi: 10.1046/j.1365-3040.1999.00391.x.
- Norby, R. J. *et al.* (2005) 'Forest response to elevated CO₂ is conserved across a broad range of productivity', *Proceedings of the National Academy of Sciences*, 102(50), pp. 18052–18056. doi: 10.1073/pnas.0509478102.
- Norby, R. J. *et al.* (2010) 'CO₂ enhancement of forest productivity constrained by limited nitrogen availability', *Proceedings of the National Academy of Sciences of the United States of America*, 107, pp. 19368–19373. doi: 10.1073/pnas.1006463107.
- Norby, R. J. *et al.* (2016) 'Model-data synthesis for the next generation of forest free-air CO₂enrichment (FACE) experiments', *New Phytologist*, 209(1), pp. 17–28. doi: 10.1111/nph.13593.
- Norby, R. J. and Zak, D. R. (2011) 'Ecological Lessons from Free-Air CO₂ Enrichment (FACE) Experiments', *Annual Review of Ecology, Evolution, and Systematics*, 42(1), pp. 181–203. doi: 10.1146/annurev-ecolsys-102209-144647.
- Nowak, R. S., Ellsworth, D. S. and Smith, S. D. (2004) 'Functional responses of plants to elevated atmospheric CO₂- Do photosynthetic and productivity data from FACE experiments support early predictions?', *New Phytologist*, 162(2), pp. 253–280. doi: 10.1111/j.1469-8137.2004.01033.x.
- O'Connell, A. M. (1988) *Nutrient Dynamics in Decomposing Litter in Karri Forests of South-Western Australia*, *Journal of Ecology*. Available at: <https://about.jstor.org/terms>.
- Okada, M. *et al.* (2001) 'Free-air CO₂ enrichment (FACE) using pure CO₂ injection: System description', *New Phytologist*, 150(2), pp. 251–260. doi: 10.1046/j.1469-8137.2001.00097.x.
- Pan, Y. *et al.* (2009) 'Separating effects of changes in atmospheric composition, climate and land-use on carbon sequestration of U.S. Mid-Atlantic temperate forests'. doi: 10.1016/j.foreco.2009.09.049.
- Pan, Y. *et al.* (2011) 'A large and persistent carbon sink in the world's forests', *Science*. doi: 10.1126/science.1201609.
- Parfitt, R. L. (1979) 'The availability of P from phosphate-goethite bridging complexes. Desorption and uptake by ryegrass', *Plant and Soil*. Martinus Nijhoff, The Hague/Kluwer Academic Publishers, 53(1–2), pp. 55–65. doi: 10.1007/BF02181879.
- Pataki, D. E. *et al.* (2003) 'Tracing Changes in Ecosystem Function under Elevated Carbon Dioxide Conditions', *BioScience*, 53(9), p. 805. doi: 10.1641/0006-3568(2003)053[0805:tciefu]2.0.co;2.
- Phillips, O. L. *et al.* (2009) 'Drought sensitivity of the amazon rainforest', *Science*, 323(5919), pp. 1344–1347. doi: 10.1126/science.1164033.
- Phillips, R. P., Bernhardt, E. S. and Schlesinger, W. H. (2009) 'Elevated CO₂ increases root exudation from loblolly pine (*Pinus taeda*) seedlings as an N-mediated response', *Tree Physiology*, 29, pp. 1513–1523. doi: 10.1093/treephys/tpp083.

- Pregitzer, K. *et al.* (2006) 'Soil respiration in northern forests exposed to elevated atmospheric carbon dioxide and ozone', *Oecologia*, 148(3), pp. 503–516. doi: 10.1007/s00442-006-0381-8.
- Prentice, I. C. *et al.* (2001) 'The Carbon Cycle and Atmospheric Carbon Dioxide', in Houghton, J. T. *et al.* (eds) *Climate Change 2001: The Scientific Basis*. Cambridge: Cambridge University Press, pp. 183–237.
- Pritchard, S. G. *et al.* (2008) 'Fine root dynamics in a loblolly pine forest are influenced by free-air-CO₂-enrichment: a six-year-minirhizotron study', *Global Change Biology*, 14, pp. 588–602. doi: 10.1111/j.1365-2486.2007.01523.x.
- Pumpanen, J. *et al.* (2008) 'Respiration in Boreal Forest Soil as Determined from Carbon Dioxide Concentration Profile', *Soil Science Society of America Journal*, 72(5), p. 1187. doi: 10.2136/sssaj2007.0199.
- Le Quéré, C. *et al.* (2009) 'Trends in the sources and sinks of carbon dioxide', *Nature Geoscience*, 2(831). doi: 10.1038/ngeo689.
- Raich, J. and Tufekcioglu, A. (2000) 'Vegetation and Soil Respiration: Correlations and Controls', *Biogeochemistry*, 48(1), pp. 71–90.
- Rasse, D. P., Rumpel, C. and Dignac, M.-F. (2005) 'Is soil carbon mostly root carbon? Mechanisms for a specific stabilisation', *Plant and Soil*. Springer, pp. 341–356. doi: 10.2307/24124940.
- Reich, P. B. *et al.* (2006) 'Nitrogen limitation constrains sustainability of ecosystem response to CO₂.', *Nature*, 440(7086), pp. 922–5. doi: 10.1038/nature04486.
- Reich, P. B., Hungate, B. A. and Luo, Y. (2006) 'Carbon-Nitrogen Interactions in Terrestrial Ecosystems in Response to Rising Atmospheric Carbon Dioxide', *Annual Review of Ecology, Evolution, and Systematics*, 37, pp. 611–636. doi: 10.1146/annurev.ecolsys.37.091305.110039.
- Rogers, H. H., Runion, G. B. and Krupa, S. V. (1994) 'Plant responses to atmospheric CO₂ enrichment with emphasis on roots and the rhizosphere', *Environmental Pollution*, 83(1–2), pp. 155–189. doi: 10.1016/0269-7491(94)90034-5.
- Rosswall, T. (1982) 'Microbiological regulation of the biogeochemical nitrogen cycle', *Plant and Soil*. Martinus Nijhoff/Dr. W. Junk Publishers, 67(1–3), pp. 15–34. doi: 10.1007/BF02182752.
- Ruehr, N. K. and Buchmann, N. (2009) 'Soil respiration fluxes in a temperate mixed forest: Seasonality and temperature sensitivities differ among microbial and root-rhizosphere respiration', *Tree Physiology*, 30(2), pp. 165–176. doi: 10.1093/treephys/tp106.
- Rütting, T. and Andresen, L. C. (2015) 'Nitrogen cycle responses to elevated CO₂ depend on ecosystem nutrient status', *Nutr Cycl Agroecosyst*. doi: 10.1007/s10705-015-9683-8.
- Ryan, M. G. and Law, B. E. (2005) 'Interpreting, measuring, and modeling soil respiration', *Biogeochemistry*. Kluwer Academic Publishers, 73(1), pp. 3–27. doi: 10.1007/s10533-004-5167-7.
- Savage, K. E. *et al.* (2013) 'Long-term changes in forest carbon under temperature and nitrogen amendments in a temperate northern hardwood forest', *Global Change Biology*, 19, pp. 2389–2400. doi: 10.1111/gcb.12224.
- Saxe, H., Ellsworth, D. S. and Heath, J. (1998) 'Tree and forest functioning in an enriched CO₂ atmosphere', *New Phytologist*, 139(3), pp. 395–436. doi: 10.1046/j.1469-8137.1998.00221.x.
- Schepaschenko, D. G. *et al.* (2015) 'Estimation of forest area and its dynamics in Russia based on synthesis of remote sensing products', *Contemporary Problems of Ecology*, 8(7), pp. 811–817. doi: 10.1134/S1995425515070136.
- Schindlbacher, A., Zechmeister-Boltenstern, S. and Jandl, R. (2009) 'Carbon losses due to soil warming: Do autotrophic and heterotrophic soil respiration respond equally?', *Global Change Biology*, 15(4), pp. 901–913. doi: 10.1111/j.1365-2486.2008.01757.x.
- Schlesinger, W. H. (1991) *Biogeochemistry: an Analysis of Global Change*. Academic Press. doi: 10.1016/C2012-0-01654-7.

- Schlesinger, W. H. and Andrews, J. A. (2000) 'Soil respiration and the global carbon cycle', 48, pp. 7–20. doi: 10.1023/A:1006247623877.
- Schneider, M. K. *et al.* (2004) 'Ten years of free-air CO₂ enrichment altered the mobilization of N from soil in *Lolium perenne* L. swards', *Global Change Biology*, 10(8), pp. 1377–1388. doi: 10.1111/j.1365-2486.2004.00803.x.
- Soussan, J., Shrestha, B. K. (Bharat K. . and Uprety, L. P. (Laya P. (1995) *The social dynamics of deforestation : a case study from Nepal*. Parthenon Pub. Group.
- Stinson, G. *et al.* (2011) 'An inventory-based analysis of Canada's managed forest carbon dynamics, 1990 to 2008', *Global Change Biology*, 17(6), pp. 2227–2244. doi: 10.1111/j.1365-2486.2010.02369.x.
- Suseela, V. *et al.* (2012) 'Effects of soil moisture on the temperature sensitivity of heterotrophic respiration vary seasonally in an old-field climate change experiment', *Global Change Biology*, 18(1), pp. 336–348. doi: 10.1111/j.1365-2486.2011.02516.x.
- Swift, M. J. (Michael J., Heal, O. W. and Anderson, J. M. (Jonathan M. (1979) *Decomposition in terrestrial ecosystems*. Blackwell.
- Tao, S. *et al.* (2016) 'Global patterns and determinants of forest canopy height', *Ecology*. Ecological Society of America, 97(12), pp. 3265–3270. doi: 10.1002/ecy.1580.
- Tingey, D. T., Phillips, D. L. and Johnson, M. G. (2000) 'Elevated CO₂ and conifer roots : effects on growth, life span and turnover', *New Phytologist*, 147, pp. 87–103.
- Tiseo, I. (2021) *Atmospheric CO₂ concentrations worldwide 1959-2020* | Statista. Available at: <https://www.statista.com/statistics/1091926/atmospheric-concentration-of-co2-historic/> (Accessed: 14 March 2021).
- Tomè, E. *et al.* (2016) 'Mycorrhizal contribution to soil respiration in an apple orchard', *Applied Soil Ecology*. doi: 10.1016/j.apsoil.2016.01.016.
- Trueman, R. J. and Gonzalez-Meler, M. A. (2005) 'Accelerated belowground C cycling in a managed agriforest ecosystem exposed to elevated carbon dioxide concentrations', *Global Change Biology*, 11(8), pp. 1258–1271. doi: 10.1111/j.1365-2486.2005.00984.x.
- Van Veen, J. A. *et al.* (1987) 'Turnover of carbon, nitrogen and phosphorus through the microbial biomass in soils incubated with 14-C-, 15-N- and 32-P-labelled bacterial cells', *Soil Biology and Biochemistry*, 19, pp. 559–565. doi: 10.1016/0038-0717(87)90099-X.
- Vitousek, P. (1982) 'Nutrient Cycling and Nutrient Use Efficiency', *The American Naturalist*. The University of Chicago Press/The American Society of Naturalists, pp. 553–572. doi: 10.2307/2461143.
- Wand, S. J. E. *et al.* (1999) 'Responses of wild C₄ and C₃ grass (Poaceae) species to elevated atmospheric CO₂ concentration: a meta-analytic test of current theories and perceptions', *Global Change Biology*, 5, pp. 723–741.
- Wang, B. *et al.* (2014) 'Soil moisture modifies the response of soil respiration to temperature in a desert shrub ecosystem', *Biogeosciences*, 11, pp. 259–268. doi: 10.5194/bg-11-259-2014.
- Waring, R. H. and Running, S. W. (2007) *Forest ecosystems : analysis at multiple scales*. 3rd edn. Elsevier/Academic Press.
- Wei, W., Weile, C. and Shaopeng, W. (2010) 'Forest soil respiration and its heterotrophic and autotrophic components: Global patterns and responses to temperature and precipitation', *Soil Biology and Biochemistry*. doi: 10.1016/j.soilbio.2010.04.013.
- Wisniewski, J. and Sampson, R. N. (1993) *Terrestrial Biospheric Carbon Fluxes: Quantification of Sinks and Sources of CO₂*. Edited by J. Wisniewski and R. N. Sampson. Bad Harzburg: Kluwer Academic Publishers. doi: 10.1007/978-94-011-1982-5.
- Zaehle, S. (2013) 'Terrestrial nitrogen-carbon cycle interactions at the global scale', *Philosophical Transactions of the Royal Society B* 368. doi: 10.1098/rstb.2013.0125.
- Zaehle, S. *et al.* (2014) 'Evaluation of 11 terrestrial carbon-nitrogen cycle models against observations

from two temperate Free-Air CO₂ enrichment studies', *The New phytologist*, 202(3), pp. 803–22. doi: 10.1111/nph.12697.

Zak, D. R. *et al.* (2000) 'Elevated atmospheric CO₂, fine roots and the response of soil microorganisms: a review and hypothesis', *New Phytologist*, 147(1), pp. 201–222. doi: 10.1046/j.1469-8137.2000.00687.x.

Zak, D. R. *et al.* (2011) 'Forest productivity under elevated CO₂ and O₃: positive feedbacks to soil N cycling sustain decade-long net primary productivity enhancement by CO₂', *Ecology Letters*, 14, pp. 1220–1226. doi: 10.1111/j.1461-0248.2011.01692.x.

Zhou, X., Wan, S. and Luo, Y. (2007) 'Source components and interannual variability of soil CO₂ efflux under experimental warming and clipping in a grassland ecosystem', *Global Change Biology*, 13(4), pp. 761–775. doi: 10.1111/j.1365-2486.2007.01333.x.

Chapter 2: Methodology

This chapter gives an overview of the site selected for study and the field and the analytical methods used to produce the results set out in Chapters 3 to 5 and aims to provide general information about the study area and the methodological approaches used. Detailed descriptions about the site and the FACE Facility can be found at Hart *et al.*, (2019) and Mackenzie *et al.*, (2021).

2.1 Site Description

2.1.1 Birmingham's Institute of Forest Research (BIFoR)

Birmingham's Institute of Forest Research (BIFoR) is temperate deciduous woodland, located within Mill Haft at Staffordshire, England (52° 48' 3.6" N, 2° 18' 0" W). Mill Haft is part of Norbury Park Estate and has been woodland since pre-1881, appearing to be unchanged ever since. The total BIFoR FACE experimental area covers 7.3 ha, while the great forest covers 19.1 ha (Figure 2-1). A detailed site description can be found in Mackenzie *et al.* (2021).

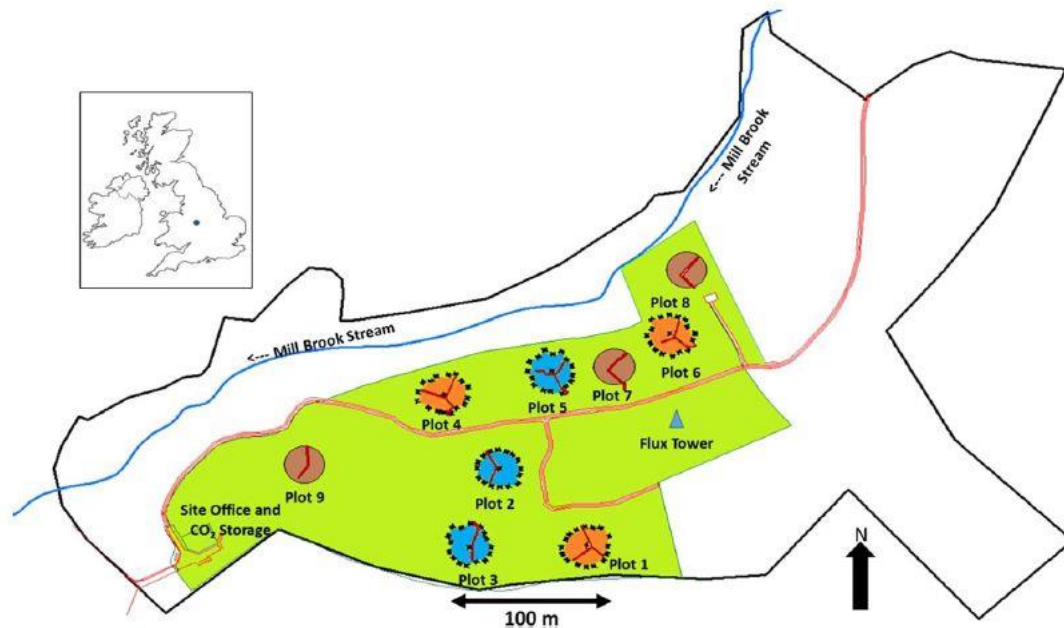


Figure 2- 1: Schematic map of the BIFoR FACE facility with Mill Haft wood. The green coloured area highlights the total experimental area controlled by the University of Birmingham, while the thick black line area represents the greater forest area. The circles coloured in orange, blue, and brown represent the eCO₂, ambient, and ghost arrays, respectively. The red line represents the main access road, while the blue line represents the Mill Brook stream flowing through the northern side of the woodland from NNE to WSW. The blue triangle represents a 40 m flux tower (adapted from Hart *et al.*, 2019).

BIFoR has a temperate maritime climate, with a mean annual temperature of 8 °C and mean annual precipitation of 800 mm (Mackenzie *et al.*, 2021). Briefly, the soil is brown earth luvisol with a sandy-clay texture and a mean soil pH of 4.5 at the top 10 cm. Mean soil total N and P in the top 10 cm are 0.28% and 18 mg P kg⁻¹, respectively, indicating that BIFoR is a low nutrient woodland, and total organic matter content is 3.67%.

The dominant overstorey species at the BIFoR FACE facility is old-growth (>160 years) *Quercus robur* (pedunculate oak), approximately 25 m height, covering approximately 45% of the array area. The woodland has a dense multi-layered canopy unaffected by the construction of the FACE infrastructure (Hart *et al.*, 2019). The understorey is interspersed with *Corylus avellana* (common hazel), *Acer pseudoplatanus* (sycamore), *Ilex aquifolium* (holly), *Crataegus monogyna*, and *C.*

laevigata (hawthorn). Pre-treatment oak leaf analysis showed that the mean N:P ratio was ~16, indicating a possible N and P co-limitation in the ecosystem (Mackenzie et al., 2021).

2.1.2 BIFoR Free Air CO₂ Enrichment (FACE) facility

A detailed FACE facility description can be found in Hart *et al.* (2019). Briefly, the BIFoR FACE facility comprises six 30 m diameter infrastructure arrays (elevated CO₂, n = 3; ambient, n = 3) and three non-infrastructure arrays (undisturbed, n = 3). Each treatment is replicated three times and operates on two different canopy levels, as suggested by Fillion, Dutilleul, and Potvin (2000). The infrastructure is approximately 25 m height, depending on each array's canopy height. Figure 2-2 depicts a schematic example of a BIFoR FACE array with infrastructure. CO₂ is mixed with air before its release and subsequently is released from the upwind quadrant of 15-m radius treatment patches. The CO₂ release rates are adjusted every second, and the emitter pipe valve, which is based on wind direction, is adjusted every 4 seconds.

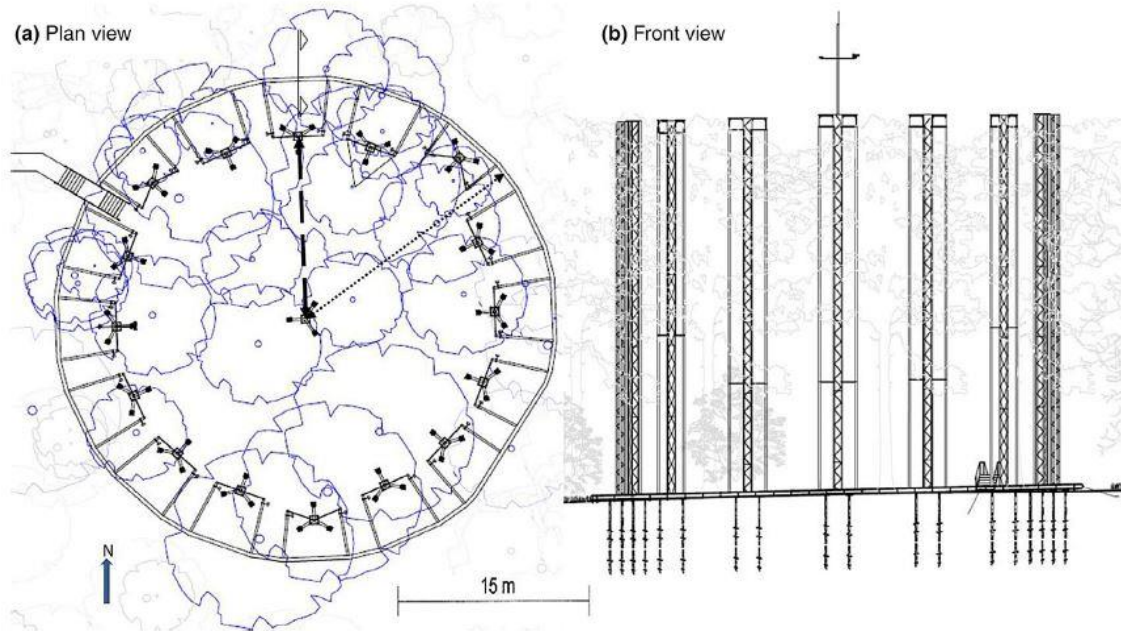


Figure 2- 2: Schematic representation of a BIFoR FACE infrastructure array. (a) Plan view of a 30 m diameter experimental patch with the structures at its circumference. The dotted line represents the center's radius to the outer plenum edge ($R \sim 20$ m). In contrast, the dashed line represents the radius from the centre to the research array's inner edge ($R \sim 15$ m). (b) The front view depicts the screw pile system penetrating the bedrock, providing secure anchoring and bypassing the need for supporting the towers with guy cables (Hart *et al.*, 2019).

CO₂ fumigation began on the 3rd April 2017 until 27th October 2017 (Year 1) and on the 1st April 2018 until 31st October 2018 (Year 2). Both years, the beginning and the end of the fumigation followed the forest's phenology, coexisting with the beginning of budburst and leaf fall, respectively. The fumigation system operated from 05:00 to 22:00, depending on the solar angle. For Year 1 (Figure 2-3), the eCO₂ arrays were within the 10% of target for 81.6% of the scheduled operation time and 20% of the target within 96.7% (Hart *et al.*, 2019). Contamination of the ambient arrays by CO₂ from the eCO₂ arrays was rare and short-lived, with ambient arrays being 10% of the control setpoint 98.8% of the time.

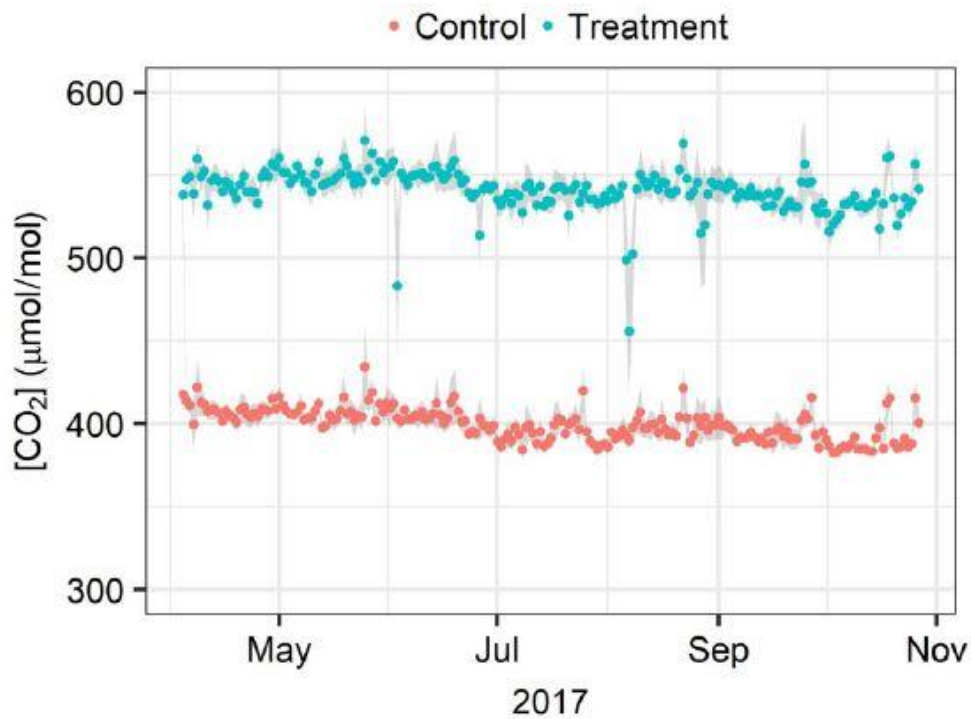


Figure 2- 3: Daily atmospheric CO₂ averages in ambient (red dots) and eCO₂ (blue dots) arrays at BIFoR FACE during Season 1 (4th April – 27th October 2017) (adapted from Hart *et al.*, 2019).

2.2 Field Methods

2.2.1 Soil respiration

2.2.1.1 Experimental design

To assess the soil respiration at BIFoR FACE, 18 experimental blocks were established across the site, 9 in ambient arrays and 9 in eCO₂ arrays (Figure 2-4), as proposed by Heinemeyer *et al.* (2007). Collars were installed in June 2016 (9 months before CO₂ fertilization), minimizing soil disturbance on soil respiration measurements, and left during the summer period for settlement.

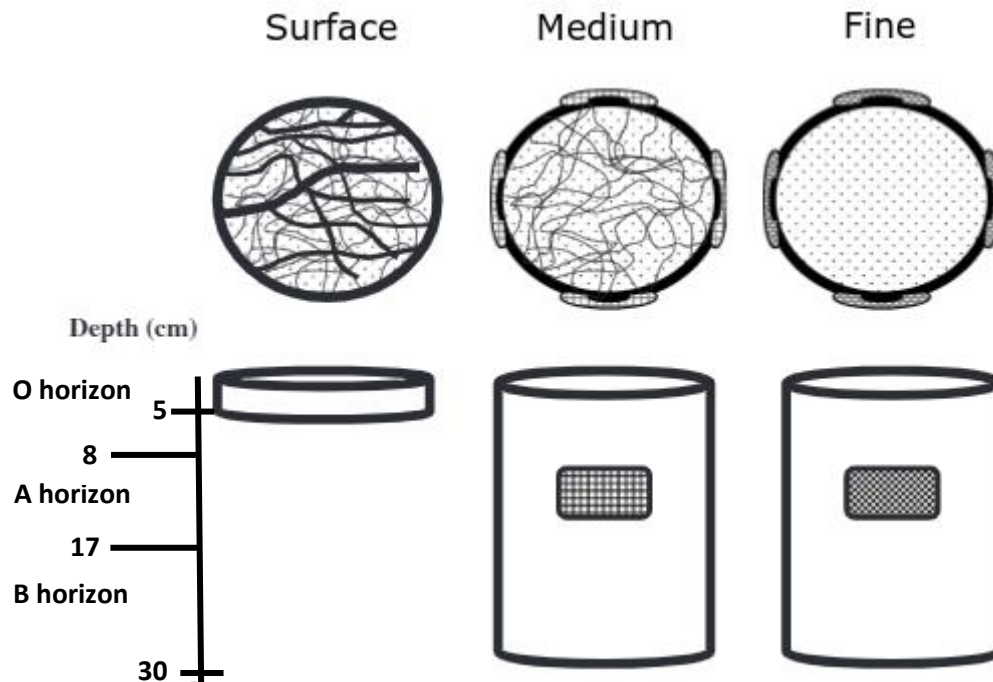


Figure 2- 4: Schematic representation of the soil respiration experimental blocks used at BIFoR FACE (adapted from Heinemeyer et al., 2007). Surface collars were only 5 cm deep inserted in the soil allowing roots, hyphal, and microbial growth. Medium and fine collars were inserted 30 cm deep in the soil, excluding fine roots from entering the collar. The fine collars were allowing only microbial growth.

Each block consisted of one PVC shallow collar (Drainage Superstore, Plymouth, UK) and two deeper collars with different mesh treatments. All collars were 200 mm in diameter, the shallow collars (*surface* collars hereafter) were 5 cm in height, and the deeper ones were 30 cm in height. The shallow collar was inserted only 3 cm in the soil, pressed firmly onto the litter layer with three 20 cm long stainless steel rods attached at the bottom of the collar to prevent dislocation by human or animal activity. The stainless steel rods ensured no roots were severed while an airtight seal was achieved, avoiding potential lateral diffusion of CO₂. These collars did not interfere with fine roots, mycorrhizal, or microbial dynamics and growth. The two deeper collars were inserted at approximately 25 cm depth, preventing fine root ingrowth, which is concentrated mainly in the soil's upper centimetres (Jackson, Mooney, and Schulze, 1997). Deeper collars had four rectangular (5 x 5 cm) windows cut into their sides

which were covered with nylon meshes, with grids size of 41 μm (Ek, 1997) (*medium* collars hereafter) and 1 μm (*fine* collars hereafter), allowing or excluding ectomycorrhizal hyphal ingrowth, respectively. In summary, there are three surface, three medium, and three fine collars in every ambient and eCO₂ array (18 collars of each treatment across the site).

As mentioned in Chapter 1, assessing the contribution of various soil components to the total soil respiration is of paramount importance towards understanding the C dynamics belowground and their possible imbalance due to CO₂ fertilization. With the experimental design as described above, partitioning the soil respiration into total (R_s), autotrophic (R_a), heterotrophic (R_h), fine root (R_r), and hyphal (R_m) respiration were enabled. R_s and R_h were measured directly from the surface and fine collars, respectively. R_a was calculated by subtracting the fine collars' values from those of the surface collars. R_r was calculated by subtracting the medium collars' values from the surface collars, and lastly, R_m was calculated by subtracting the fine collars' values from the medium collars. For enabling a better understanding, the equations used for the soil respiration partitioning calculations can be found below:

$$\text{Total soil respiration } (R_s) = \text{Surface collars} \quad \text{Equation 2 – 1}$$

$$\text{Heterotrophic respiration } (R_h) = \text{Fine collars} \quad \text{Equation 2 – 2}$$

$$\text{Autotrophic respiration } (R_a) = \text{Surface} - \text{Fine collars} \quad \text{Equation 2 – 3}$$

$$\text{Fine root respiration } (R_r) = \text{Surface} - \text{Medium collars} \quad \text{Equation 2 – 4}$$

$$\text{Hyphal respiration } (R_m) = \text{Medium} - \text{Fine collars} \quad \text{Equation 2 – 5}$$

2.2.1.2 Soil respiration measurements

Soil respiration rates were measured with a close-path infrared gas analyser (IRGA) control unit (LI-8100A, LI-COR, Nebraska, USA) coupled with a multiplexer (LI-8150, LI-COR, Nebraska, USA), allowing all nine collars to be measured using opaque long-term chambers (8100-104, LI-COR, Nebraska, USA), autonomously and continuously for one ambient and one eCO₂ array simultaneously. The first measurement took place in October 2016 (4 months after the collar installation) and continued until October 2018 (end of Year 2 of the CO₂ fumigation). The measurements were collected on hourly intervals for two continuous weeks, allowing the monitoring of soil respiration variability associated with daily cycles. The instruments were moved to the next ambient and eCO₂ arrays on a fortnightly basis, enabling the monitoring of soil respiration associated with spatial variability.

CO₂ travels from the production sites to the atmosphere principally by diffusion through air-filled pores and cracks in the soil. However, it can also be impelled by local climatological changes in pressure due to wind or volumetric displacement by rain. The LI-8100A avails the rate of CO₂ increase in the chamber to estimate the rate at which CO₂ diffuses into the air outside the chamber; thus, for accurate estimates, conditions in and out of the chamber must be similar. These conditions contain the concentration gradients driving diffusion, barometric pressure, soil moisture, and temperature.

As the chamber closes to measure, it creates an increase in CO₂ mole fraction, making the CO₂ diffusion gradient between the soil surface layer and the air inside and outside of the chamber differ. The instrument estimates and corrects the diffusion rate using an analytical technique that considers the effects of increasing chamber CO₂

concentration on the diffusion gradient, facilitating the initial rate of CO₂ increase estimate that followed immediately after the chamber closed.

Although previous studies have shown that chambers can change gas concentration gradients in the soil, causing errors in CO₂ flux estimates (Healy *et al.*, 1996), this is prevented by limiting the measurement time to 2 minutes, limiting CO₂ concentration changes to vary significantly, and keeping the chamber effect to the minimum. Furthermore, chambers are designed with pressure vents to block pressure gradients and wind incursions outside of the chamber. The chamber's automated movement prevents possible mechanical disturbances during measurements. The soil area inside and outside of the chamber is exposed to the same environmental conditions, as the chamber moves away from the soil measurement area when a measurement is not in progress.

The instrument automatically provides the calculation of fluxes and performs the essential corrections by default. A detailed description of the system's theory of operation can be found at *LI-8100 Automated Soil CO₂ Flux System & LI-8150 Multiplexer Instruction Manual* (2007). Briefly, the equation used for calculating the flux is:

$$F_c = \frac{10 * V * P_0 \left(1 - \frac{W_0}{1000}\right)}{R * S(T_0 + 273.15)} * \frac{\partial C'}{\partial t} \quad \text{Equation 2 - 6}$$

Where F_c is the soil CO₂ efflux rate ($\mu\text{mol m}^{-2} \text{s}^{-1}$), V is the volume (cm^3), P_0 is the initial pressure (kPa), W_0 is the initial water vapour mole fraction (mmol mol^{-1}), S is the soil surface area (cm^2), R is the gas constant ($8.314 \text{ Pa m}^3 (\text{K}^{-1} \text{mol}^{-1})$), T_0 is the initial

air temperature (°C), and $(\partial C')/\partial t$ is the initial rate of change in water-corrected CO₂ mole fraction ($\mu\text{mol mol}^{-1}$).

Data quality was assessed using the SoilFluxProTM software (LI-COR, Nebraska, USA). Since the infrared gas analyser-multiplexer-long-term-chamber path is closed, negative fluxes were removed from the dataset. Furthermore, fluxes with a coefficient of variation (%) of linear flux greater than 3.5, and fluxes with poor fitting were also removed. The software calculates both the linear and the exponential soil flux automatically; however, certain variables were adjusted from the manufacturer's default settings to fit our experimental needs. The surface area of the 20 cm diameter collars was 314.16 cm², the long-term chamber volume was 4076.1 cm³, while the IRGA and the multiplexer volume were set to default values. The volume of the cables (237 cm³) connecting the chambers with the multiplexer was also included. Due to soil variability, each chamber-collar surface's overall volume was unique for each collar and was measured frequently to ensure accurate fluxes, as advised by the manufacturer. All observations were 2 minutes in length, with the first 20 sec excluded from the flux calculation since it is a period that ensures the gas mixing inside the chamber. An additional 15 sec and 45 sec were added before and after the observation duration, respectively, to ensure that the cables transferring the gas to the IRGA were flushed clean and avoid any potential carryover to the following observation.

2.2.2. Environmental factors

Soil volumetric water content (VWC) and soil temperature (T_s) were measured one meter from each of the three experimental soil respiration blocks per array, with

permanently installed shallow CS655 probes inserted in the top 12 cm soil (Campbell Scientific, Logan, UT, USA). These data were recorded in 15-min intervals by a data logger in each plot (Campbell Sci CR1000, Campbell Scientific).

2.2.3 Soil Bioavailable nutrients

Ion-exchange resin membranes (IEMs hereafter) (Membranes International Inc., New Jersey, USA) were used to assess inorganic N, as ammonium (NH_4^+) and nitrate (NO_3^-), and P, as phosphate (PO_4^{3-}), availability, using a similar approach as Hasegawa, Macdonald and Power (2016). This is a simple, commonly used method offering an integrated measure of nutrient availability through the whole incubation period (Abrams and Jarrell, 1992; Qian and Schoenau, 2002; Bowatte *et al.*, 2008) as opposed to nutrient availability measurements from soil extracts and soil solutions that provide instantaneous measurements of nutrient availability, echoing the concentrations available at the time of the sampling (Abrams and Jarrell, 1992; Bowatte *et al.*, 2008).

Five anion IEMs (AMI 7001; 2 cm x 12 cm) and five cation IEMs (CMI 7000; 2 cm x 12 cm) were inserted in the top 12 cm of the soil next to each soil respiration experimental block in each array. From January 2017, three AMI and three CMI were inserted in the soil at eight locations within each array; three sets of each were located next to the soil respiration experimental blocks. The rest five sets were randomly located within each array. IEMs were incubated in situ for approximately a month before retrieval.

2.2.4 Soil sampling

2.2.4.1 Experimental design

Samples were collected in March 2017 (a month before the CO₂ treatment started) and then in March, July, and November 2018 (Year 2). No samples were collected during Year 1 of the experiment due to logistical constraints such as time, resources, and human power availability. Before the commencement of soil sampling, three permanent soil plots (2 x 2 m²) for soil core extraction have been marked out within each array (eCO₂, ambient, and ghost). The soil plot locations are specified in Fig. 2-5. Each soil plot was subsequently subdivided into a grid with a plastic frame representing the available core extraction area. For each soil plot, a corresponding plot outside each array was marked for backfilling core extraction.

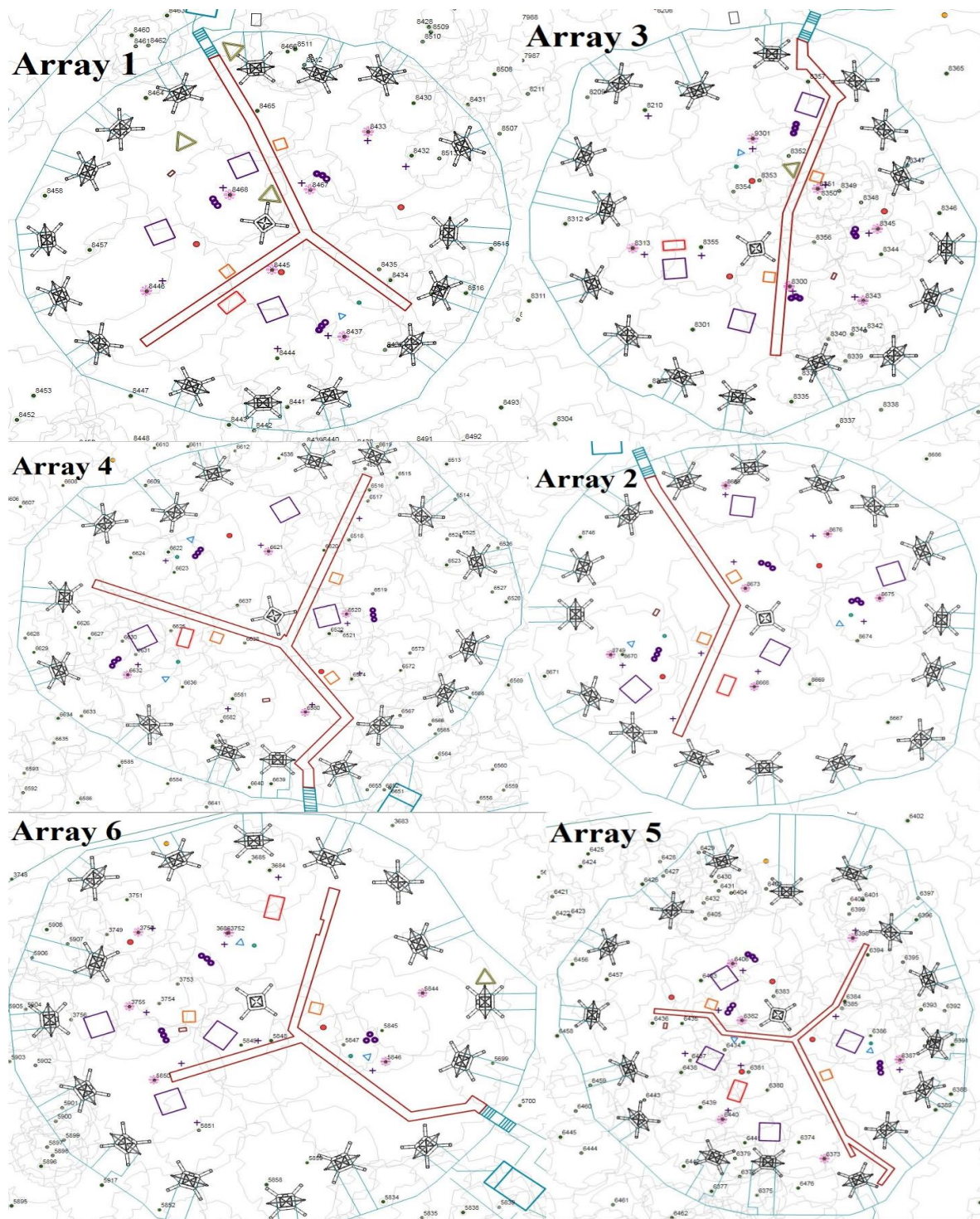


Figure 2- 5: Maps of all six FACE arrays ($n = 3$ ambient and $n = 3$ eCO₂) shown as the initially assigned pairs (ambient-eCO₂). The purple squares denote the soil sampling plots ($n = 3$ per array, except array 2 and 5 where $n = 4$), the purple circles denote the soil respiration experimental blocks ($n = 3$ per array), and the purple crosses denote the ion-exchange soil resin membrane locations ($n = 8$ per array).

2.2.4.2 Soil core extraction

A 55 mm-diameter soil core (30 cm depth) was extracted from each soil plot from each of the nine arrays ($n = 27$ soil cores across the site). All soil cores were sampled on the same day and kept in a cool box as generally advised for temperate soils (Hart *et al.*, 1994) and widely used when there are constraints on possessing soil samples directly after sampling. For each soil core taken from the soil plots in each array, the same depth and diameter core was taken from the backfilling plots outside of the arrays. The backfilling cores were excavated to the same depth as the soil cores, separated by horizons, and sieved with a 2 mm mesh sieve. Roots and pebbles were removed from the backfilling cores. Both locations from where soil and backfilling cores were extracted were marked with a 20 cm long plastic tube. A summary of the samples taken over the four different sampling campaigns is set out in Table 2-1.

Table 2- 1: Summary of the number of samples taken, analysis, and methods used for all four soil campaigns at BIFoR FACE.

n (per sampling campaign)					
		Baseline	Season 2		
Variable	Method	March (2017)	March (2018)	July (2018)	November (2018)
Soil moisture	Loss of ignition	81	81	81	81
Bulk density	55 mm diameter x 30 cm length core	27	27	27	27
Microbial biomass	Chloroform fumigation	81	81	81	81
Total organic C	Analytik Jena	162	162	162	162
Total organic N	Analytik Jena	162	162	162	162
NH ₄ ⁺	Skalar San ++	81	81	81	81
NO ₃ ⁻	Skalar San ++	81	81	81	81
PO ₄ ³⁻	Molybdenum blue method	162	162	162	162

2.3 Laboratory Methods

2.3.1 Soil Bioavailable nutrients

Upon retrieval, IEMs were washed thoroughly with deionized water to remove any soil particles and then extracted for PO_4^{3-} , NH_4^+ and NO_3^- using the following modification of Rayment and Lyons (2011)'s and Bowatte *et al.* (2008)'s methods, respectively. Each AMI and CMI from each sample location were extracted with 0.5 M HCl, shaken at 180 rpm for two hours, and then the membranes were removed from the solution and discarded. From January 2017 and onwards, the three CMI from each location were bulked together as one sample, and equivalently for the three AMI, and then the same process was followed as described before.

Concentrations of NH_4^+ and NO_3^- were analysed by a continuous flow analyser (San ++ Continuous Flow Analyser, Skalar, Breda, The Netherlands). The automated procedure for NH_4^+ determination is based on the modified Berthelot reaction (Krom, 1980; Searle, 1984). Ammonia is chlorinated to monochloramine, which reacts with salicylate to 5-aminosalicylate. After oxidation and oxidative coupling, a green coloured complex is formed. The absorption of the formed complex is measured at 660 nm. Six standards were used for performing the calibration curve, reference material was used every 30 samples, and a drift check material was used every ten samples to assess potential variation over the analysis time. The software performs drift and water correction automatically.

Moreover, the automated procedure for the determination of NO_3^- is based on the cadmium reduction method (Navone, 1964; Gal, Frenzel, and Möller, 2004). The sample is buffered at pH 8.2 and passed through a column containing granulated copper-cadmium to reduce the NO_3^- to nitrite (NO_2^-). The NO_2^- (originally present plus reduced NO_3^-) is determined by diazotising with sulphanilamide and coupling with N-

(1-naphthyl)ethylenediamine dihydrochloride to form a highly coloured azo dye which is measured at 530 nm. Six standards were used for performing the calibration curve, reference material was used every 30 samples, and a drift check material was used every ten samples to assess potential variation over the analysis time. The software performs drift and water correction automatically.

Concentrations of PO_4^{3-} were analysed spectroscopically (UV-Vis Jenway 6850, Cole-Palmer, UK) using the molybdenum blue method (Boltz and Mellon, 1948; Worsfold *et al.*, 2005). Ammonium heptamolybdate and potassium antimony (III) oxide tartrate react in an acidic medium with diluted phosphate solutions to form an antimony-phospho-molybdate complex. This complex is reduced to an intensely blue-coloured complex by L(+)-ascorbic acid and measured at 880 nm. Six standards were used for performing the calibration curve, reference material was used every 30 samples, and a drift check material was used every ten samples to assess potential variation over the analysis time. Standards and samples were prepared in 4 mL cuvettes and were left for 15 minutes for colour development.

Detection limits for all three analyses can be found in Table 2-2 as provided by Skalar and as calculated via the I method (Shrivastava and Gupta, 2011). The biota-available N and P ratios were determined as ratios of NH_4^+ -N, NO_3^- -N, and PO_4^{3-} -P. The data presented in this study are reported in monthly averages in $\mu\text{g NH}_4^+\text{-N cm}^{-2} \text{ d}^{-1}$, $\mu\text{g NO}_3^-\text{-N cm}^{-2} \text{ d}^{-1}$, and $\mu\text{g PO}_4^{3-}\text{-P cm}^{-2} \text{ d}^{-1}$, respectively.

Table 2- 2: Summary of detection limits and wavelengths used during the soil bioavailable nutrient analysis, inorganic N, and microbial P analyses provided by the manufacturer (for NH_4^+ and NO_3^-) and as calculated (for PO_4^{3-}). The units reported are mg NH_4^+ -N, NO_3^- -N, and PO_4^{3-} -P/L. Detection limits for all three analyses were calculated using 0.5M HCl as the matrix.

Analysis	Wavelength	Detection limits			
		Instrument's specification	Limit of detection	Limit of quantitation	Limit of blank
NH_4^+	660 nm	0.2	0.143	0.426	0.089
NO_3^-	530 nm	0.02	-0.041	0.015	-0.052
PO_4^{3-}	880 nm	NA	-0.015	-0.012	-0.015

2.3.2 Daily IEM Loading Capacity Assessment

A daily IEM loading capacity assessment was performed to assess the IEMs' loading capacity simulating field conditions in the laboratory environment for 60 days with 5-day intervals. A mixed stock solution was prepared to represent an average 5-day-concentration of the months with the highest concentration recorded, during the baseline period, 7 mg NH_4^+ -N/L, 12 mg NO_3^- -N/L, and 1 mg PO_4^{3-} -P/L, respectively. One AMI and one CMI (2 x 4 cm) were inserted in pre-labeled sample vials with 50 mL mixed stock solution. The samples were shaken for 24 h at 180 rpm. After 24 h, the day-equivalent set of samples IEMS were extracted with 0.5 M HCl, shaken for two h at 180 rpm, and both extract and residual were frozen until analysis. The rest of the IEMS were transferred in new vials, the freshly mixed stock solution was added and shaken for 24 h following the process described above. Residual samples were frozen until analysis. The assessment was performed in triplicates.

It was observed that the NH_4^+ ions (Figure 2-6A) are adsorbed linearly for the first 35 days of incubation in the soil; for the following ten days, the CMI adsorbance capacity stays similar, and in the final ten days, the CMI adsorbance capacity is increased again. For the first 40 days, the CMIs could successfully adsorb over 99.09% of the

NH_4^+ ions suspended in the stock solution; the following days, the CMI adsorbance remained over 94%. Furthermore, in the first 40 days, the difference between the stock solution and the extracts' concentration of $\text{NH}_4^+\text{-N}$ were differing from 6.5-14%, with the overall difference reaching 36%, suggesting that the CMI do not release the whole amount of ions that initially were adsorbed on them.

Similar patterns were observed for the NO_3^- ions adsorbance capacity (Figure 2-6B). The linear adsorbance pattern, the plateau, and the slight increase the final ten days being present with the only difference that the adsorbance linearity was present for five days longer than the $\text{NH}_4^+\text{-N}$. Moreover, for the first 40 days, the AMIs were able to adsorb over 99.99% of the $\text{NO}_3^-\text{-N}$ ions suspended in the stock solution and down to 96.1% for the whole period. Furthermore, in the first 45 days, the difference between the stock solution and the extracts' concentration of NO_3^- were differing from 1.6-10%, with the overall difference reaching 21%, suggesting that the AMIs are not releasing the whole amount of ions that initially were adsorbed on them.

Finally, for $\text{PO}_4^{3-}\text{-P}$ ions, the adsorbance capacity (Figure 2-6C) was linear until the first 40 days, and after that, a dramatic decrease in the adsorbance capacity was observed. In that time frame, the AMIs successfully adsorbed from 94-99.9% of the PO_4^{3-} ions suspended in the mixed stock solution, as indicated by the residuals concentrations, but for the 45-60 days, the adsorbance capacity was reduced to 55-82%. Moreover, in the first 45 days, the deviation between the stock solution and the extracts' concentration of $\text{PO}_4^{3-}\text{-P}$ differed from 19-71%, with the extracts having higher concentrations than the initial stock solution. The deviation range was wider for 45-60 days, 24-81%, suggesting that the AMIs are getting saturated with $\text{PO}_4^{3-}\text{-P}$ ions and cannot adsorb more.

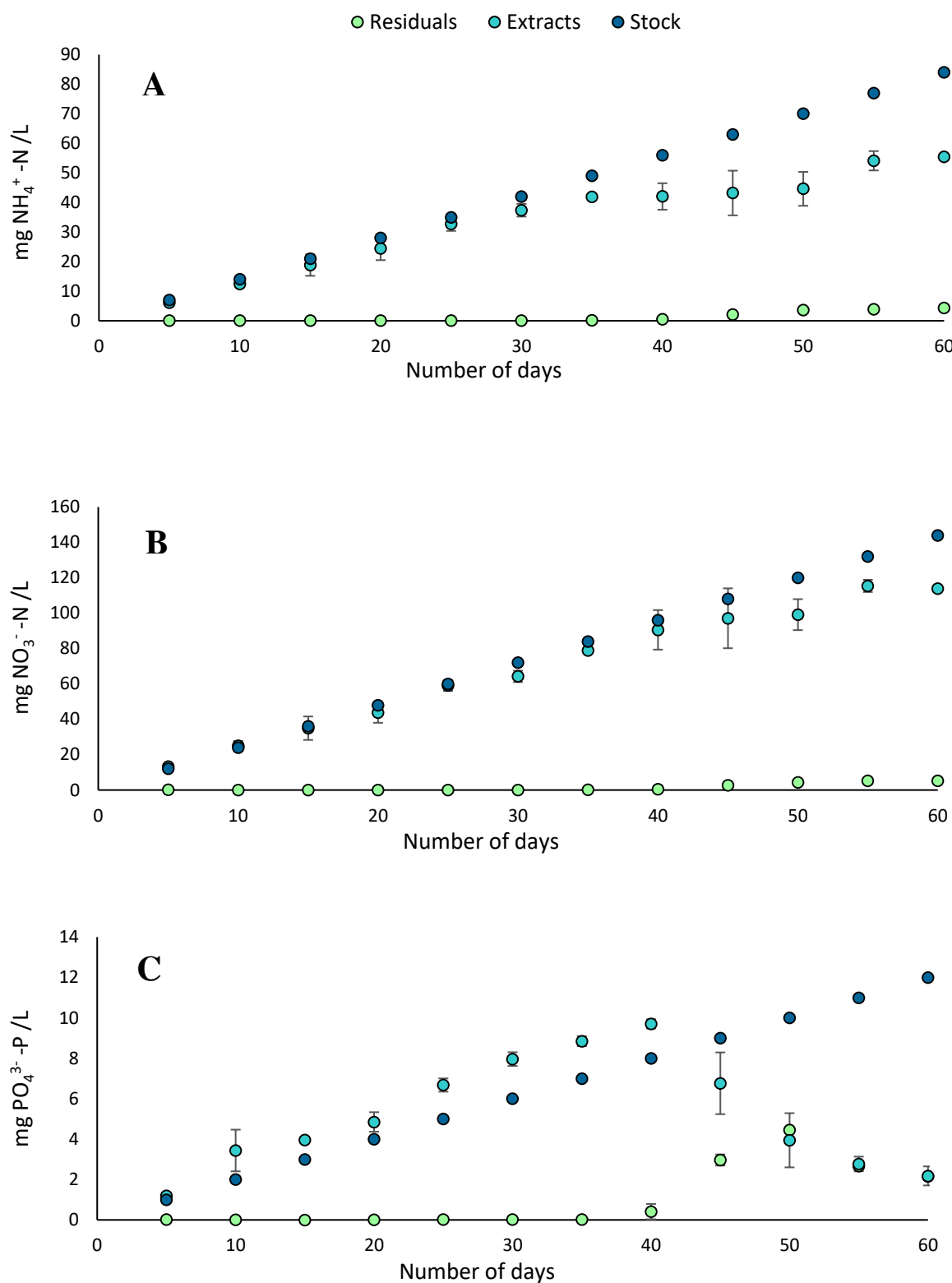


Figure 2- 6: Daily IEM loading capacity assessment for NH_4^+ (A), NO_3^- (B), and PO_4^{3-} (C). The light blue circles represent the extracted from IEMS concentrations, the dark blue circles represent the stock solution concentrations, and the green circles represent the residuals concentrations. The concentrations are in mg/L, and the error bars represent the standard deviation.

2.3.3 Extraction time assessment

Another assessment was performed to assess the IEMs' extraction time of different concentrations. Three different concentration ranges were used (Low, Medium, High) for all three ions ($\text{NH}_4^+\text{-N}$: 7, 50, 80 mg/L; $\text{NO}_3^-\text{-N}$: 12, 80, 150 mg/L; $\text{PO}_4^{3-}\text{-P}$: 1, 7, 12 mg/L). One AMI and one CMI (2 x 4 cm) were inserted in pre-labelled sample vials with 50 mL mixed stock solution of each concentration range. The samples were shaken for 24 h at 180 rpm. After the 24 h, the IEMS were extracted with 0.5 M HCl, shaken for 2, 6, 10, and 24 h at 180 rpm, and both extract and residual were frozen until analysis. The assessment was performed in triplicates.

In Figure 2-7A, the different concentrations and extraction times are shown for NH_4^+ . For the low concentration, the CMIs were able to adsorb 99.2-99.4% of the initial concentration, and the 2 h extraction was the most suitable one, providing 95% retrieval from the CMI. For the medium concentration, the CMI adsorbance capacity was similar to the one observed at the low concentration (99.2-99.4%), although the most suitable extraction time was 24 h, providing 93% retrieval. On the contrary, the CMI adsorbance capacity for the high concentration was significantly lower (73-79%), and the most suitable extraction time was 10 h, providing 81% retrieval.

In Figure 2-7B, the different concentrations and extraction times are shown for NO_3^- . For the low concentration, the AMIs were able to adsorb 100% of the initial concentration, and the 24 h extraction was the most suitable one, offering 92.5% retrieval from the AMIs. For the medium concentration, the AMI adsorbance capacity was similar to the one observed at the low concentration (99.8%), although the most suitable extraction time was the 10 h, offering 90% retrieval. Furthermore, the AMI adsorbance capacity for the high concentration was slightly lower (86-87%), and the most suitable extraction time was 24 h, providing 90% retrieval.

In Figure 2-7C, the different concentrations and extraction times are shown for PO_4^{3-} . The AMIs were able to adsorb 98-99% of the initial concentration for the low concentration, and the two h extraction was the most suitable one, offering 92% retrieval from the AMIs. For the medium concentration, the AMI adsorbance capacity was similar to the one observed at the low concentration (97-98%), although the most suitable extraction time was the 24 h, offering over 90% retrieval. However, for the high PO_4^{3-} -P concentration, all four extraction times performed relatively the same, and AMIs could not release the PO_4^{3-} P ions in the solution.

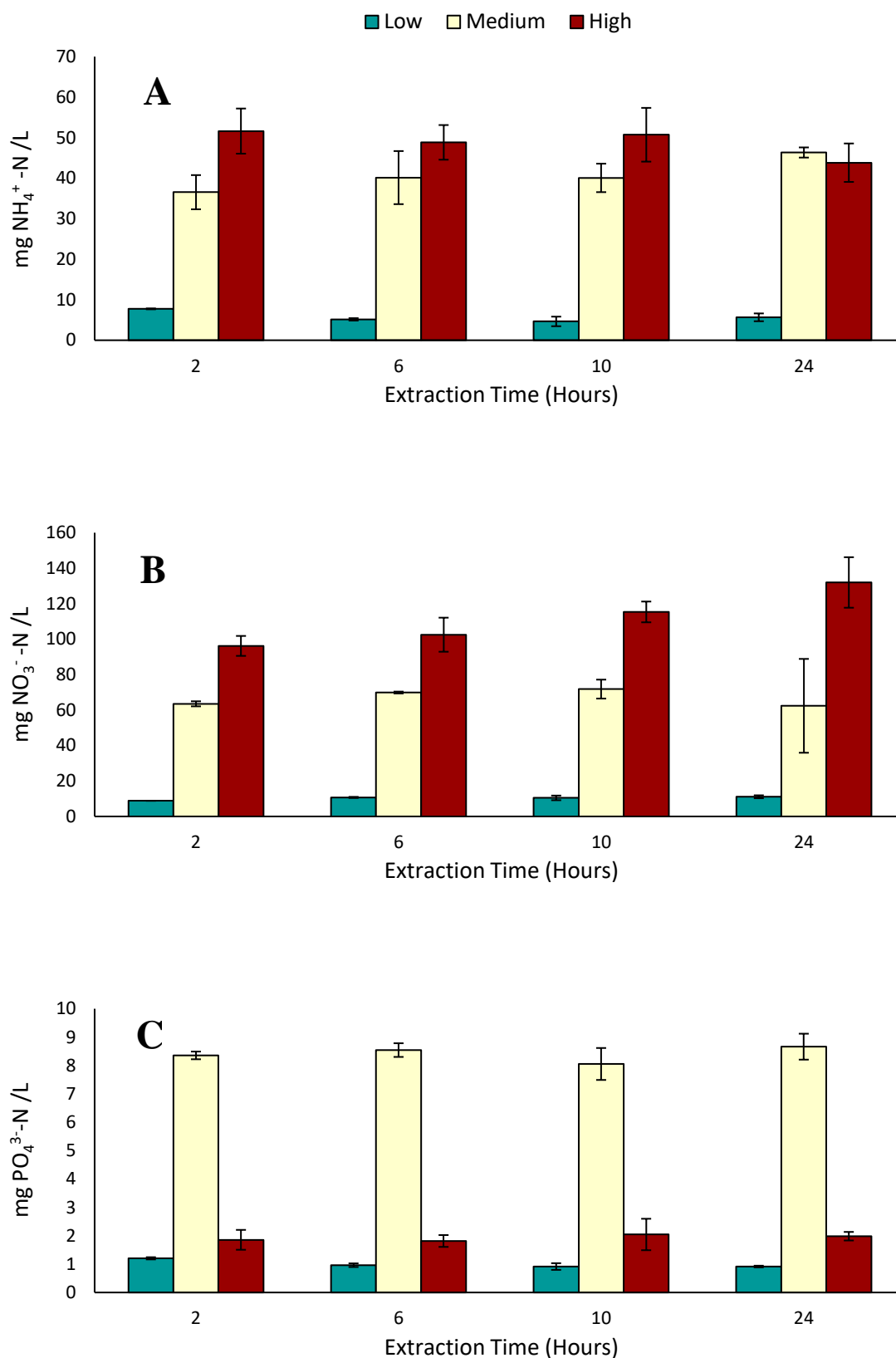


Figure 2- 7: Extraction time assessment for NH_4^+ (A), NO_3^- (B) and PO_4^{3-} (C). The green bars represent the lower concentrations, the yellow bars represent the medium concentrations, and the red bars represent the high concentrations for all three bioelements. The error bars represent the standard deviation.

2.3.4 Soil analysis

After sampling, all samples were returned to the laboratory for further analysis. Before analysis, each core was weighted and separated into three horizons (O, A, and B). Each horizon was sieved (2 mm sieve), and roots and pebbles were removed. From each horizon, subsamples were taken for soil moisture, microbial biomass total organic C and N, NH_4^+ , NO_3^- and PO_4^{3-} , DNA extraction, and archiving purposes for future analysis. Figure 2-8 is the schematic representation of the initial steps taken in the laboratory for all soil campaigns. Detailed descriptions for all analyses can be found later in this Chapter. Root and DNA analyses were performed by Clare Ziegler and Aileen Baird, respectively, for their Ph.D. project purposes; thus, these datasets are not presented in this thesis.

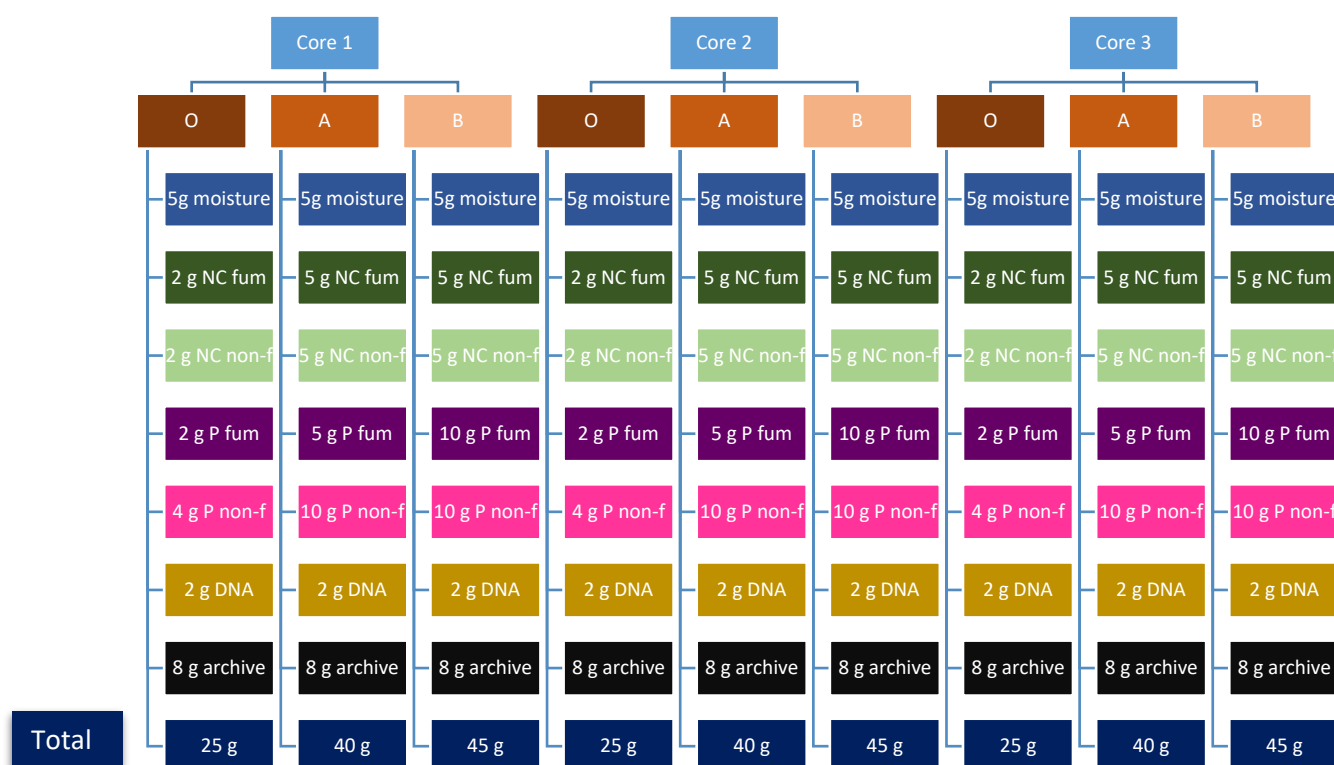


Figure 2- 8: Tree diagram depicting an example of the cores extracted in one array and the subsequent subsampling for the different analyses.

2.3.4.1 Soil moisture and bulk density

Soil moisture was determined gravimetrically by drying a 5g subsample from each horizon, at 106 °C for 48 hours and was calculated as follows:

$$\text{Soil moisture} = \frac{(W_w + t) - (W_d + t)}{(W_d + t) - t} \quad \text{Equation 2 – 7}$$

where W_w is the weight of wet soil (g), W_d is the weight of dry soil (g), and t is the tare's weight (g).

The soil moisture enabled the calculation of soil bulk density from:

$$\rho_d = \frac{M_s}{V_t} \quad \text{Equation 2 – 8}$$

where ρ_d is soil bulk density (g cm^{-3}), M_s is the mass of dry soil (g) per core volume, and V_t is the total volume of the soil core (cm^3).

2.3.4.2 Microbial biomass

To investigate the immobilization and mobilization of bioelements, specifically C and N, in the soil and their potential changes under elevated CO_2 , four subsamples were taken from each horizon. Two of the subsamples mentioned above were fumigated with chloroform (CHCl_3) following the methods described at Brookes, Powlson, and Jenkinson, 1982; Brookes *et al.*, 1985; Beck *et al.*, 1997 and the other two were used

as a control for the CHCl_3 fumigation process. One of the chloroform fumigated-nonfumigated pair of subsamples was analysed for total organic C and N (*CN pair* hereafter), and the other pair (*PO_4^{3-} pair* hereafter) was analysed for PO_4^{3-} -P (Table 2-3). Depending on the horizon and the subsequent analysis (CN or PO_4^{3-}), the subsamples' weights differed and can be found in the table. The CHCl_3 fumigated samples were put in a vacuum desiccator with a beaker containing 40 ml ethanol-free CHCl_3 and a moist paper towel to prevent the soils' desiccation. The desiccator was evacuated until the CHCl_3 boiled vigorously, and this process was repeated three times. On the fourth evacuation, once the CHCl_3 had boiled for two minutes, the valve was closed, and the desiccator was placed in the dark for 48 hours, preventing the CHCl_3 from breaking down. The non- CHCl_3 fumigated samples were also incubated in the dark next to the desiccator.

Table 2- 3: Summary of the different horizons' masses used for the CHCl_3 fumigation analysis.

Subsamples weights (g)				
Analysis	Horizons			
CN		O	A	B
	CHCl_3 fumigated	2	5	5
	CHCl_3 nonfumigated	2	5	5
PO_4^{3-}				
	CHCl_3 fumigated	2	5	10
	CHCl_3 nonfumigated	4	10	10

2.3.4.3 Total organic C and N

Immediately after 48 hours of CHCl_3 fumigation, both CHCl_3 fumigated, and non-fumigated samples for the CN analysis were extracted with 10 ml of 0.5 M K_2SO_4 ,

shaken for 2 hours at 200 rpm, and centrifuged for 5 minutes at 3999 rpm. Subsequently, all samples were syringe-filtered with a 0.45 mm syringe filter. The samples were stored overnight in the fridge until their next day's analysis.

2.3.4.4 Inorganic N

The non-CHCl₃ fumigated samples mentioned above were also analysed for soil extracted NH₄⁺ and NO₃⁻ by a continuous flow analyser (San ++ Continuous Flow Analyser, Skalar, Breda, The Netherlands) as described in section 2.3.1, with the only modification that 0.5 M K₂SO₄ was used for the standard preparation instead of deionised water and as a carrier to keep the matrix the same.

2.3.4.5 Microbial P

Immediately after 48 hours of CHCl₃ fumigation, in both CHCl₃ fumigated and non-fumigated samples for the PO₄³⁻ analysis, an AMI (2 x 4 cm size) and 15 ml of deionised water were inserted in each sample, as adapted from Sharpley (2000). The samples were shaken for 2 hours at 200 rpm. Subsequently, the AMIs were removed, washed, and extracted following the same process described in section 2.3.1 *Soil bioavailable nutrients* with the modification that the HCl extraction lasted 24 hours instead of 2. The samples were analysed spectroscopically (UV-Vis Jenway 6850, Cole-Palmer, UK) as described in section 2.3.1.

2.4 Statistical Methods

All analyses were carried out using R 3.6.2 and Rstudio 1.2.5033 (RStudio Team, 2019). The mixed-effects models were performed using R package lme4 (Bates *et al.*, 2015), and the coefficient of determination was calculated using the R package MuMIn

(Barton, 2014). For all analyses, effects were considered to be strongly significant if the model-reported P-value < 0.05.

Many semi-empirical approaches are modeling soil respiration response to environmental variables due to the C flux's global significance between ecosystems and the atmosphere (Raich, Potter and Bhagawati, 2002). Soils are associated with high heterogeneity and do not abide under a single functional unit, as in the case of photosynthesis, in which the functional unit is the leaf (Kutsch, Bahn and Heinemeyer, 2010). In soils, various organisms and enzymes are decomposing a variety of chemical substances, and only a few soil microbes have been studied. Hence, soil respiration modelling often follows a holistic approach, modelling soil respiration responses as a whole.

The most commonly used semi-empirical modelling approaches are the exponential Q_{10} relationship (Hoff, 1898), the Arrhenius equation, and its subsequent modification by Lloyd and Taylor (1994) or gap-filling strategies (Gomez-Casanovas *et al.*, 2013). However, both approaches include only soil temperature as a predictor variable of soil respiration; the Q_{10} approach does not always provide the best fit of the soil respiration responses, while the Arrhenius might not apply under changing substrate availability circumstances (Kutsch, Bahn and Heinemeyer, 2010).

When studying soil respiration responses *in situ*, both biotic and abiotic factors, such as photosynthesis, soil moisture, and soil temperature, co-vary. Hence, when soil respiration variation is attributed to a single variable, background correlations with other variables can rumple the relationship. Moreover, our study includes unavoidably the spatial dimension since forest soils are heterogeneous. Thus, we concluded that the optimum approach that could describe the soil respiration responses was to use a

semi-empirical relationship in which soil moisture, soil temperature, soil respiration, and their interactions with eCO₂ were used to predict soil respiration responses. Moreover, our approach includes both the spatial and temporal elements in the soil respiration predictions.

2.4.1 Chapter 3 – Additional methodology

2.4.1.1 Environmental drivers and R_s

To assess the potential eCO₂ effect on environmental drivers, daily averages of the VWC and T_s were analysed in a mixed-effect model framework treating eCO₂ as a fixed effect with 'array'. Data collected before the eCO₂ enrichment (up to 3rd April 2017) were analysed in a separate mixed-effects model framework to assess potential differences before eCO₂ enrichment due to soil's inherent spatial variability.

Before performing the mixed-effect models for investigating the effect of R_s' environmental variables, we needed to establish the variables' relationships with R_s. Linear and quadratic relationships between R_s and VWC were tested, and linear and exponential relationships between R_s and T_s. The best models were chosen based on the Akaike information criteria (AIC).

Mixed-effects models were also used to investigate the effect of environmental drivers, season, eCO₂, and their interactions on R_s, aggregated in daily averages. For this mixed-effects framework, the variables above (eCO₂, VWC, T_s, and season) were treated as fixed effects while 'array', 'collar/sensor', and 'number of days since the beginning of the measurements' were treated as random effects. Before the eCO₂ enrichment (up to 3rd April 2017), data collected were analysed separately to assess

potential differences before eCO₂ enrichment due, presumably to spatial inhomogeneities in R_s.

The AIC tool was used to identify the two best-fitted models, and an ANOVA was used to determine which of the two models was the best fitted. Finally, the coefficient of determination (R²) was calculated to assess the model's predictive capacity.

2.4.1.2 Annual R_s estimates

Due to the experimental setup (measuring one ambient array and one treatment array for two weeks) and given the seasonal and temporal variability of R_s, a modelled approach was used to calculate the annual R_s. Daily averages of the R_s data were estimated using the model of best fit from the *Environmental drivers'* section, predicting the R_s of the rest of the arrays at all periods for the whole study period. VWC and T_s from each array aggregated in daily averages were used as predictors. Subsequently, daily averages of observed and predicted R_s values were merged, producing a complete R_s dataset.

2.4.1.3 Bioavailable nutrients

For nutrient analysis, the replication unit was the FACE array (n=3 for each of ambient and treatment), and all data were aggregated in monthly timestamps. The effect of eCO₂ on bioavailable nutrient concentrations was assessed using linear-mixed-effects models, for which 'array' and 'number of days since the beginning of the measurements' were random factors. Data collected before the eCO₂ enrichment were analysed separately to assess initial pretreatment differences. Subsequently, linear-mixed-effects models were undertaken with CO₂ and two covariates – T_s and VWC –

and their interactions ($e\text{CO}_2 \cdot T_s$, $e\text{CO}_2 \cdot \text{VWC}$, and $e\text{CO}_2 \cdot T_s \cdot \text{VWC}$) as fixed effects to evaluate the role of soil conditions in responses to elevated CO_2 . In this mixed-effects framework, 'array' and 'number of days since the beginning of the measurements' were used as random factors.

2.4.2 Chapter 4 – Additional methodology

2.4.2.1 Environmental drivers and R_s

To assess the potential $e\text{CO}_2$ effect on environmental drivers, daily averages of the VWC and T_s were analysed in a mixed-effect model framework treating $e\text{CO}_2$ as a fixed effect with 'array'. Before performing the mixed-effect models for investigating the effect of R_s environmental variables, we needed to establish the variables' relationships with R_s . Linear and quadratic relationships between R_s and VWC were tested, and linear and exponential relationships between R_s and T_s . The best models were chosen based on the Akaike information criteria (AIC).

Mixed-effects models were also used to investigate the effect of environmental drivers, season, $e\text{CO}_2$, and their interactions on R_s , aggregated in daily averages. For this mixed-effects framework, the variables above ($e\text{CO}_2$, VWC, T_s) were treated as fixed effects while 'array', 'collar/sensor', and 'number of days since the beginning of the measurements' were treated as random effects. Finally, the AIC tool was used to identify the two best-fitted models, and an ANOVA was used to determine which of these two models was finally the best. Moreover, the coefficient of determination (R^2) was calculated to assess the model's predictive capacity.

2.4.2.2 Annual R_s estimates

Due to the experimental setup (measuring one ambient array and one treatment array for two weeks) and R_s ' seasonal and temporal variability, a modelled approach was used to calculate the annual R_s . Daily averages of the R_s data were estimated using the best fit model from the *Environmental drivers'* section, predicting the R_s of the rest of the arrays at all periods for the whole study period. VWC and T_s from each array aggregated in daily averages were used as predictors. Subsequently, daily averages of observed and predicted R_s values were merged, producing a complete R_s dataset.

2.4.2.3 Soil bioavailable nutrients

For nutrient analysis, the replication unit was the FACE array ($n=3$ for each of ambient and eCO_2), and all data were aggregated in monthly timestamps. The effect of eCO_2 on bioavailable nutrient concentrations was assessed using linear-mixed-effects models, for which 'array' and 'number of days since the beginning of the measurements' were random factors. Data collected before the eCO_2 enrichment (Pre-treatment) and Year 1 were analysed separately in Chapter 3.

Mixed-effects models were used to determine whether the relationships between T_s and VWC with the nutrient availabilities were linear or exponential. The appropriate models were chosen via an ANOVA. Subsequently, mixed-effects models were undertaken with eCO_2 and three covariates – T_s , VWC, and P – and their interactions ($eCO_2 \cdot T_s$, $eCO_2 \cdot VWC$, and $eCO_2 \cdot P$) as fixed effects to evaluate the role of climatic conditions in responses to eCO_2 . Utilising the Akaike Information Criterion (AIC) tool, the two models with the lowest AIC were chosen. An ANOVA was used to determine which model of the two mentioned above was finally the best-fitted one.

2.4.2.4 Microbial biomass and inorganic N

Similarly, for the soil intensives' analysis, the replication unit was the FACE array (n=3 for each of ambient and eCO₂). We utilised again the linear-mixed-effects models to assess the eCO₂ effect on microbial biomass and inorganic N, for which 'array' and 'campaign' were random factors, while 'soil horizon', 'season' and 'eCO₂' were fixed factors.

2.4.3 Chapter 5 – Additional methodology

Due to experimental design failure (fine root ingrowth in root exclusion collars), only descriptive statistics (e.g. average, minimum and maximum values) were performed for Chapter 5 for all the partition components of soil respiration (R_h, R_a, R_r, and R_m). The total soil respiration (R_s) was not investigated in Chapter 5 as it was extensively studied in Chapters 3 and 4. For more details, please see Chapter 5.

2.5 References

- Abrams, M. M. and Jarrell, W. M. (1992) 'Bioavailability Index for Phosphorus Using Ion Exchange Resin Impregnated Membranes', *Soil Science Society of America Journal*, 56(5), pp. 1532–1537. doi: 10.2136/sssaj1992.03615995005600050033x.
- Barton, K. (2014) 'MuMIn: multi-model inference. R package version 3.1-96'.
- Bates, D. *et al.* (2015) 'Fitting Linear Mixed-Effects Models Using **lme4**', *Journal of Statistical Software*. American Statistical Association, 67(1). doi: 10.18637/jss.v067.i01.
- Beck, T. *et al.* (1997) *An inter-laboratory comparison of ten different ways of measuring soil microbial biomass C*, *Soil Biol. B&hem.*
- Boltz, D. F. and Mellon, M. G. (1948) 'Spectrophotometric Determination of Phosphorus as Molybdiphosphoric Acid', *Analytical Chemistry*. American Chemical Society, 20(8), pp. 749–751. doi: 10.1021/ac60020a021.
- Bowatte, S. *et al.* (2008) 'In situ ion exchange resin membrane (IEM) technique to measure soil mineral nitrogen dynamics in grazed pastures', *Biology and Fertility of Soils*, 44(6), pp. 805–813. doi: 10.1007/s00374-007-0260-4.
- Brookes, P. C. *et al.* (1985) 'Chloroform fumigation and the release of soil nitrogen: A rapid direct extraction method to measure microbial biomass nitrogen in soil', *Soil Biology and Biochemistry*. Pergamon, 17(6), pp. 837–842. doi: 10.1016/0038-0717(85)90144-0.

Brookes, P. C., Powlson, D. S. and Jenkinson, D. S. (1982) 'Measurement of microbial biomass phosphorus in soil', *Soil Biology and Biochemistry*, 14, pp. 319–329. doi: 10.1007/BF02280183.

Ek, H. (1997) 'The influence of nitrogen fertilization on the carbon economy of *Paxillus involutus* in ectomycorrhizal association with *Betula pendula*', *New Phytologist*, 135(1), pp. 133–142. doi: 10.1046/j.1469-8137.1997.00621.x.

Filion, M., Dutilleul, P. and Potvin, C. (2000) 'Optimum experimental design for free-air carbon dioxide enrichment (FACE) studies', *Global Change Biology*, 6(7), pp. 843–854. doi: 10.1046/j.1365-2486.2000.00353.x.

Gal, C., Frenzel, W. and Möller, J. (2004) 'Re-examination of the cadmium reduction method and optimisation of conditions for the determination of nitrate by flow injection analysis', *Microchimica Acta*, 146(2), pp. 155–164. doi: 10.1007/s00604-004-0193-7.

Gomez-Casanovas, N. *et al.* (2013) 'Gap filling strategies and error in estimating annual soil respiration', *Global Change Biology*, 19(6), pp. 1941–1952. doi: 10.1111/gcb.12127.

Hart, K. M. *et al.* (2019) 'Characteristics of free air carbon dioxide enrichment of a northern temperate mature forest', *Global Change Biology*, 26(2), p. gcb.14786. doi: 10.1111/gcb.14786.

Hart, S. *et al.* (1994) 'Nitrogen mineralization, immobilization, and nitrification', in *Methods of soil analysis. Part 2: Microbiological and Biochemical Properties*. Madison, Wisconsin: Soil Science Society of America, pp. 985–1018.

Hasegawa, S., Macdonald, C. A. and Power, S. A. (2016) 'Elevated carbon dioxide increases soil nitrogen and phosphorus availability in a phosphorus-limited Eucalyptus woodland', *Global Change Biology*, 22(4), pp. 1628–1643. doi: 10.1111/gcb.13147.

Healy, R. W. *et al.* (1996) 'Numerical evaluation of static-chamber measurements of soil-atmosphere gas exchange: Identification of physical processes', *Soil Science Society of America Journal*. Soil Science Society of America, pp. 740–747. doi: 10.2136/sssaj1996.03615995006000030009x.

Heinemeyer, A. *et al.* (2007) 'Forest soil CO₂ flux: Uncovering the contribution and environmental responses of ectomycorrhizas', *Global Change Biology*, 13(8), pp. 1786–1797. doi: 10.1111/j.1365-2486.2007.01383.x.

Hoff, J. H. van't (1898) *Lectures on Theoretical and Physical Chemistry. Part 1: Chemical dynamics*. London.

Jackson, R. B., Mooney, H. A. and Schulze, E. D. (1997) 'A global budget for fine root biomass, surface area, and nutrient contents', *Proceedings of the National Academy of Sciences of the United States of America*, 94(14), pp. 7362–7366. doi: 10.1073/pnas.94.14.7362.

Krom, M. (1980) 'Spectrophotometric determination of Ammonia: a study of a modified Berthelot reaction using salicylate and dichloroisocyanurate', *Analyst*, 105(1249), pp. 305–316. doi: 10.1021/ie50220a003.

Kutsch, W. L., Bahn, M. and Heinemeyer, A. (2010) *Soil carbon dynamics: An integrated methodology, Soil Carbon Dynamics: An Integrated Methodology*. Cambridge University Press. doi: 10.1017/CBO9780511711794.

LI-8100 Automated Soil CO₂ Flux System & LI-8150 Multiplexer Instruction Manual (2007) LICOR.

Li, G. C., Mahler, R. L. and Everson, D. O. (1990) 'Effects of plant residues and environmental factors on phosphorus availability in soils', *Communications in Soil Science and Plant*

Analysis, 21(5–6), pp. 471–491. doi: 10.1080/00103629009368246.

Lloyd, J. and Taylor, J. A. (1994) 'On the Temperature Dependence of Soil Respiration', *Functional Ecology*. JSTOR, 8(3), p. 315. doi: 10.2307/2389824.

MacKenzie, R. *et al.* (2021) 'BIFoR FACE: Water-soil-vegetation-atmosphere research in a temperate deciduous forest catchment, including under elevated CO₂', *Hydrological Processes*. doi: 10.22541/au.160157598.86879557.

Navone, R. (1964) 'Proposed Method for Nitrate in Potable', *American Water Works Association*, 56(6), pp. 781–783.

Qian, P. and Schoenau, J. J. (2002) 'Practical applications of ion exchange resins in agricultural and environmental soil research', *Canadian Journal of Soil Science*, 82, pp. 9–21. Available at: www.nrcresearchpress.com (Accessed: 5 February 2020).

Raich, J. W., Potter, C. S. and Bhagawati, D. (2002) 'Interannual variability in global soil respiration, 1980–94', *Global Change Biology*, 8(8), pp. 800–812. doi: 10.1046/j.1365-2486.2002.00511.x.

Rayment, G. and Lyons, D. J. (2011) *Soil chemical methods: Australasia (Australian soil and land survey handbook series: v.3)*, *Australian soil and land survey handbook series*. CSIRO Publishing.

Searle, P. L. (1984) 'The berthelot or indophenol reaction and its use in the analytical chemistry of nitrogen: A review', *Analyst*. The Royal Society of Chemistry, 109(5), pp. 549–568. doi: 10.1039/AN9840900549.

Shrivastava, A. and Gupta, V. (2011) 'Methods for the determination of limit of detection and limit of quantitation of the analytical methods', *Chronicles of Young Scientists*, 2(1), pp. 21–25. doi: 10.4103/2229-5186.79345.

Team, Rs. (2019) 'RStudio: Integrated Development for R.' Boston, MA: RStudio, Inc.

Worsfold, P. J. *et al.* (2005) 'Sampling, sample treatment and quality assurance issues for the determination of phosphorus species in natural waters and soils.', *Talanta*, 66(2), pp. 273–93. doi: 10.1016/j.talanta.2004.09.006.

Chapter 3: Short-term carbon cycling and nutrient availability responses of a mature oak woodland under elevated CO₂

3.1 Abstract

Significant uncertainties are intertwined with future carbon (C) uptake and storage by terrestrial ecosystems. The University of Birmingham's Institute of Forest Research (BIFoR) was established in 2016, and one of its main scopes is to study the effects of elevated atmospheric CO₂ (eCO₂) on a temperate mature woodland utilizing its Free-Air CO₂ Enrichment (FACE) facility. BIFoR FACE is the first whole-ecosystem FACE experiment studying a mature deciduous temperate woodland and simulates global atmospheric concentrations expected to pertain ca. 2050. During the first year of eCO₂ enrichment, eCO₂ was observed to affect soil respiration positively, but the effect was not statistically significant. The annual estimates of soil respiration were stimulated by approximately 21% (1,341 vs. 1,624 g C m⁻² y⁻¹ in ambient and eCO₂ arrays, respectively). However, the eCO₂ effect was significant only when considering the synergic interaction of soil temperature and soil moisture.

Moreover, NO₃⁻-N availability showed a prompt and sustained decrease, up to 37% in monthly averages, in eCO₂ arrays, whereas eCO₂ did not affect NH₄⁺-N and PO₄³⁻-P availability in the soil. The belowground responses observed in this study were more likely driven by increased carbon allocation belowground and utilisation from the extensive network of roots, ectomycorrhizal fungi, and soil heterotrophs. However, the ecological significance of these responses for mature ecosystems under eCO₂ and their persistence through time require further research.

3.2 Introduction

Anthropogenic CO₂ emissions have resulted in an over 50% increase in atmospheric CO₂ concentrations since the pre-industrial era (annual mean for 2019: 411.5 ppm, *Daily CO₂*, 2019), and this rise is predicted to continue (Stocker *et al.*, 2013). According to future projections, the extent and the rate of this increase are not only dependent on the anthropogenic emissions (UNFCCC, 2005) but also on the capacity of ecosystems to take up carbon (C) and store it (Friedlingstein *et al.*, 2006; Friedlingstein *et al.*, 2014). The terrestrial biosphere plays a pivotal role in climate change and C cycling and is associated with the highest uncertainty regarding its response to (i.e., feedback on) environmental change (Lovenduski and Bonan, 2017; Quéré *et al.*, 2018).

Forest ecosystems are of high importance for the C cycle since it is estimated that ~ 860 ± 60 Pg C are currently being stored in the world's forests (Pan *et al.*, 2011). Northern temperate forests are the primary regulators (Schimel, Stephens and Fisher, 2015) of the terrestrial C sink, sequestering ~ 0.7 Pg C y⁻¹; one-third of the total uptake (Pan *et al.*, 2011). From a theoretical perspective, mature forests are close to equilibrium regarding their growth/turnover and litter inputs/soil respiration rates resulting in a comparatively constant C storage (Sousa, 1984). However, disturbances can cause this equilibrium to move, altering the C storage capacity of the ecosystem. One such disturbance is increasing atmospheric CO₂, which may 'fertilise' forest ecosystems, leading to an uptake of anthropogenic CO₂ into the plant and soil biomass (Zhu *et al.*, 2016). Although currently, forest ecosystems serve as a CO₂ sink (Pan *et al.*, 2011; Quéré *et al.*, 2018), the future projections of forest ecosystems' C storage capacity are highly uncertain (Ciais, Sabine and Bala, 2013).

Soil respiration (R_s) is the production of CO_2 from the soil when plant roots, microbes, hyphae, and soil fauna respire and is the second-largest flux of C between terrestrial ecosystems and the atmosphere (Raich and Schlesinger, 1992; Zhao *et al.*, 2017). Globally, it is estimated that soil respiration accounts for the release of 75-100 Pg C yr^{-1} , an order of magnitude larger than anthropogenic fossil fuel combustion (Boden, Marland and Andres, 2012). Hence, small changes in soil CO_2 effluxes may provoke significant changes in the net C balance, potentially shifting the C sink into a C source, at least temporarily, with substantial implications for the global C cycle (Cox *et al.*, 2000). Mainly, deciduous forests release approximately 1.18 Pg C yr^{-1} via the process of soil respiration (Warner *et al.*, 2019).

R_s is one of the least-studied elements of the terrestrial C cycle due to spatial and temporal sampling limitations and the high cost of measurement instruments (Savage, Davidson, and Richardson, 2008). Moreover, R_s is highly variable both temporally and spatially (Bond-Lamberty and Thomson, 2010), adding great uncertainty to global C cycle models. Although it is generally accepted that R_s may be enhanced by elevated atmospheric CO_2 , it is possible that the enhancement mentioned above may be negated by other constraints, making its role in climate feedback debatable (Qi, Xu and Wu, 2002; Davidson and Janssens, 2006). Understanding the nutrient mechanisms in mature forest ecosystems' capacity to sequester additional C is of great global concern and requires further investigation.

Many studies have shown that the magnitude and persistence of CO_2 fertilization effects on enhanced plant growth are linked with soil nutrient availability. The highest growth responses were seen in experiments where soil N availability was high (Reich, Hungate and Luo, 2006; Reich and Hobbie, 2013). Soil N availability is widely recognised as a crucial factor of productivity responses under elevated CO_2 (de Graaff

et al., 2006; Reich, Hungate and Luo, 2006; Norby and Zak, 2011), with progressive N limitation predicted to be a critical mechanism limiting C fertilization responses over time (Luo *et al.*, 2004). Effects of elevated CO₂ on soil N availability have been reported to be both positive and negative (Zak *et al.*, 2000), and more specifically in FACE experiments, show no change (Finzi *et al.*, 2002; Zak *et al.*, 2003) or a decrease (Hovenden *et al.*, 2008; Lagomarsino *et al.*, 2008).

Contrary to the high interest that has been given to the effects of elevated CO₂ on the N cycle, impacts of elevated CO₂ on P availability, or both N and P availability, have been given less attention. Field studies that have investigated the effects of elevated CO₂ on P availability were conducted in combination with N fertilization of a subset of the FACE plots and have reported both increases (Khan *et al.*, 2010) and decreases (Lagomarsino *et al.*, 2008). The only FACE experiment investigating the impacts of elevated CO₂ on both N and P availability without nutrient fertilisation has reported increases in the availability of both nutrients under eCO₂ (Hasegawa, Macdonald and Power, 2016).

However, eCO₂ affects R_s and nutrient availability via direct and indirect channels by affecting environmental variables, such as soil moisture (volumetric water content; VWC) and soil temperature (T_s). The eCO₂ effect on VWC is uncertain since studies have reported either small increases (Leuzinger and Korner, 2007; Manderscheid, Erbs and Weigel, 2014; Andresen *et al.*, 2018; Moser *et al.*, 2018), marginal increases, or no increase at all (Drake *et al.*, 2016). A potential rise in VWC will sequentially lead to a decrease in the topsoil availability of specific nutrients that are prone to leaching (McKinley *et al.*, 2009; Siemens *et al.*, 2012), an increase in plant C input to the soil, and faster decomposition due to alleviation of the water stress (Marhan *et al.*, 2010).

Moreover, increased VWC can alter microbial activity, C and N mineralization, and weathering (Kuzyakov *et al.*, 2019), which will impact R_s .

Although most of the previous FACE experiments were conducted in young stands or relatively homogenous plantations (King *et al.*, 2004), mature forests may respond differently to elevated CO_2 . Old-growth forests cannot be assumed to respond in the same way as young stands. Old-growth forests may have thoroughly explored and exploited their belowground resources, limiting the possibility of increased C allocation belowground (Körner, 2006). Moreover, nutrient cycles in mature forests are more tightly coupled than in young forests (Zaehle *et al.*, 2014). Mature trees may also have less flexibility in nutrient use (Körner *et al.*, 2005).

We continuously measured R_s at hourly intervals across the first year of CO_2 enrichment in a mature deciduous temperate woodland in the present study. We collected approximately 40,000 high-frequency automated measurements, offering meticulous scrutiny of R_s and its relationships with environmental drivers, including eCO_2 . We also assessed the availability of ammonium (NH_4^+-N), nitrate (NO_3^--N), and phosphate ($PO_4^{3-}-P$) at monthly intervals over the same period by deploying, collecting, and analysing over 1,000 ion-exchange membranes. Here we aim to establish the heterogeneity of R_s , VWC, T_s , and nutrient availability at BIFoR FACE before the eCO_2 enrichment and subsequently to answer the following questions:

- Does the eCO_2 affect R_s , soil moisture, and soil temperature on a mature oak woodland?
- How do bioavailable soil nutrients respond to eCO_2 ?

3.3 Methodology

3.3.1 Experimental site

The University of Birmingham's Institute of Forest Research (BIFoR) FACE is a temperate deciduous forest located within Mill Haft woodland in Staffordshire, England (52° 48' 3.6" N, 2° 18' 0" W). Mill Haft is part of Norbury Park Estate and has been woodland since pre-1881, appearing to be unchanged ever since. Mean precipitation during the overall studied period was 872.4 mm. Annual mean minimum and maximum temperatures for 2016 were 13, -3, and 32 °C, respectively, and for 2017 were 10, -5.5, and 28 °C.

A detailed site description can be found in (MacKenzie *et al.*, 2021). Briefly, the soil is brown earth cambisol with a sandy-clay texture and a mean soil pH of 4.5 at the top 10 cm. Mean soil total N and P in the top 10 cm are 0.28% and 18 mg P kg⁻¹, respectively, indicating that BIFoR is a low nutrient woodland, and total organic matter content is 3.67%.

The dominant overstorey species at the BIFoR FACE facility is old-growth (>160 years) *Quercus robur* (pedunculate oak), approximately 25 m in height. The woodland has a dense multi-layered canopy unaffected by constructing the FACE infrastructure (Hart *et al.*, 2019). The understorey is interspersed with *Corylus avellana* (common hazel), *Acer pseudoplatanus* (sycamore), *Ilex aquifolium* (holly), *Crataegus monogyna*, and *C. laevigata* (two native species of hawthorn).

3.3.2 BIFoR FACE facility

A detailed FACE facility description can be found in Hart *et al.*, (2019). Briefly, the BIFoR FACE facility comprises six 30 m diameter infrastructure arrays (elevated CO₂,

n = 3; ambient controls, n = 3) and three non-infrastructure arrays. Each eCO₂ array (+150 ppm above ambient) was paired with an ambient array at the early planning phase of the experiment after the baseline studies determined several forest characteristics (MacKenzie *et al.*, 2021). eCO₂ enrichment began on 3 April 2017 until 27 October 2017 (budburst to leaf fall, approximately) and will continue for each growing season until 2026. The fumigation system operated from 05:00 to 22:00, depending on the solar angle. During the eCO₂ enrichment period, eCO₂ arrays were within the 10% of target for 81.6% of the scheduled operation time and 20% of the target within 96.7% of scheduled operation time (Hart *et al.*, 2019). Contamination of the ambient arrays by CO₂ from the eCO₂ arrays was rare and short-lived, with control arrays being 10% of the control setpoint 98.8% of the time. Figure 3-1 shows the canopy greenness index from the PhenoCam installation date (May 2016) until Year 1 (December 2017).



Figure 3- 1: Canopy “greenness index” at BIFoR FACE measured from PhenoCam showing the 90th percentile of the daily green chromatic coordinate (GCC) of the canopy phenology nine months before the eCO₂ switch-on until the end of the first year of eCO₂ enrichment. Data are shown from May 2016 (9 months before the eCO₂ enrichment) until December 2017 (end of the first year of eCO₂ enrichment). The grey lines indicate gaps in the dataset due to technical failures of the PhenoCam, while the red lines enclose the period of eCO₂ enrichment (<https://phenocam.sr.unh.edu/webcam/sites/millhaft/>)

3.3.3 Measurements

3.3.3.1 Soil respiration, R_s

Three PVC (Drainage Superstore, CMO Ltd, Plymouth, UK) collars for monitoring the R_s were established within each of the six infrastructure arrays ($n = 3$, eCO₂ arrays $n = 3$, ambient arrays). Each of these 20-cm-diameter collars was inserted 5 cm into the soil and permitted the R_s measurement. The collars were installed in spring 2016 and left for establishment through the growing season; the soil collars were permanently installed to reduce soil disturbance by repeated measurements and ensure that the same soil was measured over time (King *et al.*, 2004).

Automated measurements of R_s were taken simultaneously at 1-hour intervals at all three surface collars in a fumigated array and its paired ambient control array, using 20-cm-diameter long-term chambers interfaced with a multiplexer and an infra-red gas analyser (IRGA) (Li-8100-104 long-term chambers, Li-8150 multiplexer and Li-8100A IRGA; LI-COR). The observation length was 2 min with 20 s dead-band, a 15 s pre-purge, and a 45 s post purge, giving a total measurement cycle of 3 min 20 s. The measurements began on October 19, 2016 (5 months before the beginning of eCO₂ enrichment). We report data until December 31, 2017 (2 months after the switch-off of eCO₂ enrichment at the end of the first treatment growing season). The LI-COR systems were moved every two weeks between replicating paired eCO₂ and ambient arrays and returning to the same array pair on a 4-week rotation.

All data went through quality checks before analysis using SoilFluxPro software, version 4.0.1 (LI-COR, Nebraska, USA). Data points with negative linear fluxes or data points with a linear flux coefficient of variation higher than 3.5 were removed from the dataset, as these were indicative of leaks in the chamber. Data points with a linear flux coefficient of variation between 1.5 and 3.5 were manually checked for assessing the

fit quality. Of 69,216 data points during the first year of operation, 39,557 data points were used for analysis. There was a moderate data loss (43%), primarily due to equipment failures (water condensation in the electric plates) and, to a lesser extent, due to poor-quality fits. Daily and monthly averages of these data are reported in this study in $\mu\text{mol CO}_2 \text{ m}^{-2} \text{ s}^{-1}$, while annual averages are reported in $\text{g C m}^{-2} \text{ y}^{-1}$.

3.3.3.2 Environmental drivers

Soil volumetric water content (VWC) and soil temperature (T_s) were measured with permanently installed shallow CS655 probes inserted in the top 12 cm soil (Campbell Scientific, Logan, UT, USA). VWC probes were sited one metre from each of the three experimental R_s collars in each array. The VWC data were recorded in 15-min intervals by a data logger in each plot (CR1000, Campbell Scientific) and are reported in daily averages.

The temperature sensitivity (Q_{10}) of R_s was calculated using the following equations

$$\ln R_s = kT + C$$

$$Q_{10} = e^{10k}$$

where k is the regression slope of \ln -transformed respiration against measured temperature, and C is an empirical constant (Kutsch, Bahn and Heinemeyer, 2010). Q_{10} was calculated for Pre-treatment and Year 1 separately to observe any eCO_2 effect.

3.3.3.3 Biota available (bioavailable) inorganic N and P

Ion-exchange resin membranes (Membranes International Inc., New Jersey, USA) were used to measure the available inorganic N, as ammonium ($\text{NH}_4^+\text{-N}$) and nitrate ($\text{NO}_3^-\text{-N}$), and P, as phosphate ($\text{PO}_4^{3-}\text{-P}$). Between May and October 2016, five anion exchange membranes (AMI 7001; 2 cm x 12 cm) and five cation exchange membranes (CMI 7000; 2 cm x 12 cm) were inserted in the top 12 cm of the soil within ~50 cm of each R_s collar in each array. Following a statistical analysis of replicate variability, the sampling design was modified. From January 2017, three anion- and three cation-exchange resin membranes were inserted in the soil at eight locations within each array; three sets of each were located next to the R_s collars, and the other five sets were randomly located within each array. Membranes were deployed in situ for approximately one month before retrieval. To assess the resin membranes' loading capacity, a capacity lab test was performed for 60 days, testing daily (see Chapter 2). Up to 40 days of resin membrane incubation, 99% of $\text{NH}_4^+\text{-N}$, $\text{NO}_3^-\text{-N}$, and $\text{PO}_4^{3-}\text{-P}$ was absorbed in the membrane; beyond 40 days, the absorbance capacity decreased, but never to less than 90%.

Upon retrieval, membranes were washed thoroughly with deionised water to remove any soil particles and then extracted for PO_4^{3-} , NH_4^+ and NO_3^- [modified from Rayment and Lyons, (2011) and Bowatte *et al.*, (2008), respectively]. Each membrane was extracted with 0.5 M HCl, shaken at 180 rpm for two hours, and then the membranes were removed from the solution and discarded. From January 2017 and onwards, the three membranes from each location were bulked together as one sample, and the same process was followed as described above.

Concentrations of NH_4^+ and NO_3^- were analysed by a continuous flow analyser (San++ Continuous Flow Analyser, Skalar, Breda, The Netherlands), and concentrations of

PO_4^{3-} were analysed by ultraviolet-visible spectroscopy (Jenway 6850) using the molybdenum blue method (Worsfold *et al.*, 2005). The data presented in this study are reported as monthly averages, per unit area of the membrane, in $\mu\text{g NH}_4^+-\text{N cm}^{-2} \text{ d}^{-1}$, $\mu\text{g NO}_3^--\text{N cm}^{-2} \text{ d}^{-1}$, and $\mu\text{g PO}_4^{3-}-\text{P cm}^{-2} \text{ d}^{-1}$, respectively, and the ratios of these.

3.3.4 Statistical analysis

All analyses were carried out using R 3.6.2 and Rstudio 1.2.5033 (Rstudio Team, 2019). The mixed-effects models were performed using R package lme4 (Bates *et al.*, 2015), and the coefficient of determination was calculated using the R package MuMIn (Barton, 2014). For all analyses, effects were considered to be significant if the model-reported P-value < 0.05.

3.3.4.1 Environmental drivers and R_s

Treatment effects were derived directly by comparing the daily means of R_s for eCO_2 and ambient arrays using a one-way ANOVA. The Pre-treatment period and Year 1 were assessed separately to establish potential significant differences before eCO_2 enrichment and significant treatment effects, respectively. Interactions between eCO_2 and environmental drivers (VWC and T_s) were evaluated using a two-way ANOVA for both periods. The more complicated interactions between both environmental drivers were assessed using a three-way ANOVA. However, as described in *Chapter 2*, trying to investigate treatment effects in such dataset, where we have clustered repeated measurements across time, there is both spatial and temporal variability to account for, without compromising the real variability and dealing with potential imbalances in the number of measurements (very common for field datasets as such), mixed-effects

models are more advantageous than ANOVA. Hence in all mixed-effects models performed, 'array,' 'location within the array,' and 'number of days since the beginning of the experiment' to account for the correlations between repeated measurements within each collar/array were added as random effects. All mixed-effects models performed in this Chapter daily averages of R_s (per collar), VWC, and T_s (per sensor, respectively) were used.

Mixed-effects models were used to investigate potential pre-eCO₂ enrichment differences in the pre-assigned as 'ambient' and 'elevated' arrays. Although there was no eCO₂ enrichment during the Pre-treatment period, please allow been named as such for easier understanding. eCO₂, its interaction with VWC and T_s , and the complex interaction between all three variables were used as fixed effects. The relationships between R_s and VWC as well as R_s and T_s were linear during the Pre-treatment period. Akaike Information Criteria (AIC) tool was used to determine which of the models mentioned above was most likely the best model for this dataset. The two models with the lowest AIC score were compared using the ANOVA¹ function to compute the Chi-squares between the two models for investigating the model fit. Finally, the coefficient of determination (R^2) was calculated to assess the variance captured by the model.

Similarly, the same principles as described above were used for investigating the eCO₂ effects during Year 1 of eCO₂ enrichment at BIFoR FACE. eCO₂, its interaction with VWC and T_s , and the complex interaction between all three variables were used as fixed effects. However, during Year 1, only R_s and T_s ' relationship was linear, whereas R_s and VWC was quadratic. The AIC tool was utilised again to choose the

¹ Although the function is called ANOVA it is a likelihood ration test (LRT) and not to be confused with the statistical method.

most likely best model amongst the ones mentioned above, while the ANOVA function was used for concluding the best-fitted model.

3.3.4.2 Bioavailable nutrients

For nutrient analysis, the replication unit was the FACE array ($n=3$ for each of ambient and eCO_2), and all data were aggregated in monthly timestamps. The effect of eCO_2 only on bioavailable nutrient concentrations was assessed using linear-mixed-effects models, for which 'array' and 'number of days since the beginning of the measurements' were random factors. Data collected before the eCO_2 enrichment were analysed separately to assess initial pretreatment differences. Subsequently, linear-mixed-effects models were undertaken with CO_2 and two covariates – T_s and VWC – and their interactions ($eCO_2 \cdot T_s$, $eCO_2 \cdot VWC$, and $eCO_2 \cdot T_s \cdot VWC$) as fixed effects to evaluate the role of soil conditions in responses to elevated CO_2 . In this mixed-effects framework, 'array' and 'number of days since the beginning of the measurements' were used as random factors.

3.3.5 Estimate of annual R_s

Due to the experimental setup (measuring one ambient array and one eCO_2 array for two weeks) and given the seasonal and temporal variability of R_s , a modelled approach was used to calculate the seasonal R_s , utilising the best-fitted models described in section 3.3.4.1 *Environmental drivers and R_s* . Daily averages of the R_s data were estimated using the best-fitted models for Pre-treatment and Year 1, predicting the R_s of the rest of the arrays at all periods for the whole study period. VWC and T_s from each array aggregated in daily averages were used as predictors. Subsequently, daily

averages of observed and predicted R_s values were merged, producing a complete R_s dataset.

3.4 Results

3.4.1 R_s response to environmental drivers and eCO_2

R_s exhibited high variability throughout the study period, following seasonal patterns related to VWC, T_s , and precipitation patterns (Fig. 3-2). The pre-treatment period started in mid-autumn (19th October) 2016 and lasted until the early spring (2nd April) of 2017. During that period, no eCO_2 was introduced in the woodland; however, all arrays were pre-assigned as 'ambient' and ' eCO_2 '. The dashed lines on Fig. 3-2 enclose the eCO_2 enrichment period (3rd April – 27th October 2017; *Year 1* hereafter).

R_s increased during the growing season (concurring with eCO_2 enrichment) in both ambient and eCO_2 treatments, as the T_s increased and VWC decreased. Both daily and monthly averages indicated that R_s was frequently higher in the eCO_2 arrays. The greatest differences appeared to be during August and September 2017 (August 3.74 $\mu\text{mol CO}_2 \text{ m}^{-2} \text{ s}^{-1}$ in ambient vs. 4.89 $\mu\text{mol CO}_2 \text{ m}^{-2} \text{ s}^{-1}$ in eCO_2 ; September 2.98 $\mu\text{mol CO}_2 \text{ m}^{-2} \text{ s}^{-1}$ in ambient vs. 4.34 $\mu\text{mol CO}_2 \text{ m}^{-2} \text{ s}^{-1}$ in eCO_2). Precipitation was observed to lead to a pulse effect on R_s commensurate with an increase in VWC. Both VWC and T_s had a strong and clear seasonal pattern, while precipitation was sporadic and highly variable (Fig. 3-2b, c).

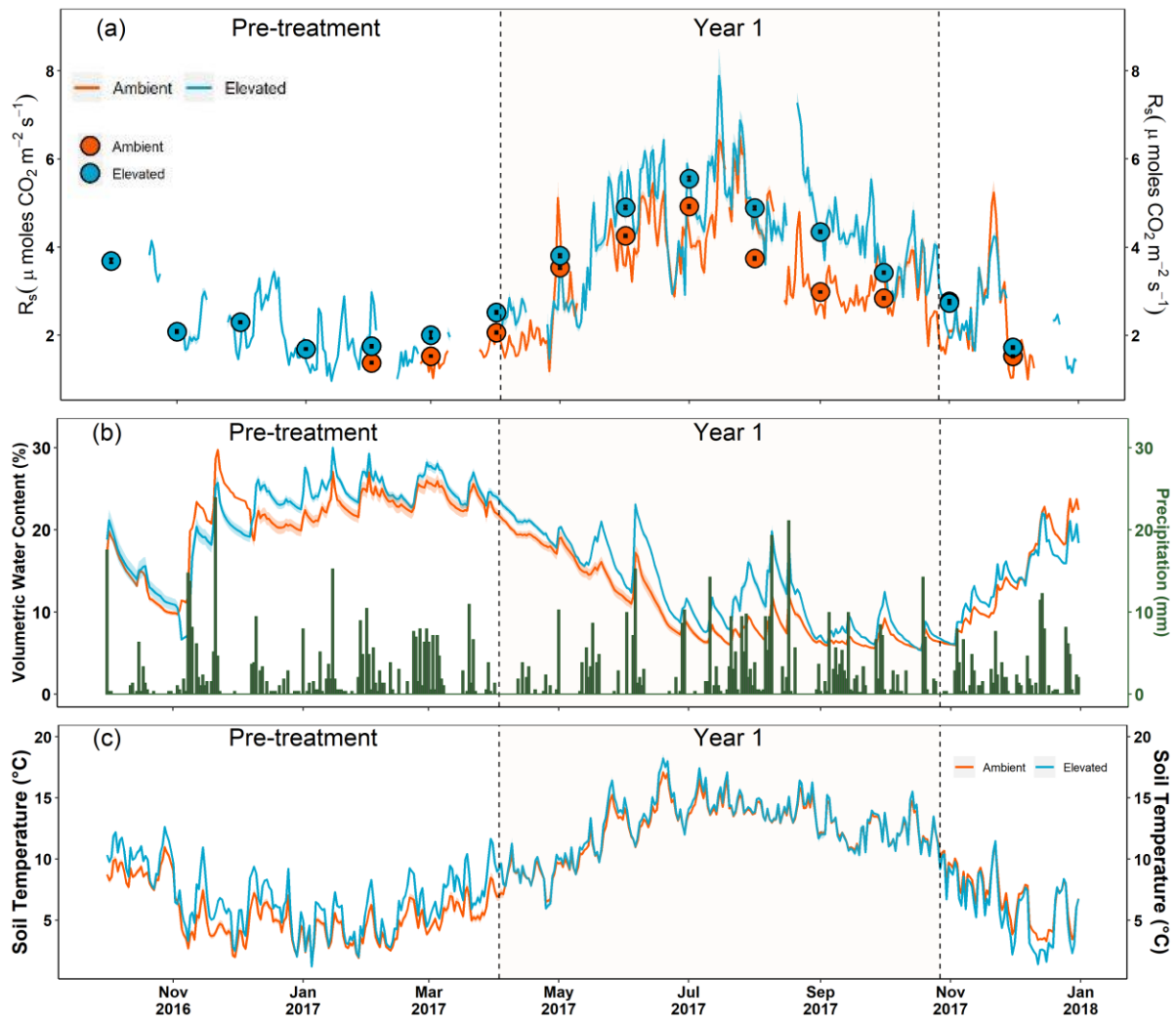


Figure 3-2: Seasonal variation of R_s (a), VWC and precipitation (b), and T_s (c) at BIFoR FACE during the Pre-treatment and first year of eCO_2 enrichment (October 2016 – October 2017). The blue coloured lines/solid points denote the eCO_2 arrays, while the orange lines/solid points denote the ambient arrays. The lighter coloured ribbons around the lines and the error bars indicate the SE for R_s , VWC, and T_s . All data describe daily averages, except the solid points in (a), which reflect the R_s monthly averages. The vertical dashed lines enclose the period when the eCO_2 enrichment was switched on (Year 1, 3rd April – 27th October 2017), whereas the period before reflects the Pre-treatment period (19th October 2016 – 2nd April 2017).

We also investigated the R_s response to rain events during Year 1 at BIFoR FACE (Fig. 3-3). For example, we present approximately nine rain events for 2.5 months (24th July – 1st August 2017). R_s responded rapidly to rain events, and the magnitude of the R_s rate increase was dependent on the conditions of the soils before the event. The drier and warmer the soils were before a rain event, the greater the increase on R_s .

Two rain events are studied here as an example; both events were chosen as they happened while the R_s measurements were already in that location for a few days at least. Thus any potential R_s difference observed can be attributed to the rain events rather than the R_s spatial variability. For example, Event A, a small rain event (1 mm) in mid-July, almost doubled the R_s under both ambient and eCO₂ conditions from ~ 3 to 6 and from ~ 4 to 8 $\mu\text{mol CO}_2 \text{ m}^{-2} \text{ s}^{-1}$, respectively. Before this event, the soils at BIFoR FACE were warm and dry, having received less than 0.3 mm precipitation during the previous 11-day-period. However, no further increase on R_s was observed during greater rain events (Event B end of July), when the soils were wetter because precipitation events were more frequent and the soil temperatures were lower.

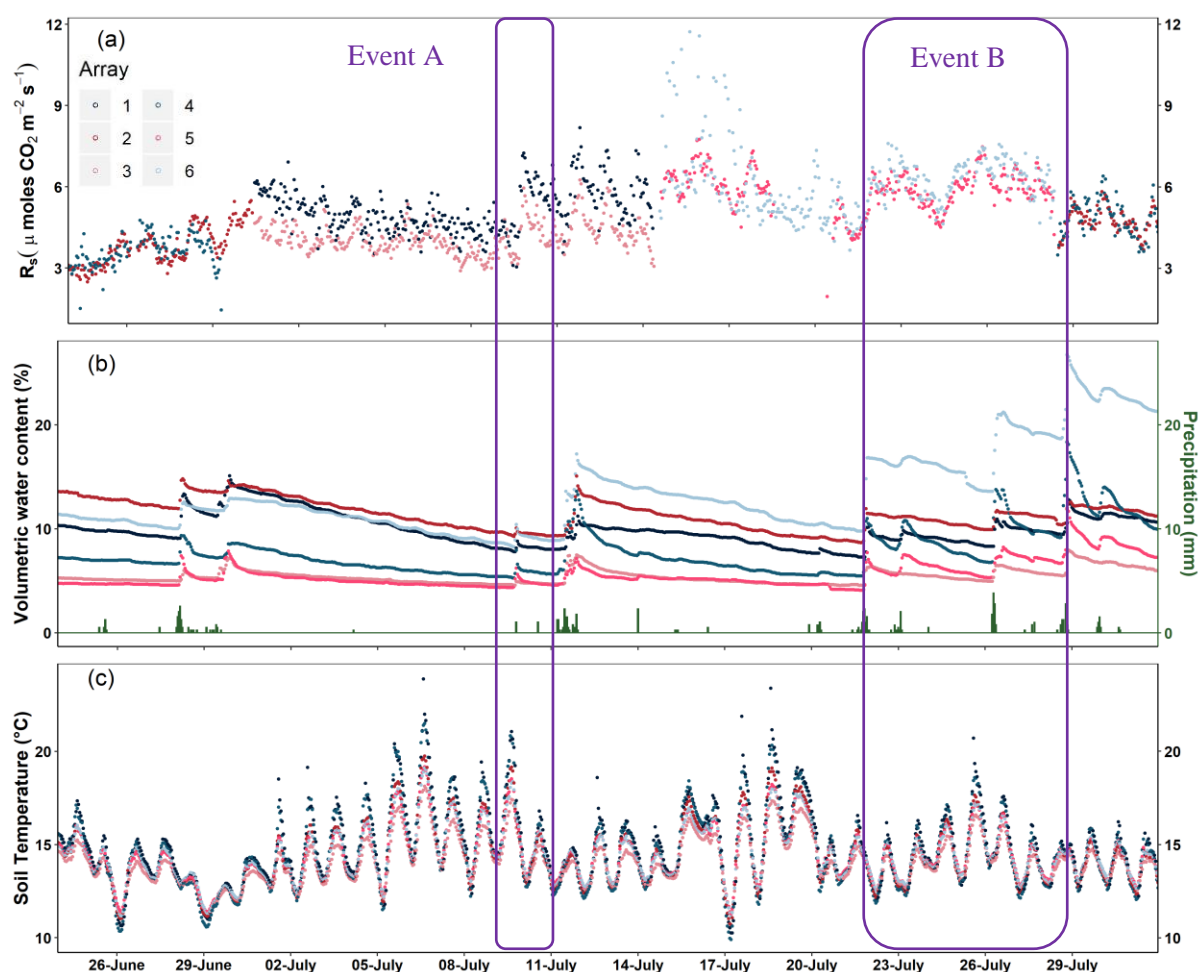


Figure 3- 3: (a) Example responses of R_s to precipitation events during Year 1 of eCO_2 enrichment at BIFoR FACE. Warm colours reflect ambient arrays, while cold colours reflect eCO_2 arrays. Note that not all arrays were measured for R_s simultaneously; instead, an ambient and an eCO_2 array were measured for a two-weekly period. (b) VWC (lines) and precipitation (bars), and (c) T_s during the same period. All data presented in hourly averages.

Table 3-1 shows the average (mean \pm standard deviation), minimum and maximum VWC, T_s , and R_s during Pre-treatment and Year 1 (2017), as well as the number of observations and the Q_{10} values both ambient and eCO_2 arrays. The mean VWC, T_s , and R_s were slightly higher in eCO_2 arrays during both Pre-treatment and Year 1, with the variables having a greater range and variability in eCO_2 arrays. Q_{10} was higher in ambient arrays before and after the eCO_2 enrichment (Pre-treatment: 2.96 in ambient vs. 2.66 in eCO_2 arrays; Year 1: 3.08 in ambient vs. 2.64 in eCO_2).

Simple mixed-effects models were used to investigate significant differences in daily VWC, T_s , R_s between ambient and eCO₂ arrays for both Pre-treatment and Year 1. All three variables (VWC, T_s , R_s) were statistically similar between the pre-assigned as ‘ambient’ and ‘eCO₂’ arrays during the Pre-treatment period (p-value 0.78, 0.38, and 0.4, respectively; Table 3-1), as well as during Year 1 (p-value 0.35, 0.15 and 0.29, respectively; Table 3-1).

Table 3- 1: Mean, number of observations (*n*), minimum and maximum VWC, T_s , and R_s for Pre-treatment and Year 1 in ambient and eCO₂ arrays based on daily averages (mean \pm sd), as well as Q_{10} values and p-values from simple mixed-effects models. Significance values are based on the mixed-effects model approach with eCO₂ as the main effect and array, location within an array, and the number of days since the beginning of the measurement as random effects.

Variable	Mean		Minimum		Maximum		n		p-value
Ambient		eCO ₂	Ambient	eCO ₂	Ambient	eCO ₂	Ambient	eCO ₂	
Pre-treatment									
VWC	21.00±4.57	21.76±5.18	9.75	6.63	29.74	30.03	184	184	0.78
T _s	5.47±2.13	6.80±2.55	1.75	1.23	10.97	12.62	184	184	0.38
R _s	1.55±0.26	2.07±0.71	1.03	0.97	2.09	4.14	24	104	0.40
Q ₁₀	2.96	2.66							
Year 1									
VWC	10.60±4.80	12.93±5.20	5.48	5.35	21.75	23.68	208	208	0.35
T _s	12.39±2.28	12.66±2.43	6.51	5.98	17.08	18.23	208	208	0.15
R _s	3.51±1.15	4.32±1.23	1.19	1.47	6.63	7.89	190	195	0.29
Q ₁₀	3.08	2.64							

The synergic effects of eCO₂ treatment on R_s with the environmental drivers (VWC and Ts) were also explored using more complex models that incorporated interaction effects. The dual impact of eCO₂ and each environmental driver and their triadic interaction can be found in Table 3-2. During Pre-treatment, no interaction was statistically significant; however, the model with the lowest AIC was the eCO₂*Ts. This model explained 64% of the observed variability on R_s. The model was validated for homoscedasticity, normality, and linearity of residuals, and linearity of the random effects (see section 3.8 Supplementary Material, Figure S3-2 and Table S3-5 for the model's coefficients).

During Year 1, the eCO₂*Ts interaction and the eCO₂*VWC*Ts interaction were statistically significant (p-value 0.008 and <0.001, respectively). These two interaction models were also the ones with the lowest AIC and could explain 61 and 63% of R_s' variability. The ANOVA function was used to determine which of the two models was the best fitted; the latter model was the best one (P-value < 0.001). Finally, the model was validated for homoscedasticity, normality, linearity of residuals, and linearity of the random effects (see section 3.8 Supplementary Material, Figure S3-3, and Table S3-5 the model's coefficients).

Table 3- 2: Analysis of R_s and its drivers' variance during Pre-treatment and Year 1 at BIFoR FACE. The degrees of freedom for each explanatory variable is 1, $P < 0.1$ is shown in bold.

Predictors	DF _{den}	F-value	p-value	R_c^2	AIC
<i>Pre-treatment</i>					
eCO ₂	2.83	1.90	0.27	0.68	735.70
eCO ₂ *VWC	9.37	0.18	0.68	0.66	700.16
eCO ₂ *T _s	296.34	1.88	0.17	0.64	616.58
eCO ₂ *VWC*T _s	323.79	0.08	0.78	0.63	645.74
<i>Year 1</i>					
eCO ₂	4.02	1.50	0.29	0.31	4217.25
eCO ₂ *VWC	1170.3	1.21	0.27	0.50	4002.80
eCO ₂ *T _s	1155.9	6.92	0.008	0.61	3540.43
eCO ₂ *VWC*T _s	1162.06	35.02	<0.001	0.63	3530.30

Where DF_{den}: denominator's degrees of freedom, F-value: F-test determination, R_c^2 : coefficient of determination and AIC: Akaike Information tool

Utilising the models' from above, we were able to estimate the R_s by imputing data for the arrays that were not measured each fortnight or periods where no data existed and create a "complete" dataset. Thus, at all times, we have $n=3$ with two arrays being predicted values and the third one being the observed values for ambient and eCO₂ arrays, respectively.

Figure 3-4 shows the R_s response to VWC and T_s in both ambient and eCO₂ arrays using daily averages of the "gap-filled" dataset. R_s in ambient arrays increased as T_s increased, and VWC decreased, with the highest values observed at high T_s and low VWC (Fig. 3-4a). In low temperatures, R_s were similar regardless of VWC, indicating that T_s was a limiting factor. In eCO₂ arrays, the highest R_s were observed when both T_s and VWC increased; however, the VWC range in eCO₂ arrays was much greater than in ambient arrays (Fig. 3-4b).

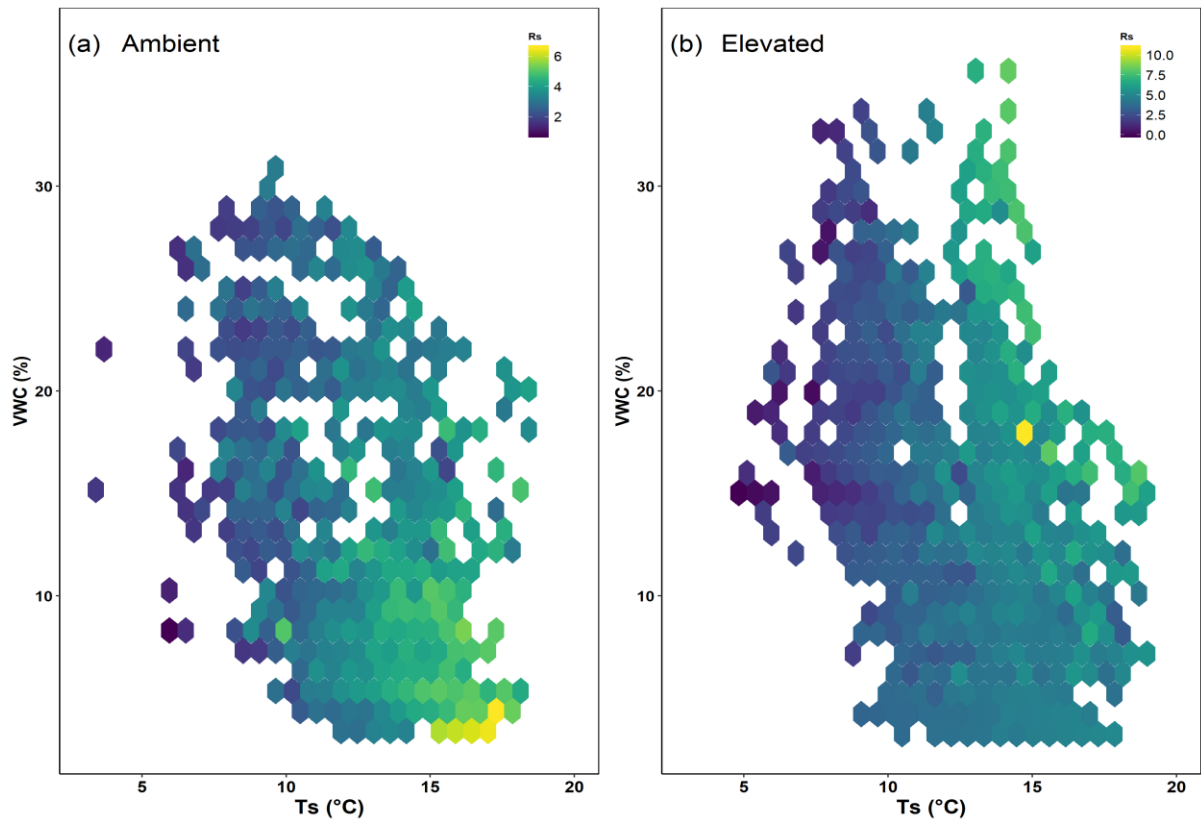


Figure 3- 4: R_s response to T_s and VWC in ambient (a) and eCO_2 (b) conditions at BIFoR FACE during the first year of operation. Hexagons reflect daily averages per collar of the “gap-filled” dataset utilising the model’s prediction.

3.4.2 Estimates of annual R_s

As mentioned in the section above, the best-fitted models were utilised to predict R_s ’ missing values for the studied period. Figure 3-5a and b show the observed R_s values against the predicted R_s values in ambient and eCO_2 arrays during both Pre-treatment and Year 1 of eCO_2 enrichment at BIFoR FACE. Note that in Fig. 3-5a during the Pre-treatment period, the model cannot capture the temporal variability due to missing data. The observed values are daily averages of one array each fortnight, whereas the predicted values are daily averages of three arrays for ambient and eCO_2 arrays, respectively. The objective of the model was to “fill the gaps” between R_s

measurements with defensible estimates. Observed and predicted R_s were strongly correlated (Fig. 3-5c; $p < 0.001$ for both ambient and eCO_2 arrays; $R = 0.84$ and 0.88 , respectively); the equation's slope was 1 and 0.96 for ambient and eCO_2 arrays, respectively.

R_s ' mean annual flux was estimated as the predicted and observed daily averages of R_s data above (Fig. 3-5d). The mean annual (i.e., October 2016- November 2017) R_s at BIFoR FACE in ambient arrays was $1,341 \pm 21 \text{ g C m}^{-2} \text{ y}^{-1}$ (mean \pm se), while in eCO_2 arrays was approximately 21.1% higher ($1,624 \pm 24 \text{ g C m}^{-2} \text{ y}^{-1}$; mean \pm se).

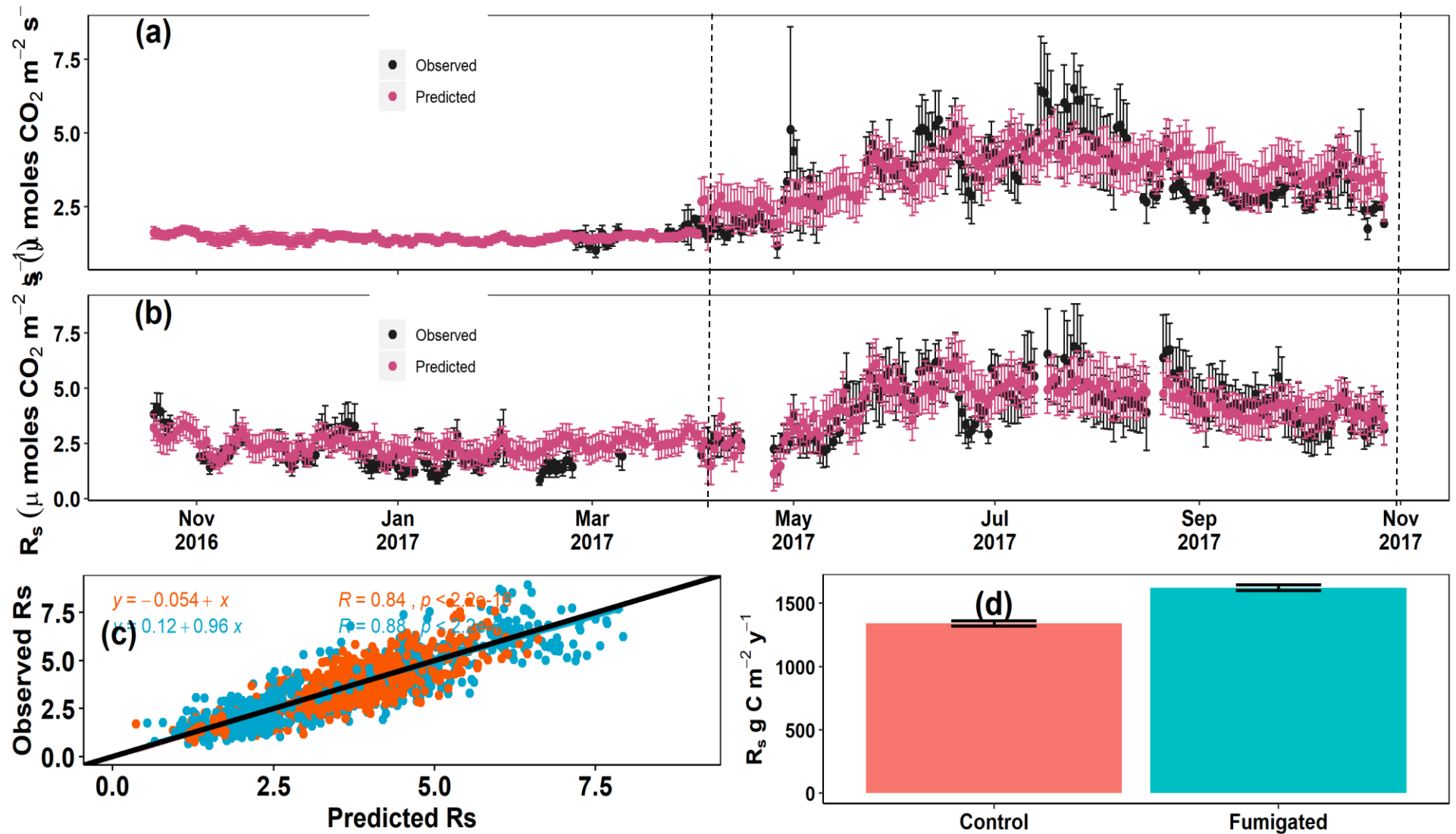


Figure 3- 5: a) Observed and predicted R_s measurements under ambient conditions, b) Observed and predicted R_s measurements under eCO_2 conditions. The black solid points denote the daily-average (mean \pm sd) observed R_s measurements, while the pink solid points denote the predicted R_s values. The dashed lines enclose the Year 1 of eCO_2 enrichment. c) Predicted and observed R_s correlation for eCO_2 (blue line) and ambient (orange line) arrays. The blue solid points denote the eCO_2 arrays, while the orange solid points denote the ambient arrays. d) Mean annual R_s in $\text{g C m}^{-2} \text{ y}^{-1}$ in ambient (orange) and eCO_2 (blue) arrays during the first year at BIFoR FACE. The error bars denote the standard error.

3.4.3 Biota available (bioavailable) inorganic N and P

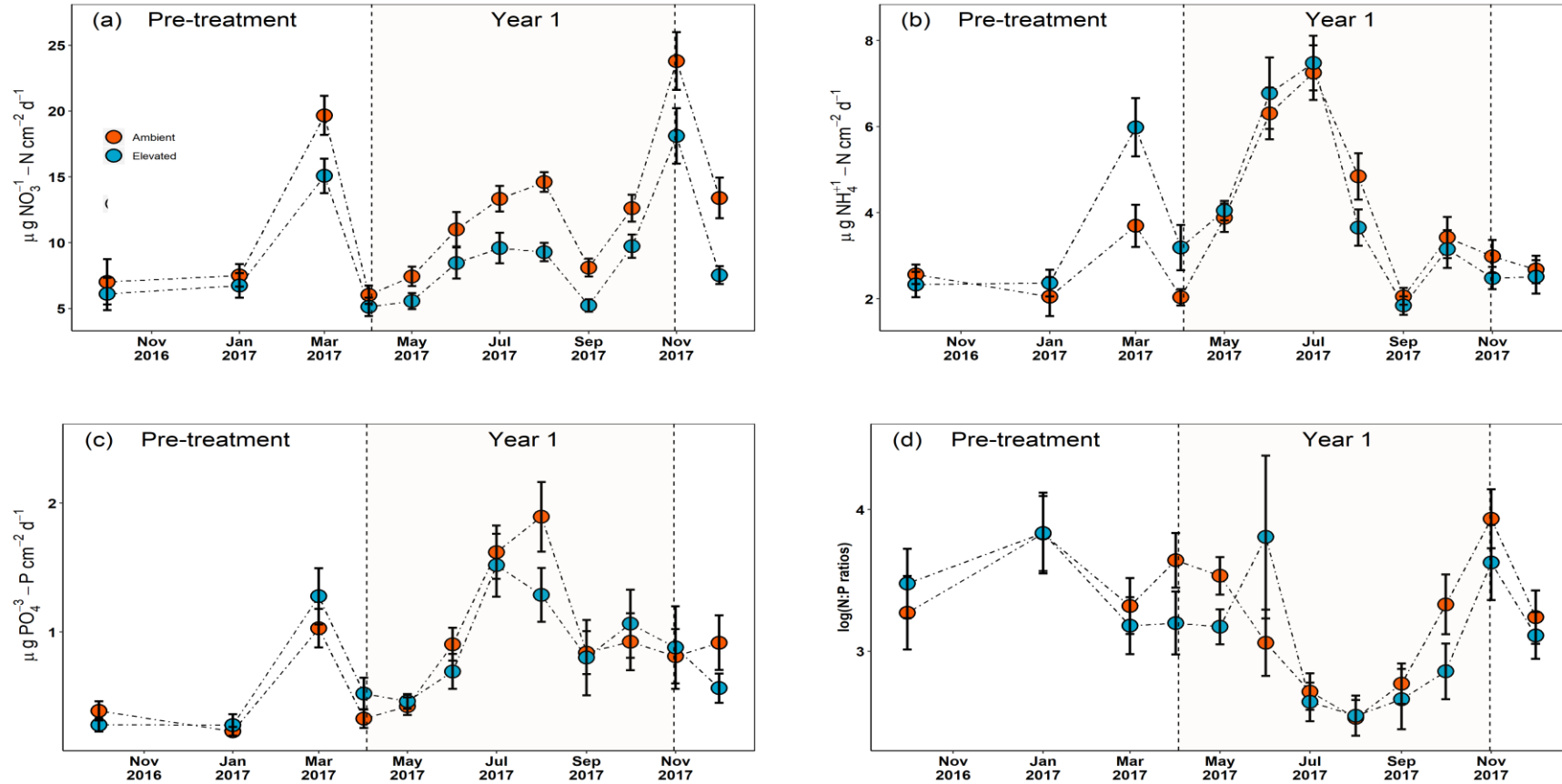


Figure 3- 6: Temporal changes in ion exchange resin membranes (a) $\text{NO}_3^- - \text{N}$, (b) $\text{NH}_4^+ - \text{N}$ and (c) $\text{PO}_4^{3-} - \text{P}$ concentrations, (d) $\log(\text{N:P ratios})$, (mean \pm se, $n = 3$). The orange solid points reflect the nutrient availability in the ambient arrays, whereas the blue solid points reflect the nutrient availability in the eCO₂ arrays. The shaded area denotes eCO₂ treatment (Year 1, 3rd April – 27th October 2017), whereas the period before reflects the Pre-treatment period (1st October 2016 – 2nd April)

All three soil bioavailable nutrients (NO_3^- -N, NH_4^+ -N, and PO_4^{3-} -P) exhibited strong seasonality, with availability increasing as the T_s increased and VWC decreased (Fig. 3-6a, b, and c). All three bioavailable nutrients had low availabilities at the beginning of the eCO_2 enrichment (April 2017; NO_3^- -N 6.0 ± 0.7 in ambient vs. $5.1 \pm 0.7 \mu\text{g NO}_3^-$ -N $\text{cm}^{-2} \text{d}^{-1}$ in eCO_2 arrays; NH_4^+ -N 3.9 ± 0.3 in ambient vs. $3.2 \pm 0.5 \mu\text{g NH}_4^+$ -N $\text{cm}^{-2} \text{d}^{-1}$ in eCO_2 arrays; PO_4^{3-} -P 0.3 ± 0.1 in ambient vs. $0.5 \pm 0.1 \mu\text{g PO}_4^{3-}$ -P $\text{cm}^{-2} \text{d}^{-1}$ in eCO_2 arrays), while their highest availabilities were observed in summer for NH_4^+ -N (July 2017; 7.3 ± 0.6 in ambient vs. $7.5 \pm 0.6 \mu\text{g NH}_4^+$ -N $\text{cm}^{-2} \text{d}^{-1}$ in eCO_2 arrays) and PO_4^{3-} -P (August 2017; 1.9 ± 0.3 in ambient vs. $1.3 \pm 0.2 \mu\text{g PO}_4^{3-}$ -P $\text{cm}^{-2} \text{d}^{-1}$ in eCO_2 arrays) and in autumn for NO_3^- -N (November 2017; 23.8 ± 2.2 in ambient vs. $18.1 \pm 2.1 \mu\text{g NO}_3^-$ -N $\text{cm}^{-2} \text{d}^{-1}$ in eCO_2 arrays).

NO_3^- -N had the lowest availability at the beginning of eCO_2 enrichment (April 2017) and increased as the growing season progressed (Fig. 3-6a). The eCO_2 arrays had persistently lower NO_3^- -N availability throughout the eCO_2 enrichment with the greatest difference observed in August 2017 (14.6 ± 0.8 in ambient vs. $9.3 \pm 0.7 \mu\text{g NO}_3^-$ -N $\text{cm}^{-2} \text{d}^{-1}$ in eCO_2 arrays, respectively). NH_4^+ -N and PO_4^{3-} -P exhibited a similar pattern response in both ambient and eCO_2 arrays, with no great differences observed in their availability between ambient and eCO_2 arrays. Accordingly, N:P ratios decreased as the availability of the nutrients increased.

Table 3- 3: Soil nutrients availability and N:P ratios during the Pre-treatment and Year 1 at ambient and eCO₂ arrays (mean ± sd), and summary of mixed-effects models of the eCO₂ effect on nutrient availability. All nutrients units are per unit area of membrane in µg cm⁻² d⁻¹(refer to section 3.3.4.2 Bioavailable nutrients for method). p-value < 0.1 is shown in bold.

	eCO ₂ effect					
Variable	Ambient	eCO ₂	DF _{num}	DF _{den}	F-value	p-value
<i>Pre-treatment</i>						
NO ₃ ⁻ - N	11.4 ± 7.0	9.1 ± 4.7	1	16	0.64	0.44
NH ₄ ⁺ - N	2.8 ± 1.1	3.5 ± 1.9	1	16	0.99	0.33
PO ₄ ³⁻ - P	0.6 ± 0.4	0.6 ± 0.7	1	16	0.05	0.82
log(N:P) ratio	3.5 ± 0.7	3.5 ± 0.9	1	4	0.02	0.89
<i>Year 1</i>						
NO ₃ ⁻ - N	10.4 ± 3.6	7.3 ± 2.9	1	38	9.08	0.005
NH ₄ ⁺ - N	4.3 ± 2.1	4.9 ± 2.0	1	38	0.202	0.66
PO ₄ ³⁻ - P	1.0 ± 0.6	0.9 ± 0.7	1	3.62	0.50	0.52
log(N:P) ratio	3.1 ± 0.6	2.9 ± 0.7	1	3.96	0.06	0.82

Where DF_{num}: numerator's degrees of freedom, DF_{den}: denominator's degrees of freedom, F-value: F-test determination

Table 3-3 shows the averages during Pre-treatment and Year 1 of all three soil bioavailable nutrients and N:P ratios in ambient and eCO₂ arrays. Although during the Pre-treatment periods, differences in the availability of all three soil nutrients and the N:P ratios were observed between the preassigned as ambient and eCO₂ arrays, none of these differences were found to be statistically significant. During Year 1 of eCO₂ enrichment, eCO₂ had a statistically significant effect only on NO₃⁻-N availability, decreasing the NO₃⁻-N availability by up to 37% under eCO₂ conditions. However, NH₄⁺-N, PO₄³⁻ and N:P ratios were statistically similar between ambient and eCO₂ conditions.

T_s had a statistically significant effect on all three bioavailable nutrients (NO₃⁻-N, NH₄⁺-N, and PO₄³⁻-P) as well as the N:P ratio (Table 3-4). VWC had a statistically significant

effect on N:P ratios, whereas no statistically significant effects were observed in the three bioavailable nutrients. The interactions between eCO₂ and the environmental variables (VWC and T_s) did not significantly affect the bioavailable nutrients or the N:P ratios.

Table 3- 4: Summary of mixed-effects models of the environmental variables and their interactions with eCO₂ on bioavailable soil nutrients. Fixed factors are VWC, T_s, and their interactions with eCO₂. The degrees of freedom for each explanatory variable is 1. P-value < 0.1 is shown in bold.

		Predictors			
Response variables		VWC	T _s	eCO ₂ *VWC	eCO ₂ *T _s
NO ₃ ⁻ -N	F	3.72	16.14	0.19	2.77
	Df _{den}	20.69	36	20.69	36
	P-value	0.07	0.0003	0.67	0.10
NH ₄ ⁺ -N	F	1.85	48.30	0.33	1.10
	Df _{den}	36	32.75	36	32.75
	P-value	0.18	<0.001	0.57	0.30
PO ₄ ³⁻ -P	F	3.77	25.16	0.93	2.64
	Df _{den}	35.78	31.82	35.78	31.82
	P-value	0.06	<0.001	0.34	0.11
N:P ratios	F	5.53	10.96	0.55	2.51
	Df _{den}	34.69	31.99	34.69	31.99
	P-value	0.02	0.002	0.46	0.12

3.5 Discussion

Soils at BIFoR FACE exhibited strong seasonal patterns in soil moisture, temperature, and respiration during approximately six months before the first eCO₂ enrichment as well as the first year of eCO₂ enrichment (Fig. 3-2). No significant differences were observed in soil respiration, temperature, moisture, and bioavailable soil nutrients

between ambient and eCO₂ arrays during the Pre-treatment period. However, following fumigation, eCO₂ had a positive effect on soil respiration but only when additional factors of soil temperature and soil moisture were taken into account (Table 3-2). Soil temperature had a stronger effect than soil moisture on both respiration and nutrient availability. eCO₂ also had a statistically significant negative effect on NO₃⁻-N availability but affected neither NH₄⁺-N nor PO₄³⁻ availability.

3.5.1 Soil respiration and environmental drivers

The annual estimates of soil respiration during the first year of eCO₂ enrichment were 1,341±21 vs. 1,624±24 g C m⁻² y⁻¹ in ambient and eCO₂ arrays. These estimates are within the range of observations (500-2,100 g C m⁻² y⁻¹) reported for similar temperate forests (Campbell and Law, 2005). Soil respiration in the BIFoR FACE was observed to be at a higher range than other temperate forests; however, this is expected since mature forests have higher soil respiration than initiation young and old-growth forests. Our annual estimates are higher than the global mean value for deciduous broadleaf forests, ~850 g C m⁻² y⁻¹ (Xu and Shang, 2016) as well as other deciduous broadleaf forests (509-867 g C m⁻² y⁻¹ Hibbard et al., 2005; 663-913 g C m⁻² y⁻¹ Giasson et al., 2013). However, it is essential to note that the deciduous broadleaf forests included in Hibbard et al., (2005) were much younger than BIFoR FACE (31-75 years). In contrast, the Harvard forest soils in Giasson et al., (2013) are heavily influenced by prior land use (agricultural, pasture and woodlots use) and natural disturbances.

The seasonal patterns of soil respiration support our annual respiration estimates at BIFoR FACE, showing consistent higher soil respiration in eCO₂ arrays during Year 1 of eCO₂ enrichment (Fig. 3-2). These results are further supported by the mixed-effects models' outcome, where the eCO₂ interaction with soil temperature and the eCO₂ interaction with soil temperature and moisture were statistically significant.

Previous FACE experiments in forest ecosystems have observed different magnitudes of increase (Duke: 15.2%; FACTS-I: 29.4%, FACTS-II: 12.6% for *P. tremuloides* and 42.5% for *Betula/Populus*; POPFACE: 35.6% for *P. eur*, 49.5% for *P. alba* and 35.7% for *P. nigra*) or even a decrease (ORNL: 3%) in soil respiration rates during their first year of eCO₂ enrichment (King *et al.*, 2004; Bernhardt *et al.*, 2006). However, all these forest ecosystems were either plantations or young forests on disturbed soils. Moreover, in large open-top chambers studying the effects of eCO₂ in oak saplings, an increase of 22 and 37% was observed; however, the saplings were exposed to higher eCO₂ concentrations (Norby, 1996). EucFACE is the only FACE experiment conducted in mature woodland. The observed increase in annual soil respiration observed was approximately 7% (Drake *et al.*, 2018), similar to that observed at BIFoR FACE.

The models used for the soil respiration estimates were the eCO₂ and soil temperature interaction for the Pre-treatment period and the triple interaction between eCO₂, soil temperature, and moisture for Year 1. Both models predicted 64 and 63% of the variability (Table 3-2). Our modelling estimates are defensible since the correlation between predicted and observed soil respiration values was statistically significant in ambient and eCO₂ arrays. Two plausible reasons explain the relatively moderate performance observed in our modelling approach. Although soil moisture is an essential regulator of soil respiration, our study site is a mesic ecosystem, where soil moisture was not strongly limiting soil respiration rates most of the time. Secondly, although including soil moisture as a predictive variable may increase the model's predictive power, albeit it increases the prevalence of unreasonable fits, especially as the gap fraction between measurements increases (Gomez-Casanovas *et al.*, 2013). Such modelling approaches can perform better under small data-gap fractions, and

the unreasonable fits increase as the gap fractions increase. However, it is essential to note that the model's performance decreases when there is a plethora of temporal variability with limited spatial variability. Although our gap fraction was approximately 13%, it is essential to note that the gap fraction was spatial due to the experimental design and instrumental limitations (one ambient and one eCO₂ measured per hour for two weeks).

eCO₂ was observed to alter soil respiration response to the combined soil moisture and soil temperature effects. In ambient arrays, high respiration was observed under high temperature and low soil moisture. However, in eCO₂ arrays, despite soil temperature being the primary driver of soil respiration, our analysis highlights soil moisture importance (Fig. 3-4, Table 3-2). When soil moisture was included in our mixed-model analysis, the model's predictive capability increased by 2% (61 vs. 63% predictive capacity, respectively).

Soil moisture did not follow soil temperature and soil respiration's aforementioned seasonal pattern (Fig. 3-2). Soil moisture followed a seasonal course which is characteristic of temperate forests, with high levels in late autumn, winter, and spring, and lower levels in summer and early autumn (Davidson, Belk and Boone, 1998; Savage and Davidson, 2001; DeForest *et al.*, 2006; Turner and Henry, 2010; Contosta, Frey and Cooper, 2011). An optimum water content where soil respiration rates peaked (~ 10% volumetric water content) was observed (see section 3.8 *Supplementary Material Fig. S3-1*), but as the soil moisture increased further, soil respiration was suppressed. Our findings are in agreement with previous studies, which show that intermediate water content is commonly found to be optimum for soil respiration (Davidson, Belk and Boone, 1998; Davidson *et al.*, 2000; Drewitt *et al.*, 2002; Davidson and Janssens, 2006; Giasson *et al.*, 2013). High water content can

reduce root growth and function, primarily because of decreased oxygen availability in the soil pores (Kutsch, Bahn and Heinemeyer, 2010). On the other hand, dry soil conditions decrease the root water content, followed by a decrease in root cell turgor pressure. Consequently, since root cell turgor pressure is essential for plant growth, this will reduce metabolic activity and, finally, decrease soil respiration rates (Kutsch, Bahn and Heinemeyer, 2010).

Soil respiration seasonal cycles followed soil temperature's seasonal cycles, with soil respiration being highest in summer and lowest in winter (Fig. 3-2). Soil respiration peaks during the growing season when the soil temperature is high, and root exudates of labile C are likely to be abundant. In contrast, soil respiration tends to reach its lowest levels during winter when the soil temperature is low and labile C is limited (Contosta, Frey and Cooper, 2011). The observed pattern agrees with previous studies in temperate forest ecosystems (Davidson, Belk and Boone, 1998; Jaeger, C.H. III *et al.*, 1999; Bohlen *et al.*, 2001; Hogberg *et al.*, 2001; Knoepp and Swank, 2002; Bowden *et al.*, 2004; Mo *et al.*, 2005; DeForest *et al.*, 2006; Contosta, Frey and Cooper, 2011).

Temperature sensitivity Q_{10} was 3.08 in ambient vs. 2.64 in eCO₂ arrays during Year 1 at BIFoR FACE, lower than other deciduous forests (3.83; Giasson *et al.*, 2013) and the global average (3.46; Bond-Lamberty and Thomson, 2010). Moreover, the lower Q_{10} in eCO₂ arrays indicated that soil respiration under eCO₂ conditions was less sensitive to soil temperature. However, Q_{10} has been criticized since it is calculated via seasonal variations in temperature (see also *Chapter 2*), it is challenging to distinguish the temperature effect from other seasonal factors, such as carbon allocation to roots, solar radiation, and soil moisture (Davidson, Janssens and Lou, 2006; Almagro *et al.*, 2009; Jia *et al.*, 2013; Han *et al.*, 2014; Y. Wang *et al.*, 2014),

and Q_{10} has been observed to decrease as soil moisture increased in forest soils (Gutiñas *et al.*, 2013), thus distinguishing whether the Q_{10} decrease was due to eCO_2 or due to increased soil moisture under eCO_2 conditions, was challenging.

Although investigating soil responses to environmental factors individually might provide a simpler approach, *in situ*, the environmental factors interact in a more complex and dynamic way with soil respiration. However, in either very low or very high soil temperatures, soil moisture's effect on soil respiration was almost negligible, suggesting that soil temperature is the primary driver of soil respiration. It is commonly observed in temperate ecosystems that soil temperature is the primary driver of soil respiration (Lloyd and Taylor, 1994; Giasson *et al.*, 2013; Finzi *et al.*, 2014), and soil moisture becomes a controlling factor only at very high or very low levels (Lellei-Kovács *et al.*, 2011).

Soil respiration responded rapidly to rain events. The magnitude of the soil respiration increase depended on the antecedent soil conditions, with greater soil respiration effects after a prolonged dry period. This observation is in agreement with other studies (Unger *et al.*, 2010). The rainfall effect was greater if it was after a prolonged dry and warm period, almost doubling the soil respiration, even if the rainfall event was approximately 1 mm. However, no further increase in soil respiration was observed when the rainfall event was after a period of high soil moisture, even under high precipitation event (> 3mm). The pulses of soil respiration, often referred to as the Birch Effect (Birch, 1964), as a response to rainfall events can be explained due to physical CO_2 displacement from soil pore spaces (Liu *et al.*, 2002; Maier *et al.*, 2010). Moreover, after a rainfall event, previously unavailable C substrates that had accumulated when soils were dry may become available to microbes due to an increase in soil moisture (Denef, Six, Bossuyt, *et al.*, 2001; Denef, Six, Paustian, *et*

al., 2001; Six *et al.*, 2004; Göransson *et al.*, 2013). Another plausible hypothesis for the soil respiration pulse observed after a rainfall event is the osmolytes used by microbes to resist desiccation during dry conditions being metabolized (Fierer and Schimel, 2003; Xiang *et al.*, 2008; Williams and Xia, 2009) or due to microbial cell lysis due to excess turgor pressure, leading to a release of carbohydrates and other labile C solutes, and their subsequent consumption by surviving microbes (Xu, Baldocchi and Tang, 2004; Schimel, Balser and Wallenstein, 2007; Borken and Matzner, 2009; Warren, 2014).

According to the ecosystem's mass balance, the observed increase in soil CO₂ effluxes must be equated by additional C inputs, such as litterfall or the C loss from soil pools (Giardina and Ryan, 2002). It is already well established that alterations in C inputs to soils, such as litterfall, can explain soil respiration responses to eCO₂ (Drake *et al.*, 2011). However, the immediate soil respiration responses observed within days after the eCO₂ enrichment, combined with the period that the eCO₂ enrichment started (deciduous trees do not shed leaves early on the growing season), imply that the soil CO₂ efflux stimulation cannot be attributed to increased litterfall inputs in the eCO₂ arrays. Therefore, we suggest that the prompt and sustained soil respiration response to eCO₂ was due to increased C allocation belowground to roots and mycorrhizae.

3.5.2 Response of bioavailable nutrients to eCO₂

During the first year of eCO₂ enrichment at BIFoR FACE, eCO₂ had a statistically significant effect on NO₃⁻-N availability, decreasing the availability by 27%, on average, in eCO₂ arrays (Fig. 3-6 and Table 3-3-3). In contrast, eCO₂ had no statistically significant effect on NH₄⁺-N and PO₄³⁻-P availability, nor on N:P ratios. All three soil nutrients and N:P ratios exhibited strong seasonal patterns, with their availability

higher in summer and lower in winter. Soil temperature had a statistically significant effect on all three nutrients and N:P ratios; however, soil moisture had a statistically significant effect on N:P ratios (Table 3-4). Neither soil temperature nor soil moisture's interaction with eCO₂ was statistically significant.

All three soil nutrients and N:P ratios exhibited the same response pattern towards a combined effect of soil moisture, soil temperature, and monthly cumulative rainfall (see section 3.8 Supplementary material Fig. S3-4). Nutrient availability increased as soil temperature and cumulative precipitation increased while soil moisture decreased. The higher the soil temperature and rainfall for the same soil moisture level, the higher the nutrient availability. However, the higher the precipitation for the same soil temperature level, the higher the availability, while soil moisture's effect appeared almost negligible in both ambient and eCO₂ arrays.

The effect of eCO₂ on NO₃⁻-N availability is highly uncertain since it has been observed to increase, decrease or have no significant impact (Bassirirad *et al.*, 1996; BassiriRad *et al.*, 1997; BassiriRad *et al.*, 1997; Hasegawa, Macdonald and Power, 2016). Soil NO₃⁻-N availability under eCO₂ could be affected due to N mineralization and microbial immobilization (Díaz *et al.*, 1993; Hungate, 1999) or dinitrogen fixation (Hartwig *et al.*, 1996). Moreover, it could be affected due to leaching or plant uptake pathways such as total plant N pools (Owensby, Coyne and Auen, 1993), root uptake kinetics (Bassirirad *et al.*, 1996), root length density, and root system size (Newton *et al.*, 1996).

Uptake and assimilation of both N forms are essential for plant growth and require the expenditure of energy. It is well documented that NO₃⁻-N requires considerably more energy for uptake and assimilation than NH₄⁺-N because NO₃⁻-N must be metabolically

reduced to ammonia before it can be assimilated (Haynes and Goh, 1978; Blacqui re, Hofstra and Stulen, 1987; Glass and Siddiqi, 1995). Thus, the distinct root preference for NH_4^+ -N uptake is especially pronounced in tree species, possibly as an adaptation mechanism to forest soils that are relatively low on NO_3^- -N content (Bassirirad *et al.*, 1996). Specifically for oaks, it has been observed that, during the seedling stage, there is a slight NH_4^+ -N preference (Stadler, Gebauer and Schulze, 1993). However, a shift towards NO_3^- -N preference has been observed in sites where nitrification is more rapid (Singh, Singh and Gupta, 2014). However, studies have shown increased uptake NO_3^- -N capacity without changes in root N concentration, indicating that the increased uptake was due to increased carbohydrates allocation to the roots (Bassirirad *et al.*, 1996). Thus, NO_3^- -N uptake and utilization may be disproportionally enhanced by eCO_2 compared to NH_4^+ -N due to higher energy root status (BassiriRad *et al.*, 1997).

Another pathway explaining the decrease in NO_3^- -N availability in eCO_2 arrays is uptake by ectomycorrhizal hyphae. Mycorrhizal hyphae form symbiotic relationships with the plants exchanging nitrogen and phosphorus for organic carbon. There is speculation that forests with ectomycorrhizal associations operate in an organic nutrient economy due to the decelerated litter decomposition rates, which result in greater amounts of soil organic matter being accumulated (Phillips, Brzostek and Midgley, 2013). Hence, ectomycorrhizal hyphae can acquire more nitrogen from soil organic matter, providing more available N to the plants. Certain ectomycorrhizal hyphae species have been observed to grow better on NO_3^- than NH_4^+ (Aouadj *et al.*, 2000; Scheromm *et al.*, 1990). Moreover, many ectomycorrhizal hyphae have been observed to acquire NO_3^- -N and metabolize it as an N source (Nygren, 2008). However, there are limited studies on ectomycorrhizal hyphae and eCO_2 , but a few of them report inconsistencies on ectomycorrhizal hyphae responses under eCO_2

regarding both colonization (Garcia *et al.*, 2008; Wang *et al.*, 2015) and biomass (Gutknecht, Field and Balser, 2012).

Microbial processes, such as nitrification, immobilization, and denitrification, may also explain the observed decrease in NO_3^- -N availability in eCO_2 arrays could be through microbial. Nitrification is a step-wise process and is two different autotrophic bacterial groups perform each step. Nitrification is affected by various environmental factors, such as oxygen, temperature, moisture, the abundance of NH_4^+ , population, diversity of nitrifying microorganisms, and substrates' availability to those organisms (Yuan *et al.*, 2005). Nitrification is observed to be inhibited at higher soil moisture ranges (>60%); however, soil moisture at BIFoR FACE was observed to be consistently lower than 30%. Both soil temperature and moisture did not reach levels that could halt nitrification during eCO_2 enrichment. The NH_4^+ availability was similar under both ambient conditions and eCO_2 conditions; thus the inhibition of nitrification a plausible explanation for the observed decrease in NO_3^- -N availability is unlikely. In the short term, no eCO_2 effect has been observed on nitrification (Rütting and Andresen, 2015) and autotrophic nitrifiers (Hu *et al.*, 2016). Although gross nitrification has been observed to decrease in FACE experiments, the datasets are small in size; thus, caution must be taken when interpreting these results (Rütting and Andresen, 2015). Thus the observed decrease in NO_3^- -N availability could be attributed to increased microbial and plant uptake under eCO_2 enrichment.

It has been observed that in the short term, microbes are responsible for substantially faster initial uptake of all N forms and, more specifically, a higher capacity for NO_3^- -N (Kuzyakov and Xu, 2013). Although the overall microbial biomass increased only by 7% under eCO_2 conditions, based on a meta-analysis by de Graaff *et al.*, (2006), NO_3^- immobilization has increased under eCO_2 conditions (Zak *et al.*, 2000). However, it is

still unclear the effect of eCO₂ on microbial processes, since the findings in the literature regarding microbial biomass, N mineralization, and microbial immobilization under eCO₂ conditions report both large increases and decreases in all three processes mentioned above (Hungate, 1999; Zak *et al.*, 2000).

Another plausible explanation for the decrease in NO₃⁻-N availability under eCO₂ is increased nitrous oxide (N₂O) emissions from soil. Although in the short-term, eCO₂ enrichment did not affect nitrate-reducing organisms (Marhan *et al.*, 2011), eCO₂ can enhance the N₂O emissions from 27 up to 50% (Ineson, Coward and Hartwig, 1998; Kee Lam *et al.*, 2010). N₂O emissions can be enhanced under eCO₂ by increased root-derived available C, thus providing energy for denitrification, stimulating root biomass, and exudates for denitrifiers (Ineson, Coward and Hartwig, 1998; Kettunen *et al.*, 2007). Such increases in N₂O are considered to offset CO₂ sequestration by more than 70% (Liu and Greaver, 2009), significantly impacting the terrestrial C sink.

Studies have shown that NO₃⁻-N availability was severely affected under eCO₂ due to increased leaching, and the effect was exacerbated under the combination of eCO₂ and N addition (Liu *et al.*, 2008). Temperate forests are predicted to face a gradual decline in their stability as the atmospheric N deposition increases, leading to nitrogen saturation (Schulze, 1989; MacDonald *et al.*, 2002). These N-saturated forests are predicted to undergo an initial rise in soil N availability, mainly in NO₃⁻-N, followed by substantial leaching. Thus, considerable leaching might accelerate nutrient limitations in ecosystems affected by chronic N deposition, subsequently affecting the amount of C sequestered and stored in these ecosystems and leading to more significant climate change impacts.

It has been generally observed that net N mineralization rates increase with temperature (Rustad *et al.*, 2001; Shaw and Harte, 2001; Melillo *et al.*, 2002; Wang *et al.*, 2006), thus higher rates of $\text{NH}_4^+\text{-N}$ are bioavailable as the growing season progresses. Although soil moisture can significantly affect net N mineralization (Sierra, 1997; Paul *et al.*, 2003), the maximum net N mineralization rate occurs when soil moisture is near field water holding capacity (Stanford and Epstein, 1974). In contrast, nitrification is generally accepted to be halted at high soil moisture conditions. In contrast, the effect of soil temperature on nitrification follows a bell-shaped curve with optimum conditions at 30-35 °C (Sahrawat, 2008). Nonetheless, our dataset exceeded the optimum conditions neither for soil temperature nor for soil moisture.

Furthermore, increased soil temperature and soil moisture have been observed to increase $\text{PO}_4^{3-}\text{-P}$ availability (Li, Mahler and Everson, 1990). N mineralization is a more robust process than nitrification. A plethora of bacteria, fungi, and free-living organisms contribute to the decomposition of organic matter and, subsequently, N mineralization. Moreover, decomposition takes place both under aerobic and anaerobic conditions, whereas nitrification requires well-aerated soils.

Substantial enhancement has been observed on N mineralization rates under eCO_2 conditions; the literature on FACE experiments is inconclusive regarding the eCO_2 effect on $\text{NH}_4^+\text{-N}$ availability and consumption (Rütting and Andresen, 2015). Our results contradict the results of other studies of eCO_2 in mature forests that have observed an increase in $\text{NH}_4^+\text{-N}$ availability (Hasegawa, Macdonald and Power, 2016; Schleppi, Körner and Klein, 2019). Moreover, it has been reported that plants' demand for phosphorus increases due to growth stimulation under eCO_2 conditions (Gentile *et al.*, 2012; Zhang *et al.*, 2014). Moreover, the symbiotic relationship between mycorrhizal fungi and host plants can be stimulated under eCO_2 since fungi will

increase their P foraging activities in exchange for the increased root carbohydrate supply (Kiers *et al.*, 2011). Mycorrhizal fungi have been reported to enlarge their network under eCO₂ conditions; thus, nutrient absorption increases (Staddon, Gregersen and Jakobsen, 2004). Moreover, increased P immobilization by microbes under eCO₂ conditions has also been reported (Jin *et al.*, 2014). However, literature P availability in forest ecosystems under eCO₂ is limited and conflicting, since both no effects (Johnson *et al.*, 2004) or positive effects (Dijkstra *et al.*, 2012; Hasegawa, Macdonald and Power, 2016) have been reported.

3.5.3 Interactions of carbon and nutrient cycling to eCO₂

Environmental variables such as soil moisture, soil temperature, precipitation, nutrient demand, and supply are key processes contributing to the observed soil respiration. Other factors such as plant growth (De Vries, Brunsting and Van Laar, 1974), plant metabolism (Wit, Brouwer and Vries, 1970; Wieser and Bahn, 2004), root production and growth (Högberg and Read, 2006; Kutsch, Bahn and Heinemeyer, 2010; An *et al.*, 2017) root system micro-environment (Lambers, Atkin and Millenaar, 2002; Heinemeyer *et al.*, 2007; Kutsch, Bahn and Heinemeyer, 2010), and free-living mycorrhizosphere biota (Raich and Tufekcioglu, 2000; Mitra *et al.*, 2014; Brady and Weil, 2017), are crucial contributors to soil respiration. However, from an ecosystemic perspective, carbon and nutrient cycles are interlinked and interact with each other.

This study observed a prompt and sustained response of soil respiration to eCO₂ combined with soil temperature and moisture. Given the data available to this study, we hypothesised that the increased soil respiration response under eCO₂ is plausible to be attributed to increased carbon allocation belowground to roots, mycorrhiza

hyphae, and free-living microbes. We also observed a significant decrease in NO_3^- -N availability which was obvious just after a month of eCO_2 enrichment and was sustained until the end of the first year of eCO_2 enrichment. Interestingly, no differences were observed in NH_4^+ -N availability in ambient and eCO_2 arrays, and the environmental conditions recorded at BIFoR FACE did not reach limiting levels for the nitrification process. Moreover, given that this was an initial short-term response, we can reject the hypothesis that the observed decrease in NO_3^- -N availability under eCO_2 was due to increased N_2O emissions.

Ergo the suggested pathway for our observed responses during the first year of eCO_2 enrichment at BIFoR FACE is increased carbon allocation through roots to the soil, thus increasing the carbon substrate available to microorganisms. Soil microorganisms and plants utilised the extra carbon, and in order to meet their metabolic demands, they increased their nutrient uptake in the form of NO_3^- -N.

3.5.4 Future implications

Expectations are that maybe mature forests respond differently to eCO_2 enrichment than young forests due to different developmental C needs and internal-plant C allocations (Körner, 2006). During the early tree stages, more effort is allocated to increasing height and foliage development. During later stages in tree development, stem growth and root development may become the priority for resource allocation (Peichl and Arain, 2007). Moreover, the magnitude of the eCO_2 effect on mature forests may be constrained by nutrient availability. Mature and old-growth forests are operating under a self-supporting system in terms of nutrition, with nutrient availability rates controlled by microbial activity (Ingestad, 1982). If the nutrient demand rates exceed the nutrient availability rates under eCO_2 , the possibility of increased carbon

allocation belowground for an attempt to advance foraging nutrients may be restricted in mature forest ecosystems.

Although this study focused only on the first year of eCO₂ enrichment at a mature temperate woodland and continuous observation is essential since different processes have different timescales. Short-term responses are not always sustained, and they tend to disappear or alter after a few years (Drake *et al.*, 2018; Ochoa-Hueso, Piñeiro and Power, 2019). However, if the observed responses in this study are sustained, the ecosystem can undergo a progressive nitrogen limitation (PNL) (Finzi *et al.*, 2006). PNL under eCO₂ can occur as a swift mineral N immobilization by plant uptake, leading to mineral N soil depletion from the labile pools, resulting in slower N mineralization rates and a subsequent decrease in N availability (Luo *et al.*, 2004). Moreover, PNL can occur due to an increased microbial N demand due to the increased microbial C availability, leading to increased N immobilization by microorganisms, and decreased N availability to plants (Luo *et al.*, 2004). If mature forests are faced with nutrient limitations under eCO₂, the net primary production will not respond anymore to eCO₂. This is crucial since, for the past 20 years, temperate forests have played an essential role as CO₂ sinks. Thus the forests' capacity to uptake and store carbon long-term might be compromised, pausing greater uncertainties to climate change.

3.6 Conclusions

The purpose of this study was to monitor the soil respiration and the bioavailability of soil nutrients in a mature temperate woodland during its first year of eCO₂ enrichment to +150 ppm above ambient conditions. This is the first time that belowground responses of soil eCO₂ fluxes and nutrient dynamics of mature temperate woodland are under high-resolution scrutiny, both temporally and spatially. Moreover, this study

provided the advantage to study the responses of the woodland under the 2050 atmospheric CO₂ scenario as a coetaneous event.

Temperate deciduous forest ecosystems exhibit strong seasonality in their physiology, environmental variables, and, subsequently, their biochemical responses. During winter, deciduous forests do not have leaves, soil moisture is high, and soil temperature is low. Accordingly, soil respiration rates and soil nutrient bioavailability are low. Thus, seasonality had a significant effect on both soil respiration rates and soil nutrient bioavailability.

Soil temperature had a statistically significant effect on all three bioavailable soil nutrients (NO₃⁻-N, NH₄⁺-N, and PO₄³⁻-P), and all nutrients' availability increased as soil temperature increased. However, soil moisture had a negative effect on NH₄⁺-N and PO₄³⁻-P availability, with the effect being more prominent for NH₄⁺-N availability. NO₃⁻-N availability responded negatively to soil moisture under low water content, albeit NO₃⁻-N availability increased as the soil moisture increased. Soil moisture's effect on all three nutrients was not statistically significant. Both soil moisture and soil temperature had a statistically significant effect on N:P ratios. Soil temperature had a negative impact on N:P ratios, while soil moisture had almost no effect on N:P ratios in low and medium water content. However, as soil moisture increased to high water content, the effect on N:P ratios was negative.

Addressing the research questions posed at the beginning, we suggest the following.

- Does eCO₂ affect soil respiration, soil moisture, and soil temperature on a mature oak woodland?

Although soil respiration was higher in eCO₂ arrays (up to 46% increase in monthly averages), eCO₂ had no statistically significant effect on soil respiration. The annual

soil respiration was approximately 21.1% higher in eCO₂ arrays, feeding back to the atmosphere and an additional 283 g C m⁻² y⁻¹. Per contra, although soil moisture and soil temperature were slightly higher under eCO₂ conditions, they were statistically similar between ambient and eCO₂ conditions. Moreover, soil respiration rain pulses were more prominent under eCO₂ conditions than under ambient conditions.

The interactions between eCO₂, soil moisture, and soil temperature had a statistically significant effect on soil respiration; thus, soil respiration responses to the environmental variables were altered under eCO₂ conditions. The effect of soil temperature on soil respiration was more pronounced under eCO₂ conditions. The effect of soil moisture was more prominent under eCO₂ conditions, and the tipping point in which soil moisture's effect switches from positive to negative was shifted to higher water content. Thus, the highest respiration rates under eCO₂ conditions were reported under high soil temperatures regardless of the water content.

- How do bioavailable soil nutrients respond to eCO₂?

eCO₂ had a statistically significant effect on NO₃⁻-N availability, decreasing the seasonal availability by 27% on average. No statistically significant eCO₂ effect was observed on NH₄⁺-N and PO₄³⁻-P availability nor on the N:P ratios. eCO₂ interactions with both soil moisture and soil temperature were statistically similar under ambient and eCO₂ conditions. Although soil moisture, soil temperature, and rainfall had an interactive and dynamic effect on nutrient availability, it appeared that soil temperature and cumulative monthly precipitation were the main drivers of soil nutrient availability.

Combining the overall belowground responses observed during the first year of eCO₂ enrichment at BIFoR FACE, we suggest that those responses are most likely attributed to increased rhizosphere activity under eCO₂ conditions due to an increase in

belowground carbon allocation. The major environmental drivers for such belowground responses are soil moisture and soil temperature, which were statistically similar under ambient and eCO₂ conditions. Thus, these responses are more likely to be driven by an increased photosynthate transport belowground, increasing the root respiration and the mycorrhizal and microbial respiration due to increased carbon supply. For the increased soil respiration response to be accommodated, the NO₃⁻ demand increased. It could either be attributed either to increased plant demand and subsequent uptake through the mycorrhiza's symbiotic relationship or to increased microbial activity and subsequent immobilization. Both pathways can affect the ecosystem's long-term responses differently, and ultimately the forest's potential to sequester more carbon.

3.7 References

- Almagro, M. *et al.* (2009) 'Temperature dependence of soil CO₂ efflux is strongly modulated by seasonal patterns of moisture availability in a Mediterranean ecosystem', *Soil Biology and Biochemistry*, 41(3), pp. 594–605. doi: 10.1016/j.soilbio.2008.12.021.
- An, J. Y. *et al.* (2017) 'Litterfall production and fine root dynamics in cool-temperate forests', *PLOS ONE*, 12(6), p. e0180126. doi: 10.1371/journal.pone.0180126.
- Andresen, L. C. *et al.* (2018) 'Biomass responses in a temperate European grassland through 17 years of elevated CO₂', *Global Change Biology*, 24(9), pp. 3875–3885. doi: 10.1111/gcb.13705.
- Aouadj, R., Es-Sgaouri, A. and Button, B. (2000) 'Etude de la stabilite et de quelques proprietes de la nitrate reductase du champignon ectomycorhizien *Pisolithus tinctorius*', *Cryptogamie, Mycologie*, 21(3), pp. 187–202. doi: 10.1016/S0181-1584(00)01044-7.
- Barton, K. (2014) 'MuMIn: multi-model inference. R package version 3.1-96'.
- Bassirirad, H. *et al.* (1996) 'Differential responses of root uptake kinetics of NH₄⁺ and NO₃⁻ to enriched atmospheric CO₂ concentration in field-grown loblolly pine', *Plant, Cell and Environment*, 19(3), pp. 367–371. doi: 10.1111/j.1365-3040.1996.tb00260.x.
- BassiriRad, Hormoz *et al.* (1997) 'Changes in root NH₄⁺ and NO₃⁻ absorption rates of loblolly and ponderosa pine in response to CO₂ enrichment', *Plant and Soil*, 190(1), pp. 1–9. doi: 10.1023/A:1004206624311.
- BassiriRad, H. *et al.* (1997) 'Growth and root NO₃⁻ and PO₄³⁻ uptake capacity of three desert species in response to atmospheric CO₂ enrichment', *Australian Journal of Plant Physiology*, 24(3), pp. 353–358. doi: 10.1071/PP96109.

- Bates, D. *et al.* (2015) 'Fitting Linear Mixed-Effects Models Using **lme4**', *Journal of Statistical Software*. American Statistical Association, 67(1). doi: 10.18637/jss.v067.i01.
- Bernhardt, E. S. *et al.* (2006) 'Long-term effects of free air CO₂ enrichment (FACE) on soil respiration', *Biogeochemistry*, 77(1), pp. 91–116. doi: 10.1007/s10533-005-1062-0.
- Blacqui re, T., Hofstra, R. and Stulen, I. (1987) 'Ammonium and nitrate nutrition in *Plantago lanceolata* and *Plantago major* L. ssp. *major* - I. Aspects of growth, chemical composition and root respiration', *Plant and Soil*, 104(1), pp. 129–141. doi: 10.1007/BF02370635.
- Boden, T. a, Marland, G. and Andres, R. J. (2012) 'Global, Regional, and National Fossil-Fuel CO₂ Emissions (1751 - 2009)', *Carbon Dioxide Information Analysis Center Oak Ridge National Laboratory USA Oak Ridge TN Department of Energy*. doi: 10.3334/CDIAC/00001.
- Bohlen, P. J. *et al.* (2001) 'Plant-Soil-Microbial Interactions in a Northern Hardwood Forest', *Ecology*. Wiley, 82(4), p. 965. doi: 10.2307/2679896.
- Bond-Lamberty, B. and Thomson, A. (2010) 'Temperature-associated increases in the global soil respiration record', *Nature*, 464. doi: 10.1038/nature08930.
- Borken, W. and Matzner, E. (2009) 'Reappraisal of drying and wetting effects on C and N mineralization and fluxes in soils', *Global Change Biology*, 15(4), pp. 808–824. doi: 10.1111/j.1365-2486.2008.01681.x.
- Bowatte, S. *et al.* (2008) 'In situ ion exchange resin membrane (IEM) technique to measure soil mineral nitrogen dynamics in grazed pastures', *Biology and Fertility of Soils*, 44(6), pp. 805–813. doi: 10.1007/s00374-007-0260-4.
- Bowden, R. D. *et al.* (2004) 'Chronic nitrogen additions reduce total soil respiration and microbial respiration in temperate forest soils at the Harvard Forest', *Forest Ecology and Management*, 196(1), pp. 43–56. doi: 10.1016/j.foreco.2004.03.011.
- Brady, N. and Weil, R. (2017) *The nature and properties of soil*. 15th edn. Pearson.
- Campbell, J. L. and Law, B. E. (2005) 'Forest soil respiration across three climatically distinct chronosequences in Oregon', *Biogeochemistry*, 73, pp. 109–125. doi: 10.1007/s10533-004-5165-9.
- Ciais, P., Sabine, C. and Bala, G. (2013) 'Chapter 6: Carbon and other biogeochemical cycles', *Climate Change 2013: The Physical Science Basis*.
- Contosta, A. R., Frey, S. D. and Cooper, A. B. (2011) 'Seasonal dynamics of soil respiration and N mineralization in chronically warmed and fertilized soils', *Ecosphere*, 2(3), p. art36. doi: 10.1890/ES10-00133.1.
- Cox, P. M. *et al.* (2000) 'Acceleration of global warming due to carbon-cycle feedbacks in a coupled climate model', *Nature*, 408(6809), pp. 184–187. doi: 10.1038/35041539.
- Daily CO₂ (2019). Available at: <https://www.co2.earth/daily-co2> (Accessed: 26 March 2020).
- Davidson, E. A. *et al.* (2000) 'Effects of soil water content on soil respiration in forests and cattle pastures of eastern Amazonia', *Biogeochemistry*, 48(1), pp. 53–69. doi: 10.1023/A:1006204113917.
- Davidson, E. A., Belk, E. and Boone, R. D. (1998) 'Soil water content and temperature as independent or confounded factors controlling soil respiration in a temperate mixed hardwood forest.', *Global Change Biology*, 4, pp. 217–227.
- Davidson, E. A. and Janssens, I. A. (2006) 'Temperature sensitivity of soil carbon decomposition and feedbacks to climate change', *Nature*, 440, pp. 165–173. doi: 10.1038/nature04514.

- Davidson, E. A., Janssens, I. A. and Lou, Y. (2006) 'On the variability of respiration in terrestrial ecosystems: Moving beyond Q_{10} ', *Global Change Biology*, 12(2), pp. 154–164. doi: 10.1111/j.1365-2486.2005.01065.x.
- DeForest, J. L. *et al.* (2006) 'Phenophases alter the soil respiration-temperature relationship in an oak-dominated forest', *International Journal of Biometeorology*, 51(2), pp. 135–144. doi: 10.1007/s00484-006-0046-7.
- Denef, K., Six, J., Paustian, K., *et al.* (2001) 'Importance of macroaggregate dynamics in controlling soil carbon stabilization: Short-term effects of physical disturbance induced by dry-wet cycles', *Soil Biology and Biochemistry*, 33(15), pp. 2145–2153. doi: 10.1016/S0038-0717(01)00153-5.
- Denef, K., Six, J., Bossuyt, H., *et al.* (2001) 'Influence of dry-wet cycles on the interrelationship between aggregate, particulate organic matter, and microbial community dynamics', *Soil Biology and Biochemistry*, 33(12–13), pp. 1599–1611. doi: 10.1016/S0038-0717(01)00076-1.
- Díaz, S. *et al.* (1993) 'Evidence of a feedback mechanism limiting plant response to elevated carbon dioxide', *Nature*, 364(6438), pp. 616–617. doi: 10.1038/364616a0.
- Dijkstra, F. A. *et al.* (2012) 'Climate change alters stoichiometry of phosphorus and nitrogen in a semiarid grassland', *New Phytologist*, 196(3), pp. 807–815. doi: 10.1111/j.1469-8137.2012.04349.x.
- Drake, J. E. *et al.* (2011) 'Increases in the flux of carbon belowground stimulate nitrogen uptake and sustain the long-term enhancement of forest productivity under elevated CO_2 ', *Ecology Letters*, 14(4), pp. 349–357. doi: 10.1111/j.1461-0248.2011.01593.x.
- Drake, J. E. *et al.* (2016) 'Short-term carbon cycling responses of a mature eucalypt woodland to gradual stepwise enrichment of atmospheric CO_2 concentration', *Global Change Biology*, 22(1), pp. 380–390. doi: 10.1111/gcb.13109.
- Drake, J. E. *et al.* (2018) 'Three years of soil respiration in a mature eucalypt woodland exposed to atmospheric CO_2 enrichment', *Biogeochemistry*, 139(1), pp. 85–101. doi: 10.1007/s10533-018-0457-7.
- Drewitt, G. B. *et al.* (2002) 'Measuring forest floor CO_2 fluxes in a Douglas-fir forest', *Agricultural and Forest Meteorology*. Elsevier, 110(4), pp. 299–317. doi: 10.1016/S0168-1923(01)00294-5.
- Fierer, N. and Schimel, J. P. (2003) 'A Proposed Mechanism for the Pulse in Carbon Dioxide Production Commonly Observed Following the Rapid Rewetting of a Dry Soil', *Soil Science Society of America Journal*, 67(3), pp. 798–805. doi: 10.2136/SSSAJ2003.7980.
- Finzi, A. C. *et al.* (2002) 'The nitrogen budget of a pine forest under free air CO_2 enrichment', *Oecologia*. Springer Berlin Heidelberg, 132(4), pp. 567–578. doi: 10.1007/s00442-002-0996-3.
- Finzi, A. C. *et al.* (2006) 'Progressive Nitrogen Limitation of Ecosystem Processes Under Elevated CO_2 in a Warm-Temperate Forest', *Ecology*, 87(1), pp. 15–25. doi: 10.1890/04-1748.
- Finzi, A. C. *et al.* (2014) 'Net primary production and soil respiration in New England hemlock forests affected by the hemlock woolly adelgid', *Ecosphere*, 5(8), p. art98. doi: 10.1890/ES14-00102.1.
- Friedlingstein, P. *et al.* (2006) 'Climate-Carbon Cycle Feedback Analysis: Results from the C 4 MIP Model Intercomparison', *Journal of Climate*, 19, pp. 3337–3353.
- Friedlingstein, P. *et al.* (2014) 'Uncertainties in CMIP5 Climate Projections due to Carbon Cycle Feedbacks', *Journal of Climate*, 27, pp. 511–526. doi: 10.1175/JCLI-D-12-00579.1.

- Garcia, M. O. *et al.* (2008) 'Mycorrhizal dynamics under elevated CO₂ and nitrogen fertilization in a warm temperate forest', *Plant and Soil*, 303(1–2), pp. 301–310. doi: 10.1007/s11104-007-9509-9.
- Gentile, R. *et al.* (2012) 'Effects of long-term exposure to enriched CO₂ on the nutrient-supplying capacity of a grassland soil', *Biology and Fertility of Soils*, 48(3), pp. 357–362. doi: 10.1007/s00374-011-0616-7.
- Giardina, C. P. and Ryan, M. G. (2002) 'Total belowground carbon allocation in a fast-growing Eucalyptus plantation estimated using a carbon balance approach', *Ecosystems*, 5(5), pp. 487–499. doi: 10.1007/s10021-002-0130-8.
- Giasson, M.-A. *et al.* (2013) 'Soil respiration in a northeastern US temperate forest: a 22-year synthesis', *Ecosphere*, 4(11), p. 140. doi: 10.1890/ES13.00183.1.
- Glass, A. D. M. and Siddiqi, M. Y. (1995) 'Nitrogen absorption by plant roots', in Srivastava, H. S. and Singh, R. P. (eds) *Nitrogen Nutrition in Higher Plants*. New Delhi: Associated Pub. Co, p. 445.
- Gomez-Casanovas, N. *et al.* (2013) 'Gap filling strategies and error in estimating annual soil respiration', *Global Change Biology*, 19(6), pp. 1941–1952. doi: 10.1111/gcb.12127.
- Göransson, H. *et al.* (2013) 'Bacterial growth and respiration responses upon rewetting dry forest soils: Impact of drought-legacy', *Soil Biology and Biochemistry*, 57, pp. 477–486. doi: 10.1016/j.soilbio.2012.08.031.
- de Graaff, M. A. *et al.* (2006) 'Interactions between plant growth and soil nutrient cycling under elevated CO₂: A meta-analysis', *Global Change Biology*, 12(11), pp. 2077–2091. doi: 10.1111/j.1365-2486.2006.01240.x.
- Gutiññas, M. E. *et al.* (2013) 'Sensitivity of soil respiration to moisture and temperature', *Journal of Soil Science and Plant Nutrition*, 13(2), pp. 445–461.
- Gutknecht, J. L. M., Field, C. B. and Balser, T. C. (2012) 'Microbial communities and their responses to simulated global change fluctuate greatly over multiple years', *Global Change Biology*, 18(7), pp. 2256–2269. doi: 10.1111/j.1365-2486.2012.02686.x.
- Han, G. *et al.* (2014) 'Ecosystem photosynthesis regulates soil respiration on a diurnal scale with a short-term time lag in a coastal wetland', *Soil Biology and Biochemistry*. doi: 10.1016/j.soilbio.2013.09.024.
- Hart, K. M. *et al.* (2019) 'Characteristics of free air carbon dioxide enrichment of a northern temperate mature forest', *Global Change Biology*, 26(2), p. gcb.14786. doi: 10.1111/gcb.14786.
- Hartwig, U. A. *et al.* (1996) 'Symbiotic nitrogen fixation: one key to understand the response of temperate grassland-ecosystems to elevated CO₂?', in Körner, C. and Bazzaz, F. A. (eds) *Carbon Dioxide, populations and communities*. San Diego: Academic Press, pp. 253–264. doi: 10.1007/3-540-31237-4_18.
- Hasegawa, S., Macdonald, C. A. and Power, S. A. (2016) 'Elevated carbon dioxide increases soil nitrogen and phosphorus availability in a phosphorus-limited Eucalyptus woodland', *Global Change Biology*, 22(4), pp. 1628–1643. doi: 10.1111/gcb.13147.
- Haynes, R. J. and Goh, K. M. (1978) 'Ammonium and nitrate nutrition of plants', *Biological Reviews*. Wiley, 53(4), pp. 465–510. doi: 10.1111/j.1469-185x.1978.tb00862.x.
- Heinemeyer, A. *et al.* (2007) 'Forest soil CO₂ flux: Uncovering the contribution and environmental responses of ectomycorrhizas', *Global Change Biology*, 13(8), pp. 1786–1797. doi: 10.1111/j.1365-2486.2007.01383.x.

- Hibbard, K. A. *et al.* (2005) 'An analysis of soil respiration across northern hemisphere temperate ecosystems', *Biogeochemistry*, 73(1), pp. 29–70. doi: 10.1007/s10533-004-2946-0.
- Högberg, P. *et al.* (2001) 'Large-scale forest girdling shows that current photosynthesis drives soil respiration', *Nature*, 411(6839), pp. 789–792. doi: 10.1038/35081058.
- Högberg, P. and Read, D. J. (2006) 'Towards a more plant physiological perspective on soil ecology', *Trends in Ecology and Evolution*, 21(10), pp. 548–554. doi: 10.1016/j.tree.2006.06.004.
- Hovenden, M. J. *et al.* (2008) 'Warming prevents the elevated CO₂-induced reduction in available soil nitrogen in a temperate, perennial grassland', *Global Change Biology*, 14(5), pp. 1018–1024. doi: 10.1111/j.1365-2486.2008.01558.x.
- Hu, H. W. *et al.* (2016) 'Effects of climate warming and elevated CO₂ on autotrophic nitrification and nitrifiers in dryland ecosystems', *Soil Biology and Biochemistry*, 92, pp. 1–15. doi: 10.1016/j.soilbio.2015.09.008.
- Hungate, B. A. (1999) 'Ecosystem Responses to Rising Atmospheric CO₂: Feedbacks through the Nitrogen Cycle', in Luo, Y. and Mooney, H. A. (eds) *Physiological Ecology, Carbon Dioxide and Environmental Stress*. Academic Press, pp. 265–285. doi: 10.1016/B978-012460370-7/50011-5.
- Ineson, P., Coward, P. A. and Hartwig, U. A. (1998) 'Soil gas fluxes of N₂O, CH₄ and CO₂ beneath *Lolium perenne* under elevated CO₂: The Swiss free air carbon dioxide enrichment experiment', *Plant and Soil*, 198(1), pp. 89–95. doi: 10.1023/A:1004298309606.
- Ingestad, T. (1982) 'Relative addition rate and external concentration; Driving variables used in plant nutrition research', *Plant, Cell & Environment*, 5(6), pp. 443–453. doi: 10.1111/1365-3040.ep11611714.
- Jaeger, C.H. III *et al.* (1999) 'Seasonal Partitioning of Nitrogen by Plants and Soil Microorganisms in an Alpine Ecosystem', *Ecology*, 80(6), p. 1883. doi: 10.2307/176666.
- Jia, X. *et al.* (2013) 'Temperature Response of Soil Respiration in a Chinese Pine Plantation: Hysteresis and Seasonal vs. Diel Q₁₀', *PLoS ONE*, 8(2). doi: 10.1371/journal.pone.0057858.
- Jin, J. *et al.* (2014) 'Increased microbial activity contributes to phosphorus immobilization in the rhizosphere of wheat under elevated CO₂', *Soil Biology and Biochemistry*, 75, pp. 292–299. doi: 10.1016/j.soilbio.2014.04.019.
- Johnson, D. W. *et al.* (2004) 'Effects of elevated CO₂ on nutrient cycling in a sweetgum plantation', *Biogeochemistry*, 69(3), pp. 379–403. doi: 10.1023/B:BIOG.0000031054.19158.7c.
- Kee Lam, S. A. *et al.* (2010) 'Soil gas fluxes of N₂O, CO₂ and CH₄ under elevated carbon dioxide under wheat in northern China', in *19th World Congress of Soil Science, Soil Solutions for a Changing World*.
- Kettunen, R. *et al.* (2007) 'Can a mixed stand of N₂-fixing and non-fixing plants restrict N₂O emissions with increasing CO₂ concentration?', *Soil Biology and Biochemistry*, 39(10), pp. 2538–2546. doi: 10.1016/j.soilbio.2007.04.023.
- Khan, F. N. *et al.* (2010) 'Tree exposure to elevated CO₂ increases availability of soil phosphorus', *Pakistan Journal of Botany*, 42(2), pp. 907–916.
- Kiers, E. T. *et al.* (2011) 'Reciprocal rewards stabilize cooperation in the mycorrhizal symbiosis', *Science*, 333(6044), pp. 880–882. doi: 10.1126/science.1208473.
- King, J. S. *et al.* (2004) 'A multiyear synthesis of soil respiration responded to elevated

atmospheric CO₂ from four forest FACE experiments', *Global Change Biology*, 10, pp. 1027–1042. doi: 10.1111/j.1365-2486.2004.00789.x.

Knoepp, J. D. and Swank, W. T. (2002) 'Using soil temperature and moisture to predict forest soil nitrogen mineralization', *Biology and Fertility of Soils*, 36(3), pp. 177–182. doi: 10.1007/s00374-002-0536-7.

Körner, C. *et al.* (2005) 'Carbon Flux and Growth in Mature Deciduous Forest Trees Exposed to Elevated CO₂', *Science*, 309(5739), pp. 1360–1362. doi: 10.1126/science.1113977.

Körner, C. (2006) 'Plant CO₂ responses: an issue of definition, time and resource supply', *New Phytologist*, 172, pp. 393–411. doi: 10.1111/j.1469-8137.2006.01886.x.

Kutsch, W. L., Bahn, M. and Heinemeyer, A. (2010) *Soil carbon dynamics: An integrated methodology*, *Soil Carbon Dynamics: An Integrated Methodology*. Cambridge University Press. doi: 10.1017/CBO9780511711794.

Kuzyakov, Y. *et al.* (2019) 'Review and synthesis of the effects of elevated atmospheric CO₂ on soil processes: No changes in pools, but increased fluxes and accelerated cycles', *Soil Biology and Biochemistry*. doi: 10.1016/j.soilbio.2018.10.005.

Kuzyakov, Y. and Xu, X. (2013) 'Competition between roots and microorganisms for nitrogen: mechanisms and ecological relevance', *New Phytologist*, 198(3), pp. 656–669. doi: 10.1111/nph.12235.

Lagomarsino, A. *et al.* (2008) 'Assessment of soil nitrogen and phosphorous availability under elevated CO₂ and N-fertilization in a short rotation poplar plantation', *Plant and Soil*, 308(1–2), pp. 131–147. doi: 10.1007/s11104-008-9614-4.

Lambers, H., Atkin, O. and Millenaar, F. (2002) 'Respiratory Patterns in Roots in Relation to Their Functioning', in Waisel, Y., Eshel, A., and Kafkafi, U. (eds) *Plant Roots: The Hidden Half*. Marcel Dekker, Inc., pp. 521–552. doi: 10.1201/9780203909423.pt6.

Lellei-Kovács, E. *et al.* (2011) 'Thresholds and interactive effects of soil moisture on the temperature response of soil respiration', *European Journal of Soil Biology*, 47(4), pp. 247–255. doi: 10.1016/j.ejsobi.2011.05.004.

Leuzinger, S. and Körner, C. (2007) 'Water savings in mature deciduous forest trees under elevated CO₂', *Global Change Biology*, 13(12), pp. 2498–2508. doi: 10.1111/j.1365-2486.2007.01467.x.

Li, G. C., Mahler, R. L. and Everson, D. O. (1990) 'Effects of plant residues and environmental factors on phosphorus availability in soils', *Communications in Soil Science and Plant Analysis*, 21(5–6), pp. 471–491. doi: 10.1080/00103629009368246.

Liu, J. X. *et al.* (2008) 'CO₂ enrichment increases nutrient leaching from model forest ecosystems in subtropical China', *Biogeosciences Discussions*, 5(3), pp. 2679–2706. Available at: www.biogeosciences.net/5/1783/2008/ (Accessed: 22 April 2020).

Liu, L. and Greaver, T. L. (2009) 'A review of nitrogen enrichment effects on three biogenic GHGs: the CO₂ sink may be largely offset by stimulated N₂O and CH₄ emission', *Ecology Letters*. John Wiley & Sons, Ltd, 12(10), pp. 1103–1117. doi: 10.1111/j.1461-0248.2009.01351.x.

Liu, X. *et al.* (2002) 'Response of soil CO₂ efflux to water manipulation in a tallgrass prairie ecosystem', *Plant and Soil*. Springer, 240(2), pp. 213–223. doi: 10.1023/A:1015744126533.

Lloyd, J. and Taylor, J. A. (1994) 'On the Temperature Dependence of Soil Respiration', *Functional Ecology*. JSTOR, 8(3), p. 315. doi: 10.2307/2389824.

Lovenduski, N. S. and Bonan, G. B. (2017) 'Reducing uncertainty in projections of terrestrial

carbon uptake', *Environmental Research Letters*, 12(4). doi: 10.1088/1748-9326/aa66b8.

Luo, Y. *et al.* (2004) 'Progressive nitrogen limitation of ecosystem responses to rising atmospheric carbon dioxide', *BioScience*, 54, pp. 731–739.

MacDonald, J. A. *et al.* (2002) 'Nitrogen input together with ecosystem nitrogen enrichment predict nitrate leaching from European forests', *Global Change Biology*, 8(10), pp. 1028–1033. doi: 10.1046/j.1365-2486.2002.00532.x.

MacKenzie, R. *et al.* (2021) 'BIFoR FACE: Water-soil-vegetation-atmosphere research in a temperate deciduous forest catchment, including under elevated CO₂', *Hydrological Processes*. doi: 10.22541/au.160157598.86879557.

Maier, M. *et al.* (2010) 'Pore-space CO₂ dynamics in a deep, well-aerated soil', *European Journal of Soil Science*, 61(6), pp. 877–887. doi: 10.1111/j.1365-2389.2010.01287.x.

Manderscheid, R., Erbs, M. and Weigel, H. J. (2014) 'Interactive effects of free-air CO₂ enrichment and drought stress on maize growth', *European Journal of Agronomy*, 52, pp. 11–21. doi: 10.1016/j.eja.2011.12.007.

Marhan, S. *et al.* (2010) 'Indirect effects of soil moisture reverse soil C sequestration responses of a spring wheat agroecosystem to elevated CO₂', *Global Change Biology*, 16(1), pp. 469–483. doi: 10.1111/j.1365-2486.2009.01949.x.

Marhan, S. *et al.* (2011) 'Abundance and activity of nitrate reducers in an arable soil are more affected by temporal variation and soil depth than by elevated atmospheric CO₂', *FEMS Microbiology Ecology*, 76(2), pp. 209–219. doi: 10.1111/j.1574-6941.2011.01048.x.

McKinley, D. C. *et al.* (2009) 'Does deep soil N availability sustain long-term ecosystem responses to elevated CO₂?', *Global Change Biology*, 15(8), pp. 2035–2048. doi: 10.1111/j.1365-2486.2008.01836.x.

Melillo, J. M. *et al.* (2002) 'Soil warming and carbon-cycle feedbacks to the climate system', *Science*. Science, 298(5601), pp. 2173–2176. doi: 10.1126/science.1074153.

Mitra, B. *et al.* (2014) 'Does vegetation structure regulate the spatial structure of soil respiration within a sagebrush steppe ecosystem?', *Journal of Arid Environments*, 103, pp. 1–10. doi: 10.1016/j.jaridenv.2013.12.006.

Mo, W. *et al.* (2005) 'Seasonal and annual variations in soil respiration in a cool-temperate deciduous broad-leaved forest in Japan', *Agricultural and Forest Meteorology*, 134(1–4), pp. 81–94. doi: 10.1016/j.agrformet.2005.08.015.

Moser, G. *et al.* (2018) 'Explaining the doubling of N₂O emissions under elevated CO₂ in the Giessen FACE via in-field 15N tracing', *Global Change Biology*, 24(9), pp. 3897–3910. doi: 10.1111/gcb.14136.

Newton, P. C. D. *et al.* (1996) 'Interaction of soil moisture and elevated CO₂ on the above-ground growth rate, root length density and gas exchange of turves from temperate pasture', *Journal of Experimental Botany*, 47(299), pp. 771–779.

Norby, R. J. (1996) 'Oaks in a high-CO₂ world', *Annales des Sciences Forestieres*, 53, pp. 413–429.

Norby, R. J. and Zak, D. R. (2011) 'Ecological Lessons from Free-Air CO₂ Enrichment (FACE) Experiments', *Annual Review of Ecology, Evolution, and Systematics*, 42(1), pp. 181–203. doi: 10.1146/annurev-ecolsys-102209-144647.

Nygren, C. (2008) *Functional Diversity in Nutrient Acquisition by Ectomycorrhizal Fungi*. Swedish University of Agricultural Sciences.

- Ochoa-Hueso, R., Piñeiro, J. and Power, S. A. (2019) 'Decoupling of nutrient cycles in a *Eucalyptus* woodland under elevated CO₂', *Journal of Ecology*. Edited by H. Chen. Blackwell Publishing Ltd, 107(6), pp. 2532–2540. doi: 10.1111/1365-2745.13219.
- Owensby, C. E., Coyne, P. I. and Auen, L. M. (1993) 'Nitrogen and phosphorus dynamics of a tallgrass prairie ecosystem exposed to elevated carbon dioxide', *Plant, Cell and Environment*, 16(7), pp. 843–850. doi: 10.1111/j.1365-3040.1993.tb00506.x.
- Pan, Y. *et al.* (2011) 'A large and persistent carbon sink in the world's forests', *Science*. doi: 10.1126/science.1201609.
- Paul, K. I. *et al.* (2003) 'Defining the relation between soil water content and net nitrogen mineralization', *European Journal of Soil Science*, 54(1), pp. 39–48. doi: 10.1046/j.1365-2389.2003.00502.x.
- Peichl, M. and Arain, M. A. (2007) 'Allometry and partitioning of above- and belowground tree biomass in an age-sequence of white pine forests', *Forest Ecology and Management*. Elsevier, 253(1–3), pp. 68–80. doi: 10.1016/j.foreco.2007.07.003.
- Phillips, R. P., Brzostek, E. and Midgley, M. G. (2013) 'The mycorrhizal-associated nutrient economy: A new framework for predicting carbon-nutrient couplings in temperate forests', *New Phytologist*, 199(1), pp. 41–51. doi: 10.1111/nph.12221.
- Qi, Y., Xu, M. and Wu, J. (2002) 'Temperature sensitivity of soil respiration and its effects on ecosystem carbon budget: Nonlinearity begets surprises', *Ecological Modelling*, 153. doi: 10.1016/S0304-3800(01)00506-3.
- Quéré, C. *et al.* (2018) 'Global Carbon Budget 2018', *Earth System Science Data*, 10(4), pp. 2141–2194. doi: 10.5194/essd-10-2141-2018.
- Raich, J. and Tufekcioglu, A. (2000) 'Vegetation and Soil Respiration: Correlations and Controls', *Biogeochemistry*, 48(1), pp. 71–90.
- Raich, J. W. and Schlesinger, W. H. (1992) 'The global carbon dioxide flux in soil respiration and its relationship to vegetation and climate', *Tellus*, 44B, pp. 81–99. Available at: <https://onlinelibrary.wiley.com/doi/pdf/10.1034/j.1600-0889.1992.t01-1-00001.x> (Accessed: 6 September 2019).
- Rayment, G. and Lyons, D. J. (2011) *Soil chemical methods: Australasia (Australian soil and land survey handbook series: v.3)*, *Australian soil and land survey handbook series*. CSIRO Publishing.
- Reich, P. B. and Hobbie, S. E. (2013) 'Decade-long soil nitrogen constraint on the CO₂ fertilization of plant biomass', *Nature Climate Change*, 3(3), pp. 278–282. doi: 10.1038/nclimate1694.
- Reich, P. B., Hungate, B. A. and Luo, Y. (2006) 'Carbon-Nitrogen Interactions in Terrestrial Ecosystems in Response to Rising Atmospheric Carbon Dioxide', *Annual Review of Ecology, Evolution, and Systematics*, 37, pp. 611–636. doi: 10.1146/annurev.ecolsys.37.091305.110039.
- Rustad, L. E. *et al.* (2001) 'A meta-analysis of the response of soil respiration, net nitrogen mineralization, and aboveground plant growth to experimental ecosystem warming', *Oecologia*, 126(4), pp. 543–562. doi: 10.1007/s004420000544.
- Rütting, T. and Andresen, L. C. (2015) 'Nitrogen cycle responses to elevated CO₂ depend on ecosystem nutrient status', *Nutr Cycl Agroecosyst*. doi: 10.1007/s10705-015-9683-8.
- Sahrawat, K. L. (2008) 'Factors Affecting Nitrification in Soils', *Communications in Soil Science and Plant Analysis*, 39, pp. 1436–1446. doi: 10.1080/00103620802004235.

Savage, K. E. and Davidson, E. A. (2001) 'Interannual variation of soil respiration in two New England forests', *Global Biogeochemical Cycles*, 15(2), pp. 337–350. doi: 10.1029/1999GB001248.

Scheromm, P., Plassard, C. and Salsac, L. (1990) 'Effect of nitrate and ammonium nutrition on the metabolism of the ectomycorrhizal basidiomycete, *Hebeloma cylindrosporum* Romagn', *New Phytologist*, 114(2), pp. 227–234. doi: 10.1111/j.1469-8137.1990.tb00394.x.

Schimel, J., Balser, T. C. and Wallenstein, M. (2007) 'Microbial stress-response physiology and its implications for ecosystem function', *Ecology*, pp. 1386–1394. doi: 10.1890/06-0219.

Schleppi, P., Körner, C. and Klein, T. (2019) 'Increased Nitrogen Availability in the Soil Under Mature *Picea abies* Trees Exposed to Elevated CO₂ Concentrations', *Frontiers in Forests and Global Change*, 2, p. 59. doi: 10.3389/ffgc.2019.00059.

Schulze, E. D. (1989) 'Air pollution and forest decline in a spruce (*Picea abies*) forest', *Science*, pp. 776–783. doi: 10.1126/science.244.4906.776.

Shaw, M. R. and Harte, J. (2001) 'Response of nitrogen cycling to simulated climate change: Differential responses along a subalpine ecotone', *Global Change Biology*, 7(2), pp. 193–210. doi: 10.1046/j.1365-2486.2001.00390.x.

Siemens, J. *et al.* (2012) 'Elevated air carbon dioxide concentrations increase dissolved carbon leaching from a cropland soil', *Biogeochemistry*, 108(1–3), pp. 135–148. doi: 10.1007/s10533-011-9584-0.

Sierra, J. (1997) 'Temperature and soil moisture dependence of N mineralization in intact soil cores', *Soil Biology and Biochemistry*, 29(9–10), pp. 1557–1563. doi: 10.1016/S0038-0717(96)00288-X.

Singh, J. S., Singh, S. . and Gupta, S. R. (2014) *Ecology, Environmental Science & Conservation*. First. New Delhi: S. Chand Publishing.

Six, J. *et al.* (2004) 'A history of research on the link between (micro)aggregates, soil biota, and soil organic matter dynamics', *Soil and Tillage Research*, 79(1), pp. 7–31. doi: 10.1016/j.still.2004.03.008.

Sousa, W. P. (1984) 'The Role of Disturbance in Natural Communities', *Annual Review of Ecology and Systematics*, 15(1), pp. 353–391. doi: 10.1146/annurev.es.15.110184.002033.

Staddon, P. L., Gregersen, R. and Jakobsen, I. (2004) 'The response of two *Glomus* mycorrhizal fungi and a fine endophyte to elevated atmospheric CO₂, soil warming and drought', *Global Change Biology*, 10(11), pp. 1909–1921. doi: 10.1111/j.1365-2486.2004.00861.x.

Stadler, J., Gebauer, G. and Schulze, E.-D. (1993) 'The Influence of Ammonium on Nitrate Uptake and Assimilation in 2-Year-Old Ash and Oak Trees - A Tracer-Study with 15 N', *Isotopenpraxis Isotopes in Environmental and Health Studies*, 29(1–2), pp. 85–92. doi: 10.1080/10256019308046139.

Stanford, G. and Epstein, E. (1974) 'Nitrogen Mineralization-Water Relations in Soils', *Soil Science Society of America Journal*, 38(1), pp. 103–107. doi: 10.2136/sssaj1974.03615995003800010032x.

Stocker, T. F. *et al.* (2013) 'Technical Summary', in Stocker, T. F. *et al.* (eds) *Climate Change 2013: The Physical Science Basis. Contribution of Working Group I to the Fifth Assessment Report of the Intergovernmental Panel on Climate Change*. Cambridge, United Kingdom and New York, NY, USA: Cambridge University Press.

Team, Rs. (2019) 'RStudio: Integrated Development for R.' Boston, MA: RStudio, Inc.

Turner, M. M. and Henry, H. A. L. (2010) 'Net nitrogen mineralization and leaching in response to warming and nitrogen deposition in a temperate old field: The importance of winter temperature', *Oecologia*, 162(1), pp. 227–236. doi: 10.1007/s00442-009-1435-5.

UNFCCC (2005) *Adoption of the Paris Agreement*.

Unger, S. *et al.* (2010) 'The influence of precipitation pulses on soil respiration - Assessing the " Birch effect" by stable carbon isotopes', *Soil Biology and Biochemistry*, 42(10), pp. 1800–1810. doi: 10.1016/j.soilbio.2010.06.019.

De Vries, F. W. T. P., Brunsting, A. H. M. and Van Laar, H. H. (1974) 'Products, requirements and efficiency of biosynthesis a quantitative approach', *Journal of Theoretical Biology*, 45(2), pp. 339–377. doi: 10.1016/0022-5193(74)90119-2.

Wang, B. *et al.* (2014) 'Soil moisture modifies the response of soil respiration to temperature in a desert shrub ecosystem', *Biogeosciences*, 11, pp. 259–268. doi: 10.5194/bg-11-259-2014.

Wang, C. *et al.* (2006) 'Temperature and soil moisture interactively affected soil net N mineralization in temperate grassland in Northern China', *Soil Biology and Biochemistry*, 38(5), pp. 1101–1110. doi: 10.1016/j.soilbio.2005.09.009.

Wang, X. *et al.* (2015) 'Ectomycorrhizal colonization and growth of the hybrid larch F1 under elevated CO₂ and O₃', *Environmental Pollution*. Elsevier Ltd, 197, pp. 116–126. doi: 10.1016/j.envpol.2014.11.031.

Warner, D. L. *et al.* (2019) 'Spatial Predictions and Associated Uncertainty of Annual Soil Respiration at the Global Scale', *Global Biogeochemical Cycles*, 33(12), pp. 1733–1745. doi: 10.1029/2019GB006264.

Warren, C. R. (2014) 'Response of organic N monomers in a sub-alpine soil to a dry-wet cycle', *Soil Biology and Biochemistry*, 77, pp. 233–242. doi: 10.1016/j.soilbio.2014.06.028.

Wieser, G. and Bahn, M. (2004) 'Seasonal and spatial variation of woody tissue respiration in a *Pinus cembra* tree at the alpine timberline in the central Austrian Alps', *Trees - Structure and Function*, 18(5), pp. 576–580. doi: 10.1007/s00468-004-0341-z.

Williams, M. A. and Xia, K. (2009) 'Characterization of the water soluble soil organic pool following the rewetting of dry soil in a drought-prone tallgrass prairie', *Soil Biology and Biochemistry*, 41(1), pp. 21–28. doi: 10.1016/j.soilbio.2008.08.013.

Wit, C. T. de, Brouwer, R. and Vries, F. W. T. P. de (1970) 'The simulation of photosynthetic systems', in Setlik, I. (ed.) *Prediction and Measurement of Photosynthetic Productivity*. Wageningen, pp. 47–70.

Worsfold, P. J. *et al.* (2005) 'Sampling, sample treatment and quality assurance issues for the determination of phosphorus species in natural waters and soils.', *Talanta*, 66(2), pp. 273–93. doi: 10.1016/j.talanta.2004.09.006.

Xiang, S. R. *et al.* (2008) 'Drying and rewetting effects on C and N mineralization and microbial activity in surface and subsurface California grassland soils', *Soil Biology and Biochemistry*, 40(9), pp. 2281–2289. doi: 10.1016/j.soilbio.2008.05.004.

Xu, L., Baldocchi, D. D. and Tang, J. (2004) 'How soil moisture, rain pulses, and growth alter the response of ecosystem respiration to temperature', *Global Biogeochemical Cycles*, 18(4), p. n/a-n/a. doi: 10.1029/2004GB002281.

Xu, M. and Shang, H. (2016) 'Contribution of soil respiration to the global carbon equation', *Journal of Plant Physiology*, 203, pp. 16–28. doi: 10.1016/j.jplph.2016.08.007.

Yuan, F. *et al.* (2005) 'Characterization of nitrifying bacteria communities of soils from different

ecological regions of China by molecular and conventional methods', *Biology and Fertility of Soils*, 41(1), pp. 22–27. doi: 10.1007/s00374-004-0802-y.

Zaehle, S. *et al.* (2014) 'Evaluation of 11 terrestrial carbon-nitrogen cycle models against observations from two temperate Free-Air CO₂ enrichment studies', *The New phytologist*, 202(3), pp. 803–22. doi: 10.1111/nph.12697.

Zak, D. . *et al.* (2000) 'Atmospheric CO₂ and the composition and function of soil microbial communities', *Ecological Applications*, 10(1), pp. 47–59.

Zak, D. R. *et al.* (2000) 'Elevated atmospheric CO₂, fine roots and the response of soil microorganisms: a review and hypothesis', *New Phytologist*, 147(1), pp. 201–222. doi: 10.1046/j.1469-8137.2000.00687.x.

Zak, D. R. *et al.* (2003) 'Soil nitrogen cycling under elevated CO₂: A synthesis of forest face experiments', *Ecological Applications*, 13(6), pp. 1508–1514. doi: 10.1890/03-5055.

Zhang, C. *et al.* (2014) 'Effects of simulated nitrogen deposition on soil respiration components and their temperature sensitivities in a semiarid grassland', *Soil Biology and Biochemistry*. Elsevier Ltd, 75, pp. 113–123. doi: 10.1016/j.soilbio.2014.04.013.

Zhao, Z. *et al.* (2017) 'Model prediction of biome-specific global soil respiration from 1960 to 2012', *Earth's Future*, 5(7), pp. 715–729. doi: 10.1002/2016EF000480.

Zhu, Z. *et al.* (2016) 'Greening of the Earth and its drivers', *Nature Climate Change*. Nature Publishing Group, 6(8), pp. 791–795. doi: 10.1038/nclimate3004.

3.8 Supplementary material

The data presented in Fig. S3-1 are only during the eCO₂ enrichment period (April – October 2017), to assess both ambient and eCO₂ conditions and exclude the winter period (low T_s and high VWC) in an attempt to isolate each drivers effect. A positive effect of VWC on R_s rates (Fig. 3a) was identified under low VWC levels (<10%) under ambient conditions, followed by a plateau response until ~ 14%. As the VWC levels increased further than those levels, the effect of VWC on R_s was negative. Although it appears as the VWC in higher levels halted R_s, the VWC levels were not that high as to prohibit R_s, thus this response suggests an interaction with T_s. Under eCO₂ conditions, the R_s responses followed the same pattern as in ambient conditions, but the R_s rates were higher. Moreover, the plateau response in the medium VWC levels under ambient conditions was not observed under eCO₂ conditions. Instead, VWC had a positive effect on R_s rates under eCO₂ conditions until ~15% water content followed by negative feedback as the VWC levels increase. Antithetically, the effect of T_s on R_s,

under ambient conditions, was positive across the whole range of T_s during Year 1 (Fig. S3-1b). The R_s response on T_s under eCO_2 conditions was the same as in ambient conditions, but the R_s rates were higher. However, as T_s increased above 15 °C it had a negative effect on R_s rates, suggesting an interaction with VWC.

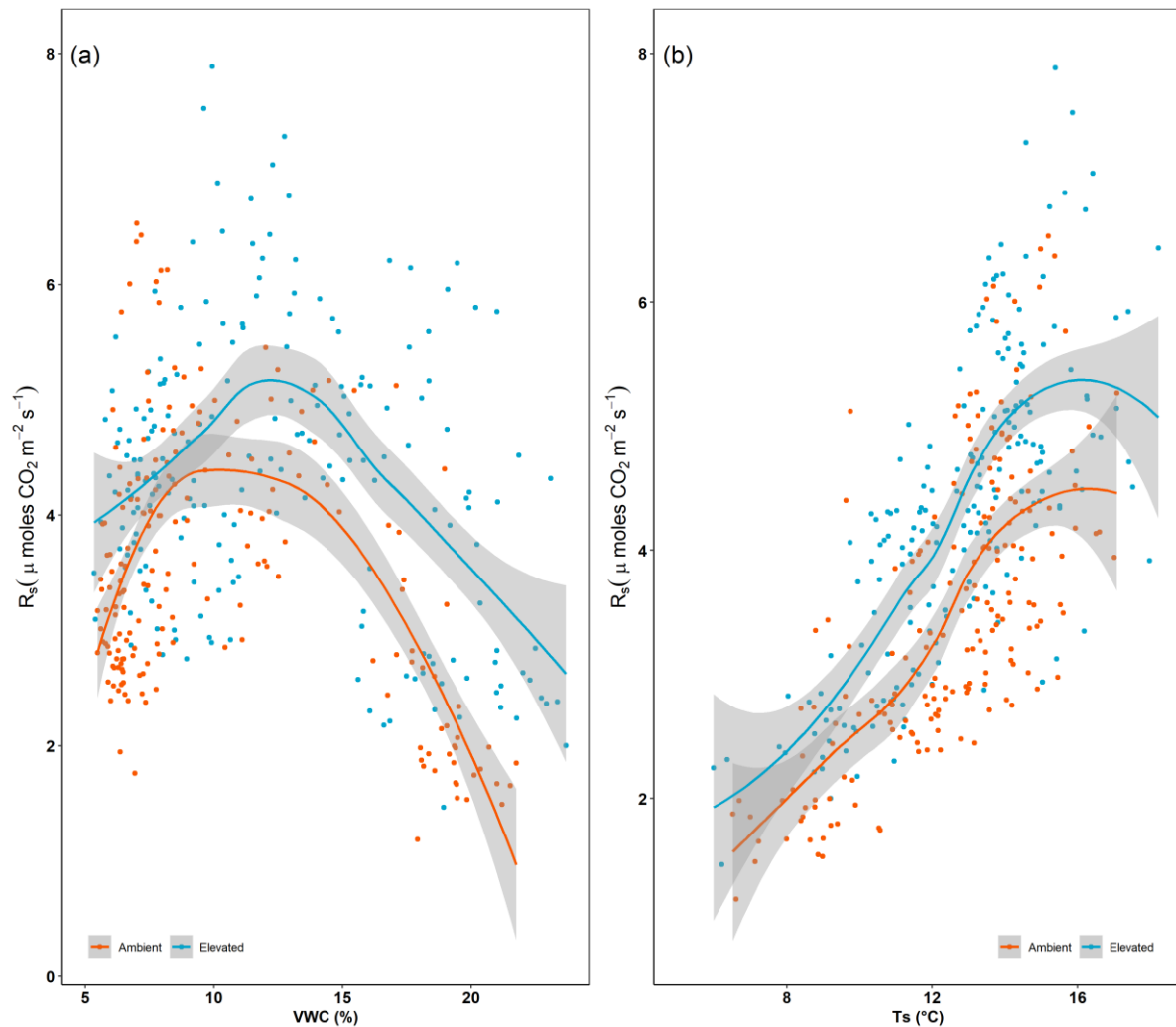


Figure S3- 1: R_s response (LOESS) on VWC (a) and T_s (b) in both eCO_2 and ambient conditions during Year 1. The blue solid points represent the eCO_2 arrays, while the orange solid points represent the ambient arrays.

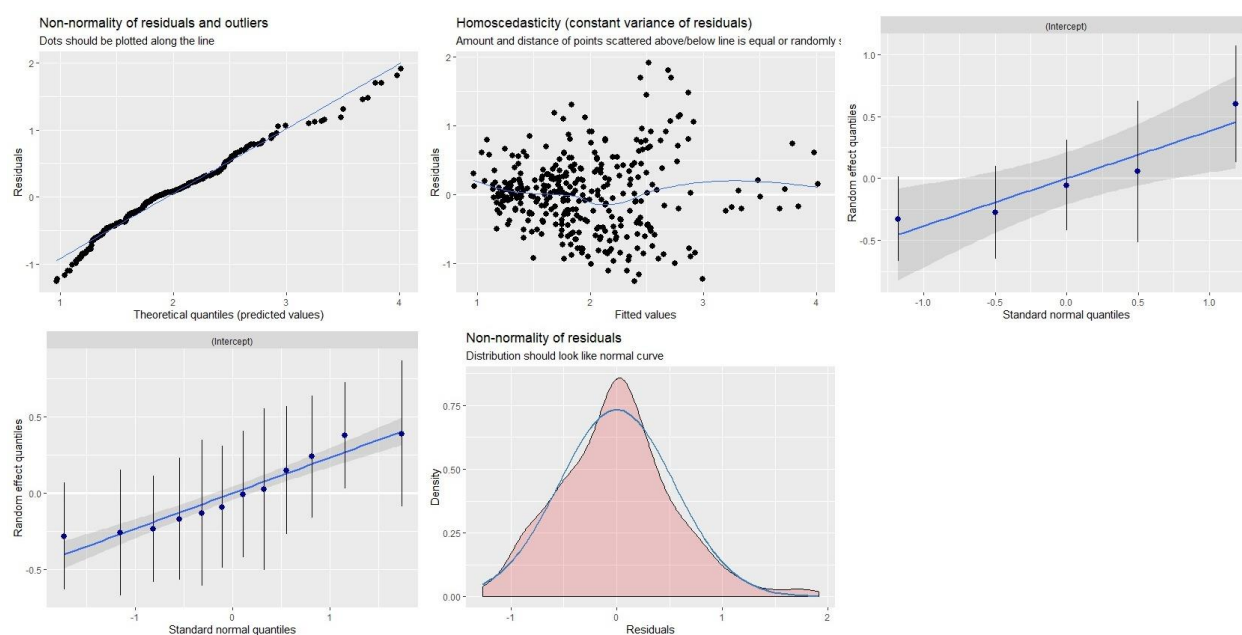


Figure S3- 2: Model validation for estimating soil respiration during Pre-treatment for homoscedasticity, normality of residuals, and outliers and random effects.

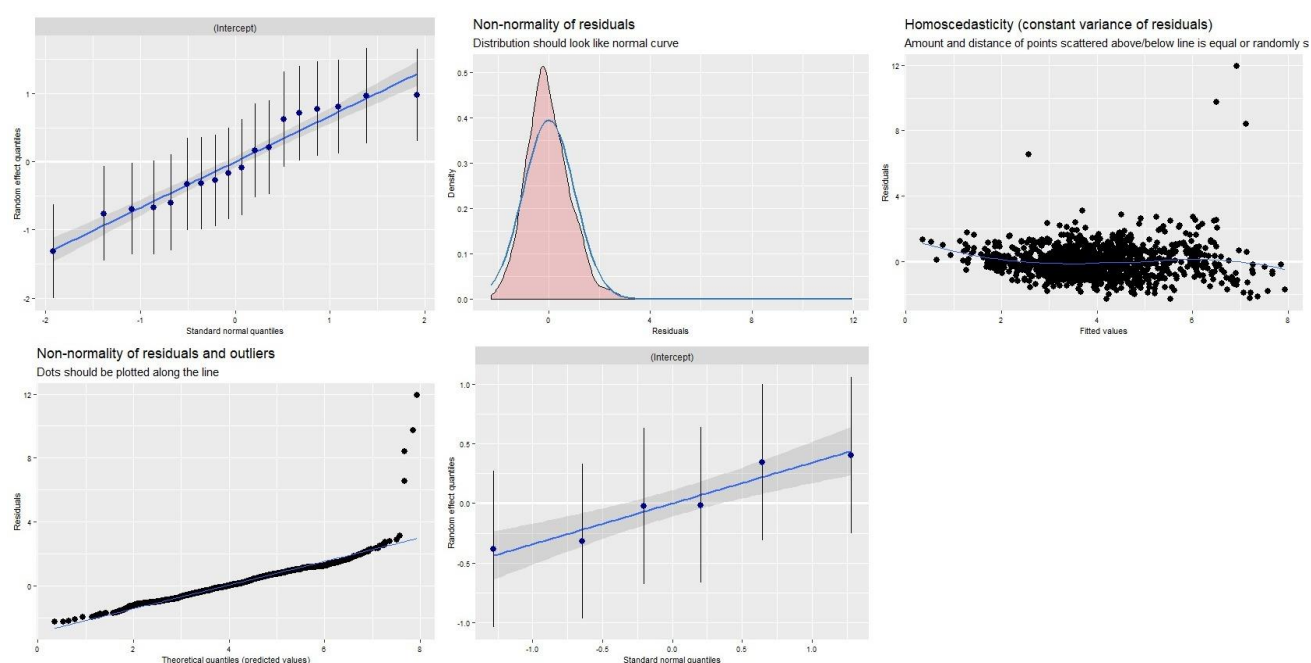


Figure S3- 3: Model validation for estimating soil respiration during Year 1 for homoscedasticity, normality of residuals, and outliers and random effects.

Table S3-1 shows the mean regression coefficients for the best-fitted models for Pre-treatment and Year 1.

Table S3- 1: Fixed effects parameter estimates (coefficients) for the best-fitted model for Pre-treatment and Year 1.

	Estimate	Std. Error	t-value
<i>Pre-treatment</i>			
Intercept	1.15	0.66	1.74
eCO ₂	0.33	0.74	0.45
T _s	0.05	0.07	0.67
eCO ₂ :T _s	0.10	0.07	1.37
<i>Year 1</i>			
Intercept	0.65	0.54	-1.19
eCO ₂	2.86	0.79	3.60
VWC	0.003	0.002	1.55
T _s	0.3525	0.03	11.90
eCO ₂ :VWC	-0.01	0.002	-6.14
eCO ₂ :T _s	-0.18	0.04	-4.14
VWC: T _s	-0.0003	0.0002	-1.79
eCO ₂ * VWC* T _s	0.001	0.0002	5.92

Fig. S3-4 shows the soil bioavailable nutrient and N:P ratios responses to VWC, T_s, and precipitation at BIFoR FACE during Year 1. All three nutrients (NO₃⁻-N, NH₄⁺-N, and PO₄³⁻-P), as well as the N:P ratios, exhibited the same pattern in response to all three environmental variables, under both ambient and eCO₂ conditions. The highest nutrient availability was observed under low VWC, high T_s, and high precipitation, whereas the lowest nutrient availability was observed under high VWC, low T_s, and low precipitation. Moreover, under the same T_s and precipitation, the nutrient availability regardless of the VWC level, suggesting that the main drivers for nutrient availability were T_s and precipitation.

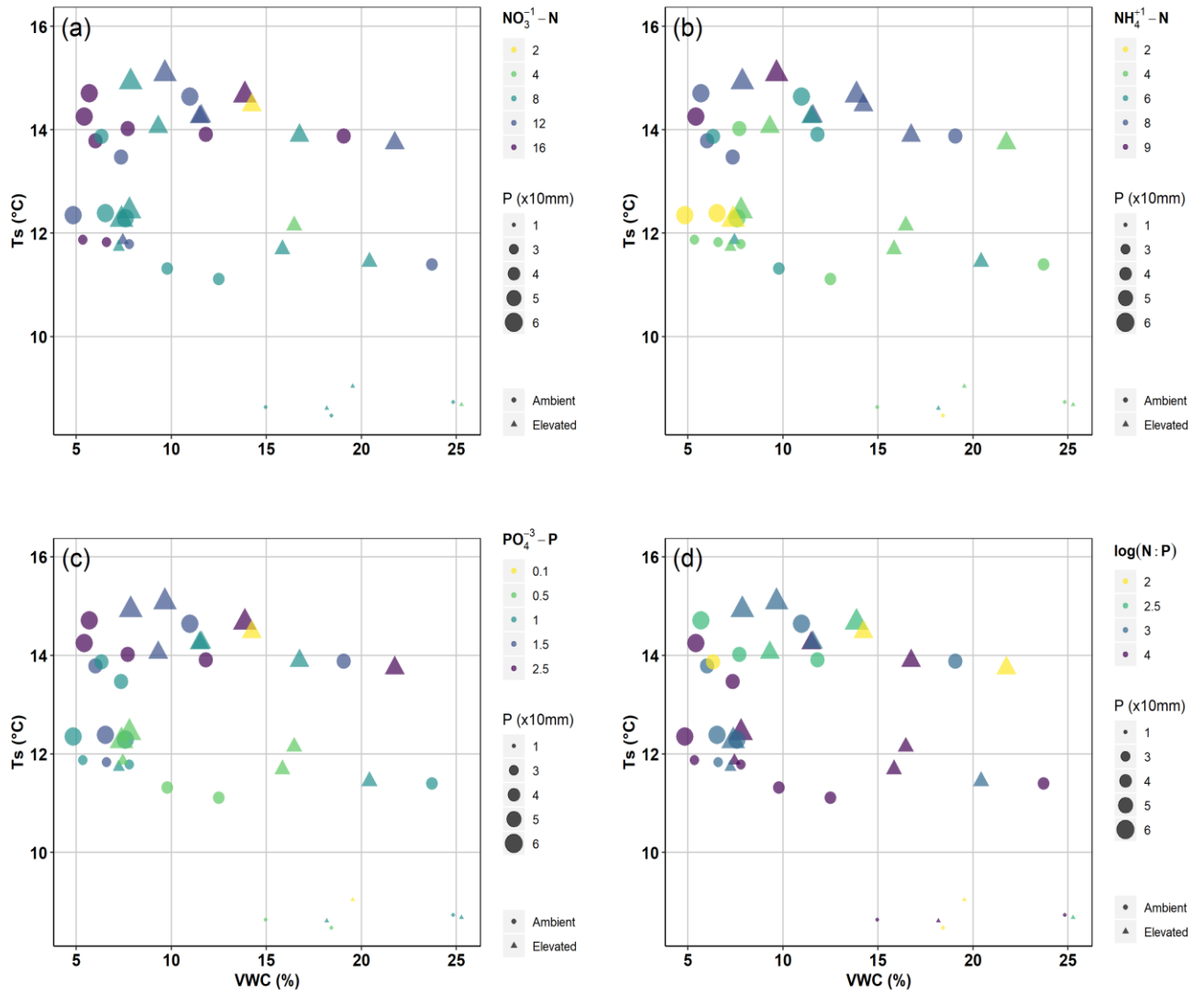


Figure S3- 4: (a) $NO_3^- - N$, (b) $NH_4^+ - N$, (c) $PO_4^{3-} - P$ availability, and (d) N:P ratios in correlation with VWC, T_s , and P at BIFoR FACE during Year 1 of eCO_2 enrichment. The triangles reflect the eCO_2 conditions while the circles reflect the ambient conditions. The colour luminance reflects the monthly cumulative precipitation in *10 mm, which increases as the precipitation increases. The size of the shapes reflects the availability of soil nutrients and N:P ratios, which increase as the availability increases.

Chapter 4: Dominance of extreme events over elevated CO₂: the responses of forest belowground processes in a Free Air CO₂ Enrichment experiment

4.1 Abstract

Elevated CO₂ (eCO₂) and extreme events (such as heatwaves and droughts) are closely associated with climate change, potentially impacting belowground processes such as soil respiration and nutrient cycling. However, the relative importance of the eCO₂ or extreme events remains unknown. Here, we evaluate the impact of extreme events (extreme climatic and biological events) on belowground processes during a Free Air CO₂ Enrichment (FACE) at a mature temperate woodland. The drought had a severe effect on soil respiration, suppressing soil respiration by 47 and 40% in ambient and eCO₂ arrays, respectively, compared with the previous year. eCO₂ dampened the extreme event's impact by increasing soil respiration by ~36% in eCO₂ arrays. A winter moth outbreak led to a short-lived manifold increase in soil nutrient availability during autumn for all three nutrients, with the effect being more prominent under eCO₂.

4.2 Introduction

Anthropogenic emissions of carbon dioxide (CO₂) are the highest ever recorded, with over a twofold increase in the past 170 years (IPCC, 2014a). Concurrently, both the land surface temperature and precipitation are documented to follow ascending patterns over the same period, with the effect being more prominent in the Northern

Hemisphere (IPCC, 2014b). Future projections predict different magnitudes, albeit in agreement, of the continuous increase in atmospheric CO₂ concentration and its relationships with land surface temperature and precipitation to be directly correlated (Collins *et al.*, 2013). Increases in the frequency and/or intensity of extreme weather, climate, and biological events (EE) observed in the recent decades have been linked to the changes mentioned above in the climate (Classen *et al.*, 2005; Easterling *et al.*, 2017). These extreme-event stressors and/or their interactions increase the risks of severe or irreversible impacts on natural ecosystems since they are modifying hydrological systems, altering populations' life cycles and activities, and shifting species migration (IPCC, 2014b). Therefore, EE can dramatically influence the regional C cycle by altering the structure, composition, and functioning of terrestrial ecosystems and possibly shifting a current C sink to a C source (Frank *et al.*, 2015).

However, the rate of atmospheric CO₂ increase is not only conditional on the anthropogenic emissions (UNFCCC, 2005) but also on the ecosystems' efficiency to uptake carbon (C) and store it (Friedlingstein *et al.*, 2006, 2014). Forest ecosystems are immensely significant for the C cycle since it is estimated that $\sim 860 \pm 60$ Pg C are currently being stored in the world's forests (Pan *et al.*, 2011), with the Northern temperate forests being the primary regulators (Schimel, Stephens and Fisher, 2015). Moreover, forests are expected to endure the most significant net effects of climate change on the terrestrial C balance than other ecosystems (Frank *et al.*, 2015). EE and their impact on the global C cycle might enhance the positive climate-C cycle feedbacks (Reichstein *et al.*, 2013); however, increases in EE are predicted to cause significant losses of natural forests due to lagged forest migration (Malcolm *et al.*, 2002), increase in wildfires (Westerling *et al.*, 2006), increases in insect infestations and pathogen-related diseases (Kirilenko and Sedjo, 2007), and increase in forests'

production due to elevated CO₂ (eCO₂) "fertilization effect" (Idso and Kimball, 2001). Nonetheless, the mechanisms and the impacts of EE on the global C cycle are still not well understood due to inherently scarce data availability and the associated high uncertainties in the climate models (Seneviratne *et al.*, 2012).

Soil respiration (R_s), one of the least-studied elements of the terrestrial C cycle, is observed to be enhanced by eCO₂, high soil temperature, and after precipitation events (Birch effect), while is halted by low soil moisture (Orchard and Cook, 1983; Davidson *et al.*, 2000; Pregitzer *et al.*, 2008; Drake *et al.*, 2018). Nonetheless, the magnitude and tenacity of the eCO₂ and environmental variables' effects are highly dependable on the soil nutrient availability (Zak *et al.*, 2000, 2003; Finzi *et al.*, 2002; Hovenden *et al.*, 2008; Lagomarsino *et al.*, 2008). This is of high significance, especially for old-growth forests that might thoroughly have explored and exploited their belowground resources, limiting the possibility of increased C allocation belowground due to an increase in access to limiting nutrients (Körner, 2006). Moreover, nutrient cycles in mature forests are more coupled than young forests (Zaehle *et al.*, 2014), and mature trees have exhibited less flexibility in nutrient use (Körner *et al.*, 2005). Thus, understanding the nutrient mechanisms in mature forest ecosystems' capacity to sequester additional C is of great global concern and requires further investigation.

A series of extreme events happened at BIFoR FACE during the second year of eCO₂ enrichment; Beast from the East with low temperatures and snowfall until late March, a winter moth outbreak in mid-May, followed a six-week heatwave spell that lasted until early August. This is the first time that such a combination of extreme events occurred within a large-scale climate change experiment, thus provided the unique opportunity to study the combined impact of these extreme events *in situ* under eCO₂.

We measured R_s at hourly intervals continuously across the second year of CO₂ enrichment at BIFoR FACE. We collected approximately 40k high-frequency automated measurements, offering precise inspection of the R_s and the relationships with the environmental drivers and the potential interactions with eCO₂. Furthermore, we assessed the availability of ammonium (NH₄⁺-N), nitrate (NO₃⁻-N), and phosphate (PO₄³⁻-P) at monthly intervals over the same period. We also performed three soil sampling campaigns assessing the microbial biomass throughout the second year of CO₂ enrichment.

4.3 Methodology

4.3.1 Site and extreme events description

A detailed description of the experimental site, Birmingham's Institute of Forest Research Free-Air Carbon Dioxide Enrichment (BIFoR FACE) facility, environmental drivers (VWC, T_s and P), R_s , and soil biota available inorganic N and P can be found in Chapter 2 and 3 of the thesis. This Chapter focuses on data collected during the Dormant period (28th October 2017 – 25th March 2018) and Year 2 of eCO₂ enrichment (26th March 2018 – 31st October 2018), unless stated otherwise.

Briefly, BIFoR FACE is a temperate deciduous old-growth (>160 years) oak woodland located within Mill Haft at Staffordshire, England. The soil is brown earth luvisol with a sandy-clay texture and mean soil pH of 4.5 at the top 10 cm. Mean soil total N and P in the top 10 cm are 0.28% and 18 mg P kg⁻¹, respectively, indicating that BIFoR is a low nutrient woodland, and total organic matter content is 3.67%.

A detailed FACE facility description can be found in Hart *et al.* (2019). Briefly, the BIFoR FACE facility comprises six 30 m diameter infrastructure arrays (elevated CO₂

(eCO₂ hereafter), n = 3; controls (*Ambient*, hereafter), n = 3) and three non-infrastructure arrays. Year 1 of eCO₂ enrichment began on 3rd April 2017 until 27th October 2017, while Year 2 began on the 26th March 2018 until 31st October 2018. eCO₂ enrichment took place from budburst to leaf fall approximately, and only during light hours, depending on the solar angle. During the first year of eCO₂ enrichment, eCO₂ arrays were within the 10% of target for 81.6% of the scheduled operation time and 20% of the target within 96.7% of scheduled operation time (Hart *et al.*, 2019). Contamination of the ambient arrays by CO₂ from the eCO₂ arrays was rare and short-lived, with ambient arrays being 10% of the control setpoint 98.8% of the time.

Figure 4-1 shows the schematic diagram of the study period timeline of Chapters 3 and 4 and the extreme events during Year 2 of eCO₂ enrichment at BIFoR FACE. The Pre-treatment period reflects the period before eCO₂ enrichment (19th October 2016 - 2nd April 2017), and Year 1 reflects the period when eCO₂ treatment was switched on (3rd April – 27th October 2017). Dormant reflects the period in-between Year 1 and Year 2 of eCO₂ enrichment (no eCO₂ enrichment during that period; 28th October 2017 – 25th March 2018). Finally, Year 2 reflects the second year of eCO₂ enrichment at BIFoR FACE (26th March 2018 – 31st October 2018).

Environmentally, 2018 was a unique year. The conditions varied greatly throughout the year, with the beginning of it having 0.2°C below the last 30-year average (*Met Office*, 2018). Three cold waves were experienced in a short period (late February until late March 2018); the Anticyclone Hartmut (known as the "Beast from the East"), Storm Emma followed by the mini Beast from the East. All three events were characterised by unusually low temperatures, strong winds, and heavy snowfall (*Beast from the East - Met Office*, 2018). The cold waves were displaced by warmer end of April and May 2018, with temperatures being 1° and 1.7° C above average (*Weather*

review - Spring 2018 | theWeather Club, 2018). Late May/first week of June, BIFoR FACE experienced a winter moth (*Operopthera brumata*) outbreak causing a severe defoliation event. Lastly, the summer of 2018 was the warmest English summer alongside 1976, 2003, and 2006 (*2018 - A Record Breaking Year | theWeather Club*, 2018). From late June until early August 2018, UK experienced a six-week spell with an average temperature of 17.1 °C.

Figure 4-2 shows the air temperature, rainfall, snowfall, and sun hours from the closest to BIFoR FACE weather station (3.2 miles from BIFoR FACE, Gnosall, UK) since 2009 (*Gnosall, Staffordshire, United Kingdom Weather Averages | Monthly Average High and Low Temperature | Average Precipitation and Rainfall days | World Weather Online*, no date). The red box highlights the year 2018 for all the presented parameters. 2018 has the highest average temperature recorded (20 °C) since 2014. The driest month in 2018 was June, with monthly rainfall of 35.07 mm, whereas in all the previous years, the driest conditions were not during the summer season. Moreover, during 2018, the greatest amount of snow recorded since 2011, exceeding 15 cm coverage and the sun hours, remained higher than 200 from May until October 2018.

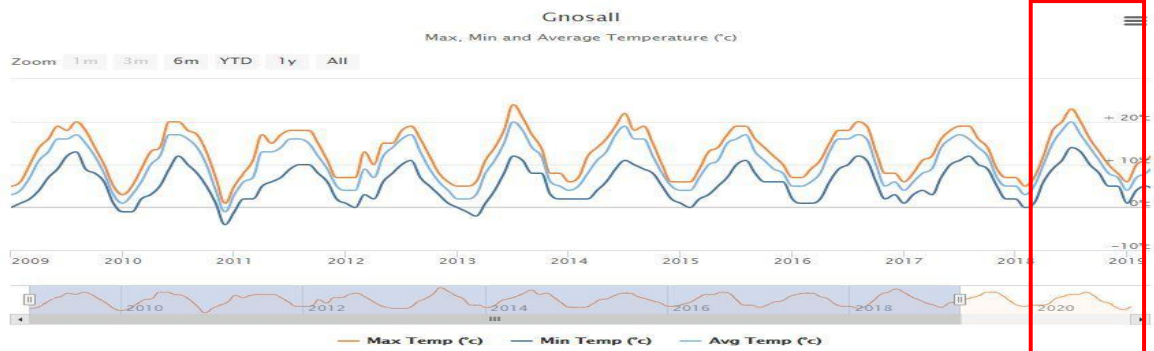
Study period timeline

Important timestamps

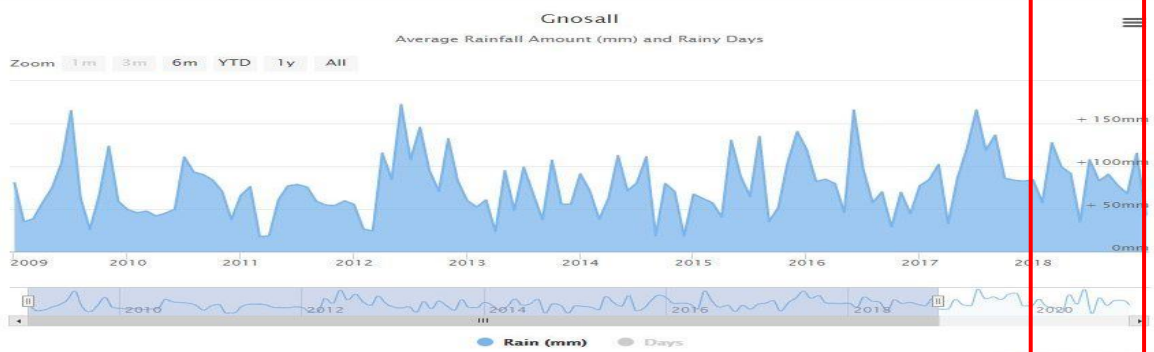


Figure 4- 1: Schematic diagram of the study period timeline (October 2016 – October 2018) and important extreme events.

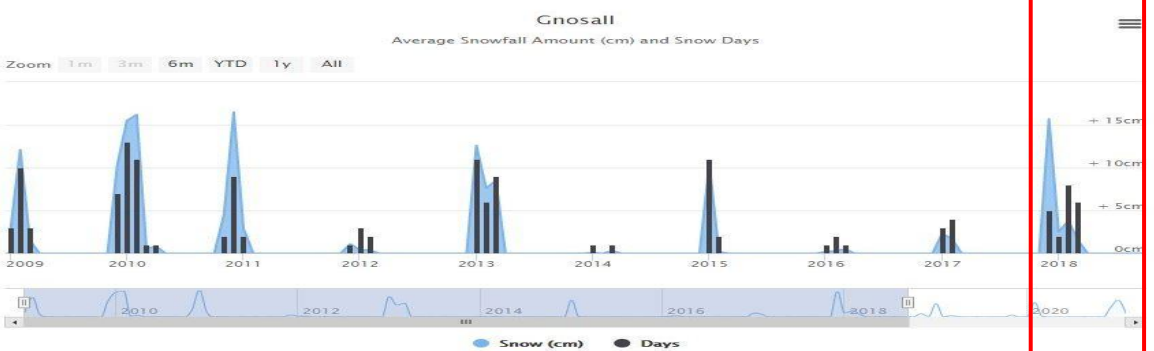
Max, Min and Average Temperature



Rainfall and Rain Days



Snowfall and Snow Days



Sun Hours and Sun Days

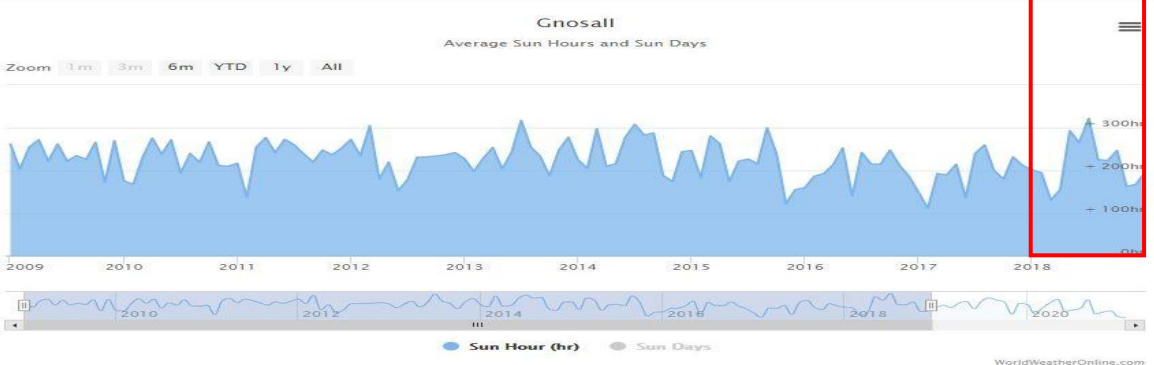


Figure 4- 2: Weather parameters (ait temperature, rainfall, snowfall and snow days, and sun hours) from a weather station 3.2 miles from BIFoR FACE from 2009 until 2018 (Gnosall, Staffordshire, United Kingdom Weather Averages | Monthly Average High and Low Temperature | Average Precipitation and Rainfall days | World Weather Online, no date).

Figure 4-3 shows the canopy greenness index (GCC) from the PhenoCam installed at BIFoR FACE from October 2016 (Pre-treatment) until the end of Year 2 (October 2018). Daily GCC during Year 1 peaked at 0.46; however, during Year 2 reached 0.44, and the decrease was steeper than the one observed the year before.

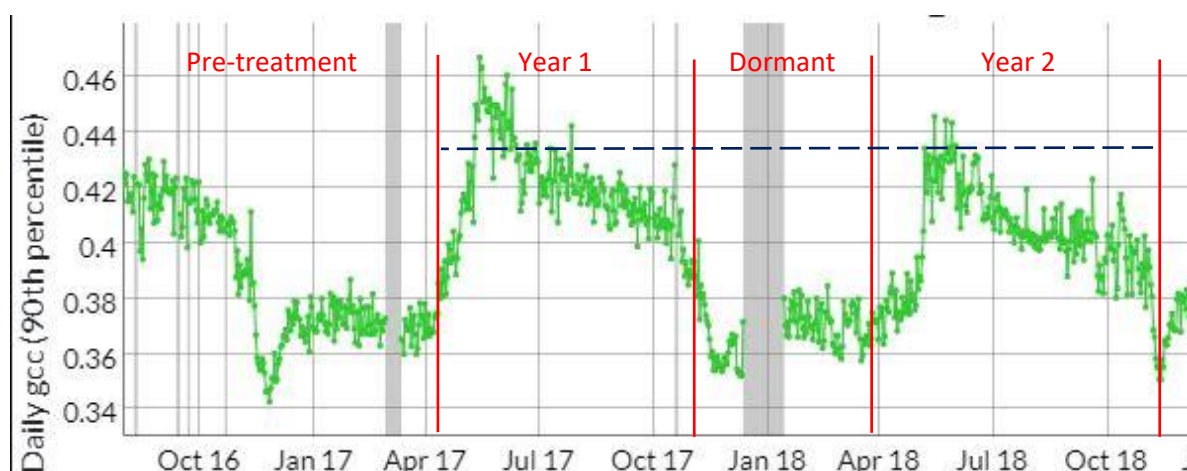


Figure 4- 3: Canopy "greenness index" at BIFoR FACE measured from PhenoCam showing the 90th percentile of the daily green chromatic coordinate (GCC) of the canopy phenology nine months before the eCO₂ switch-on until the end of the second year of eCO₂ enrichment. Data inside the red lines show the first and second years of the eCO₂ enrichment. The dashed line indicated the difference in the GCC between Year 1 and Year 2 of eCO₂ enrichment due to the extreme events. The grey lines indicate gaps in the dataset due to technical failures of the PhenoCam, while the red lines enclose the period of eCO₂ enrichment (<https://phenocam.sr.unh.edu/webcam/sites/millhaft/>)

4.3.2 Measurements

4.3.2.1 R_s

Three surface PVC (Drainage Superstore, CMO Ltd, Plymouth, UK) collars for monitoring the R_s were established within each of the six infrastructure arrays (n = 3, eCO₂ arrays, and n = 3, ambient arrays). The 20-cm-diameter collar was inserted 5 cm into the soil and permitted the measurement of the total R_s. The collars were installed in spring 2016 and left for establishment through the growing season; the soil collars were permanently installed to reduce soil disturbance by repeated

measurements and ensure that the same soil was measured over time (King *et al.*, 2004).

Automated measurements of R_s were taken at 1-hour intervals at all three surface collars in an eCO₂ array and its paired ambient array simultaneously, using 20-cm-diameter long-term chambers interfaced with a multiplexer and an infra-red gas analyser (IRGA) (Li-8100-104 long-term chambers, Li-8150 multiplexer, and Li-8100A IRGA; LI-COR). The observation length was 2 min with 20 s dead-band, a 15 s pre-purge, and a 45 s post purge, giving a total measurement cycle of 3 min 20 s per collar. The measurements began on 19th October 2016 (5 months before the beginning of eCO₂ enrichment), and we report data until 31st October 2018 (end of Year 2 of eCO₂ enrichment). The LI-COR systems were moved every two weeks between replicate paired eCO₂ and ambient arrays, returning to the same array pair on a 4-week rotation.

All data went through quality checks before analysis using SoilFluxPro software, version 4.0.1 (LI-COR, Nebraska, USA). Data points with negative linear fluxes or data points with a linear flux coefficient of variation higher than 3.5 were removed from the dataset, as these were indicative of leaks in the chamber. Data points with a linear flux coefficient of variation between 1.5 and 3.5 were manually checked for assessing the fit quality. Of a total of 43,776 data points during the second year of operation, 27,217 data points were used for analysis. There was a moderate data loss (38%), mostly due to equipment failures (water condensation in the electric plates) and, to a less extent, due to poor-quality fits. Daily and monthly averages of these data are reported in this study in $\mu\text{mol CO}_2 \text{ m}^{-2} \text{ s}^{-1}$.

4.3.2.2 Environmental drivers

Soil volumetric water content (VWC) and soil temperature (T_s) were measured with permanently installed shallow CS655 probes inserted in the top 12 cm soil (Campbell Scientific, Logan, UT, USA). VWC probes were sited one meter from each of the three experimental R_s collars in each array. The VWC data were recorded in 15-min intervals by a data logger in each plot (CR1000, Campbell Scientific) and reported daily.

The temperature sensitivity (Q_{10}) of R_s was calculated using the following equations

$$\ln R_s = kT + C$$

$$Q_{10} = e^{10k}$$

where k is the regression slope of ln-transformed respiration against measured temperature, and C is an empirical constant (Kutsch, Bahn and Heinemeyer, 2010).

4.3.2.3 Bioavailable inorganic N and P

Ion-exchange resin membranes (Membranes International Inc., New Jersey, USA) were used to measure the available inorganic N, as ammonium ($\text{NH}_4^+\text{-N}$) and nitrate ($\text{NO}_3^-\text{-N}$), and P, as phosphate ($\text{PO}_4^{3-}\text{-P}$). Three anion- (AMI 7001; 2 cm x 12 cm) and three cation-exchange (CMI 7000; 2 cm x 12 cm) resin membranes were inserted in the soil at eight locations within each array; three sets of each were located next to the R_s collars, and the other five sets were randomly located within each the array. Resin membranes were deployed in situ for approximately one month before retrieval.

Upon retrieval, resin membranes were washed thoroughly with deionised water to remove any soil particles and then extracted for PO_4^{3-} , NH_4^+ and NO_3^- (modified from Rayment and Lyons (2011) and Bowatte *et al.* (2008), respectively. The three resin membranes from each location were bulked together as one sample, extracted with 0.5 M HCl, shaken at 180 rpm for two hours, and then the resin membranes were removed from the solution and discarded.

Concentrations of NH_4^+ and NO_3^- were analysed by a continuous flow analyser (San++ Continuous Flow Analyser, Skalar, Breda, The Netherlands), and concentrations of PO_4^{3-} were analysed by ultraviolet-visible spectroscopy (Jenway) using the molybdenum blue method (Worsfold *et al.*, 2005). The data presented in this study are reported as monthly averages in $\mu\text{g NH}_4^+\text{-N cm}^{-2} \text{ d}^{-1}$, $\mu\text{g NO}_3^-\text{-N cm}^{-2} \text{ d}^{-1}$, and $\mu\text{g PO}_4^{3-}\text{-P cm}^{-2} \text{ d}^{-1}$, respectively, and the ratios of these.

4.3.2.4 Microbial biomass and inorganic N

Three soil sampling campaigns took place during Year 2 of eCO_2 enrichment, one in spring (6th March 2018), one in summer (9th July 2018), and one in autumn (26th November 2018). For each campaign, one soil core (30 cm long x 55 mm \varnothing) was collected from three soil plots in each of the ambient and eCO_2 arrays (18 cores in total). Each core was subsequently separated into O, A, and B horizons (54 samples).

From each sample, six subsamples were taken; one for determining soil moisture gravimetrically, four for determining microbial biomass C, N, and P, and inorganic $\text{NH}_4^+\text{-N}$ and $\text{NO}_3^-\text{-N}$, and one for DNA analysis (data not shown). For determining the gravimetric volume content, ~5 g of soil were weighted in a tin cup and kept in an oven

for 48 h at 105 °C. After 48 h, the samples were reweighed, and the gravimetric volume content was calculated using the following equation:

$$\text{Gravimetric volume content} = \frac{(\text{wt of wet soil+tare})-(\text{wt of dry soil+tare})}{(\text{wt of dry soil+tare})-\text{tare}}$$

For assessing microbial biomass C, N, and P and inorganic NH_4^+ -N and NO_3^- -N, four subsamples were taken and separated into chloroform fumigated and non-fumigated. For both fumigated and non-fumigated samples, the weights differed by horizon (2 g for O horizon and 5 g for A and B horizons). The chloroform fumigated samples were transferred into glass vials and were placed in a vacuum desiccator with 20 mL of ethanol-free chloroform. The desiccator was evacuated until the chloroform was boiling vigorously, and this process was repeated three times. The desiccator was left in the dark for 48 hours on the fourth evacuation, with the valve closed to prevent chloroform from breaking down. In the meantime, the non-fumigated samples were incubating in the dark next to the vacuum desiccator.

After 48 hours, one set of chloroform fumigated and non-fumigated samples were extracted with 10 mL of 0.5 M K_2SO_4 , syringe filtered, and the filtered extracted was analysed for total organic carbon (TOC) and total organic nitrogen (TON) using Analytik Jena Multi N/C series (Analytik Jena, Jena, Germany). Only the non-fumigated samples were analysed for inorganic NO_3^- -N and NH_4^+ using the same method described previously in the *Biota available (bioavailable) inorganic N and P* section.

The other chloroform fumigated and non-fumigated set of samples was used to analyse $\text{PO}_4^{3-}\text{-P}$. After 48 hours of incubating, an anion-exchange resin membrane (AMI 7001, Membranes International Inc., New Jersey, USA; 2 cm x 4 cm) was added to the sample with 15 mL deionised water and were shaken for 2 hours at 200 rpm. After 2 hours, the samples were kept for further total P analysis (data not shown), while the anion-exchange resin membranes were washed and transferred in new sample tubes. Anion-exchange resin membranes were extracted with 0.5 M HCl and shaken for 24 hours at 180 rpm. After 24 hours, the anion-exchange resin membranes were discarded, while the solution was used to determine the $\text{PO}_4^{3-}\text{-P}$ using the same method as described previously in the *Biota available (bioavailable) inorganic N and P* section.

4.3.3 Statistical analysis

All analyses were carried out using R 3.6.2 and Rstudio 1.2.5033 (RStudio Team, 2019). The mixed-effects models were performed using R package lme4 (Bates *et al.*, 2015), and the coefficient of determination was calculated using the R package MuMIn (Barton, 2014). For all analyses, effects were considered to be strongly significant if the model-reported p-value < 0.05 and marginally significant if p-value < 0.1.

4.3.3.1 Environmental drivers and R_s

Treatment effects were derived directly by comparing the daily means of R_s for eCO₂ and ambient arrays using a one-way ANOVA. The dormant period and Year 2 were assessed separately to establish potential significant differences during switch-on and -off eCO₂ enrichment and significant treatment effects. Interactions between eCO₂

and environmental drivers (VWC and T_s) were evaluated using mixed-effects models. In all mixed-effects models performed, 'array,' 'location within the array,' and 'number of days since the beginning of the experiment' to account for the correlations between repeated measurements within each collar/array were added as random effects. All mixed-effects models performed in this Chapter daily averages of R_s (per collar), VWC, and T_s (per sensor, respectively) were used.

The relationships between R_s and VWC as well as R_s and T_s were linear during the Dormant period. The AIC tool was used to determine which of the models mentioned above was most likely the best model for this dataset. The two models with the lowest AIC score were compared using the ANOVA function to compute the Chi-squares between the two models for investigating the model fit. Finally, the coefficient of determination (R^2) was calculated to assess the variance captured by the model.

Similarly, the same principles as described above were used for investigating the eCO_2 effects during Year 2 of eCO_2 enrichment at BIFoR FACE. eCO_2 , its interaction with VWC and T_s , and the complex interaction between all three variables were used as fixed effects. However, during Year 2, only R_s and T_s ' relationship was linear, whereas R_s and VWC was quadratic. The AIC tool was utilised again to choose the most likely best model amongst the ones mentioned above, while the ANOVA function was used for concluding the best-fitted model.

4.3.3.2 Estimate of annual R_s

Due to the experimental setup (measuring one ambient array and one eCO_2 array for two weeks) and given the seasonal and temporal variability of R_s , a modelled approach was used to calculate the seasonal R_s , utilising the best-fitted models described in

section 4.3.3.1 *Environmental drivers and R_s* . Daily averages of the R_s data were estimated using the best-fitted models for Dormant and Year 2, predicting the R_s of the rest of the arrays at all periods for the whole study period. VWC and T_s from each array aggregated in daily averages were used as predictors. Subsequently, daily averages of observed and predicted R_s values were merged, producing a complete R_s dataset.

4.3.3.3 Soil bioavailable nutrients

For nutrient analysis, the replication unit was the FACE array ($n=3$ for each ambient and eCO_2), and all data were aggregated in monthly timestamps. The effect of eCO_2 only on bioavailable nutrient concentrations was assessed using linear-mixed-effects models, for which 'array' and 'number of days since the beginning of the measurements' were random factors. Data collected before the eCO_2 enrichment were analysed separately to assess potential hereditary eCO_2 differences. Subsequently, linear-mixed-effects models were undertaken with CO_2 and two covariates – T_s and VWC – and their interactions ($eCO_2 \cdot T_s$, $eCO_2 \cdot VWC$, and $eCO_2 \cdot T_s \cdot VWC$) as fixed effects to evaluate the role of soil conditions in responses to elevated CO_2 . In this mixed-effects framework, 'array' and 'number of days since the beginning of the measurements' were used as random factors.

4.3.3.4 Microbial biomass and inorganic N

Similarly, for the soil intensives' analysis, the replication unit was the FACE array ($n=3$ for each of ambient and eCO_2). We utilised the linear-mixed-effects models again to assess the eCO_2 effect on microbial biomass and inorganic N, for which 'array' and

'campaign' were random factors, while 'soil horizon', 'season' and 'eCO₂' were fixed factors.

4.4 Results

4.4.1 R_s response to environmental drivers and eCO₂

R_s exhibited high variability throughout the study period, following seasonal patterns related to VWC, T_s, and precipitation patterns (Fig. 4-4). A detailed description of the Pre-treatment period and Year 1 can be found in Chapter 3. The Dormant period started on 28th October 2017 and lasted until early spring (25th March 2018). During that period, no eCO₂ was introduced in the woodland. The dashed lines on Fig. 4-4 enclose the eCO₂ enrichment period (Year 1 3rd April – 27th October 2017; Year 2 26th March – 31st October 2018). The dotted black rectangle encloses the defoliation event, while the dotted orange rectangle encloses the heatwave event.

R_s increased at the beginning of the growing season (concurring with eCO₂ enrichment) in both ambient and eCO₂ treatments. T_s increased, and VWC decreased, followed by a steep decrease as the VWC decreased from approximately 20 to 10% in mid-May (Fig. 4-4a-c). R_s increased again as VWC and T_s increased during the defoliation event, only to decrease further during the summer when T_s was over 15 °C, VWC dropped below 10%, and there were no Pr events. R_s increased again in the autumn as the VWC started to rise again, and Pr events were more frequent.

Both daily and monthly averages indicated that R_s was frequently higher in the eCO₂ arrays. The greatest differences appeared to be during May and August 2018 (May 1.56 μmol CO₂ m⁻² s⁻¹ in ambient vs. 3.33 μmol CO₂ m⁻² s⁻¹ in eCO₂; August 2.14 μmol CO₂ m⁻² s⁻¹ in ambient vs. 3.60 μmol CO₂ m⁻² s⁻¹ in eCO₂). Precipitation was observed

to lead to a pulse effect on R_s commensurate with an increase in VWC. T_s had a strong and clear seasonal pattern, whereas VWC had a steep decrease lower than 10% for approximately five months (July – October 2018). Pr was sporadic and highly variable, and no Pr events were recorded for around four weeks (Fig. 4-4b, c).

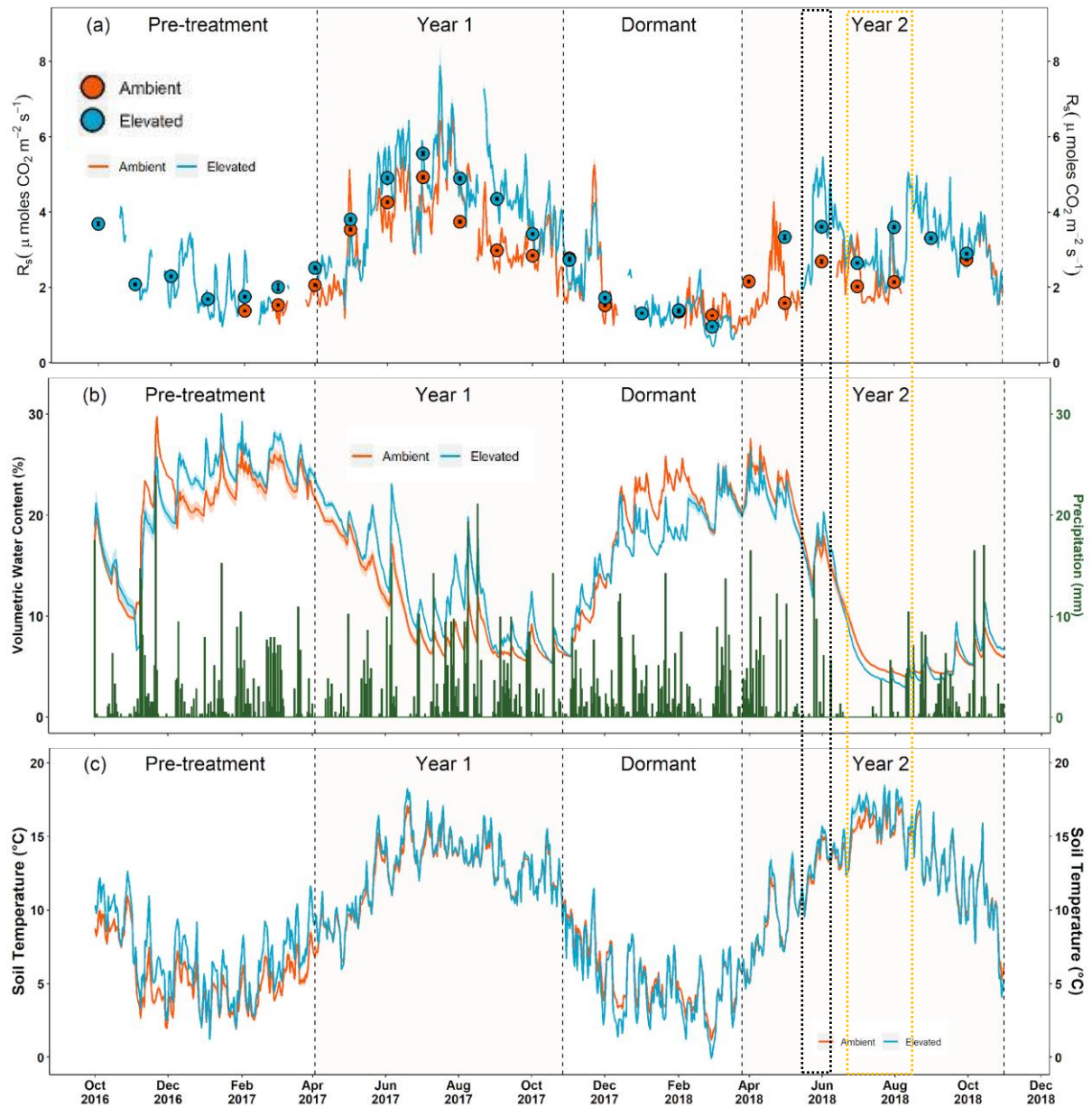


Figure 4- 4: Seasonal course of R_s (a), VWC and precipitation (b), and T_s (c) at BIFoR FACE during the first two years of eCO_2 enrichment (October 2016 – October 2018). The blue coloured lines/solid points denote the eCO_2 arrays, while the orange lines/solid points denote the ambient arrays. The lighter coloured ribbons around the lines and the error bars indicate the se for R_s , VWC, and T_s . All data describe daily averages, except the solid points in (a), which reflect the R_s monthly averages. The vertical dashed lines enclose the period when the eCO_2 enrichment was switched on (Year 1, 3rd April – 27th October 2017 and Year 2, 26th March – 31st October 2018), whereas the periods in between the dashed segments reflect

the Pre-treatment period (19th October 2016 – 2nd April 2017) and the Dormant period (28th October 2017 – 25th March 2018).

Table 4-1 shows the average (mean \pm standard deviation), minimum and maximum VWC, T_s , and R_s during Dormant and Year 2 (2018), and the Q_{10} values both ambient and eCO₂ arrays. Mean VWC, T_s , and R_s were similar between ambient and eCO₂ arrays, with T_s and R_s having a greater range and variability in eCO₂ arrays, whereas VWC had a greater range in ambient arrays. Q_{10} was higher in ambient arrays during Dormant (3.54 in ambient vs. 4.28 in eCO₂ arrays). During Year 2, eCO₂ arrays were drier and warmer, on average, than ambient arrays, while Q_{10} was higher in ambient arrays (1.40 in ambient vs. 1.23 in eCO₂ arrays).

Simple mixed-effects models were used to investigate significant differences in daily VWC, T_s , R_s between ambient and eCO₂ arrays for both Dormant and Year 2. VWC and R_s were statistically similar between ambient and eCO₂ arrays during the Dormant period (p-value 0.71 and 0.84, respectively; Table 4-1), while T_s was marginally significant (p-value 0.05). During Year 2 R_s , there was a statistical difference between ambient and eCO₂ arrays (p-value 0.02), while VWC and T_s were statistically similar (p-value 0.9 and 0.5, respectively).

Table 4- 1: Mean, minimum and maximum VWC, T_s , and R_s for Dormant and Year 2 in ambient and eCO_2 arrays based on daily averages (mean \pm sd), as well as Q_{10} values and p-values from simple mixed-effects models. Significance values are based on the mixed-effects model approach with eCO_2 as the main effect and array, location within an array, and the number of days since the beginning of the measurement as random effects. p-value <0.1 is shown in bold.

Variable	Mean		Minimum		Maximum		p-value
	Ambient	eCO ₂	Ambient	eCO ₂	Ambient	eCO ₂	
Dormant							
VWC	16.66±6.00	17.13±4.62	6.00	6.05	25.10	25.04	0.71
T _s	5.82±2.44	5.13±2.47	1.16	-0.07	11.08	11.46	0.05
R _s	1.8±0.92	1.68±0.83	0.78	0.43	5.24	4.25	0.84
Q ₁₀	3.54	4.28					
Year 2							
VWC	13.12±8.3	7.66±4.59	4.13	3.00	27.57	20.29	0.9
T _s	11.86±3.68	13.62±2.94	5.05	4.09	17.48	18.47	0.5
R _s	2.20±0.74	3.20±0.88	1.01	1.54	4.26	5.46	0.02
Q ₁₀	1.40	1.23					

Fig 4-5 shows a preliminary analysis of R_s to VWC and T_s individually. The data presented in this graph are only during the second eCO_2 enrichment period (Year 2; 26th March – 31st October 2018) to assess both ambient and eCO_2 conditions and exclude the Dormant period (low T_s and high VWC) in an attempt to isolate each drivers effect.

A positive effect of VWC on R_s rates (Fig. 4-5a) was identified under low VWC levels (<10%) under ambient conditions, followed by a plateau response until ~ 14%. As the VWC levels increased further than those levels, the effect of VWC on R_s was negative. Although it appears as the VWC in higher levels had a negative impact on R_s , the VWC levels were not that high as to prohibit R_s . Thus this response suggests an

interaction with T_s . Under eCO_2 conditions, the VWC effect on R_s was positive across the whole range of VWC.

The effect of T_s on R_s , under ambient conditions, was positive until $\sim 13^\circ C$, followed by a negative effect as the T_s increased further (Fig. 4-5b). Similarly, under eCO_2 conditions, T_s had a positive effect on R_s rates until $\sim 15^\circ C$ ($2^\circ C$ more than under ambient conditions), followed by a steeper than under ambient conditions negative effect as T_s increased further.

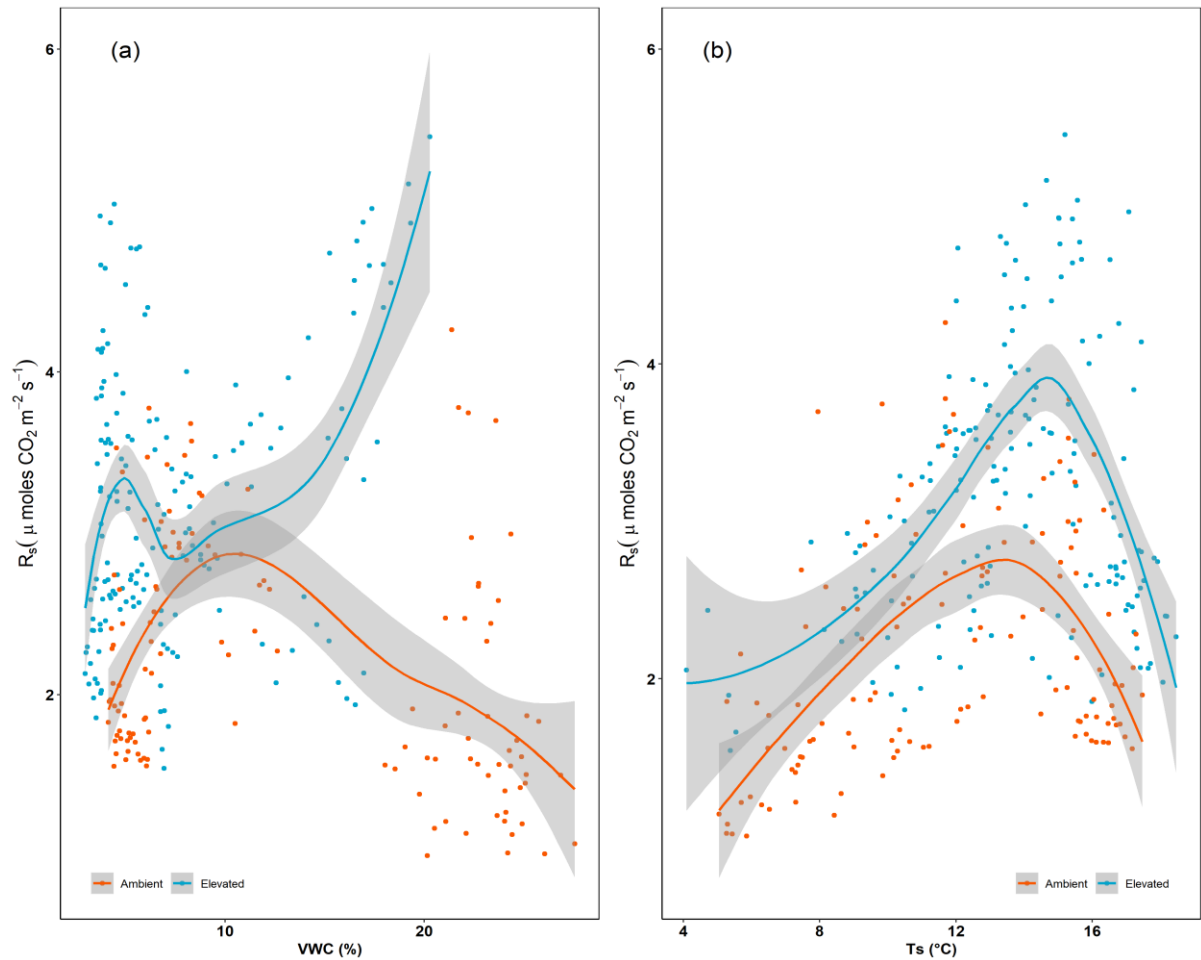


Figure 4-5: R_s response (LOESS) on VWC (a) and T_s (b) in both eCO_2 and ambient conditions during Year 2. The blue solid points represent the eCO_2 arrays, while the orange solid points represent the ambient arrays.

The synergic effects of eCO₂ treatment on R_s with the environmental drivers (VWC and T_s) were also explored using more complex models that incorporated interaction effects. The dual impact of eCO₂ and each environmental driver and their triadic interaction can be found in Table 4-2. During Dormant, eCO₂ had no statistically significant effect on R_s (p-value 0.85) but all interactions (eCO₂*VWC, eCO₂*T_s and eCO₂*VWC*T_s) were statistically significant (p-value 0.07, 0.0001 and 0.005, respectively). The two models with the lowest AIC were the eCO₂*T_s and eCO₂*VWC*T_s; however, the ANOVA function showed that the best-fitted model was the latter explaining 73% of the observed variability on R_s. The model was validated for homoscedasticity, normality, the linearity of residuals, and the random effects' linearity (see section 4.8 Supplementary Material, Figure S4-1).

During Year 2, eCO₂ had a statistically significant effect on R_s (p-value 0.02), while only the eCO₂*VWC and eCO₂*VWC*T_s interactions were statistically significant (p-value <0.001 for both). These two interaction models were also the ones with the lowest AIC and could explain 49 and 60% of R_s' variability. The ANOVA function was used to determine which of the two models was the best fitted; the latter model was the best (p-value < 0.001). Finally, the model was validated for homoscedasticity, normality, the linearity of residuals, and the random effects' linearity (see section 4.8 Supplementary Material, Figure S4-2).

Table 4- 2: Analysis of R_s and its drivers' variance during Dormant and Year 2 at BIFoR FACE. The degrees of freedom for each explanatory variable is 1, p -value < 0.1 is shown in bold.

Predictors	DF _{den}	F-value	p-value	R_c^2	AIC
<i>Dormant</i>					
eCO ₂	4.00	0.04	0.85	0.42	1607.58
eCO ₂ *VWC	579.87	3.16	0.07	0.64	1281.34
eCO ₂ *T _s	578.45	14.88	0.0001	0.70	1025.81
eCO ₂ *VWC*T _s	584.81	7.88	0.005	0.73	1047.75
<i>Year 2</i>					
eCO ₂	4.00	14.73	0.02	0.45	2289.99
eCO ₂ *VWC	855.28	73.04	<0.001	0.49	2288.20
eCO ₂ *T _s	847.8	1.01	0.31	0.49	2293.32
eCO ₂ *VWC*T _s	848.54	61.03	<0.001	0.60	2163.37

Where DF_{den}: denominator's degrees of freedom, F-value: F-test determination, R_c^2 : coefficient of determination, and AIC: Akaike Information tool

Utilising the models' from above, we were able to estimate the R_s by imputing data for the arrays that were not measured each fortnight or periods where no data existed and create a "complete" dataset. Thus, at all times, we have $n=3$ with two arrays being predicted values and the third one being the observed values for ambient and eCO₂ arrays, respectively.

4.4.2 Annual R_s estimates

As mentioned in the section above, the best-fitted models were utilised to predict R_s ' missing values for the studied period. Figure 4-6a and b show the observed R_s values against the predicted R_s values in ambient and eCO₂ arrays during both Dormant and Year 2 of eCO₂ enrichment at BIFoR FACE. Note that in Fig. 4-6a during Year 2, the model cannot capture the temporal variability due to missing data. The observed values are daily averages of one array each fortnight, whereas the predicted values

are daily averages of three arrays for ambient and eCO₂ arrays, respectively. The objective of the model was to "fill the gaps" between R_s measurements with defensible estimates. Observed and predicted R_s were strongly correlated (Fig. 4-6c; $p < 0.001$ for both ambient and eCO₂ arrays; $R = 0.76$ and 0.83 , respectively); the equation's slope was 0.96 and 1 for ambient and eCO₂ arrays, respectively.

R_s' mean annual flux was estimated as the predicted and observed daily averages of R_s data above (Fig. 4-6d). The mean annual R_s at BIFoR FACE during Year 2 in ambient arrays was $713 \pm 15 \text{ g C m}^{-2} \text{ y}^{-1}$ (mean \pm se), while in eCO₂ arrays was approximately 36.5% higher ($973 \pm 19 \text{ C m}^{-2} \text{ y}^{-1}$; mean \pm se).

4.4.3 Bioavailable nutrients

All three soil bioavailable nutrients (NO₃⁻-N, NH₄⁺-N, and PO₄³⁻-P) exhibited strong seasonality (Fig. 4-7a, b, and c), demonstrating a similar seasonal pattern with R_s and VWC (see Fig. 4-4). All three bioavailable nutrients had low availabilities at the beginning of the eCO₂ enrichment (April 2018; NO₃⁻-N 5.6 ± 0.4 in ambient vs. $5.5 \pm 0.6 \text{ } \mu\text{g NO}_3^- \text{-N cm}^{-2} \text{ d}^{-1}$ in eCO₂ arrays; NH₄⁺-N 2.0 ± 0.3 in ambient vs. $3.9 \pm 0.7 \text{ } \mu\text{g NH}_4^+ \text{-N cm}^{-2} \text{ d}^{-1}$ in eCO₂ arrays; PO₄³⁻-P 0.4 ± 0.1 in ambient vs. $0.5 \pm 0.1 \text{ } \mu\text{g PO}_4^{3-} \text{-P cm}^{-2} \text{ d}^{-1}$ in eCO₂ arrays). All three nutrients availabilities increased until June, followed by a dramatic decrease in July 2018 which was more intense in eCO₂ arrays (NO₃⁻-N 4.1 ± 0.5 in ambient vs. $2.2 \pm 0.2 \text{ } \mu\text{g NO}_3^- \text{-N cm}^{-2} \text{ d}^{-1}$ in eCO₂ arrays; NH₄⁺-N 3.9 ± 0.4 in ambient vs. $3.3 \pm 0.3 \text{ } \mu\text{g NH}_4^+ \text{-N cm}^{-2} \text{ d}^{-1}$ in eCO₂ arrays; PO₄³⁻-P 0.33 ± 0.05 in ambient vs. $0.24 \pm 0.03 \text{ } \mu\text{g PO}_4^{3-} \text{-P cm}^{-2} \text{ d}^{-1}$ in eCO₂ arrays). The decrease in ambient arrays was 76, 46, and 79% for NO₃⁻-N, NH₄⁺-N, and PO₄³⁻-P, respectively, whereas in eCO₂ arrays was 80, 60, and 85% for NO₃⁻-N, NH₄⁺-N, and PO₄³⁻-P, respectively. In August and September, all nutrient availabilities increased as VWC and Pr increased. NO₃⁻-N availability increased 7 vs. 14 times in ambient and eCO₂ arrays, respectively, NH₄⁺-

N increased 3 times in both ambient and eCO₂ arrays, while PO₄³⁻-P increased 10 vs. 20 times in ambient and eCO₂ arrays, respectively. Accordingly, N:P ratios decreased as the nutrients' availability increased and vice versa (Fig. 4-7d).

All three nutrients availabilities followed similar patterns in ambient and eCO₂ arrays, and for the majority of Year 2 was challenging to identify clear separations between ambient and eCO₂ arrays. However, the greatest differences for NO₃⁻-N availability were observed in June 2018 (17.5±1.6 in ambient vs. 11.4±0.9 µg NO₃⁻-N cm⁻² d⁻¹ in eCO₂ arrays, respectively), for NH₄⁺-N in September 2018 (NH₄⁺-N 14.5±2.5 in ambient vs. 12.6±2.1 µg NH₄⁺-N cm⁻² d⁻¹ in eCO₂ arrays, respectively), and PO₄³⁻-P was in August 2018 (PO₄³⁻-P 3.1±0.4 in ambient vs. 5.0±0.6 µg PO₄³⁻-P cm⁻² d⁻¹ in eCO₂ arrays).

Table 4-3 shows the averages during Dormant and Year 2 of all three soil bioavailable nutrients and N:P ratios in ambient and eCO₂ arrays. No statistically significant differences were observed in the availability of all three nutrients and N:P ratios during both Dormant and Year 2.

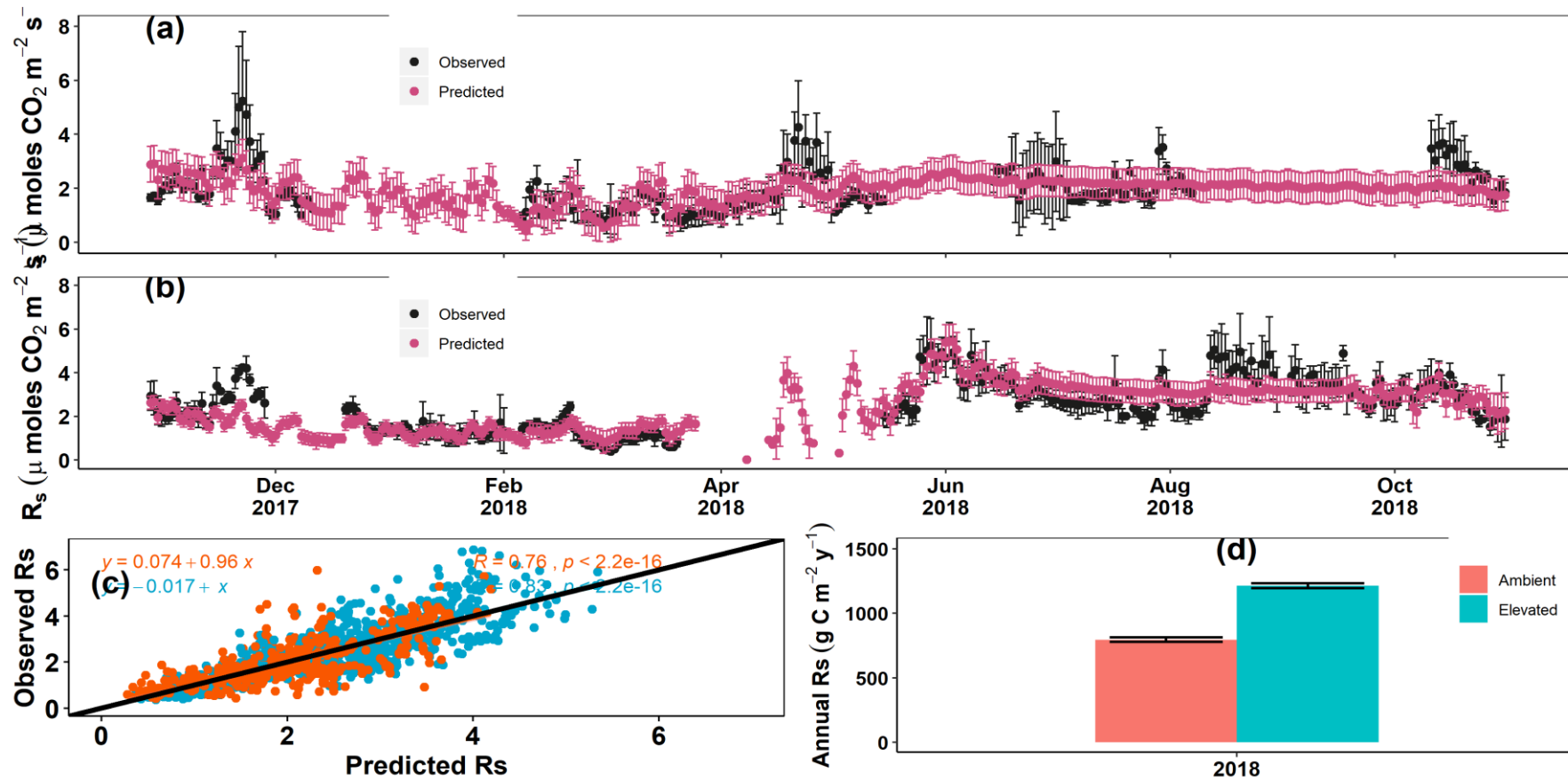


Figure 4- 6: a) Observed and predicted R_s measurements under ambient conditions, b) Observed and predicted R_s measurements under eCO_2 conditions. The black solid points denote the daily-average (mean \pm sd) observed R_s measurements, while the pink solid points denote the predicted R_s values. The dashed lines enclose Year 1 of eCO_2 enrichment. c) Predicted and observed R_s correlation for eCO_2 (blue line) and ambient (orange line) arrays. The blue solid points denote the eCO_2 arrays, while the orange solid points denote the ambient arrays. d) Mean annual R_s in $\text{g C m}^{-2} \text{ y}^{-1}$ in ambient (orange) and eCO_2 (blue) arrays during the second year at BIFoR FACE. The error bars denote the standard error.

Table 4- 3: Soil nutrients availability and N:P ratios during the Dormant and Year 2 at ambient and eCO₂ arrays (mean ± sd), and summary of mixed-effects models of the eCO₂ effect on nutrient availability. All nutrients units are per unit area of membrane in µg cm⁻² d⁻¹ (refer to section 4.3.3.3 Bioavailable nutrients for method). *p*-value < 0.1 is shown in bold.

	eCO ₂ effect				
Variable	Ambient	eCO ₂	DF _{den}	F-value	p-value
<i>Dormant</i>					
NO ₃ ⁻ - N	12.4 ± 9.6	8.9 ± 7.7	20	1.47	0.24
NH ₄ ⁺ - N	2.4 ± 1.6	2.3 ± 1.3	3.93	0.05	0.83
PO ₄ ³⁻ - P	0.7 ± 0.8	0.6 ± 0.9	3.97	0.71	0.45
log(N:P) ratio	3.4 ± 0.9	3.2 ± 1.0	3.93	0.05	0.84
<i>Year 2</i>					
NO ₃ ⁻ - N	17.9 ± 13.0	15.3 ± 12.9	40	0.43	0.52
NH ₄ ⁺ - N	6.3 ± 4.5	6.4 ± 3.4	40	0.004	0.94
PO ₄ ³⁻ - P	1.9 ± 2.0	2.1 ± 2.1	40	0.05	0.82
log(N:P) ratio	2.9 ± 0.5	2.8 ± 0.6	4	0.24	0.65

Where DF_{den}: denominator's degrees of freedom and F-value: F-test determination

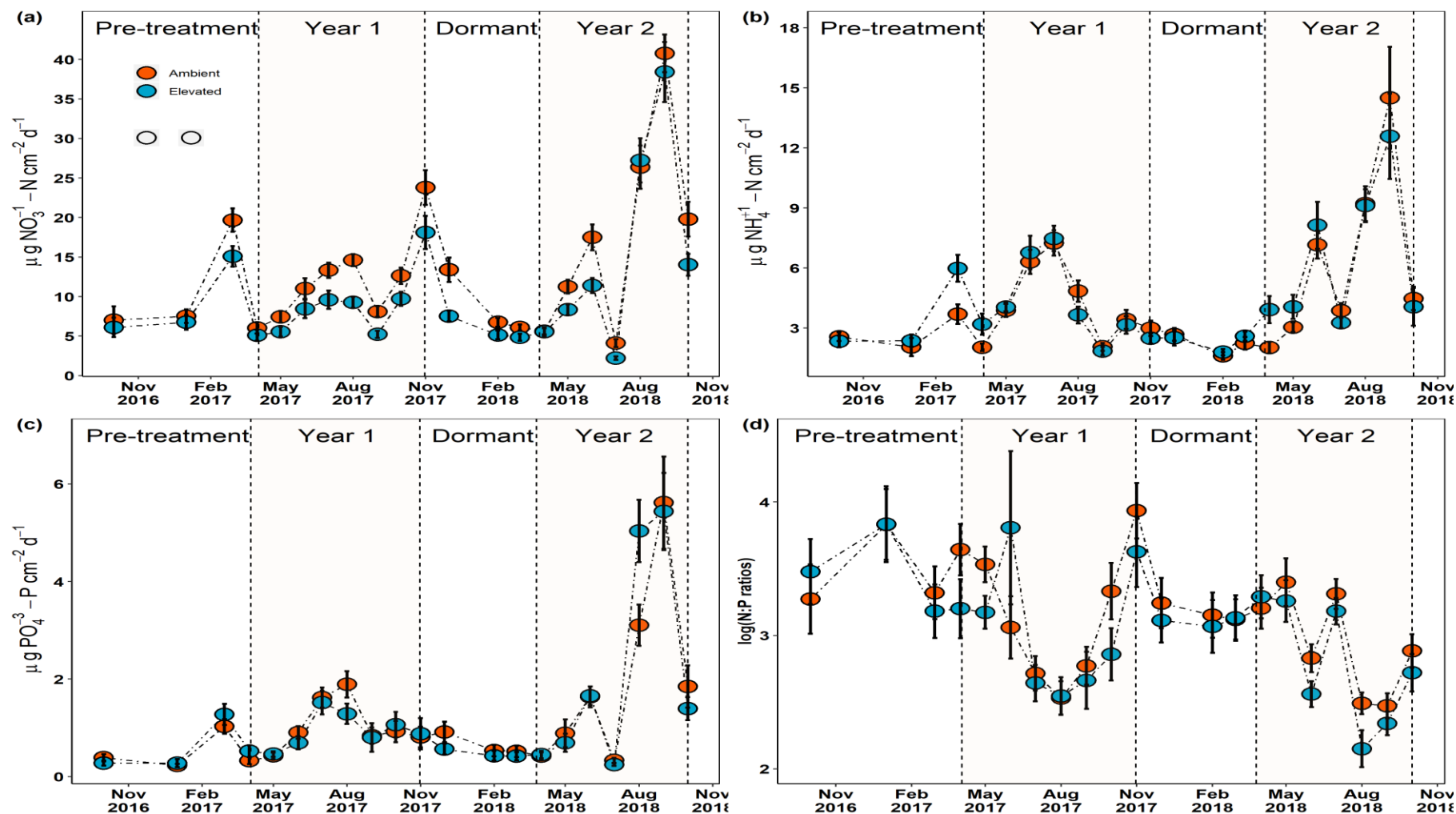


Figure 4- 7: Temporal changes in ion exchange resin membranes (a) $\text{NO}_3^- - \text{N}$, (b) $\text{NH}_4^+ - \text{N}$ and (c) $\text{PO}_4^{3-} - \text{P}$ concentrations, (d) $\log(\text{N:P ratios})$, (mean \pm se, $n = 3$). The orange solid points reflect the nutrient availability in the ambient arrays, whereas the blue solid points reflect the nutrient availability in the eCO₂ arrays. The shaded area denotes eCO₂ treatment (Year 1 and Year 2), whereas the white areas reflect the Pre-treatment and Dormant period (no eCO₂ enrichment)

VWC and Pr had a statistically significant effect on all three bioavailable nutrients (NO_3^- -N, NH_4^+ -N, and PO_4^{3-} -P) as well as the N:P ratio (Table 4-4). eCO_2 , T_s , and the interactions of eCO_2 with the environmental variables (eCO_2 *VWC, eCO_2 * T_s , and eCO_2 *Pr) had no statistically significant effect on neither nutrients availabilities nor on N:P ratios.

Table 4- 4: Summary of mixed-effects models of the eCO_2 , environmental variables, and their interactions with eCO_2 on bioavailable soil nutrients. Fixed factors are eCO_2 , VWC, T_s and their interactions with CO_2 . The degrees of freedom for each explanatory variable are 1. p-value<0.1 shown in bold.

		Predictors						
Response variables		eCO_2	VWC	T_s	Pr	eCO_2 *VW C	eCO_2 * T_s	eCO_2 * Pr
NO_3^- -N	t	-0.66	-2.19	-1.49	2.54	-0.05	0.66	0.30
	Df	40	38	3.8e ¹	38	38	3.8e ¹	38
	p-value	0.52	0.04	0.14	0.02	0.96	0.52	0.76
NH_4^+ -N	t	0.06	-2.74	2.51	1.85	0.88	-0.50	-0.24
	Df	40	37.53	38	38	36.68	38	38
	p-value	0.95	0.01	0.14	0.07	0.38	0.62	0.81
PO_4^{3-} -P	t	0.23	-2.09	-1.03	2.47	-0.35	0.43	0.06
	Df	40	37.64	3.8e ¹	38	36.81	3.8e ¹	38
	p-value	0.82	0.04	0.31	0.02	0.73	0.67	0.95
N:P ratios	t	-0.50	2.35	-0.73	- 1.46	0.09	-0.36	0.42
	Df	4	35.03	34.03	34	34.71	34.08	34
	p-value	0.65	0.03	0.47	0.15	0.93	0.72	0.67

4.4.4 Microbial biomass and inorganic N

Table 4-5 shows the summarised averages (mean±se) of gravimetric volume content, soil extractable NH_4^+ -N and NO_3^- -N, microbial biomass C, N and P, and microbial biomass C:N, C:P and N:P ratios, per soil horizon, from the three soil sampling

campaigns (March, July and November 2018) at BIFoR FACE during Year 2 of eCO₂ enrichment.

Ambient arrays were drier than eCO₂ arrays across all three soil horizons in all three soil campaigns (Table 4-5). Specifically, O horizons were 2-5 times wetter than A and 2-5 times wetter than B horizon in ambient arrays, while O horizons were 3-4 times wetter than A and 4-6 times higher than B horizons in eCO₂ arrays. March and November had comparable moisture values, while July was the driest in both ambient and eCO₂ arrays. Soil extractable NH₄⁺-N availability was higher in eCO₂ arrays for O horizons only (except in July), while for A and B horizons. NH₄⁺-N availability was higher in ambient arrays. Specifically, O horizons had 2-5 times higher NH₄⁺-N than A and 4-6 times than B horizon in ambient arrays, while O horizons had 3-5 times higher NH₄⁺-N than A and 5-6 times higher than B horizons in eCO₂ arrays. July had the highest NH₄⁺-N availability, followed by November and March in both ambient and eCO₂ arrays. Soil extractable NO₃⁻-N availability was higher ambient across all soil horizons in all three soil samplings. Specifically, O horizons had 5-6 times higher NO₃⁻-N than A and 10-18 times than B horizon in ambient arrays, while O horizons had 6-7 times higher NO₃⁻-N than A and 19-36 times higher than B horizons in eCO₂ arrays. November had the highest NO₃⁻-N availability, followed by March, while the lowest NO₃⁻-N availability was observed in July in both ambient and eCO₂ arrays.

Microbial biomass C was higher in eCO₂ arrays in O and B horizons, whereas in A horizons, microbial biomass C was higher in ambient arrays (Table 4-5). Specifically, O horizons had 2-3 times more microbial biomass C than A and 3-13 times more than B horizon in ambient arrays. O horizons were 2-7 times more microbial biomass C than A and 6-11 times more than B horizons in eCO₂ arrays. July had the highest microbial biomass C, while March and November had comparable values in ambient

and eCO₂ arrays. Microbial biomass N had the same pattern as microbial biomass C, where N was higher in eCO₂ arrays in O and B horizons.

In contrast, in A horizons, microbial biomass N was higher in ambient arrays. Specifically, O horizons had 2-4 times more microbial biomass N than A and 2-12 times more than B horizon in ambient arrays. O horizons were 2-10 times more microbial biomass N than A and 3-9 times more than B horizons in eCO₂ arrays. March and November had comparable values; however, July had approximately 4 times higher microbial biomass N in ambient and eCO₂ arrays. Similarly, microbial biomass P was higher in eCO₂ arrays in O and A horizons (except March 2018, where microbial biomass P was higher in ambient arrays in A horizon), while B horizons were similar in ambient and eCO₂ arrays. Note that there is no microbial biomass P data available for July. Specifically, O horizons had 6-7 times more microbial biomass P than A and 9-23 times more than B horizon in ambient arrays. O horizons were 5-17 times more microbial biomass O than A and 15-45 times more than B horizons in eCO₂ arrays. March had higher microbial biomass P than November in both ambient and eCO₂ arrays.

Microbial biomass C:N ratios were lower in the top layer and increased by depth in March and November, whereas in July, the top layer had higher C:N ratios and decreased by depth, with ratios being slightly higher in eCO₂ arrays (Table 4-5). C:N ratios in March and November were comparable, while in July were approximately 2 times lower for O, 7 times lower for A, and 10 and 39 times lower for B horizon in ambient and eCO₂ arrays, respectively. Microbial C:P and N:P ratios increased with depth, with ambient arrays having higher C:P and N:P ratios in O horizons. March had higher C:P and N:P ratios in the top layer, while November had higher ratios at the deeper layers. Note that there is no C:P and N:P data available for July.

eCO₂ had no statistically significant effect on neither microbial biomass nor on inorganic N (see 4.8 Supplementary Material, Table S4-1). O horizons were statistically different from A and B horizons for all variables (gravimetric volume content, soil extractable NH₄⁺-N and NO₃⁻-N, microbial C, N, and P). In contrast, A and B horizons were statistically similar. Moreover, microbial ratios were statistically equivalent across all three soil horizons. Gravimetric volume content, soil extractable NH₄⁺-N, and microbial biomass N were statistically different in March vs. July, while soil extractable NH₄⁺-N, NO₃⁻-N, microbial biomass N, and microbial C:N ratios were statistically different in July vs. November.

Table 4- 5: Summary on concentrations of gravimetric volume content, soil extractable NH_4^+ -N and NO_3^- -N, microbial biomass C, N and P, and microbial biomass C:N, C:P and N:P ratios (mean \pm se) from three soil sampling campaigns (March, July, and November 2018) per horizon under ambient (aCO₂) and eCO₂ conditions, during the Year 2 of eCO₂ enrichment at BIFoR FACE.

	Gravimetric volume content (%)		Soil extractable NH_4^+ -N (µg/g)		Soil extractable NO_3^- -N (µg/g)		Microbial biomass C (µg/g)		Microbial biomass N (µg/g)		Microbial biomass P (µg/g)		Microbial C:N		Microbial C:P		Microbial N:P	
	aCO ₂	eCO ₂	aCO ₂	eCO ₂	aCO ₂	eCO ₂	aCO ₂	eCO ₂	aCO ₂	eCO ₂	aCO ₂	eCO ₂	aCO ₂	eCO ₂	aCO ₂	eCO ₂	aCO ₂	eCO ₂
March 2018																		
O	59.1±9.5	81.6±18.1	6.6±2.1	7.8±1.0	20.0±4.1	18.9±2.3	652.5±61.0	822.5±151.2	197.3±21.4	254.7±58.7	60.2±17.7	85.3±25.3	3.4±0.3	3.5±0.3	77.6±66.0	53.3±34.4	21.5±18.0	14.3±8.6
A	25.5±2.6	21.5±1.2	2.4±0.3	1.8±0.4	4.6±1.1	2.6±0.5	180.6±38.7	115.0±12.3	50.3±13.8	26.6±3.8	10.2±1.8	5.0±1.0	4.0±0.4	4.6±0.4	46.8±26.9	74.1±50.6	13.5±8.1	22.2±17.0
B	16.2±0.5	21.3±4.9	1.9±0.2	1.4±0.2	1.9±0.3	1.0±0.3	92.7±19.8	106.4±31.9	16.5±2.7	29.5±10.9	2.6±0.9	1.9±0.7	5.9±0.9	4.0±0.3	86.9±36.2	219.9±148.9	17.2±7.6	67.0±49.2
July 2018																		
O	21.3±1.7	36.2±2.3	31.2±12.2	22.3±5.1	13.8±0.9	12.0±1.9	1016.8±140.9	1500.8±303.2	850.3±110.3	987.0±201.9	NA	NA	1.3±0.2	2.3±0.8	NA	NA	NA	NA
A	11.7±0.5	12.6±1.4	6.2±0.7	4.9±0.6	2.8±0.6	2.0±0.6	309.9±94.0	284.4±57.4	441.5±38.1	443.9±35.4	NA	NA	0.7±0.2	0.6±0.1	NA	NA	NA	NA
B	9.7±0.5	8.6±0.4	4.8±0.4	3.3±0.4	0.9±0.4	0.4±0.1	76.9±32.0	131.9±12.9	376.3±12.9	288.8±50.9	NA	NA	0.2±0.1	0.6±0.2	NA	NA	NA	NA
November 2018																		
O	47.1±8.4	74.5±14.0	7.5±2.2	12.1±4.5	35.4±8.2	25.7±4.7	630.0±128.5	1092.9±232.4	186.0±24.0	211.2±40.4	22.1±4.8	37.7±6.3	3.3±0.6	5.7±1.1	36.7±8.6	29.6±7.4	11.7±2.9	6.2±1.0
A	15.7±1.5	19.9±3.5	2.6±0.4	2.3±0.4	7.5±1.4	3.9±1.5	336.6±105.3	288.4±69.8	54.8±19.6	48.6±10.6	3.0±0.7	7.0±2.5	7.7±2.1	23.7±17.1	153.5±70.8	263.7±188.4	49.8±24.7	34.1±14.2
B	10.7±13.2	13.2±2.8	1.6±0.3	1.1±0.1	1.9±0.4	0.7±0.3	214.5±49.7	187.6±40.9	14.2±5.8	17.7±4.3	2.4±0.6	2.4±0.6	23.9±6.3	16.6±5.9	493.4±439.5	249.9±169.9	15.6±12.4	40.2±31.2

4.4.5 Year 1 vs. Year 2

A detailed description of the environmental conditions and belowground responses for Year 1 of eCO₂ enrichment can be found in *Chapter 3*. A brief description of the environmental conditions during both years can be found in Table 4-6 for accommodating comparisons. For this comparison, only the data from Year 1 and Year 2 were used, while Pre-treatment and Dormant were excluded, and they are presented as annual averages (\pm se). Year 2 had less Pr than Year 1. Moreover, VWC was higher in ambient arrays in Year 2 but lower in eCO₂ arrays than Year 1, while T_s was lower during Year 2 in ambient and eCO₂ conditions. R_s was lower during Year 2, with the decrease being more prominent in ambient arrays. Lastly, all three bioavailable nutrients had higher availabilities during Year 2, with the increase being more pronounced in eCO₂ arrays, specifically for NO₃⁻-N.

However, eCO₂ had a statistically significant effect on NO₃⁻-N availability in Year 1 (see *Chapter 3*) and R_s in Year 2 (see section 4.4.1 *R_s response to environmental drivers and eCO₂*). Moreover, both VWC and T_s in Year 2 were statistically different than Year 1, and the interactions between eCO₂ and year were statistically significant (see 4.8 Supplementary Material, Table S4-2).

Table 4- 6: Environmental variables, R_s , and bioavailable nutrients (mean \pm se) during the study period summarized in annual averages. As for Year 1 and 2, we denote only the eCO₂ enrichment period (Year 1, 3rd April – 27th October 2017 and Year 2, 26th March – 31st October 2018).

Variables	Year 1		Year 2	
	Ambient	eCO ₂	Ambient	eCO ₂
Pr (mm)	362.4		358.1	
VWC (%)	10.6 \pm 0.3	12.9 \pm 0.4	11.2 \pm 0.5	10.8 \pm 0.5
T _s (°C)	12.4 \pm 0.2	12.7 \pm 0.2	8.1 \pm 0.2	8.5 \pm 0.2
R _s (μ mol CO ₂ m ⁻² y ⁻¹)	3.5 \pm 0.1	4.3 \pm 0.1	2.1 \pm 0.1	3.2 \pm 0.1
NO ₃ ⁻ -N (μ g NO ₃ ⁻ -N cm ⁻² d ⁻¹)	10.5 \pm 1.2	7.6 \pm 0.8	17.9 \pm 4.8	15.3 \pm 4.9
NH ₄ ⁺ -N (μ g NH ₄ ⁺ -N cm ⁻² d ⁻¹)	4.3 \pm 0.8	4.3 \pm 0.8	6.3 \pm 1.7	6.4 \pm 1.3
PO ₄ ³⁻ -P (μ g PO ₄ ³⁻ -P cm ⁻² d ⁻¹)	1.0 \pm 0.2	0.9 \pm 0.2	2.0 \pm 0.7	2.1 \pm 0.8

Fig. 4-8 shows the annual R_s estimates (mean \pm se) for Year 1 and 2 at BIFoR FACE. Year 1 annual R_s was 1,341 \pm 21 g C m⁻² y⁻¹, while in eCO₂ arrays was approximately 21% higher (1,624 \pm 24 g C m⁻² y⁻¹). Year 2, the annual R_s was 714 \pm 15 g C m⁻² y⁻¹, while in eCO₂ arrays was approximately 36.5% higher (973 \pm 19 g C m⁻² y⁻¹). Ambient arrays had a 47% decrease during Year 2, while eCO₂ arrays had a 40% decrease.

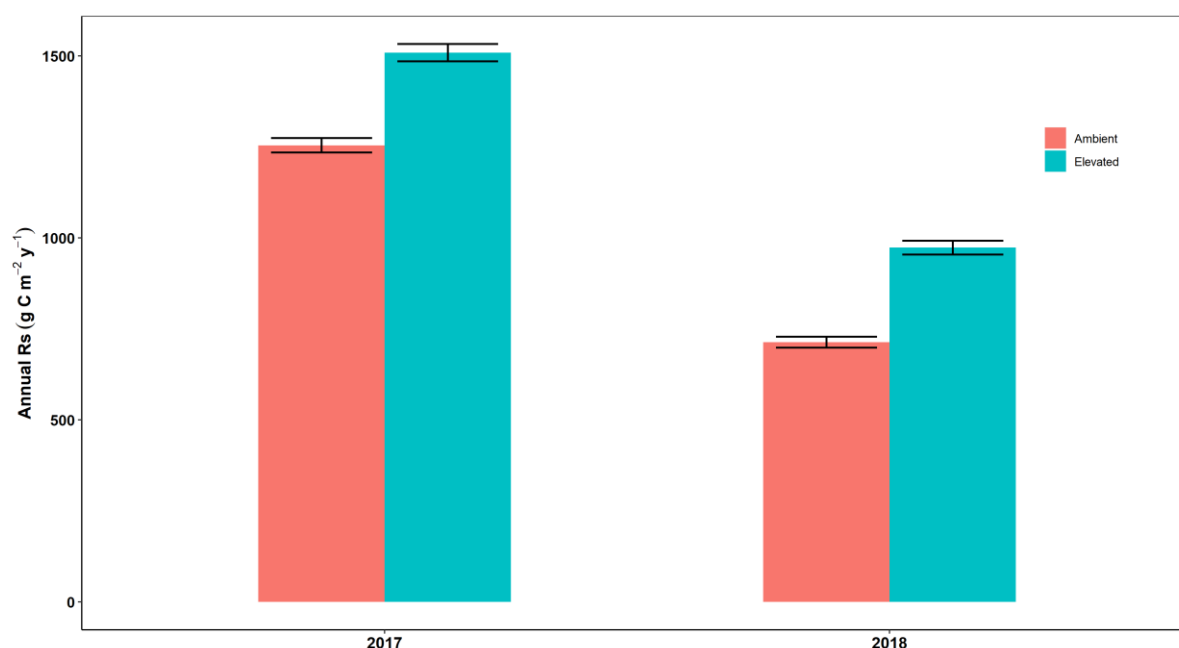


Figure 4- 8: Mean annual R_s in $\text{g C m}^{-2} \text{y}^{-1}$ in ambient (orange) and eCO_2 (blue) arrays during the first two years at BIFoR FACE. The error bars denote the standard error.

4.5 Discussion

Soils at BIFoR FACE exhibited strong seasonal patterns in soil moisture, temperature, and respiration during the second year of eCO_2 enrichment (Fig. 4-4). Year 2 of eCO_2 enrichment coincided with a series of extreme events (Beast from the East, winter moth defoliation event, 6-week heatwave), having a great impact on belowground responses at BIFoR FACE. eCO_2 had a statistically significant effect on soil respiration during Year 2 of eCO_2 enrichment (Table 4-1, p -value = 0.02), increasing by approximately 37% soil respiration on annual averages. However, no statistically significant differences were observed on bioavailable soil nutrients or microbial biomass (Table 4-3 and Table S4-1). eCO_2 had no statistically significant effect on any of the bioavailable nutrients; however, all three nutrients responded differently under eCO_2 . NO_3^- -N decreased by 15% under eCO_2 , PO_4^{3-} -P increased by 5% under eCO_2 ,

while $\text{NH}_4^+\text{-N}$ had no difference between ambient and eCO_2 arrays on annual averages.

4.5.1 Soil respiration and environmental drivers

The annual estimates of soil respiration during the first year of eCO_2 enrichment were 714 ± 15 vs. 973 ± 19 $\text{g C m}^{-2} \text{ y}^{-1}$ in ambient and eCO_2 arrays. These estimates are within the range of observations ($500\text{-}2,100$ $\text{g C m}^{-2} \text{ y}^{-1}$) reported for similar temperate forests (Campbell and Law, 2005) under non-extreme events conditions. Our estimates show that eCO_2 could mitigate the extreme event's impact on an annual average and agree with studies that have monitored soil respiration responses under synthetic drought and heatwave conditions (Roy *et al.*, 2016).

The models used for the soil respiration estimates were the triple interaction between eCO_2 , soil temperature, and moisture for both Dormant and Year 2. Both models predicted 73 and 60% of the variability (Table 4-2). Our modelling estimates are defensible since the correlation between predicted and observed soil respiration values was statistically significant in ambient and eCO_2 arrays. Both models chosen did not have the lowest AIC, but they had the highest R_c^2 . Although our analysis indicates that the primary driver during the second year of eCO_2 enrichment was soil moisture, our analysis highlights the importance of soil temperature (Fig. 4-4, Table 4-2). When soil temperature was included in our mixed-model analysis, the model's predictive capability increased by 11% (49 vs. 60% predictive capacity, respectively). Moreover, this analysis's objective was to utilise the models with the greatest predictive capacity rather than parsimony to acquire robust estimates. Thus, for this study's objectives, the models chosen for imputing missing data for soil respiration,

although they were not of the highest parsimony, offered the best possible goodness of fit (Glen, 2015).

Soil moisture had very distinctive effects on soil respiration in ambient and eCO₂ arrays (Fig. 4-5a). As the soil water content increases in ambient arrays, soil moisture becomes a limiting factor for soil respiration. However, in eCO₂ arrays, soil moisture was observed to affect Rs across the entire soil moisture range positively. Moreover, soil temperature was a limiting factor for soil respiration in levels higher than 13 and 14 °C in ambient and eCO₂ arrays, respectively, with the effect being sharper in eCO₂ arrays (Fig. 4-5b). However, in the highest soil temperature ranges, soil moisture levels also contribute to the soil respiration response and vice versa; in the highest soil moisture levels, the soil temperature also contributes to the observed response. Thus, although investigating soil responses to environmental factors individually might provide a more straightforward approach, *in situ*, the environmental factors interact in a more complex and dynamic way with soil respiration.

It is generally observed that during drought periods, soil respiration is decreased (Goulden *et al.*, 1996; Fierer and Schimel, 2002; Harper *et al.*, 2005; Borken *et al.*, 2006; Garten, Classen and Norby, 2009; Muhr and Borken, 2009; Bloor and Bardgett, 2012; Selsted *et al.*, 2012; Balogh *et al.*, 2016; Sun, Lei and Chang, 2019; Bréchet *et al.*, 2019; Ficken and Warren, 2019) due to reduced photosynthesis (Högberg *et al.*, 2001; Ruehr *et al.*, 2009; Van der Molen *et al.*, 2011), reduced C transfer from plants to soil bacteria (Zak *et al.*, 1994; Fuchslueger *et al.*, 2014) and fungi (Talbot, Allison, and Treseder, 2008), and reduced microbial and mycorrhizal exoenzyme production (Kuzyakov and Domanski, 2000; Schimel and Weintraub, 2003; Wieder, Bonan and Allison, 2013). Moreover, drought can decrease soil respiration due to soil water deficit (Orchard and Cook, 1983; Skopp, Jawson and Doran, 1990; Howard and Howard,

1993; Jassal *et al.*, 2008; Manzoni, Schimel and Porporato, 2012) or by altering the soil respiration's sensitivity to soil temperature and uncouple soil moisture, temperature, and respiration by reduction of soluble C substrate, extracellular enzyme activities and microbial processes (Selsted *et al.*, 2012; Wang *et al.*, 2014).

Seasonal temperature sensitivity Q_{10} was 1.40 in ambient vs. 1.23 in eCO₂ arrays during Year 2 at BIFoR FACE, which is lower than other forests experiencing dry conditions varying from 1.9-4.8 (Rey *et al.*, 2002; Janssens and Pilegaard, 2003; Curiel Yuste *et al.*, 2004; Borken *et al.*, 2006; Davidson, Janssens and Lou, 2006). This indicates that soil respiration in ambient arrays was more sensitive to soil temperature than in eCO₂ arrays. The low Q_{10} values observed during Year 2 of eCO₂ enrichment do not necessarily represent the temperature sensitivity differences. When Q_{10} is calculated as an annual/seasonal value, it is influenced strongly by the magnitude of the soil respirations seasonal changes (Curiel Yuste *et al.*, 2004). Moreover, under severe drought stress, the soil temperature is not a reliable soil respiration predictor; thus, Q_{10} calculations are challenging (Moncrieff and Fang, 1999). Lastly, annual/seasonal Q_{10} values do not only represent the changes in soil temperature but also changes in other seasonally oscillating variables and processes, such as soil moisture, litter inputs, microbial populations, and root biomass (Curiel Yuste *et al.*, 2004).

Previous FACE experiments in forest ecosystems have observed different magnitudes of increase (Duke: 17.4%; FACTS-I: 39.2%, FACTS-II: 49.4% for *P. tremuloides* and 59.5% for *Betula/Populus*; POPFACE: 46.7% for *P. eur*, 42.3% for *P. alba* and 34.2% for *P. nigra*, ORNL: 11.2%) in soil respiration rates during their second year of eCO₂ enrichment (King *et al.*, 2004; Bernhardt *et al.*, 2006). One needs to bear in mind two crucial points when comparing the eCO₂ induced increase observed in other FACE

experiments in the past. Firstly, all these forest ecosystems were either plantations or young forests on disturbed soils. Secondly, none of those experiments experienced various extreme events as BIFoR FACE during their second year of operation. EucFACE is the only FACE experiment conducted in mature woodland, and during their second year of eCO₂ enrichment, they observed a 9% increase in soil respiration rates (Drake *et al.*, 2018). Secondly, none of these experiments experienced such an ecosystemic perturbation during their second year of operation as BIFoR FACE.

Although the Beast from the East event technically happened before the switch-on of eCO₂ enrichment during the second year of eCO₂ enrichment at BIFoR FACE, we cannot exclude the biological importance of such an event on an ecosystemic level. The low temperatures and snowfall lasted until late March 2018, and the eCO₂ switch-on date was on 26th March. The freezing-thawing of soil leads to pulses of soil respiration (Goulden *et al.*, 1998; Larsen, Jonasson and Michelsen, 2002; Schimel, Bilbrough and Welker, 2004; Kurganova, Teepe and Lofffield, 2007) by making available decomposable organic C via microbial death (Herrmann and Witter, 2002) and thus, nutrient release. Moreover, upon thawing, organic material damaged due to frost becomes available for decomposition (Priemé and Christensen, 2001).

Another critical aspect to consider is that the Beast from the East might have triggered the moth infestation outbreak. Oak budburst was on 20th April, and the first leaf was on 25th April (approximately 20 days later than 2017). Winter moth (*Operophtera brumata*) egg hatching and the synchronised relationship with oak bud burst has been well documented (Feeny, 1970; Dongen *et al.*, 1997). The egg hatching is predominantly triggered by abiotic cues (temperature). However, for the past 30 years, a clear mistiming has been recorded between winter moth egg hatching and budburst due to changes in the weather pattern rather than increases in spring temperatures

(Visser and Holleman, 2001). Moreover, such changes in temperature patterns create asynchrony in multiple levels of the trophic chain (Visser *et al.*, 1998; Stevenson and Bryant, 2000) that can also affect the predators of winter moths, such as great tits (*Parus major*). Thus, Beast from East might have caused a delay in winter moth and great tits reproduction cycles, triggering the defoliation event.

Defoliation events have been observed to strongly increase soil respiration due to as a result of labile organic C and N inputs in the soil through frass, leaf input, and insect cadavers, which in turn increases available substrate for microbial decomposition (Lovett and Ruesink, 1995; Christenson *et al.*, 2002; Hillstrom *et al.*, 2010; I-M-Arnold *et al.*, 2016; Grüning *et al.*, 2018). However, when the defoliation events coincide or are succeeded by dry conditions, microbial decomposition can be inhibited (Jung and Lunderstadt, 2000). Moreover, eCO₂ has been observed to alter plants' chemical composition by increasing the tannin concentrations and the C/N ratios in leaves, thus reducing the leaf litter quality (Kopper and Lindroth, 2003). Accordingly, altered leaf chemical composition will alter frass composition (Madritch, Donaldson and Lindroth, 2007). That could have a severe impact on belowground processes since condensed tannins can reduce nutrient availability, decomposition rates and alter soil respiration (Parsons, Lindroth and Bockheim, 2004; Madritch, Jordan and Lindroth, 2007; Parsons, Bockheim and Lindroth, 2008; Schweitzer *et al.*, 2008).

Studying one extreme event individually on an ecosystemic level is challenging due to the lack of warning before an event and experimental data, let alone three extreme events with intertwined time barriers. Therefore, we suggest that the overall decreased soil respiration response during Year 2 was driven by the combination of extreme events, with eCO₂ dampening the extreme events' effect.

4.5.2 Bioavailable inorganic N and P

eCO₂ had no statistically significant effect on soil biota available nutrients during Year 2 of eCO₂ enrichment at BIFoR FACE. All three soil bioavailable nutrients (NH₄⁺, NO₃⁻ and PO₄³⁻) followed the same seasonal pattern; the availability of soil nutrients increased during spring/early summer, with a steep decrease in mid-summer, followed by a five- and eightfold (NH₄⁺, PO₄³⁻ and NO₃⁻, respectively) increase during autumn. Soil moisture and precipitation were found to have a statistically significant effect on soil nutrient availability, whereas soil temperature had no statistically significant effect.

Drought has been observed to slow plant growth by reducing N and P uptake, transport, and redistribution (Rouphael *et al.*, 2012), limiting ion mobility in the soil and microbial activity (Kreuzwieser and Gessler, 2010; Cregger *et al.*, 2014). Moreover, limited N and P mineralisation and inorganic N fluxes have been associated with drought events (Sardans and Peñuelas, 2004; Borken and Matzner, 2009). Although there was a substantial decrease in bioavailable nutrients in the middle of the season, we cannot claim that this observation accurately reflects the actual availability since ion exchange membranes require good contact with the soil to transfer from soil water successfully. Under such low soil moisture conditions, it is possible that the necessary soil-membrane contact was not achieved.

Following the drought event, all three soil nutrients' availability increased substantially as the rainfall increased both in intensity and frequency. Lengthy periods of drought have been linked to an accumulation of soil nutrients which subsequently are made available to soil fauna after soil rewetting (Fierer and Schimel, 2002). Moreover, soil rewetting post-drought causes a boost in decomposition and C and N mineralization (Birch, 1964), thus increasing the soil nutrient availability ephemerally. Although drying-rewetting episodes have been observed to decrease N losses in forests (Muhr,

Franke and Borken, 2010), if rainfall events intensified, N losses due to denitrification can occur (Dick, Skiba and Wilson, 2001).

4.5.3 Microbial biomass and inorganic N

Microbial biomass C and N were higher under eCO₂ conditions in all three seasons, with the highest recorded during summer, albeit not statistically significant. These results are in agreement with previous studies (Lipson, Wilson and Oechel, 2005). Microbial biomass C and N (data not available for microbial biomass P) exhibited their highest concentrations during the summer campaign. These findings agree with previous studies, where under combined eCO₂ and drought conditions, the microbial biomass C and N were more elevated than under drought or eCO₂ alone (Xue *et al.*, 2017). In our study, the mean annual microbial biomass C:N, C:P, and N:P ratios were 2.67, 57.15, and 16.6, respectively, under ambient conditions. Under eCO₂ conditions, the mean annual microbial biomass C:N, C:P, and N:P ratios were 3.7, 41.45, and 10.25, respectively. It has been observed that the microbial biomass C:N, C:P, and N:P ratios for forests are 8.2, 74, and 8.9, respectively (Cleveland and Liptzin, 2007), while the global microbial biomass C:N, C:P, and N:P ratios for temperate broadleaf forests specifically are 8.3, 46 and 4.4 (Xu, Thornton and Post, 2013).

Drought is generally observed to constrain the accumulation of microbial biomass (Zhang and Zak, 1998) due to osmotic stress resulting in cell lysis and microbial death (Turner *et al.*, 2003), and alterations in belowground inputs in the rhizosphere as a result of plant adaptation to drought stress (Milcu, Paul and Lukac, 2011). On the other hand, the eCO₂ effect is more convoluted since there is contradictory evidence of positive, negative, and no effect (Zak *et al.*, 2000; Freeman *et al.*, 2004). Even more

so, the evidence of the interactive effects of eCO₂ and drought on belowground microbial processes is rather limited (Kassem *et al.*, 2008).

Moreover, following a defoliation event, C/N ratios have been observed to decrease due to large inputs of labile C and N through frass, leaf material, and insect cadavers (Kaukonen *et al.*, 2013; I-M-Arnold *et al.*, 2016; Brouillard *et al.*, 2017; Mikkelsen *et al.*, 2017; Grüning *et al.*, 2018). Both C and N inputs during insect outbreaks are highly water-soluble. Thus they can easily and promptly penetrate deeper soil horizons (Zimmer and Topp, 2002; le Mellec, Habermann and Michalzik, 2009). N inputs via frass and fresh leaf material have been observed to increase by 300% (Grüning *et al.*, 2017) as well as the lower C/N inputs via fresh leaf material, as opposed to senescent leaf input (Kopáček *et al.*, 2010), might explain the observed decrease in July spring C/N ratios at BIFoR FACE during the second year of eCO₂ enrichment. However, one needs to be cautious when interpreting the summer soil sampling microbial biomass C:N ratios, where the ratios are observed to be lower than 3 (for the O horizons). Even though the absolute ranges of the elemental concentrations in microbial biomass can vary greatly during the different seasons, the element ratios are well-constrained (Cleveland and Liptzin, 2007). The C:N ratios for bacteria are around 5.5, whereas for fungi are 8.3, ratios of 1 and 2 are stoichiometrically impossible (Scow, 1997).

4.5.4 Year 1 vs. Year 2

Figure 4-9 shows the percentage change (mean \pm se) of soil variables between ambient and eCO₂ conditions the first two years of eCO₂ enrichment at BIFoR FACE. R_s was higher under eCO₂ for both Year 1 and Year 2 (~21 and 36%, respectively), and the change was more prominent in Year 2. The temperature sensitivity Q₁₀ was

decreased by 30 and 12% for Year 1 and 2, respectively, under eCO₂. Bioavailable NO₃⁻-N was decreased by 27 and 15% under eCO₂ during Year 1 and 2, respectively, while NH₄⁺-N had no difference. Moreover, PO₄³⁻-P had a 10% decrease during Year 1 and a 5% increase during Year 2 under eCO₂. Furthermore, there was a ~50 and 8% increase in microbial biomass C in the O and B horizons, respectively, whereas there was a 15% decrease in microbial biomass C in A horizons under eCO₂. Under eCO₂ microbial biomass, N increased by 15% in the O horizon but decreased by 2 and 17 at A and B horizons. A similar pattern was observed for microbial biomass P, with the O horizons having a 53% increase under eCO₂, while there was an 8 and 16% decrease in A and B horizons. Lastly, both, soil inorganic NH₄⁺-N and NO₃⁻-N decreased under eCO₂, with the decrease being intensified with depth.

Ultimately, R_s during Year 2 was decreased by 47 and 40% under ambient and eCO₂ conditions, respectively, compared to Year 1. Contrastingly, all soil bioavailable nutrients' concentrations were higher during Year 2 under both ambient and eCO₂ conditions. NH₄⁺-N availability increased by 47 and 49% under ambient and eCO₂ conditions, respectively. Similarly, NO₃⁻-N availability increased by 70 and 101% under ambient and eCO₂ conditions, respectively, during Year 2. Sequentially, PO₄³⁻-P availability during Year 2 increased by 100 and 133% under ambient and eCO₂ conditions, respectively.

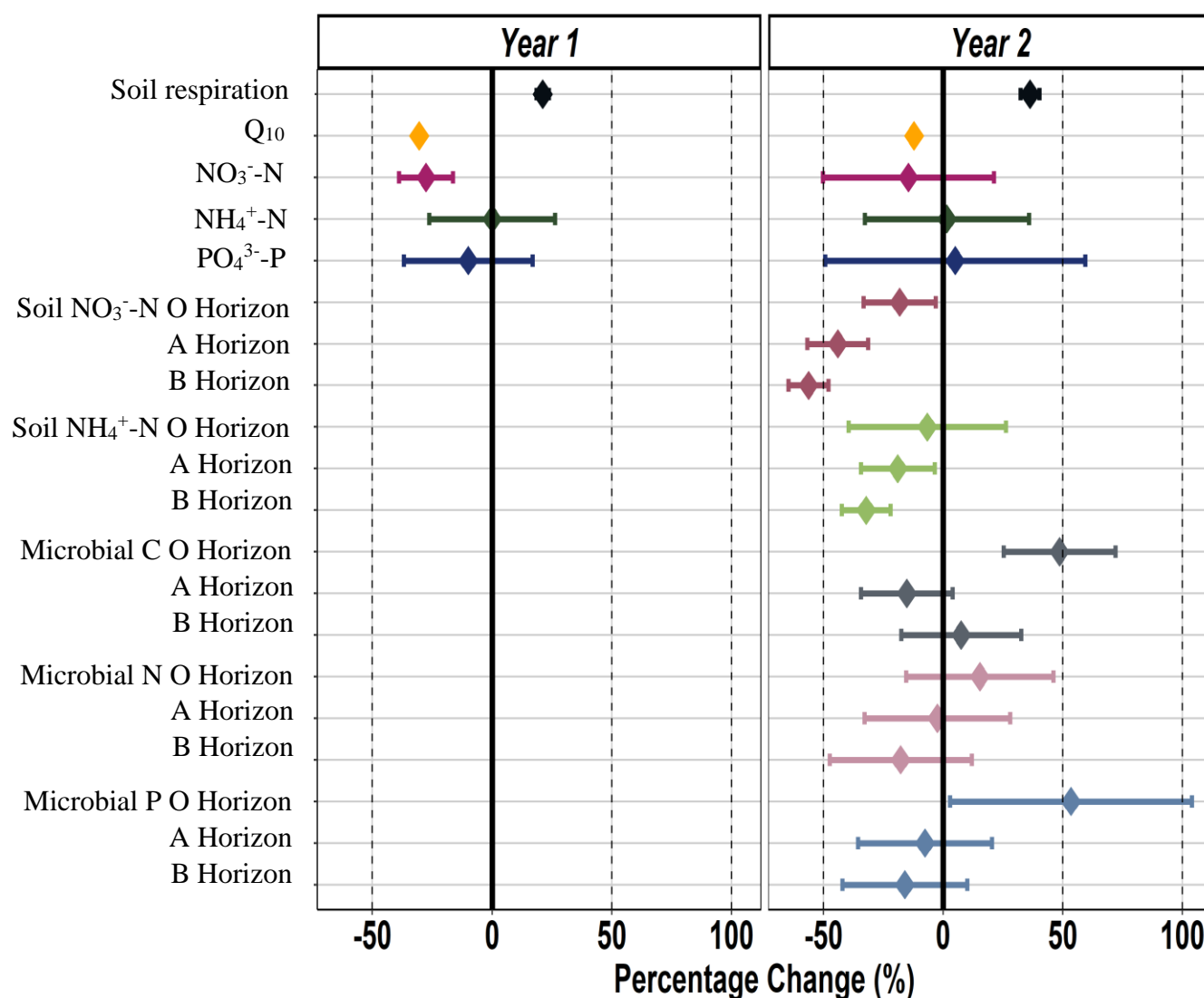


Figure 4- 9: Percentage change of R_s , soil nutrient availability (bioavailable and inorganic N), microbial biomass C, N, and P (per soil horizon) between ambient and eCO₂ conditions at BIFoR FACE the first two years of eCO₂ enrichment. The error bars denote standard error. Note that data for inorganic N and microbial biomass C, N, and P are available only for Year 2

4.5.5 Interactions of carbon and nutrient cycling

In this study, we had the opportunity to observe the effects of extreme events in a mature temperate woodland under eCO₂. We hypothesise that the substantial decrease in soil respiration observed during the second year of eCO₂ enrichment is plausible to be attributed to water deficit due to the prolonged heatwave. Moreover,

the late summer/early autumn substantial increase in nutrient availability can be attributed to the winter moth infestation event, where all the easily decomposable material deposited on the soil floor due to the infestation became available for decomposition with the increase of precipitation, which in turn increased the soil respiration.

Our data showcase that carbon and nutrient dynamics are affected differently by the different extreme events. The heatwave had a substantial impact in both carbon and nutrient cycling; however the moth outbreak, in the short-term, had a greater impact on nutrient availability rather than soil respiration. Large amounts of nutrients became available by the end of autumn, a period when the nutrient demand is not high. Although an increase in soil respiration was observed when nutrient availability was high, this was not reflected in the annual averages. Thus, the carbon cycle was dominated by the heatwave whereas the winter moth outbreak dominated the nutrient cycle.

4.5.6 Future implications

Extreme events are predicted to increase in the future (IPCC, 2007) due to climate change. eCO_2 increase is happening in a step-wise change, and its effect can be assumed constant, whereas the extreme events happen abruptly, and thus their impact is more severe. This is reflected in our observations in this study, where the series of extreme events dominated the belowground processes with eCO_2 dampening the magnitude of the extreme events. Moreover, combined extreme events tend to have less impact than the impact that the same events would have had individually (Raymond *et al.*, 2020).

Globally, droughts are predicted to dominate the terrestrial carbon cycle (Frank *et al.*, 2015). Severe drought conditions under eCO₂ can reduce the sap flow and canopy conductance, thus impacting the carbon gain (Warren, Norby and Wullschleger, 2011). Forest areas across the temperate region are predicted to be substantially negatively impacted by droughts (Schwalm *et al.*, 2010; Seneviratne *et al.*, 2012). Thus, severe drought might alleviate the eCO₂ fertilisation effect during extreme events. If trees cannot uptake the extra carbon and nutrient availability is limited, pausing severe impacts on the current forest carbon sink.

Moreover, there are considerable knowledge gaps in the physiological responses to pests on an ecosystemic scale (Kallarackal and Roby, 2012), let alone the multiple stressors combined effects. Although nutrient availability increases after a defoliation event, the time of the year and the local conditions are crucial for the nutrients' fate. Should nutrients become available during low demand time of the year and increased precipitation then the nutrient losses through leaching will increase since plants and microorganisms cannot utilise the extra amounts. Increased nutrient losses can lead to soil depletion, thus halting the extra carbon uptake.

4.6 Conclusions

In this study, we had the unprecedented opportunity to observe a parade of extreme events on a large-scale climatic experiment. The second year of eCO₂ enrichment at BIFoR FACE coincided with an unusually cold early spring, a moth outbreak causing a significant defoliation event, and a prolonged summer heatwave. eCO₂ had a significant positive effect on soil respiration relative to ambient; however, no statistically significant increase was observed in microbial biomass. Soil respiration

was suppressed by the drought, while the moth outbreak dominated the nutrient cycling. The nutrient inputs increased on the forest floor via frass, caterpillar cadavers, and fresh leaf material once the water availability increased post-drought through increased precipitation episodes.

4.7 References

- 2018 - A Record Breaking Year | theWeather Club (2018). Available at: <https://www.theweatherclub.org.uk/node/538> (Accessed: 16th November 2020).
- Balogh, J. *et al.* (2016) 'Autotrophic component of soil respiration is repressed by drought more than the heterotrophic one in dry grasslands', *Biogeosciences*. Copernicus GmbH, 13(18), pp. 5171–5182. doi: 10.5194/bg-13-5171-2016.
- Barton, K. (2014) 'MuMIn: multi-model inference. R package version 3.1-96'.
- Bates, D. *et al.* (2015) 'Fitting Linear Mixed-Effects Models Using **lme4**', *Journal of Statistical Software*. American Statistical Association, 67(1). doi: 10.18637/jss.v067.i01.
- Beast from the East - Met Office (2018). Available at: <https://www.metoffice.gov.uk/weather/learn-about/weather/atmosphere/air-masses/beast-from-the-east> (Accessed: 16th November 2020).
- Bernhardt, E. S. *et al.* (2006) 'Long-term effects of free air CO₂ enrichment (FACE) on soil respiration', *Biogeochemistry*, 77(1), pp. 91–116. doi: 10.1007/s10533-005-1062-0.
- Birch, H. F. (1964) 'Mineralisation of plant nitrogen following alternate wet and dry conditions', *Plant and Soil*. Martinus Nijhoff, The Hague/Kluwer Academic Publishers, 20(1), pp. 43–49. doi: 10.1007/BF01378096.
- Bloor, J. M. G. and Bardgett, R. D. (2012) 'Stability of above-ground and belowground processes to extreme drought in model grassland ecosystems: Interactions with plant species diversity and soil nitrogen availability', *Perspectives in Plant Ecology, Evolution and Systematics*. Urban & Fischer, 14(3), pp. 193–204. doi: 10.1016/j.ppees.2011.12.001.
- Borken, W. *et al.* (2006) 'Effects of experimental drought on soil respiration and radiocarbon efflux from a temperate forest soil', *Global Change Biology*. John Wiley & Sons, Ltd, 12(2), pp. 177–193. doi: 10.1111/j.1365-2486.2005.001058.x.
- Borken, W. and Matzner, E. (2009) 'Reappraisal of drying and wetting effects on C and N mineralization and fluxes in soils', *Global Change Biology*. John Wiley & Sons, Ltd, 15(4), pp. 808–824. doi: 10.1111/j.1365-2486.2008.01681.x.
- Bowatte, S. *et al.* (2008) 'In situ ion exchange resin membrane (IEM) technique to measure soil mineral nitrogen dynamics in grazed pastures', *Biology and Fertility of Soils*, 44(6), pp. 805–813. doi: 10.1007/s00374-007-0260-4.
- Bréchet, L. *et al.* (2019) 'Disentangling Drought and Nutrient Effects on Soil Carbon Dioxide and Methane Fluxes in a Tropical Forest', *Frontiers in Environmental Science*. Frontiers Media S.A., 7, p. 180. doi: 10.3389/fenvs.2019.00180.
- Brouillard, B. M. *et al.* (2017) 'Extent of localized tree mortality influences soil biogeochemical

response in a beetle-infested coniferous forest', *Soil Biology and Biochemistry*, 114, pp. 309-318. doi: 10.1016/j.soilbio.2017.06.016.

Campbell, J. L. and Law, B. E. (2005) 'Forest soil respiration across three climatically distinct chronosequences in Oregon', *Biogeochemistry*, 73, pp. 109-125. doi: 10.1007/s10533-004-5165-9.

Christenson, L. M. *et al.* (2002) 'The fate of nitrogen in gypsy moth frass deposited to an oak forest floor', *Oecologia*, 131(3), pp. 444-452. doi: 10.1007/s00442-002-0887-7.

Classen, A. T. *et al.* (2005) 'Insect Infestations Linked to Shifts in Microclimate', *Soil Science Society of America Journal*. Wiley, 69(6), pp. 2049-2057. doi: 10.2136/sssaj2004.0396.

Cleveland, C. C. and Liptzin, D. (2007) 'C:N:P stoichiometry in soil: Is there a "Redfield ratio" for the microbial biomass?', *Biogeochemistry*. Springer, 85(3), pp. 235-252. doi: 10.1007/s10533-007-9132-0.

Collins, M. *et al.* (2013) *Long-term Climate Change: Projections, Commitments and Irreversibility*. Cambridge University Press.

Cregger, M. A. *et al.* (2014) 'The impact of precipitation change on nitrogen cycling in a semi-arid ecosystem', *Functional Ecology*. Edited by S. Niu. Blackwell Publishing Ltd, 28(6), pp. 1534-1544. doi: 10.1111/1365-2435.12282.

Curiel Yuste, J. *et al.* (2004) 'Annual Q_{10} of soil respiration reflects plant phenological patterns as well as temperature sensitivity', *Global Change Biology*, 10(2), pp. 161-169. doi: 10.1111/j.1529-8817.2003.00727.x.

Davidson, E. A. *et al.* (2000) 'Effects of soil water content on soil respiration in forests and cattle pastures of eastern Amazonia', *Biogeochemistry*. 48(1), pp. 53-69. doi: 10.1023/A:1006204113917.

Davidson, E. A., Janssens, I. A. and Lou, Y. (2006) 'On the variability of respiration in terrestrial ecosystems: Moving beyond Q_{10} ', *Global Change Biology*. 12(2), pp. 154-164. doi: 10.1111/j.1365-2486.2005.01065.x.

Dick, J., Skiba, U. and Wilson, J. (2001) 'The effect of rainfall on NO and N₂O emissions from Ugandan agroforest soils', *Phyton*, 41(1), pp. 73-80.

Dongen, S. Van *et al.* (1997) 'Synchronization of Hatching Date with Budburst of Individual host Trees (*Quercus robur*) in the Winter Moth (*Operophtera brumata*) and its Fitness Consequences', *The Journal of Animal Ecology*, 66(1), doi: 10.2307/5969

Drake, J. E. *et al.* (2018) 'Three years of soil respiration in a mature eucalypt woodland exposed to atmospheric CO₂ enrichment', *Biogeochemistry*. Springer International Publishing, 139(1), pp. 85-101. doi: 10.1007/s10533-018-0457-7.

Easterling, D. R. *et al.* (2017) 'Climate Extremes: Observations, Modeling, and Impacts', *PNAS*, 114(19), pp. 4881-4886.

Feeny, P. (1970) 'Seasonal changes in oak leaf tannins and nutrients as a cause of spring feeding by winter moth caterpillars', *Ecology*, 51(4), pp. 565-581. doi: 10.2307/1934037

Ficken, C. D. and Warren, J. M. (2019) 'The carbon economy of drought: comparing respiration responses of roots, mycorrhizal fungi, and free-living microbes to an extreme dry-rewet cycle', *Plant and Soil*. 435(1-2), pp. 407-422. doi: 10.1007/s11104-018-03900-2.

Fierer, N. and Schimel, J. P. (2002) 'Effects of drying-rewetting frequency on soil carbon and nitrogen transformations', *Soil Biology and Biochemistry*. Pergamon, 34(6), pp. 777-787. doi: 10.1016/S0038-0717(02)00007-X.

- Finzi, A. C. *et al.* (2002) 'The nitrogen budget of a pine forest under free air CO₂ enrichment', *Oecologia*. Springer Berlin Heidelberg, 132(4), pp. 567–578. doi: 10.1007/s00442-002-0996-3.
- Frank, Dorothea *et al.* (2015) 'Effects of climate extremes on the terrestrial carbon cycle: concepts, processes and potential future impacts', *Global Change Biology*. 21(8), pp. 2861–2880. doi: 10.1111/gcb.12916.
- Freeman, C. *et al.* (2004) 'Export of dissolved organic carbon from peatlands under elevated carbon dioxide levels', *Nature*, 430(6996), pp. 195–198. doi: 10.1038/nature02707.
- Friedlingstein, P. *et al.* (2006) 'Climate-carbon cycle feedback analysis: Results from the C4MIP model intercomparison', *Journal of Climate*, 19(14), pp. 3337–3353. doi: 10.1175/JCLI3800.1.
- Friedlingstein, P. *et al.* (2014) 'Uncertainties in CMIP5 Climate Projections due to Carbon Cycle Feedbacks', *Journal of Climate*, 27, pp. 511–526. doi: 10.1175/JCLI-D-12-00579.1.
- Fuchslueger, L. *et al.* (2014) 'Experimental drought reduces the transfer of recently fixed plant carbon to soil microbes and alters the bacterial community composition in a mountain meadow', *New Phytologist*. New Phytol, 201(3), pp. 916–927. doi: 10.1111/nph.12569.
- Garten, C. T., Classen, A. T. and Norby, R. J. (2009) 'Soil moisture surpasses elevated CO₂ and temperature as a control on soil carbon dynamics in a multi-factor climate change experiment', *Plant and Soil*. Springer, 319(1–2), pp. 85–94. doi: 10.1007/s11104-008-9851-6.
- Gnosall, Staffordshire, United Kingdom Weather averages | Monthly Average High and Low Temperature | Average Precipitation and Rainfall days | World Weather Online (no date). Available at: <https://www.worldweatheronline.com/gnosall-weather-averages/staffordshire/gb.aspx> (Accessed: 6 March 2021)
- Goulden, M. L. *et al.* (1996) 'Exchange of carbon dioxide by a deciduous forest: Response to interannual climate variability', *Science*. American Association for the Advancement of Science, 271(5255), pp. 1576–1578. doi: 10.1126/science.271.5255.1576.
- Gruning, M. M. *et al.* (2017) 'Defoliating insect mass outbreak affects soil N fluxes and tree N nutrition in scots pine forests', *Frontiers in Plant Science*, 8, doi: 10.3389/fpls.2017.00954.
- Gruning, M. M. *et al.* (2018) 'Increased forest soil CO₂ and N₂O emissions during insect infestation', *Forests*, 9(10), doi: 10.3390/f9100612.
- Harper, C. W. *et al.* (2005) 'Increased rainfall variability and reduced rainfall amount decreases soil CO₂ flux in a grassland ecosystem', *Global Change Biology*. John Wiley & Sons, Ltd, 11(2), pp. 322–334. doi: 10.1111/j.1365-2486.2005.00899.x.
- Hart, K. M. *et al.* (2019) 'Characteristics of free air carbon dioxide enrichment of a northern temperate mature forest', *Global Change Biology*. John Wiley & Sons, Ltd (10.1111), p. gcb.14786. doi: 10.1111/gcb.14786.
- Herrmann, A. and Witter, E. (2002) 'Sources of C and N contributing to the flush in mineralization upon freeze-thaw cycles in soils', *Soil Biology and Biochemistry*, 34(10), pp. 1495–1505. doi: 10.1016/S0038-0717(02)00121-9
- Hillstorm, M. *et al.* (2010) 'Soil carbon and nitrogen mineralization following deposition of insect frass and greenfall from forests under elevated CO₂ and O₃', *Plant and Soil*, 336(1), pp. 75–85. doi: 10.1007/s11104-010-0449-4.
- Högberg, P. *et al.* (2001) 'Large-scale forest girdling shows that current photosynthesis drives soil respiration', *Nature*, 411(6839), pp. 789–792. doi: 10.1038/35081058.
- Hovenden, M. J. *et al.* (2008) 'Warming prevents the elevated CO₂-induced reduction in

available soil nitrogen in a temperate, perennial grassland', *Global Change Biology*, 14(5), pp. 1018–1024. doi: 10.1111/j.1365-2486.2008.01558.x.

Howard, D. M. and Howard, P. J. A. (1993) 'Relationships between CO₂ evolution, moisture content and temperature for a range of soil types', *Soil Biology and Biochemistry*, 25(11). doi: 10.1016/0038-0717(93)90008-Y.

I-M-Arnold, A. et al. (2016) 'Forest defoliator pests alter carbon and nitrogen cycles', *Royal Society Open Sciences*, 3(10). doi: 10.1098/rsos.160361

Idso, S. B. and Kimball, B. A. (2001) 'CO₂ enrichment of sour orange trees: 13 Years and counting', *Environmental and Experimental Botany*. Elsevier, 46(2), pp. 147–153. doi: 10.1016/S0098-8472(01)00093-4.

IPCC (2007) 'Summary for policy makers', in Solomon SD et al. (eds) *Climate change 2007: the physical science basis. Contribution of working group I to the fourth assessment report of the intergovernmental panel on climate change*. Cambridge: Cambridge University Press.

IPCC (2014a) *Climate Change 2014, Climate Change 2014: Synthesis Report*. doi: 10.1017/CBO9781107415324.

IPCC (2014b) 'Climate Change 2014 Synthesis Report Summary Chapter for Policymakers', *ipcc*.

Janssens, I. A. and Pilegaard, K. (2003) 'Large seasonal changes in Q₁₀ of soil respiration in a beech forest', *Global Change Biology*, 9(6), pp.911-918. doi: 10.1046/j.1365-2486.2003.00636.x.

Jassal, R. S. et al. (2008) 'Effect of soil water stress on soil respiration and its temperature sensitivity in an 18-year-old temperate Douglas-fir stand', *Global Change Biology*, 14(6), pp. 1305–1318. doi: 10.1111/j.1365-2486.2008.01573.x.

Jung, P. and Lunderstadt, J. (2000) 'Wirkung von Larvenkot von Dendrolimus pini L. (Lep., Lasiocampidae)nach Frass an Kiefer auf Keimung und Keimlingswachstum von Kiefern-Birken-und Eichensaat', *Journal of Applied Entomology*, 124(5-6), pp. 253-258. doi:10.1046/j.1439-0418.2000.00474.x.

Kallarackal, J. and Roby, T. J. (2012) 'Responses of trees to elevated carbon dioxide and climate change', *Biodiversity and Conservation*, pp. 1327-1342. doi: 10.1007/s10531-012-0254-x.

Kassem, I. I. et al. (2008) 'Effect of Elevated CO₂ and Drought on Soil Microbial Communities Associated with *Andropogon gerardii*', *Journal of Integrative Plant Biology*. John Wiley & Sons, Ltd, 50(11), pp. 1406–1415. doi: 10.1111/j.1744-7909.2008.00752.x.

Kaukonen, M. et al. (2013) 'Moth herbivory enhances resources turnover in subarctic mountain birch forests?', *Ecology*, 94(2), pp. 267-272. doi: 10.1890/12-0917.1.

King, J. S. et al. (2004) 'A multiyear synthesis of soil respiration responded to elevated atmospheric CO₂ from four forest FACE experiments', *Global Change Biology*, 10, pp. 1027–1042. doi: 10.1111/j.1365-2486.2004.00789.x.

Kirilenko, A. P. and Sedjo, R. A. (2007) 'Climate change impacts on forestry', *Proceedings of the National Academy of Sciences of the United States of America*. National Academy of Sciences, 104(50), pp. 19697–19702. doi: 10.1073/pnas.0701424104.

Kopáček, J. et al. (2010) 'Composition of Norway spruce litter and foliage in atmospherically acidified and nitrogen-saturated Bohemian Forest stands, Czech Republic', *Boreal Environment Research*, 15, pp. 413-426

Kopper, B. J. and Lindroth, R. L. (2003) 'Effects of elevated carbon dioxide and ozone on the

phytochemistry of aspen and performance of an herbivore', *Oecologia*, 134(1), pp. 95-103. doi: 10.1007/s00442-002-1090-6.

Körner, C. *et al.* (2005) 'Carbon Flux and Growth in Mature Deciduous Forest Trees Exposed to Elevated CO₂', *Science*, 309(5739), pp. 1360–1362. doi: 10.1126/science.1113977.

Körner, C. (2006) 'Plant CO₂ responses: an issue of definition, time and resource supply', *New Phytologist*, 172, pp. 393–411. doi: 10.1111/j.1469-8137.2006.01886.x.

Kreuzwieser, J. and Gessler, A. (2010) 'Global climate change and tree nutrition: Influence of water availability', *Tree Physiology*. Oxford Academic, 30(9), pp. 1221–1234. doi: 10.1093/treephys/tpq055.

Kurganova, I., Teepe, R. and Löffel, N. (2007) 'Influence of freeze-thaw events on carbon dioxide emission from soils at different moisture and land use', *Carbon Balance and Management*, 2(1). doi: 10.1186/1750-0680-2-2.

Kuzyakov, Y. and Domanski, G. (2000) 'Carbon input by plants into the soil. Review', *Journal of Plant Nutrition and Soil Science*. Wiley-VCH Verlag, 163(4), pp. 421–431. doi: 10.1002/1522-2624(200008)163:4<421::AID-JPLN421>3.0.CO;2-R.

Lagomarsino, A. *et al.* (2008) 'Assessment of soil nitrogen and phosphorous availability under elevated CO₂ and N-fertilization in a short rotation poplar plantation', *Plant and Soil*, 308(1–2), pp. 131–147. doi: 10.1007/s11104-008-9614-4.

Larsen, K. S., Jonasson, S. and Michelsen, A. (2002) 'Repeated freeze-thaw cycles and their effects on biological processes in two arctic ecosystem types', *Applied Soil Ecology*, 21(3), pp. 187-195. doi: 10.1016/S0929-1393(02)00093-8.

Lipson, D. A., Wilson, R. F. and Oechel, W. C. (2005) 'Effects of elevated atmospheric CO₂ on soil microbial biomass, activity, and diversity in a chaparral ecosystem', *Applied and Environmental Microbiology*. American Society for Microbiology (ASM), 71(12), pp. 8573–8580. doi: 10.1128/AEM.71.12.8573-8580.2005.

Lovett, G. M. and Ruesink, A. E. (1995) 'Carbon and nitrogen mineralization from decomposing gypsy moth frass', *Oecologia*, 104(2), pp. 133-138. doi: 10.1007/BF00328577

Madritch, M.D., Donaldson, J. R. and Lindroth, R. L. (2007) 'Canopy herbivory can mediate the influence of plant genotype on soil processes through frass deposition', *Soil Biology and Biochemistry*, 39(5), pp. 1192-1201. doi: 10.1016/j.soilbio.2006.12.027

Malcolm, J. R. *et al.* (2002) 'Estimated migration rates under scenarios of global climate change', *Journal of Biogeography*, 29(7), pp. 835–849. doi: 10.1046/j.1365-2699.2002.00702.x.

Manzoni, S., Schimel, J. P. and Porporato, A. (2012) 'Responses of soil microbial communities to water stress: Results from a meta-analysis', *Ecology*. John Wiley & Sons, Ltd, 93(4), pp. 930–938. doi: 10.1890/11-0026.1.

le Mellec, A., Habermann, M. and Michalzik, B. (2009) 'Canopy herbivory altering C to N ratios and soil input patterns of different organic matter fractions in a Scots pine forest', *Plant and Soil*, 325(1), pp. 255-262. doi: 10.1007/s111-009-9976-2.

Met Office (2018). Available at: https://www.metoffice.gov.uk/binaries/content/assets/metofficegovuk/pdf/weather/learn-about/uk-past-events/summaries/uk_monthly_climate_summary_winter_2018.pdf (Accessed: 16th November 2020).

Mikkelsen, K. M. *et al.* (2017) 'Ecosystem resilience and limitations revealed by soil bacterial community dynamics in a bark beetle-impacted forest', *mBio*, 8(6). doi: 10.1128/mBio.01305-

- Milcu, A., Paul, S. and Lukac, M. (2011) 'Belowground interactive effects of elevated CO₂, plant diversity and earthworms in grassland microcosms', *Basic and Applied Ecology*. Urban & Fischer, 12(7), pp. 600–608. doi: 10.1016/j.baae.2011.08.004.
- Moncrieff, J. B. and Fang, C. (1999) 'A model for soil CO₂ production and transport 2: Application to Florida Pinus elliotte plantation', *Agricultural and Forest Meteorology*, 95(4), pp. 237–256. doi: 10.1016/S0168-1923(99)00035-0
- Van der Molen, M. K. *et al.* (2011) 'Drought and ecosystem carbon cycling', *Agricultural and Forest Meteorology*. doi: 10.1016/j.agrformet.2011.01.018.
- Muhr, J. and Borken, W. (2009) 'Delayed recovery of soil respiration after wetting of dry soil further reduces C losses from a Norway spruce forest soil', *Journal of Geophysical Research*. Blackwell Publishing Ltd, 114(G4), p. G04023. doi: 10.1029/2009JG000998.
- Muhr, J., Franke, J. and Borken, W. (2010) 'Drying-rewetting events reduce C and N losses from a Norway spruce forest floor', *Soil Biology and Biochemistry*. Pergamon, 42(8), pp. 1303–1312. doi: 10.1016/j.soilbio.2010.03.024.
- Orchard, V. A. and Cook, F. J. (1983) 'Relationship between soil respiration and soil moisture', *Soil Biology and Biochemistry*. Pergamon, 15(4), pp. 447–453. doi: 10.1016/0038-0717(83)90010-X.
- Pan, Y. *et al.* (2011) 'A large and persistent carbon sink in the world's forests', *Science*. doi: 10.1126/science.1201609.
- Parsons, W. F. J., Bockheim, J. G., and Lindroth, R. L. (2008) 'Independent, interactive, and species-specific responses of leaf litter decomposition to elevated CO₂ and O₃ in a northern hardwood forest', *Ecosystems*, 11(4), pp. 505–519. doi: 10.1007/s10021-008-9148-x.
- Parsons, W. F. J., Lindroth, R. L. and Bockheim, J. G. (2004) 'Decomposition of *Betula papyrifera* leaf litter under the independent and interactive effects of elevated CO₂ and O₃', *Global Change Biology*, 10, pp. 1666–1677. doi: 10.1111/j.1365-2486.2004.00851.x.
- Pregitzer, K. S. *et al.* (2008) 'Soil respiration, root biomass, and root turnover following long-term exposure of northern forests to elevated atmospheric CO₂ and tropospheric O₃', *New Phytologist*, 180(1), pp. 153–161. doi: 10.1111/j.1469-8137.2008.02564.x.
- Prieme, A. and Christensen, S. (2001) 'Natural perturbations, drying-wetting and freezing-thawing cycles, and the emission of nitrous oxide, carbon dioxide and methane from farmed organic soils', *Soil Biology and Biochemistry*, 33(15), pp. 2083–2091. doi: 10.1016/S0038-0717(01)00140-7.
- Rayment, G. and Lyons, D. J. (2011) *Soil chemical methods : Australasia (Australian soil and land survey handbook series: v.3)*, *Australian soil and land survey handbook series*. CSIRO Publishing.
- Raymond, C. *et al.* (2020) 'Understanding and managing connected extreme events', *Nature Climate Change*, 10(7), pp. 611–621. doi: 10.1038/s41558-020-0790-4.
- Reichstein, M. *et al.* (2013) 'Climate extremes and the carbon cycle', *Nature*, 500(7462), pp. 287–295. doi: 10.1038/nature12350.
- Rey, A. *et al.* (2002) 'Annual variation in soil respiration and its components in a coppice oak forest in Central Italy', *Global Change Biology*, 8(9), pp. 851–866. doi: 10.1046/j.1365-2486.2002.00521.x.
- Rouphael, Y. *et al.* (2012) 'Effects of drought on nutrient uptake and assimilation in vegetable crops', in *Plant Responses to Drought Stress: From Morphological to Molecular Features*.

Springer-Verlag Berlin Heidelberg, pp. 171–195. doi: 10.1007/978-3-642-32653-0_7.

Roy, J. *et al.* (2016) 'Elevated CO₂ maintains grassland net carbon uptake under a future heat and drought extreme', *Proceedings of the National Academy of Sciences of the United States of America*, 113(22), pp. 6224–6229. doi: 10.1073/pnas.1524527113.

Ruehr, N. K. *et al.* (2009) 'Drought effects on allocation of recent carbon: From beech leaves to soil CO₂ efflux', *New Phytologist*. John Wiley & Sons, Ltd, 184(4), pp. 950–961. doi: 10.1111/j.1469-8137.2009.03044.x.

Sardans, J. and Peñuelas, J. (2004) 'Increasing drought decreases phosphorus availability in an evergreen Mediterranean forest', *Plant and Soil*, 267(1–2). doi: 10.1007/s11104-005-0172-8.

Schimel, D., Stephens, B. B. and Fisher, J. B. (2015) 'Effect of increasing CO₂ on the terrestrial carbon cycle', 112(2). doi: 10.1073/pnas.1407302112.

Schimel, J. P., Bilbrough, C. and Welker, J. M. (2004) 'Increased snow depth affects microbial activity and nitrogen mineralization in two Arctic tundra communities', *Soil Biology and Biochemistry*, 36(2), pp. 217–227. doi: 10.1016/j.soilbio.2003.09.008

Schimel, J. P. and Weintraub, M. N. (2003) 'The implications of exoenzyme activity on microbial carbon and nitrogen limitation in soil: A theoretical model', *Soil Biology and Biochemistry*. Elsevier Ltd, 35(4), pp. 549–563. doi: 10.1016/S0038-0717(03)00015-4.

Schwalm, C. R. *et al.* (2010) 'Assimilation exceeds respiration sensitivity to drought: A FLUXNET synthesis', *Global Change Biology*, 16(2), pp. 657–670. Doi: 10.1111/j.1365-2486.2009.01991.x.

Schweitzer, J. A. *et al.* (2008) 'Plant-soil-microorganism interactions: Heritable relationship between plant genotype and associated soil microorganisms', *Ecology*, 89(3), pp. 773–781. doi: 10.1890/07-0337.1.

Scow, K. M. (1997) 'Soil Microbial Communities and Carbon Flow in Agroecosystems', in *Ecology in Agriculture*. Elsevier, pp. 367–413. doi: 10.1016/b978-012378260-1/50012-9.

Selsted, M. B. *et al.* (2012) 'Soil respiration is stimulated by elevated CO₂ and reduced by summer drought: three years of measurements in a multifactor ecosystem manipulation experiment in a temperate heathland (CLIMAITE)', *Global Change Biology*. John Wiley & Sons, Ltd, 18(4), pp. 1216–1230. doi: 10.1111/j.1365-2486.2011.02634.x.

Seneviratne, S. I. *et al.* (2012) '3 - Changes in Climate Extremes and their Impacts on the Natural Physical Environment', in *Managing the Risks of Extreme Events and Disasters to Advance Climate Change Adaptation. A Special Report of Working Groups I and II of the Intergovernmental Panel on Climate Change (IPCC)*. Cambridge University Press, pp. 109–230. doi: 10.7916/D8-6NBT-S431.

Skopp, J., Jawson, M. D. and Doran, J. W. (1990) 'Steady-State Aerobic Microbial Activity as a Function of Soil Water Content', *Soil Science Society of America Journal*. Wiley, 54(6), pp. 1619–1625. doi: 10.2136/sssaj1990.03615995005400060018x.

Stevenson, I. R. and Bryant, D. M. (2000) 'Avian phenology: Climate change and constraints on breeding', *Nature*, 406(6794), pp. 366–367. doi: 10.1038/35019151.

Sun, S., Lei, H. and Chang, S. X. (2019) 'Drought differentially affects autotrophic and heterotrophic soil respiration rates and their temperature sensitivity', *Biology and Fertility of Soils*. Springer Verlag. doi: 10.1007/s00374-019-01347-w.

Talbot, J. M., Allison, S. D. and Treseder, K. K. (2008) 'Decomposers in disguise: Mycorrhizal fungi as regulators of soil C dynamics in ecosystems under global change', *Functional*

- Ecology*. John Wiley & Sons, Ltd, 22(6), pp. 955–963. doi: 10.1111/j.1365-2435.2008.01402.x.
- Team, Rs. (2019) 'RStudio: Integrated Development for R.' Boston, MA: RStudio, Inc.
- Turner, B. L. *et al.* (2003) 'Potential contribution of lysed bacterial cells to phosphorus solubilisation in two rewetted Australian pasture soils', *Soil Biology and Biochemistry*. Pergamon, 35(1), pp. 187–189. doi: 10.1016/S0038-0717(02)00244-4.
- UNFCCC (2005) *Adoption of the Paris Agreement*.
- Visser, M. E. *et al.* (1998) 'Warmer springs lead to mistimed reproduction in great tits (*Parus major*)', *Proceedings of the Royal Society B: Biological Sciences*, 265(1408), pp. 1867–1870. doi: 10.1098/rspb.1998.0514.
- Visser, M. E. and Holleman, L. J. M. (2001) 'Warmer springs disrupt the synchrony of oak and winter moth phenology', *Proceedings of the Royal Society B: Biological Sciences*, 268, pp. 289–294. doi: 10.1098/rspb.2000.1363.
- Wang, Y. *et al.* (2014) 'Responses of soil respiration and its components to drought stress', *Journal of Soils and Sediments*, 14(1), pp. 99–109. doi: 10.1007/s11368-013-0799-7.
- Warren, J. M., Norby, R. J. and Wullschlegel, S. D. (2011) 'Elevated CO₂ enhances leaf senescence during extreme drought in a temperate forest', *Tree Physiology*, 31(2), pp. 117–130. doi: 10.1093/treephys/tpr002.
- Weather review - Spring 2018 | theWeather Club* (2018). Available at: <https://www.theweatherclub.org.uk/index.php/node/500> (Accessed: 16th November 2020).
- Westerling, A. L. *et al.* (2006) 'Warming and earlier spring increase Western US forest wildfire activity', *Science*. American Association for the Advancement of Science, 313(5789), pp. 940–943. doi: 10.1126/science.1128834.
- Wieder, W. R., Bonan, G. B. and Allison, S. D. (2013) 'Global soil carbon projections are improved by modelling microbial processes', *Nature Climate Change*, 3(10), pp. 909–912. doi: 10.1038/nclimate1951.
- Worsfold, P. J. *et al.* (2005) 'Sampling, sample treatment and quality assurance issues for the determination of phosphorus species in natural waters and soils.', *Talanta*, 66(2), pp. 273–93. doi: 10.1016/j.talanta.2004.09.006.
- Xu, X., Thornton, P. E. and Post, W. M. (2013) 'A global analysis of soil microbial biomass carbon, nitrogen and phosphorus in terrestrial ecosystems', *Global Ecology and Biogeography*. John Wiley & Sons, Ltd, 22(6), pp. 737–749. doi: 10.1111/geb.12029.
- Xue, S. *et al.* (2017) 'Effects of elevated CO₂ and drought on the microbial biomass and enzymatic activities in the rhizospheres of two grass species in Chinese loess soil', *Geoderma*. Elsevier BV, 286, pp. 25–34. doi: 10.1016/j.geoderma.2016.10.025.
- Zaehle, S. *et al.* (2014) 'Evaluation of 11 terrestrial carbon-nitrogen cycle models against observations from two temperate Free-Air CO₂ enrichment studies', *The New phytologist*, 202(3), pp. 803–22. doi: 10.1111/nph.12697.
- Zak, D. R. *et al.* (1994) 'Plant production and soil microorganisms in late-successional ecosystems: A continental-scale study', *Ecology*. Ecological Society of America, 75(8), pp. 2333–2347. doi: 10.2307/1940888.
- Zak, D. R. *et al.* (2000) 'Elevated atmospheric CO₂, fine roots and the response of soil microorganisms: a review and hypothesis', *New Phytologist*. John Wiley & Sons, Ltd, 147(1), pp. 201–222. doi: 10.1046/j.1469-8137.2000.00687.x.
- Zak, D. R. *et al.* (2003) 'Soil nitrogen cycling under elevated CO₂: A synthesis of forest face

experiments', *Ecological Applications*, 13(6), pp. 1508–1514. doi: 10.1890/03-5055.

Zhang, Q. and Zak, J. C. (1998) 'Effects of water and nitrogen amendment on soil microbial biomass and fine root production in a semi-arid environment in West Texas', *Soil Biology and Biochemistry*, 30(1), pp. 39–45. doi: 10.1016/S0038-0717(97)00089-8.

Zimmer, M. and Topp, W. (2002) 'The role of coprophagy in nutrient release from feces of phytophagous insects', *Soil Biology and Biochemistry*, 34(8), pp. 1093-1099. doi: 10.1016/S0038-0717(02)00044-5.

4.8 Supplementary material

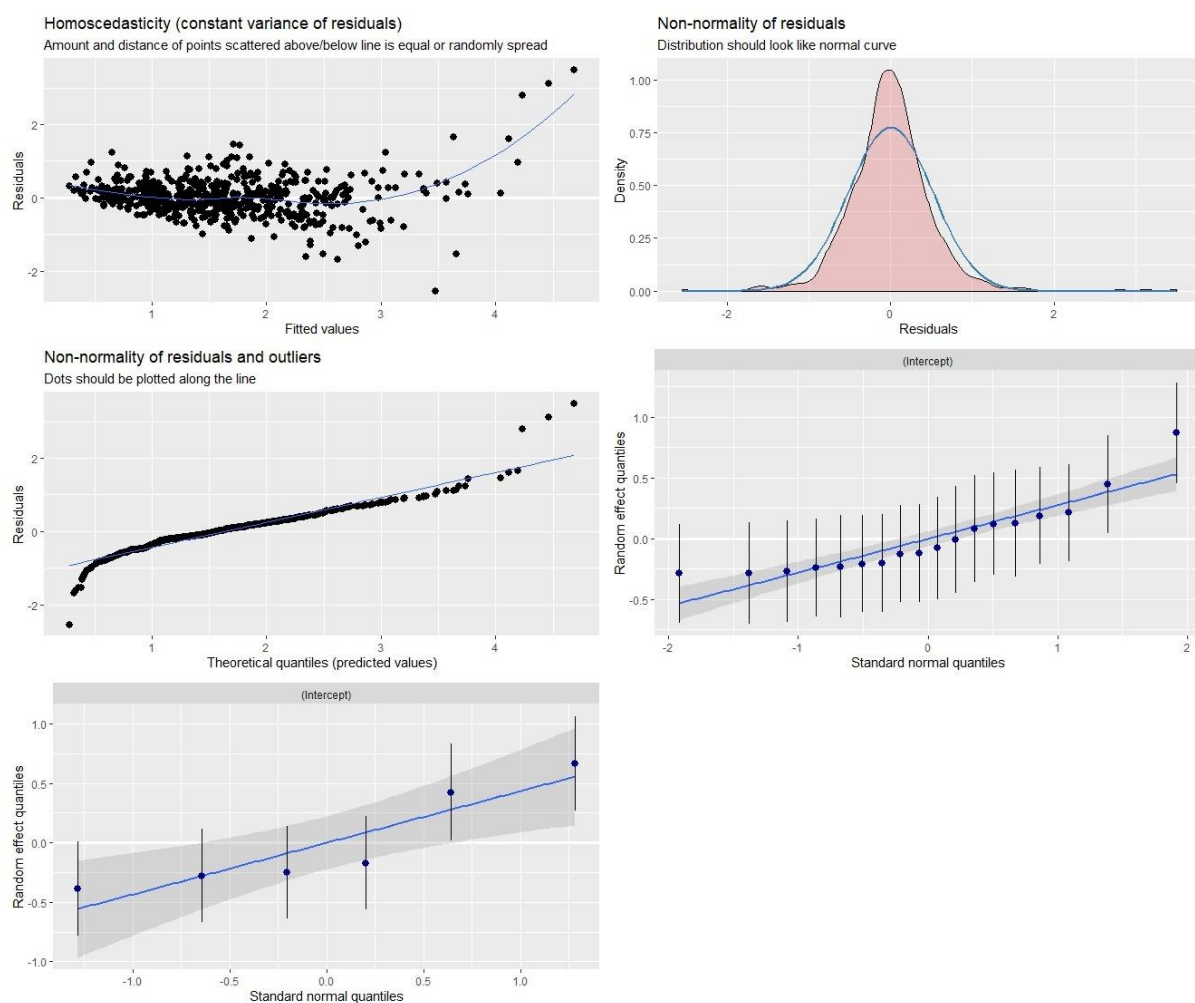


Figure S4- 1: Model validation for estimating soil respiration during Dormant for homoscedasticity, normality of residuals, and outliers and random effects.

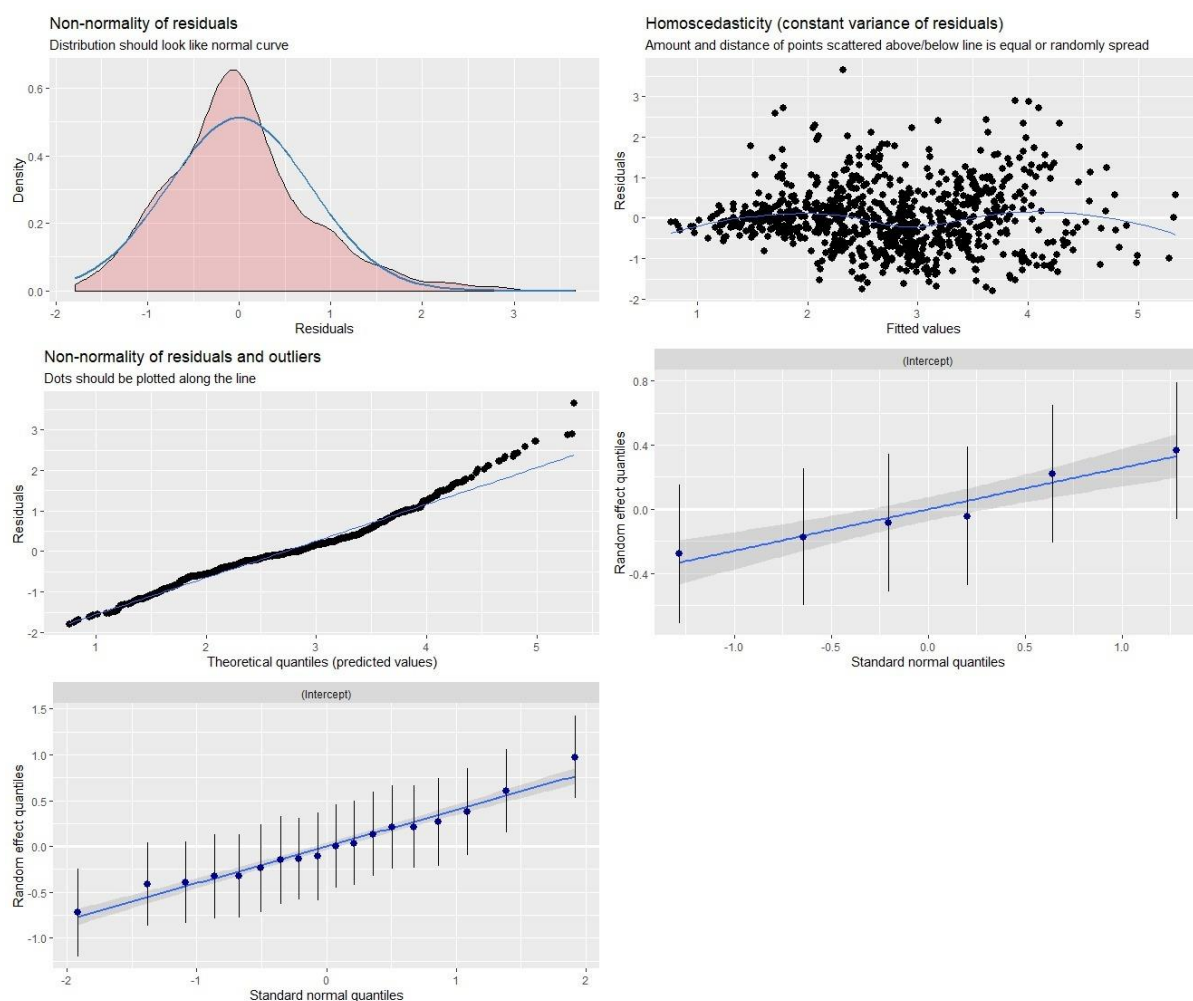


Figure S4- 2: Model validation for estimating soil respiration during Year 2 for homoscedasticity, normality of residuals, and outliers and random effects.

Figure S4-3 shows the correlations between soil nutrient availability (NO_3^- -N Fig. S4-3a; NH_4^+ -N Fig. S4-3b; and PO_4^{3-} -P Fig. S4-3c) and N:P ratios (Fig. S4-4d), and VWC, T_s and Pr at BIFoR FACE during Year 2 of eCO_2 enrichment. The highest availability for all three nutrients was observed under conditions of high precipitation low VWC and $T_s > 12^\circ\text{C}$. This indicates that Pr was a main driver during the warmer and drier period of Year 2 of eCO_2 enrichment at BIFoR FACE.

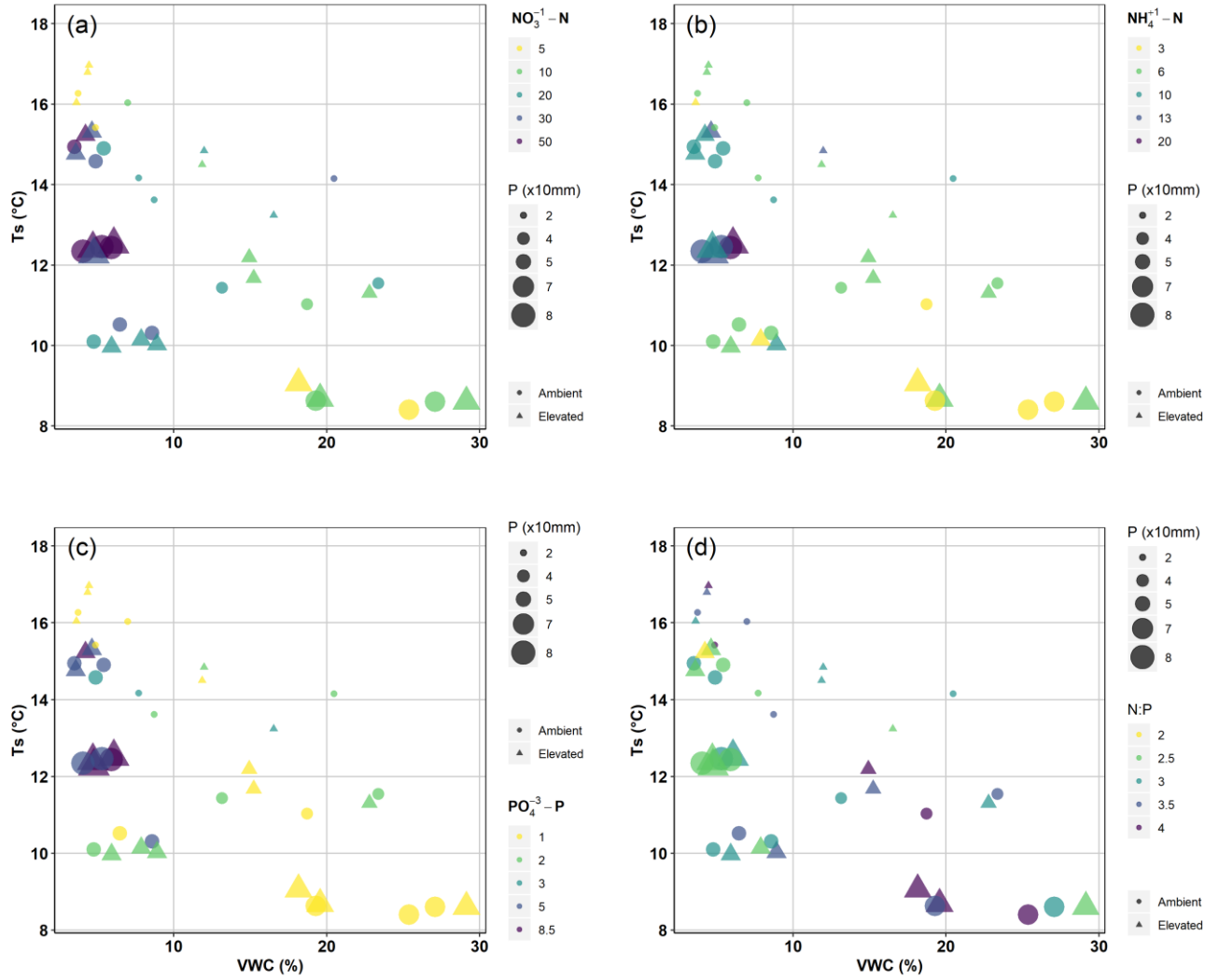


Figure S4- 3: (a) $NO_3^- - N$, (b) $NH_4^+ - N$, (c) $PO_4^{3-} - P$ availability and (d) N:P ratios in correlation with VWC, T_s and P at BIFoR FACE during Year 2 of eCO_2 enrichment. The triangles reflect the eCO_2 conditions while the circles reflect the ambient conditions. The colour luminance reflects the availability of soil nutrients and N:P ratios, which turns darker as the nutrient availability increases. The size of the shapes reflect the monthly cumulative precipitation in *10 mm, which increases as the precipitation increases.

Table S4- 1: Summary of mixed-effects models of the eCO₂, soil horizons, and sampling campaign during Year 2 of eCO₂ enrichment on gravimetric volume content, soil extractable NH₄⁺-N, soil extractable NO₃⁻-N, microbial biomass C, N and P and microbial C:N, N:P and C:P ratios. *P* < 0.1 is shown in bold.

		Covariates						
Response variables		eCO ₂	Horizons O-A	Horizons O-B	Horizons A-B	Spring-Summer	Spring-Autumn	Summer-Autumn
Gravimetric volume content	t	1.204	4.069	4.950	-0.881	-2.532	1.189	-1.343
	df	4	152	152	152	152	152	152
	P	0.295	0.0001	<0.001	1	0.034	0.704	0.538
Soil extractable NH ₄ ⁺ -N	t	-0.401	3.751	4.061	-0.310	3.257	-0.094	3.163
	df	4	152	152	152	152	152	152
	P	0.709	0.0005	0.0001	1	0.003	1	0.005
Soil extractable NO ₃ ⁻ -N	t	-1.057	7.765	9.218	-1.452	-0.920	-1.858	-2.778
	df	4	152	152	152	152	152	152
	P	0.350	<0.001	<0.001	0.439	1	0.190	0.02
Microbial biomass C	t	1.264	4.719	5.976	-1.275	1.506	-0.649	0.863
	Df	150	146	146	146	146	146	146
	P	0.208	<0.001	<0.001	0.607	0.396	1	1
Microbial biomass N	t	0.294	2.862	3.242	-0.439	6.988	0.019	6.799
	Df	154	150	150	150	150	150	150
	P	0.769	0.013	0.004	1	<0.001	1	<0.001
Microbial biomass P	t	1.071	3.379	3.795	-0.422	-	1.389	-
	Df	104	100	100	100	-	102	-
	P	0.288	0.002	0.0004	1	-	0.168	-
Microbial ratio C:N	t	0.561	-0.414	-1.727	1.320	-0.979	-1.680	-2.545
	Df	142	138	138	138	138	138	138
	P	0.576	1	0.253	0.560	0.982	0.279	0.033
Microbial ratio N:P	t	1.063	-0.192	-0.001	-0.185	-	-0.100	-
	Df	95	91	91	91	-	93	-
	P	0.290	1	1	1	-	0.921	-
Microbial ratio C:P	t	0.195	-0.298	-1.498	1.231	-	-1.280	-
	Df	95	91	91	91	-	93	-
	P	0.845	1	0.402	0.654	-	0.204	-

Table S4- 2: Analysis of variance results for VWC and T_s during Year 2 at BIFoR FACE. p -value < 0.1 is shown in bold.

Variables	DF _{num}	DF _{den}	F-value	P-value
<i>VWC</i>				
eCO ₂	1	4.0	0.375	0.574
Year	2	4076.4	250.675	<0.001
eCO ₂ * Year	2	4076.4	47.960	<0.001
<i>T_s</i>				
eCO ₂	1	4.3	1.511	0.282
Year	2	4265.4	179.933	<0.001
eCO ₂ * Year	2	4265.4	2.406	0.090

Chapter 5: A double entendre challenge - Partitioning the components of soil respiration in a mature temperate woodland under eCO₂

5.1 Abstract

Soil respiration is the second-largest C flux after photosynthesis; however, the partitioning of soil respiration to biogenic sources remains difficult. The correct quantification of the contribution of its components to total soil respiration is of pivotal importance not only for the ecosystem's potential to uptake carbon but also to assess the carbon's fate within the ecosystem. Furthermore, disentangling total soil respiration to components contribution and thus to CO₂-derived sources and their responses to abiotic factors will improve the high uncertainty associated with the climatic models' carbon cycle. Here, we attempted to quantify the soil respiration to four respiratory components (heterotrophic, autotrophic, and the further partition to root and hyphal respiration) during the first two years of Free Air CO₂ Enrichment (FACE) at a mature temperate woodland (BIFoR FACE). We observed that eCO₂ stimulated all respiratory components, except for root respiration, during the experiment's first year. This contribution was persistent during the second year through a series of extreme events (winter moth defoliation event, heatwave). The heterotrophic component was the main contributor to soil respiration in both years (over 70 and 80% during Year 1 and 2, respectively). However, the respiratory components' sensitivities to abiotic factors (soil temperature and moisture) were altered under the combined effects of eCO₂ and extreme events.

5.2 Introduction

The global average atmospheric CO₂ concentration in 2019 was 411.44 ppm and is the highest recorded in the past 800,000 years (<https://www.esrl.noaa.gov/gmd/ccgg/trends/>). Both the magnitude and the scale of the estimated atmospheric CO₂ increment have been suggested to depend on human-induced emissions, as well as on the efficiency with which ecosystems assimilate carbon (C) and store it (UNFCCC, 2005; Friedlingstein *et al.*, 2006; Friedlingstein *et al.*, 2014). Land vegetation and soil, collectively forming the terrestrial biosphere, are crucial components in the C biogeochemical cycle, currently amassing a mean of 450 Pg C as biomass stocks (Erb *et al.*, 2018). Thus, changes in the atmospheric CO₂ concentrations might have a potentially significant effect on C storage in the terrestrial biosphere due to either release or sequestration of C (Houghton, 2007).

Soil respiration (R_s), the CO₂ efflux from the forest soil, combines autotrophic root activity and associated rhizosphere organisms, heterotrophic bacteria and fungi, and soil fauna activity. R_s is divided into autotrophic respiration (R_a), which is the CO₂ produced from the metabolic activity for root growth and maintenance; and heterotrophic respiration (R_h), which is the CO₂ produced from the decomposition of organic matter used as an energy source for microbial communities (Savage *et al.*, 2013). R_a can be further partitioned to ectomycorrhizal (EM) fungi respiration (R_m) and root respiration (R_r). Although the analytical techniques used for assessing R_s have been improved (Raich and Schlesinger, 1992; Davidson *et al.*, 2002; Baldocchi, 2003), there is still little information about the individual CO₂ emissions of the respiratory components, mainly due to the difficulty in separating the root from the EM, *in situ*, thus leading to overestimation of the R_a and underestimations of the R_h (Tomè *et al.*, 2016). Moreover, temporal sampling limitations, high-cost of measurement

instruments (Savage, Davidson, and Richardson, 2008), and R_s 's high variability both temporally and spatially (Bond-Lamberty and Thomson, 2010), add significant uncertainty to global C cycle models.

R_s accounts for 60-90% of total ecosystem respiration (Longdoz, Yernaux, and Aubinet, 2000) and is the second-largest flux of C between terrestrial ecosystems and the atmosphere (Raich and Schlesinger, 1992; Zhao *et al.*, 2017). Nevertheless, R_s is one of the least-studied elements of the terrestrial C cycle due to the challenges faced in spatial and temporal sampling and the high-cost measurement instruments (Savage, Davidson and Richardson, 2008). However, each soil component (roots, fungi, free-living microbes, and soil animals) has a unique dependence on substrate quality and abiotic factors and may exhibit different behaviours under a change in their environment or climate change (Wei, Weile and Shaopeng, 2010; Ma *et al.*, 2014). Thus, it is pivotal to successfully quantify the flux from each component, better understand the drivers and the processes involved, and make more accurate model predictions.

Over the last thirty years, the terrestrial biosphere provided a net sink for approximately 20% of the CO_2 emitted by anthropogenic emissions (Quéré *et al.*, 2018), with the forest ecosystems dominating the C storage (Pan *et al.*, 2011). Forest ecosystems play a significant role in the global C cycle since 80% of all aboveground terrestrial C, and 40% of belowground C are stored in forest biomass (Goodale *et al.*, 2002). Specifically, old-growth forests can store the sequestered C at exceptionally high levels compared to young and mature forests (Keith, Mackey and Lindenmayer, 2009; Keeton *et al.*, 2011; Burrascano *et al.*, 2013; McGarvey *et al.*, 2015), thus playing a crucial role in climate mitigation (Keeton, 2019). However, old-growth forests' response under elevated atmospheric CO_2 (eCO_2) yet remains uncertain. Although

eCO₂ has been observed to increase tree growth rates in young forests (Kallarackal and Roby, 2012), no study has been conducted in mature or old-growth forests, except for the EucFACE experiment in Australia. Growth responses due to eCO₂, and subsequently forest's capacity to sequester and store C long-term, might be constrained by environmental factors, such as soil moisture and soil nutrient availability (Keeton, 2019). Since the extent to which eCO₂ has transient or long-lasting effects on the factors mentioned above is yet uncertain, the question about the carbon storage capacity within old-growth forests under climate change is yet to be answered.

In the present study, we assessed the soil respiratory components' contribution (autotrophic respiration, R_a ; heterotrophic respiration, R_h ; hyphal respiration, R_m , and root respiration, R_r) to the total soil respiration at BIFoR FACE during the first two years of CO₂ enrichment. To our knowledge, this is the first study attempting to quantify the soil respiratory components in a mature temperate woodland under elevated CO₂ (eCO₂) using high-frequency automated measurements.

5.3 Methodology

A detailed description of the experimental site, Birmingham's Institute of Forest Research Free-Air Carbon Dioxide Enrichment (BIFoR FACE) facility, environmental drivers (VWC, T_s , and P_r) soil respiration components can be found in Chapter 2 of the thesis. This Chapter focuses on data collected during the Pre-treatment period (October 2016 –March 2017), Year 1, and Year 2 of eCO₂ enrichment (April 2017 – October 2018).

Briefly, BIFoR FACE is a temperate deciduous old-growth (>160 years) oak woodland located within Mill Haft at Staffordshire, England. The soil is brown earth cambisol with a sandy-clay texture and a mean soil pH of 4.5 at the top 10 cm. Mean soil total N and P in the top 10 cm are 0.28% and 18 mg P kg⁻¹, respectively, indicating that BIFoR is a low nutrient woodland, and total organic matter content is 3.67%.

A detailed FACE facility description can be found in Hart *et al.* (2019). Briefly, the BIFoR FACE facility comprises six 30 m diameter infrastructure arrays (elevated CO₂ (eCO₂ hereafter), n = 3; controls (*Ambient*, hereafter), n = 3) and three non-infrastructure arrays. Year 1 of eCO₂ enrichment began on 3 April 2017 until 27 October 2017, while Year 2 began on the 26 March 2018 until 31 October 2018. eCO₂ enrichment took place from budburst to leaf fall approximately, and only during light hours, depending on the solar angle. During the first year of eCO₂ enrichment, eCO₂ arrays were within the 10% of target for 81.6% of the scheduled operation time and 20% of the target within 96.7% of scheduled operation time (Hart *et al.*, 2019). Contamination of the ambient arrays by CO₂ from the eCO₂ arrays was rare and short-lived, with ambient arrays being 10% of the control setpoint 98.8% of the time.

5.3.1 Measurements - Soil respiration and its partition components

Eighteen (18) experimental blocks were established across the site, 9 in ambient arrays and 9 in eCO₂ arrays (Figure 5.1), as proposed by Heinemeyer *et al.* (2007). Collars were installed in June 2016 (9 months before CO₂ fertilization), minimizing the effect of soil disturbance on soil respiration measurements, and left during the summer period for settlement; the soil collars were permanently installed to reduce soil

disturbance by repeated measurements and to ensure that the same soil was measured over time (King *et al.*, 2004).

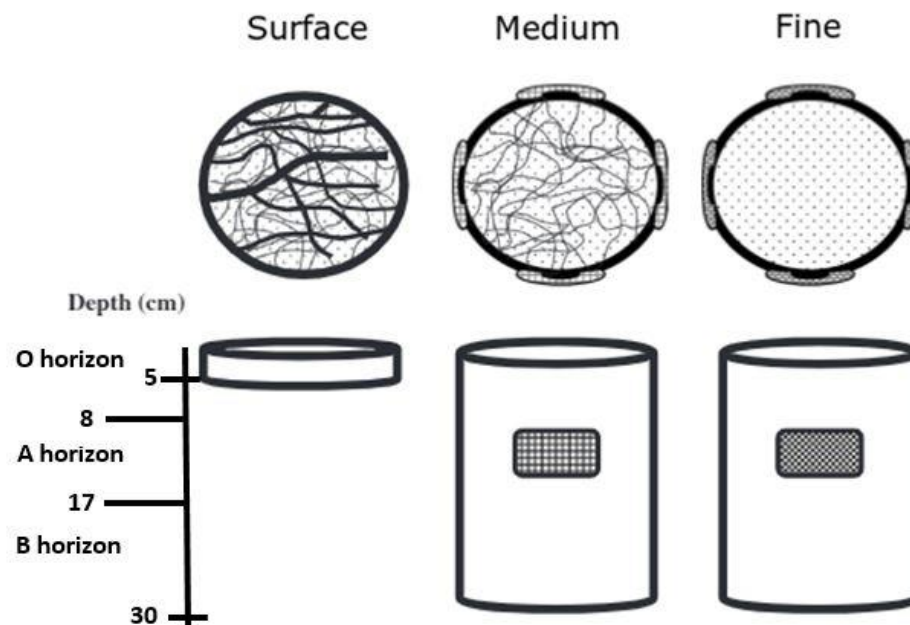


Figure 5- 1: Schematic representation of the soil respiration experimental blocks used at BIFoR FACE (adapted from Heinemeyer *et al.*, 2007). Surface collars were only 5 cm deep inserted in the soil allowing roots, hyphal, and microbial growth. Medium and fine collars were inserted 30 cm deep in the soil, excluding fine roots from entering inside the collar. The fine collars were allowing only microbial growth.

Each block consisted of one PVC shallow collar (Drainage Superstore, Plymouth, UK) and two deeper collars with different mesh treatments. All collars were 200 mm in diameter, the shallow collars (*surface* collars hereafter) were 5 cm in height, and the deeper collars were 30 cm in height. The shallow collar was inserted only 3 cm in the soil, pressed firmly onto the litter layer with three 20cm long stainless steel rods attached at the bottom of the collar to prevent dislocation by human or animal activity. The stainless steel rods ensured that no roots were severed while an airtight seal was achieved, avoiding potential lateral diffusion of CO₂. These collars did not interfere

with fine roots, mycorrhizal, or microbial dynamics and growth. The two deeper collars were inserted at approximately 25 cm depth, preventing fine root ingrowth which is concentrated mainly in the upper centimetres of the soil (Jackson, Mooney, and Schulze, 1997), and had 4 rectangular (5cm x 5 cm) windows cut into their sides which were covered with nylon meshes, with grids size of 41 μm (Ek, 1997) (*medium* collars hereafter) and 1 μm (*fine* collars hereafter) allowing or excluding ectomycorrhizal hyphal ingrowth, respectively. In summary, there are 3 surface, 3 medium, and 3 fine collars in every ambient and eCO₂ array (18 collars of each treatment across the site).

The experimental design suffered from new fine roots' growth inside the root exclusion collars (see section 5.8 *Supplementary Material*). Higher respiration rates were observed in root exclusion collars than the associated surface collars. At the end of Year 2, the exclusion collars with such behaviours were excavated carefully without causing disturbance to the neighbouring collars of the block. All the exclusion collars found to be compromised by fine root ingrowth were excluded from the analysis, leading to three medium and ten fine collars excluded from the data analyses. In total, eighteen (9 in ambient and 9 in eCO₂ arrays) surface, 15 (8 ambient and 7 in eCO₂ arrays) medium, and 8 (4 in ambient and 4 in eCO₂ arrays) fine collars were used for the data analysis.

With the experimental design as described above, partitioning the soil respiration into total (R_s), autotrophic (R_a), and heterotrophic (R_h) was enabled. The R_a was partitioned further to fine root (R_r) and hyphal (R_m) respiration. R_s and R_h were measured directly from the surface and fine collars, respectively. R_a was calculated by subtracting the values of the fine collars from those of the surface collars, R_r was calculated by subtracting the values of the medium collars from the surface collars, and lastly, R_m was calculated by subtracting the values of the fine collars from the medium collars.

To enable a better understanding, please refer to *Chapter 2* section 2.2.1.1. *Experimental design* where the equations used for the soil respiration partitioning calculations can be found.

Automated measurements of R_s were taken at 1-hour intervals at all three experimental blocks in an eCO₂ array and its paired ambient array simultaneously, using 20-cm-diameter long-term chambers interfaced with a multiplexer and an infra-red gas analyser (IRGA) (Li-8100-104 long-term chambers, Li-8150 multiplexer, and Li-8100A IRGA; Licor). The observation length was 2 min with a 20 s deadband, a 15 s pre-purge, and a 45 s post purge, giving a total measurement cycle of 3 min 20 s per collar. The measurements began on 19 October 2016 (5 months before the beginning of eCO₂ enrichment), and we report data until 31 October 2018 (end of Year 2 of eCO₂ enrichment). The LI-COR systems were moved every two weeks between replicating paired eCO₂ and ambient array and returning to the same array pair on a 4-week rotation.

All data went through quality checks before analysis using SoilFluxPro software, version 4.0.1 (LI-COR, Nebraska, USA). Data points with negative linear fluxes or data points with a linear flux coefficient of variation higher than 3.5 were removed from the dataset, as these were indicative of leaks in the chamber. Data points with a linear flux coefficient of variation between 1.5 and 3.5 were manually checked for assessing the fit quality. Of a total of 320,976 data points during the total period of operation as mentioned above, 195,124 data points were available for analysis, primarily due to equipment failures (water condensation in the electric plates) and, to a less extent, due to poor-quality fits. However, due to other experimental design failures (fine roots penetrated the root exclusion collars from the bottom and/or through the failed meshed windows), only 144,294 data points were used for this Chapter's analysis. That led to

an approximately 50% data loss in total. Daily and monthly averages of these data are reported in this Chapter in $\mu\text{mol CO}_2 \text{ m}^{-2} \text{ s}^{-1}$.

5.3.2 Statistical analysis

All analyses were carried out using R 3.6.2 and Rstudio 1.2.5033 (RStudio Team, 2019). However, due to the limitations of the experimental design's failure, only descriptive statistics were performed for this Chapter.

5.4 Results

Fig.5-2 shows R_h , R_a , R_r , and R_m 's seasonal course during the first two years of eCO_2 enrichment at BIFoR FACE. During Year 1, all soil respiratory components exhibited the same seasonal pattern, increasing until mid-summer, followed by a decrease as the growing season came to an end. Both R_a and R_h were higher in eCO_2 arrays during the first year of eCO_2 enrichment. Subsequently, R_a was further partitioned to R_r and R_m . Although R_m was observed to respond to eCO_2 as the R_h , R_r was the only soil respiratory component to exhibit higher rates in ambient arrays.

All soil respiratory components exhibited low rates during the Dormant period. During Year 2, R_h had the same response towards eCO_2 as in Year 1 (higher in eCO_2 arrays). However, the seasonal pattern was not the same. R_h in ambient arrays exhibited the lowest rates in late spring (May 2018) and gradually increased as the growing season finished. Contrary, R_h in eCO_2 arrays increased until early summer, followed by a decrease in July 2018, only to increase again. R_a was observed to follow a similar seasonal pattern as R_h ; higher rates at the beginning of the growing season, followed by a decrease in midsummer rates. Due to the experimental design limitations and

instrumental failures, no clear conclusions can be drawn once R_a was further partitioned to R_r and R_m .

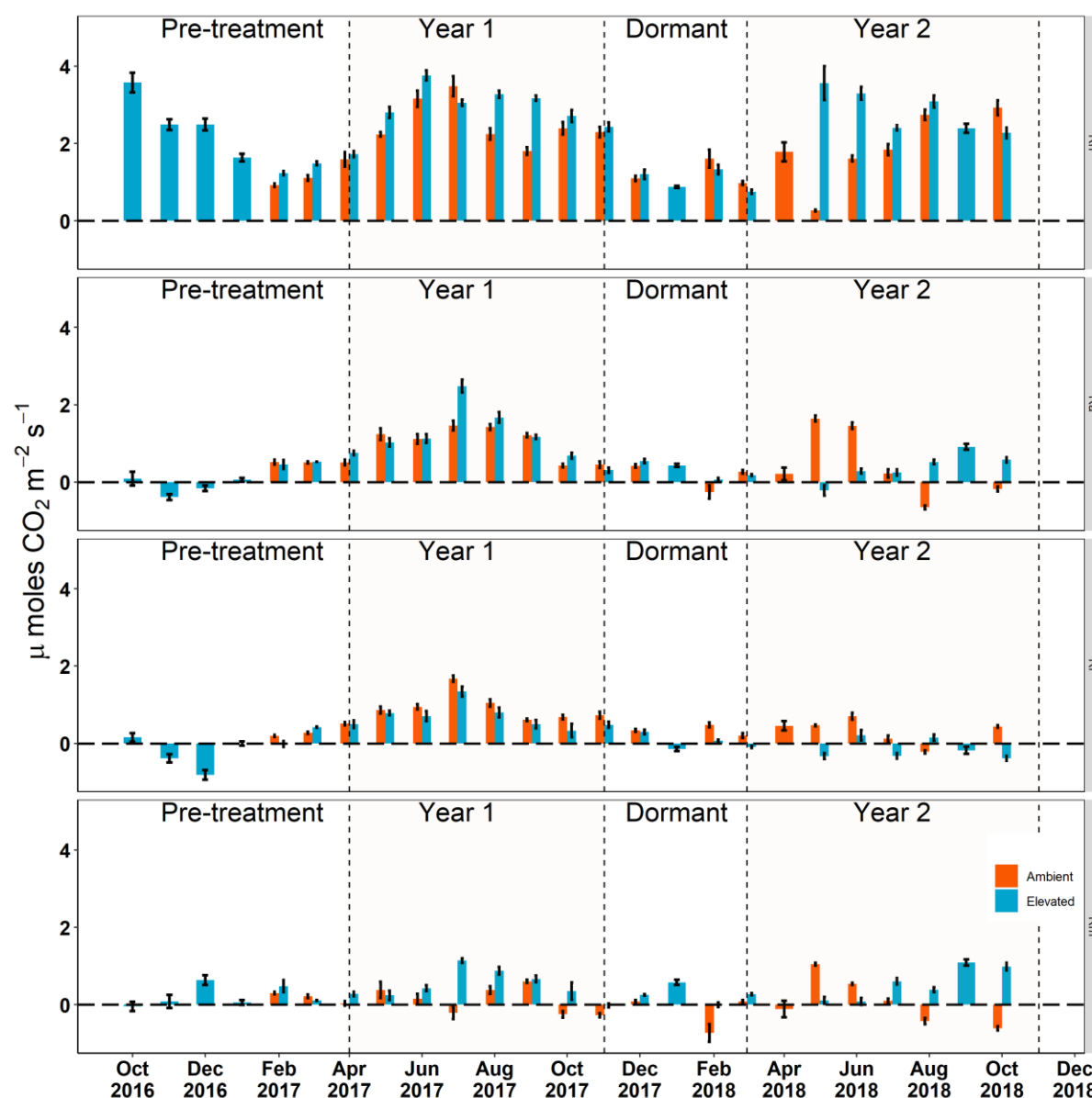


Figure 5- 2: Seasonal course of heterotrophic respiration, R_h ; autotrophic respiration R_a ; root respiration, R_r , and hyphal respiration, R_m during the Pre-treatment and first two years of eCO₂ enrichment (October 2016 – October 2018). The blue coloured bars denote the eCO₂ arrays, while the orange bars denote the ambient arrays. All data describe monthly averages, while the error bars denote standard error.

Figure 5-3 shows the percentage contribution of all soil respiratory components (R_h , R_a , R_r , and R_m) to total soil respiration, on an annual basis, in ambient and eCO₂ arrays

for the first two years of eCO₂ enrichment at BIFoR FACE. R_h was observed to be the main contributor of soil respiration, responsible for over 70 and 80% respiration rates during Year 1 and 2 of eCO₂ enrichment, respectively. By further partitioning R_a, R_r was the main contributor of R_a, accounting for over half of the R_a rates during Year 1. For Year 2, R_a partition was limited by experimental design and instrumental failures.

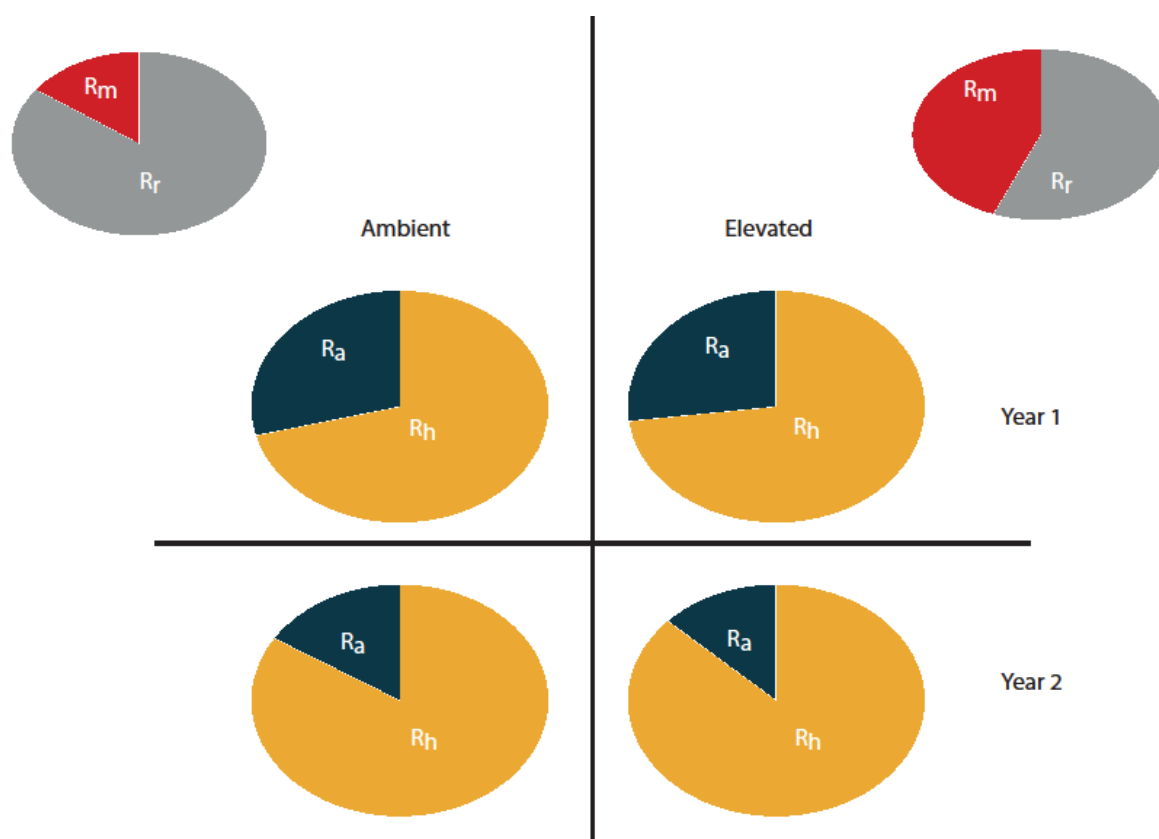


Figure 5- 3: Percentage contribution of soil respiratory components (R_h, R_a, R_r, and R_m), on an annual basis, to total soil respiration in ambient and eCO₂ arrays during the first two years of eCO₂ enrichment at BIFoR FACE. Note that partitioning R_a to R_r and R_m during Year 2 was not possible.

R_h and R_a contribution in ambient and eCO₂ arrays were similar during Year 1, with R_a contributing less in the total soil respiration in eCO₂ than in ambient arrays (R_h: 71% in ambient vs. 73% in eCO₂ arrays; R_a: 29% in ambient vs. 27% in eCO₂ arrays). Once R_a was partitioned to R_r and R_m, R_r was responsible for 85% of the R_a in ambient arrays (R_r 85% and R_m 15% in ambient arrays). Interestingly, in eCO₂ arrays, although

R_r was found to be the main R_a contributor, R_m contribution was greater than the one in ambient arrays, responsible for almost half of the R_a (R_r 56% and R_m 44% in eCO_2 arrays). In Year 2, although R_h was again the main contributor of soil respiration, the contribution was higher than Year 1 (84% vs. 87% in ambient and eCO_2 arrays, respectively), forcing R_a to contribute less (16% vs. 13% in ambient and eCO_2 arrays, respectively).

All respiratory components were observed to be higher in eCO_2 arrays during the first year of the eCO_2 enrichment, except for R_r , which was higher in ambient arrays (Fig. 5-4). Specifically, R_h , R_a , and R_m were higher by 17, 7, and 217%, respectively, in eCO_2 arrays, while R_r was 40% higher in ambient arrays. During the second year of eCO_2 enrichment, R_h was 29% higher in eCO_2 than in ambient arrays, whereas R_a was similar between ambient and eCO_2 arrays (only 0.8% higher in ambient arrays).

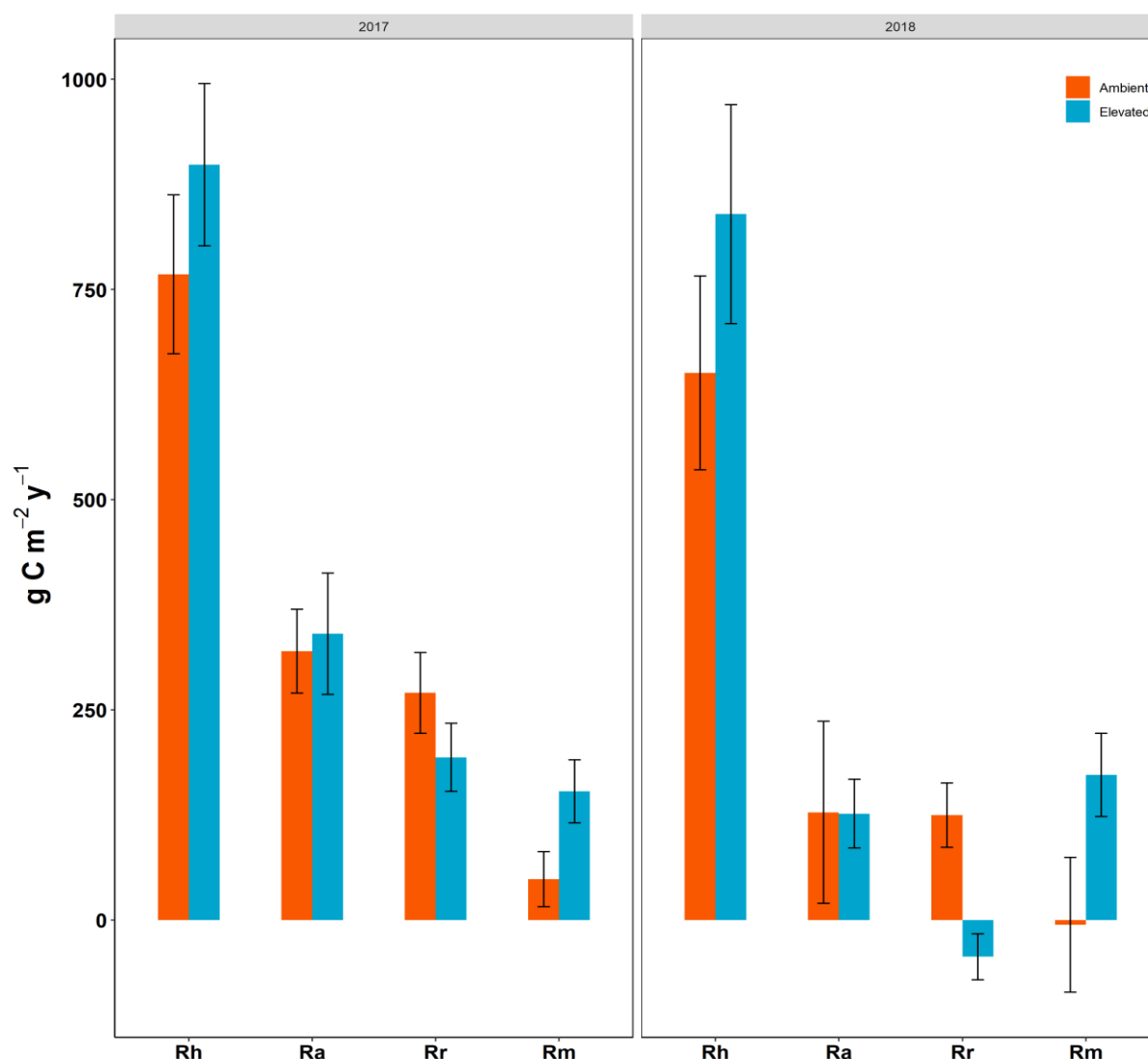


Figure 5- 4: Mean annual R_h , R_a , R_r , and R_m in ambient (orange) and eCO_2 (blue) arrays during the first two years of eCO_2 enrichment at BIFoR FACE. The error bars denote the se.

In 2017 (Year 1) all soil respiratory components had very weak negative responses on VWC (Fig. 5.5). The relationship between R_h and VWC was marginally significant in both ambient and eCO_2 arrays, while the relationship between both R_a and R_r and VWC in ambient arrays was significant. In contrast, in eCO_2 arrays, the relationships between R_a and R_r and VWC were marginally significant and not significant, respectively. R_m relationship with VWC was significant only in eCO_2 arrays, while in ambient arrays, the relationship was observed not to be significant. All respiratory

components were more sensitive to VWC in ambient arrays, except for R_m , which was more sensitive to VWC in eCO₂ arrays (see section 5.8 *Supplementary Material*, Table S5-1).

During Year 2 (2018), the soil respiratory components' responses on VWC were different from those in Year 1 (Fig. 5-5). All respiratory components were more sensitive to VWC in eCO₂ arrays (see section 5.8 *Supplementary Material*, Table S5-1). Moreover, all respiratory components (R_a , R_r , and R_m) in ambient arrays had a very weak positive response on VWC, except R_h , which had a weak negative response on VWC. The soil respiratory components' responses on VWC in eCO₂ arrays were precisely the opposite of those observed in ambient arrays. All soil respiratory components (R_a , R_r , and R_m) had a weakly positive response on VWC, except R_h , which had a moderate response on VWC. All correlations were significant, except R_a , R_r , and R_m and VWC in ambient arrays that were not significant, and R_r and VWC in eCO₂ arrays were marginally significant.

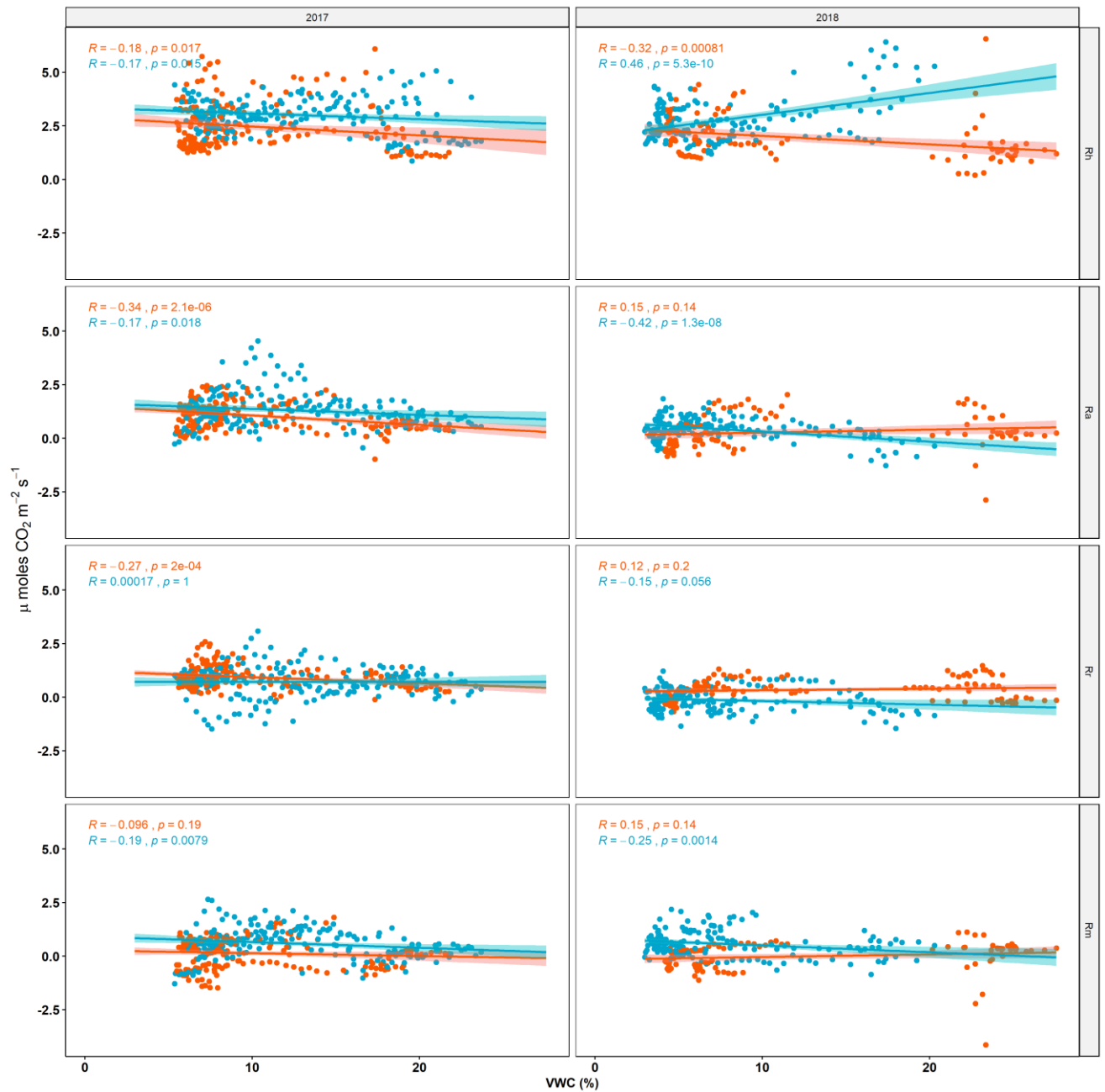


Figure 5- 5: R_h , R_a , R_r , and R_m responses on VWC in both ambient and eCO₂ arrays during the first two years of eCO₂ enrichment at BIFoR FACE. The blue solid points represent the eCO₂ arrays, while the orange solid points represent the ambient arrays.

Both R_h and R_a respiratory components were observed to have moderate but significant relationships with T_s during the first year of eCO₂ enrichment (Fig. 5-6). The relationship was stronger under eCO₂ for R_h , while T and R_a 's relationship was similar between ambient and eCO₂ arrays. R_r and soil temperature relationship were moderate and weak in ambient and eCO₂ arrays, respectively, but significant.

However, R_m was observed to have precisely the opposite pattern than R_r ; R_m and T relationship was weak and not significant in ambient arrays. The relationship was moderate but significant in eCO_2 arrays. R_h and R_r were more sensitive to T_s in ambient arrays, whereas R_a and R_m were more sensitive to T_s in eCO_2 arrays (see section 5.8 *Supplementary Material*, Table S5-1).

However, during the second year of eCO_2 enrichment, the relationship between T_s and all respiratory components changed either weak or no relationship at all (Fig. 5-6). Both R_a and R_h components had a weak and non-significant relationship with T in ambient arrays. In eCO_2 arrays, the R_h and R_a relationships with T_s were weak positive and negative, respectively, albeit both significant. The further R_a partitioning, R_r and R_m , had no relationship with T in ambient arrays. In eCO_2 arrays, the R_r relationship with T_s was weak and not significant, while R_m had a moderate relationship with T_s , but it was significant. All respiratory components were more sensitive to T in eCO_2 arrays during the second year of the experiment (see section 5.8 *Supplementary Material*, Table S5-1).

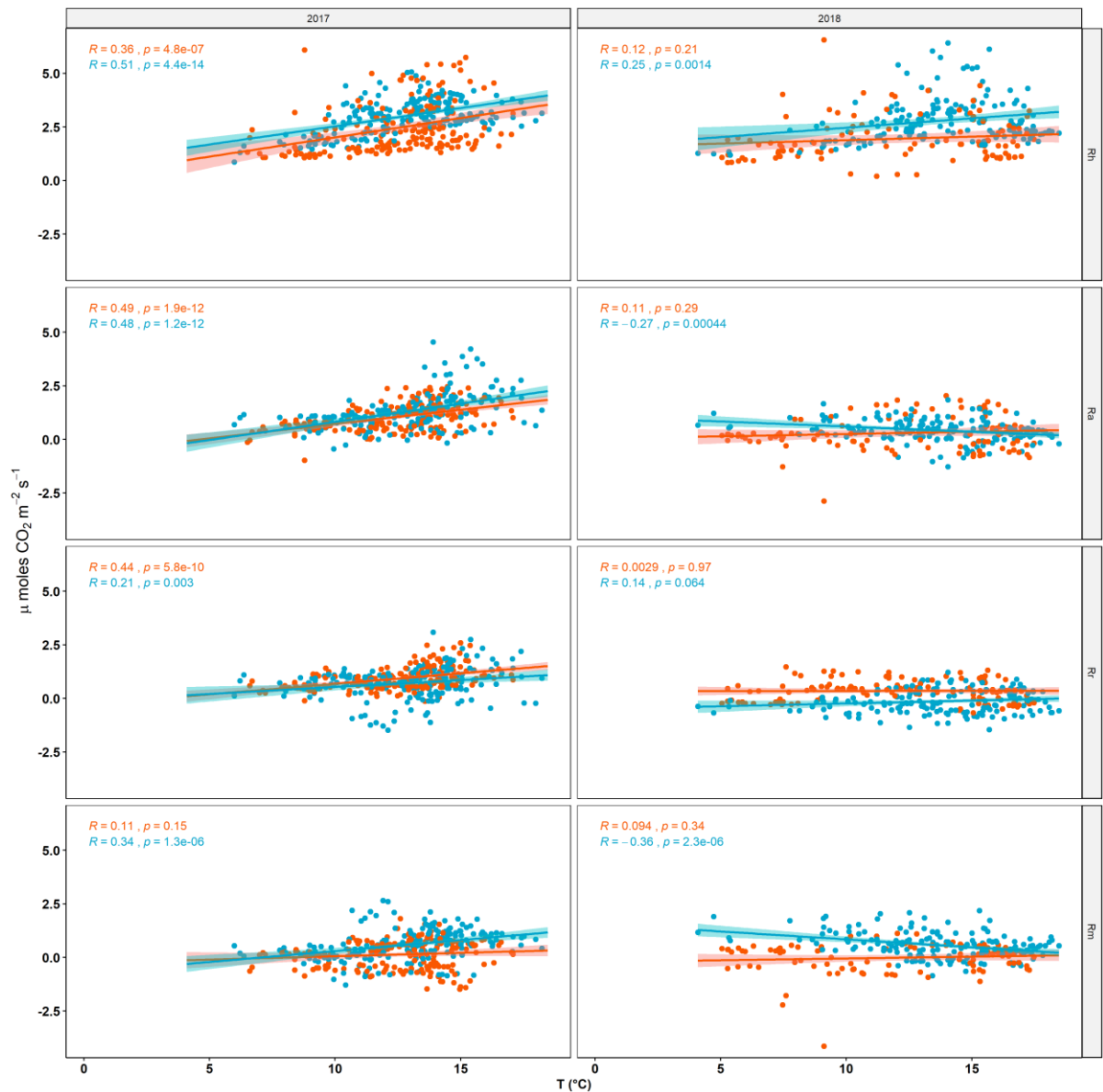


Figure 5- 6: R_h , R_a , R_i , and R_m responses on T_s in both ambient and eCO₂ arrays during the first two years of eCO₂ enrichment at BIFoR FACE. The blue solid points represent the eCO₂ arrays, while the orange solid points represent the ambient arrays.

5.5 Discussion

One of the most popular techniques for partitioning soil respiration into components, especially in forest ecosystems, is the root exclusion/ trenching technique (Bowden *et al.*, 1993; Buchmann, 2000; Ross *et al.*, 2001; Lee *et al.*, 2003; Heinemeyer *et al.*, 2007). It is a simple technique with a relatively easy and cheap installation that could be appropriate for long-term measurements, ensuring repeatability. In principle, the

technique should provide a robust estimate of the root-, hyphal- and heterotrophic-derived CO₂. In reality, though, the exclusion technique can only provide a rough estimate of the different soil components'-derived CO₂ due to multiple limitations observed between root inclusion and root exclusion soil, such as a) different microclimatic conditions (Fisher and Gosz, 1986; Ross *et al.*, 2001), b) altered nutrient cycles (Dormaar, 1990; Kuzyakov, 2002; Paterson *et al.*, 2003; Cheng and Kuzyakov, 2005), and c) experimental design failures (section 5.8 *Supplementary material* Fig. S5-7). Due to the above limitations and the other instrumental failures experienced in the two years, caution must be taken when extrapolating the results of this chapter, especially during Year 2, when the autotrophic respiration component partitioning became impossible.

This Chapter assessed soil respiration's partition to its respiratory components (heterotrophic, autotrophic, root, and mycorrhizal respiration) during the first two years of eCO₂ enrichment at BIFoR FACE. Each component was observed to have strong seasonal patterns during both years of eCO₂ enrichment (Fig. 5-2). All soil respiratory components were found to have higher fluxes during the growing seasons and lower fluxes during dormant seasons. The soil respiratory components' seasonal patterns observed in this Chapter follow similar seasonal patterns with the abiotic factors (soil moisture and soil temperature) described in *Chapters 3 and 4*, in which fluxes increased as soil temperature increased and soil moisture decreased.

Soil moisture was observed to have significant but weak effects on both autotrophic and heterotrophic respiratory components (Fig. 5-5) in both ambient and eCO₂ arrays during Year 1 of eCO₂ enrichment at BIFoR FACE. Exceptions on these observations were the root respiration in eCO₂ arrays and mycorrhizal respiration in ambient arrays, where soil moisture was observed not to affect them. Both heterotrophic and

autotrophic respiratory components were observed to have moderate but significant relationships with soil temperature during the first year of eCO₂ enrichment (Fig. 5-6), while the relationships between soil temperature and the autotrophic partition components (root and mycorrhizal components) were observed to be weaker but still significant (except R_m in ambient arrays in which the relationship was not significant).

The relationship patterns between soil moisture and soil respiratory components during Year 2 differ substantially from those observed during Year 1 (Fig. 5-5). Only the heterotrophic component had a moderate negative relationship with soil moisture, which was significant. In contrast, the autotrophic component, including root and mycorrhizal components, had very weak positive relationships with soil moisture that was not significant. In eCO₂ arrays, the exact opposite pattern was observed. Only the heterotrophic component had a moderately positive relationship with soil moisture. In contrast, the autotrophic components, including root and mycorrhizal respirations, had moderate and weak negative relationships with soil moisture, respectively. All relationships between soil moisture and soil respiratory components in eCO₂ arrays were significant during Year 2 of eCO₂ enrichment at BIFoR FACE.

During the second year of eCO₂ enrichment (extreme events year; see *Chapter 4*), all soil respiratory components had no relationship with soil temperature in ambient arrays. In eCO₂ arrays, only the heterotrophic respiration was observed to correlate with soil temperature positively; weak but significant. Soil temperature was observed to have a significant but weak negative effect on autotrophic respiration, and the same effect was observed with mycorrhizal respiration. Soil temperature did not affect root respiration in eCO₂ arrays.

During the first year of eCO₂ enrichment at BIFoR FACE, the heterotrophic and autotrophic component of soil respiration responded similarly to abiotic factors (soil moisture and soil temperature; Fig. 5-5 and 5-6 respectively), although it has been observed that both components can respond differently to biotic and abiotic controlling factors, as well as their interactions (Trueman and Gonzalez-Meler, 2005; Kuzyakov and Gavrichkova, 2010; Taneva and Gonzalez-Meler, 2011). The heterotrophic component was slightly less sensitive to soil moisture than the autotrophic component in both ambient and eCO₂ arrays during Year 1 (Gomez-Casanovas *et al.*, 2012).

Moreover, the heterotrophic component was more sensitive to soil temperature than the autotrophic component in ambient arrays (Gomez-Casanovas *et al.*, 2012), while they had the same sensitivity in eCO₂ arrays. During the second year of eCO₂ enrichment, the heterotrophic component was more sensitive to both soil moisture and temperature in both ambient and eCO₂ arrays. Interestingly our data are in agreement with studies in grasslands and prairies (Luo *et al.*, 2001; Hartley *et al.*, 2007; Bahn *et al.*, 2009), microcosms model systems (Bååth and Wallander, 2003), and forest ecosystems (Heinemeyer *et al.*, 2007; Högberg, 2010; Wei, Weile and Shaopeng, 2010).

The extreme events stressors altered the sensitivities of the soil respiratory components to abiotic factors. In ambient arrays, all respiratory components were less sensitive to soil moisture in Year 2 versus Year 1, except for the heterotrophic component, which had the same sensitivity to soil moisture both years. However, in eCO₂ arrays, all soil respiratory components were more sensitive to soil moisture in Year 2. Moreover, both autotrophic and heterotrophic components were less sensitive to soil temperature in both ambient and eCO₂ arrays in Year 2.

Although the general patterns in the relationships between the soil respiratory components and the abiotic factors were similar during the first year of eCO₂ enrichment, their sensitivities to the abiotic factors differed between ambient and eCO₂ arrays. Soil respiratory components were less sensitive to soil moisture in eCO₂ arrays, except for mycorrhizal respiration, which was less sensitive to soil moisture in ambient arrays (section 5.8 *Supplementary Material*, Table S5-1). Moreover, only the autotrophic and mycorrhizal respiration were more sensitive to soil temperature in eCO₂ arrays. During the second year of the experiment, which concurred with a series of extreme events, all soil respiratory components were more sensitive to both soil moisture and soil temperature in eCO₂ arrays.

Heterotrophic respiration was observed to be the main contributor to soil respiration in both years, accounting for almost $\frac{3}{4}$ of the total soil respiration in both ambient and eCO₂ arrays (Fig. 5-3). Our data agree with previous studies conducted in temperate forests (Matamala and Schlesinger, 2000; Subke, et al., 2006; Taneva and Gonzalez-Meler, 2011). By further attempting to partition autotrophic respiration to root and mycorrhizal respiration (only possible for the first year of eCO₂ enrichment), root respiration was the main contributor of autotrophic respiration in both ambient and eCO₂ conditions (autotrophic partitioning data available only for Year 1). Although the autotrophic/heterotrophic contribution ratio was similar between ambient and eCO₂ arrays during Year 1 of eCO₂ enrichment, the root and mycorrhizal contribution was substantially altered in eCO₂ arrays, with mycorrhizal respiration contributing 29% more to autotrophic respiration. This observation agrees with previous studies (Staddon, Gregersen and Jakobsen, 2004), where mycorrhizal abundance was observed to be stimulated under eCO₂ by increased C allocation belowground.

Heterotrophic respiration was observed to contribute more to total soil respiration during Year 2 in ambient and eCO₂ arrays. Autotrophic respiration contributed less to total soil respiration during the second year of the experiment. During the second year of eCO₂ enrichment, UK experienced a prolonged heatwave during the summer season (see *Chapter 4*). Our data agree with other studies conducting warming or drought experiments (Schimel, Balser and Wallenstein, 2007; Manzoni, Schimel and Porporato, 2012; Deslippe *et al.*, 2016; Sun, Lei and Chang, 2019). The heterotrophic component was observed to be less sensitive than the autotrophic component to drought-induced stress. Moreover, before the heatwave, the woodland suffered from a winter-moth infestation (see *Chapter 4*). Insect infestations have been observed to alter the forest floor microclimate by altering leaf litter quantity and chemical quantity (Grace, 1986; McInnes *et al.*, 1992; Findlay *et al.*, 1996; Grime *et al.*, 1996; Chapman *et al.*, 2003), deposition of insect by-products (Hollinger, 1986; Frank and Groffman, 1998; Christenson *et al.*, 2002).

Autotrophic respiration was almost halved during the second year compared to the first year of eCO₂ enrichment at BIFoR FACE. The autotrophic component has been observed to contribute less to the total soil respiration under drought stress (Balogh *et al.*, 2016; Sun, Lei and Chang, 2019). Drought stress has been observed to affect root respiration by interfering with the root physiological processes (Linn and Doran, 1984; Zhang *et al.*, 2014) by reducing the supply of photosynthates and other residues to the root systems (Carbone *et al.*, 2011; Gomez-Casanovas *et al.*, 2012).

Although heterotrophic respiration was higher in eCO₂ arrays, on an annual basis, both years of eCO₂ enrichment, autotrophic respiration was higher in eCO₂ arrays only the first year of the experiment. In the second year of the experiment, autotrophic respiration was similar between ambient and eCO₂ arrays. The two autotrophic

components, roots, and mycorrhizae had an adverse response between ambient and eCO₂ arrays, with root respiration being the only soil respiratory component lower in eCO₂ arrays.

5.6 Conclusions

This chapter aimed to monitor the soil-derived CO₂ and attempt to quantify the soil respiratory components' contribution during the first two years of eCO₂ enrichment at BIFoR FACE. During the first year of the experiment, although the ecosystem was still in flux, eCO₂ stimulated the total soil respiration, and by partitioning the respiration to two primary sources (autotrophic and heterotrophic component), we observed that both components were releasing more CO₂ under eCO₂, with the heterotrophic component having higher fluxes. Once the autotrophic component was partitioned further to root and hyphal respiration, we found that root respiration was lower in eCO₂ arrays, while hyphal respiration was higher in eCO₂ arrays.

It is generally observed that eCO₂ stimulates root respiration (Schlesinger *et al.*, 2006); however, our results disagree with this observation. Lower root respiration in eCO₂ arrays combined with over 100% hyphal stimulation and a significant decrease in nitrate availability (Chapter 3) might indicate that trees were probably under a nutrient limitation stress; thus, they shifted their carbon allocation to hyphal structures to forage more nutrients. Mature forests have very tight nutrient cycles, and they rely almost entirely upon internal nutrient recycling to meet their nutrient demands. If such a pattern (decreased nutrient availability and higher hyphal fluxes), is not a short-term response, trees might not be able to uptake extra CO₂ because of nutrient limitations.

Moreover, the soil respiratory components had different sensitivities towards the abiotic factors (soil temperature and soil moisture), and $e\text{CO}_2$ was observed to alter those sensitivities. It is essential to highlight that the different respiratory components have different carbon turnover rates and mean residence time, with root respiration having the fastest turnover and shortest mean residence time. On the other side of the spectrum, basal respiration (microbial respiration due to soil organic matter decomposition) has the slowest turnover and longest mean residence time. Thus, shifts in the relationships between soil respiratory components and abiotic factors due to $e\text{CO}_2$ can greatly impact the C cycle and the ecosystems' potential of sequestering C in the long-term.

Future predictions give a warning for an increase in the frequency and intensity of extreme events. Prolonged heatwave combined with defoliation event shifted the relative contribution of autotrophic and heterotrophic components, with the heterotrophic almost entirely dominating the total respiration. The interaction of extreme events and $e\text{CO}_2$ intensified this observation. As mentioned before, due to the different turnover rates and mean residence time that soil respiratory components have, the C cycle might be severely affected since microbial respiration releases older soil C to the atmosphere and thus posing a threat to the ecosystem's capacity of acting as a sink. However, these observations were only short-term, and it is unclear whether there is the potential of heritage effects of the extreme events to the ecosystem in the long term or whether such events have a short lifetime in the ecosystem's cycling.

5.7 References

Bååth, E. and Wallander, H. (2003) 'Soil and rhizosphere microorganisms have the same Q_{10} for respiration in a model system', *Global Change Biology*. John Wiley & Sons, Ltd, 9(12),

pp. 1788–1791. doi: 10.1046/j.1365-2486.2003.00692.x.

Bahn, M. *et al.* (2009) 'Does photosynthesis affect grassland soil-respired CO₂ and its carbon isotope composition on a diurnal timescale?', *New Phytologist*, 182(2), pp. 451–460. doi: 10.1111/j.1469-8137.2008.02755.x

Baldocchi, D. D. (2003) 'Assessing the eddy covariance technique for evaluating carbon dioxide exchange rates of ecosystems: Past, present and future', *Global Change Biology*. John Wiley & Sons, Ltd, 9(4), pp. 479–492. doi: 10.1046/j.1365-2486.2003.00629.x.

Balogh, J. *et al.* (2016) 'Autotrophic component of soil respiration is repressed by drought more than the heterotrophic one in dry grasslands', *Biogeosciences*. Copernicus GmbH, 13(18), pp. 5171–5182. doi: 10.5194/bg-13-5171-2016.

Bond-Lamberty, B. and Thomson, A. (2010) 'Temperature-associated increases in the global soil respiration record', *Nature*, 464. doi: 10.1038/nature08930.

Bowden, R. D. *et al.* (1993) 'Fluxes of Greenhouse Gases between Soils and the Atmosphere in a Temperate Forest Following a Simulated Hurricane Blowdown', *Biogeochemistry*, 21(2), pp. 61–71.

Buchmann, N. (2000) 'Biotic and abiotic factors controlling soil respiration rates in *Picea abies* stands', *Soil Biology and Biochemistry*. Pergamon, 32(11–12), pp. 1625–1635. doi: 10.1016/S0038-0717(00)00077-8.

Burrascano, S. *et al.* (2013) 'Commonality and variability in the structural attributes of moist temperate old-growth forests: A global review', *Forest Ecology and Management*, 291, pp. 458–479. doi: 10.1016/j.foreco.2012.11.020.

Carbone, M. S. *et al.* (2011) 'Seasonal and episodic moisture controls on plant and microbial contributions to soil respiration', *Oecologia*, 167(1), pp. 265–278. doi: 10.1007/s00442-011-1975-3.

Chapman, S. K. *et al.* (2003) 'Insect herbivory increases litter quality and decomposition: an extension of the acceleration hypothesis', *Ecology*, 84(11), pp. 2867–2876. doi: 10.1890/02-0046.

Cheng, W. and Kuzyakov, Y. (2015) 'Root Effects on Soil Organic Matter Decomposition', in. John Wiley & Sons, Ltd, pp. 119–143. doi: 10.2134/agronmonogr48.c7.

Christenson, L. M. *et al.* (2002) 'The fate of nitrogen in gypsy moth frass deposited to an oak forest floor', *Oecologia*, 131(3), pp. 444–452. doi: 10.1007/s00442-002-0887-7.

Davidson, E. A. *et al.* (2002) 'Minimizing artifacts and biases in chamber-based measurements of soil respiration', *Agricultural and Forest Meteorology*, 113(1–4), pp. 21–37. doi: 10.1016/S0168-1923(02)00100-4.

Deslippe, J. R. *et al.* (2016) 'Stable isotope probing implicates a species of *Cortinarius* in carbon transfer through ectomycorrhizal fungal mycelial networks in Arctic tundra', *New Phytologist*, 210(2), pp. 383–390. doi: 10.1111/nph.13797.

Dormaar, J. F. (1990) 'Effect of active roots on the decomposition of soil organic materials', *Biology and Fertility of Soils*, 10(2), pp. 121–126. doi: 10.1007/BF00336247.

Ek, H. (1997) 'The influence of nitrogen fertilization on the carbon economy of *Paxillus involutus* in ectomycorrhizal association with *Betula pendula*', *New Phytologist*, 135(1), pp. 133–142. doi: 10.1046/j.1469-8137.1997.00621.x.

Erb, K. H. *et al.* (2018) 'Unexpectedly large impact of forest management and grazing on global vegetation biomass', *Nature*, 553(7686), pp. 73–76. doi: 10.1038/nature25138.

- Findlay, S. *et al.* (1996) 'Effects of damage to living plants on leaf litter quality', *Ecological Applications*, 6(1), pp. 269–275. doi: 10.2307/2269570.
- Fisher, F. M. and Gosz, J. R. (1986) 'Effects of trenching on soil processes and properties in a New Mexico mixed-conifer forest', *Biology and Fertility of Soils*, 2(1), pp. 35–42. doi: 10.1007/BF00638959.
- Frank, D. A. and Groffman, P. M. (1998) 'Ungulate vs. landscape control of soil C and N processes in grasslands of Yellowstone National Park', *Ecology*. Ecological Society of America, 79(7), pp. 2229–2241. doi: 10.1890/0012-9658(1998)079[2229:UVLCOS]2.0.CO;2.
- Friedlingstein, P. *et al.* (2006) 'Climate-Carbon Cycle Feedback Analysis: Results from the C 4 MIP Model Intercomparison', *Journal of Climate*, 19, pp. 3337–3353.
- Friedlingstein, P. *et al.* (2014) 'Uncertainties in CMIP5 Climate Projections due to Carbon Cycle Feedbacks', *Journal of Climate*, 27, pp. 511–526. doi: 10.1175/JCLI-D-12-00579.1.
- Global Monitoring Laboratory - Carbon Cycle Greenhouse Gases (no date). Available at: <https://www.esrl.noaa.gov/gmd/ccgg/trends/> (Accessed: 3 January 2021).
- Gomez-Casanovas, N. *et al.* (2012) 'Net ecosystem exchange modifies the relationship between the autotrophic and heterotrophic components of soil respiration with abiotic factors in prairie grasslands', *Global Change Biology*, 18(8), pp. 2532–2545. doi: 10.1111/j.1365-2486.2012.02721.x.
- Goodale, C. L. *et al.* (2002) 'Forest carbon sinks in the Northern Hemisphere', *Ecological Applications*, 12(3), pp. 891–899. doi: 10.1890/1051-0761(2002)012[0891:FCSITN]2.0.CO;2.
- Grace, J. R. (1986) 'The influence of gypsy moth on the composition and nutrient content of litter fall in a Pennsylvania oak forest.', *Forest Science*, 32(4), pp. 855–870. doi: 10.1093/forestscience/32.4.855.
- Grime, J. P. *et al.* (1996) 'Evidence of a Causal Connection between Anti-Herbivore Defence and the Decomposition Rate of Leaves', *Oikos*, 77(3), p. 489. doi: 10.2307/3545938.
- Hart, K. M. *et al.* (2019) 'Characteristics of free air carbon dioxide enrichment of a northern temperate mature forest', *Global Change Biology*, 26(2), p. gcb.14786. doi: 10.1111/gcb.14786.
- Hartley, I. P. *et al.* (2007) 'The effect of soil warming on bulk soil vs. rhizosphere respiration', *Global Change Biology*, 13(12), pp. 2654–2667. doi: 10.1111/j.1365-2486.2007.01454.x.
- Heinemeyer, A. *et al.* (2007) 'Forest soil CO₂ flux: Uncovering the contribution and environmental responses of ectomycorrhizas', *Global Change Biology*, 13(8), pp. 1786–1797. doi: 10.1111/j.1365-2486.2007.01383.x.
- Högberg, P. (2010) 'Is tree root respiration more sensitive than heterotrophic respiration to changes in soil temperature?', *New Phytologist*, pp. 9–10. doi: 10.1111/j.1469-8137.2010.03366.x.
- Hollinger, D. Y. (1986) 'Herbivory and the cycling of nitrogen and phosphorus in isolated California oak trees', *Oecologia*, 70(2), pp. 291–297. doi: 10.1007/BF00379254.
- Houghton, R. A. (2007) 'Balancing the Global Carbon Budget', *Annual Review of Earth and Planetary Sciences*, 35. doi: 10.1146/annurev.earth.35.031306.140057.
- Jackson, R. B., Mooney, H. A. and Schulze, E. D. (1997) 'A global budget for fine root biomass, surface area, and nutrient contents', *Proceedings of the National Academy of Sciences of the United States of America*, 94(14), pp. 7362–7366. doi: 10.1073/pnas.94.14.7362.
- Kallarackal, J. and Roby, T. J. (2012) 'Responses of trees to elevated carbon dioxide and

- climate change', *Biodiversity and Conservation*, pp. 1327–1342. doi: 10.1007/s10531-012-0254-x.
- Keeton, W. S. *et al.* (2011) 'Late-successional biomass development in northern hardwood-conifer forests of the Northeastern United States', *Forest Science*, 57(6), pp. 489–505. doi: 10.1093/forestscience/57.6.489.
- Keeton, William S. (2019) 'Source or sink? Carbon dynamics in eastern old-growth forests and their role in climate change mitigation', in Barton, A. M. and Keeton, W. S. (eds) *Ecology and Recovery of Eastern Old-Growth Forests*. Island Press-Center for Resource Economics, pp. 267–288. doi: 10.5822/978-1-61091-891-6_14.
- Keith, H., Mackey, B. G. and Lindenmayer, D. B. (2009) 'Re-evaluation of forest biomass carbon stocks and lessons from the world's most carbon-dense forests', *Proceedings of the National Academy of Sciences of the United States of America*, 106(28), pp. 11635–11640. doi: 10.1073/pnas.0901970106.
- King, J. S. *et al.* (2004) 'A multiyear synthesis of soil respiration responded to elevated atmospheric CO₂ from four forest FACE experiments', *Global Change Biology*, 10, pp. 1027–1042. doi: 10.1111/j.1365-2486.2004.00789.x.
- Kuzyakov, Y. (2002) 'Review: Factors affecting rhizosphere priming effects', *Journal of Plant Nutrition and Soil Science*, 165(4), pp. 296–382.
- Kuzyakov, Y. and Gavrichkova, O. (2010) 'Time lag between photosynthesis and carbon dioxide efflux from soil: A review of mechanisms and controls', *Global Change Biology*, 16(12), pp. 3386–3406. doi: 10.1111/j.1365-2486.2010.02179.x.
- Lee, M. S. *et al.* (2003) 'Seasonal changes in the contribution of root respiration to total soil respiration in a cool-temperate deciduous forest', in *Plant and Soil*. Springer, pp. 311–318. doi: 10.1023/A:1026192607512.
- Linn, D. M. and Doran, J. W. (1984) 'Effect of Water-Filled Pore Space on Carbon Dioxide and Nitrous Oxide Production in Tilled and Nontilled Soils', *Soil Science Society of America Journal*, 48(6), pp. 1267–1272. doi: 10.2136/sssaj1984.03615995004800060013x.
- Longdoz, B., Yernaux, M. and Aubinet, M. (2000) 'Soil CO₂ efflux measurements in a mixed forest: Impact of chamber disturbances, spatial variability and seasonal evolution', *Global Change Biology*, Ltd, 6(8), pp. 907–917. doi: 10.1046/j.1365-2486.2000.00369.x.
- Luo, Y. *et al.* (2001) 'Acclimatization of soil respiration to warming in a tall grass prairie', *Nature*. Nature Publishing Group, 413(6856), pp. 622–625. doi: 10.1038/35098065.
- Ma, Y. *et al.* (2014) 'Stand ages regulate the response of soil respiration to temperature in a *Larix principis-rupprechtii* plantation', *Agricultural and Forest Meteorology*. doi: 10.1016/j.agrformet.2013.10.008.
- Manzoni, S., Schimel, J. P. and Porporato, A. (2012) 'Responses of soil microbial communities to water stress: Results from a meta-analysis', *Ecology*, Ltd, 93(4), pp. 930–938. doi: 10.1890/11-0026.1.
- McGarvey, J. C. *et al.* (2015) 'Carbon storage in old-growth forests of the Mid-Atlantic: Toward better understanding the eastern forest carbon sink', *Ecology*, 96(2), pp. 311–317. doi: 10.1890/14-1154.1.
- McInnes, P. F. *et al.* (1992) 'Effects of moose browsing on vegetation and litter of the boreal forest, Isle Royale, Michigan, USA', *Ecology*, 73(6), pp. 2059–2075. doi: 10.2307/1941455.
- Pan, Y. *et al.* (2011) 'A large and persistent carbon sink in the world's forests', *Science*. doi: 10.1126/science.1201609.

- Paterson, E. *et al.* (2003) 'Effects of defoliation and atmospheric CO₂ depletion on nitrate acquisition, and exudation of organic compounds by roots of *Festuca rubra*', *Plant and Soil*, 250(2), pp. 293–305. doi: 10.1023/A:1022819219947.
- Quéré, C. *et al.* (2018) 'Global Carbon Budget 2018', *Earth System Science Data*, 10(4), pp. 2141–2194. doi: 10.5194/essd-10-2141-2018.
- Raich, J. W. and Schlesinger, W. H. (1992) 'The global carbon dioxide flux in soil respiration and its relationship to vegetation and climate', *Tellus*, 44B, pp. 81–99.
- Ross, D. J. *et al.* (2001) 'Root effects on soil carbon and nitrogen cycling in a *Pinus radiata* D. Don plantation on a coastal sand', *Australian Journal of Soil Research*, 39(5), pp. 1027–1039. doi: 10.1071/SR00058.
- Savage, K., Davidson, E. A. and Richardson, A. D. (2008) 'A conceptual and practical approach to data quality and analysis procedures for high-frequency soil respiration measurements', *Functional Ecology*, 22(6), pp. 1000–1007. doi: 10.1111/j.1365-2435.2008.01414.x.
- Savage, K. E. *et al.* (2013) 'Long-term changes in forest carbon under temperature and nitrogen amendments in a temperate northern hardwood forest', *Global Change Biology*, 19, pp. 2389–2400. doi: 10.1111/gcb.12224.
- Schimel, J., Balser, T. C. and Wallenstein, M. (2007) 'Microbial stress-response physiology and its implications for ecosystem function', *Ecology*, pp. 1386–1394. doi: 10.1890/06-0219.
- Staddon, P. L., Gregersen, R. and Jakobsen, I. (2004) 'The response of two *Glomus* mycorrhizal fungi and a fine endophyte to elevated atmospheric CO₂, soil warming and drought', *Global Change Biology*, 10(11), pp. 1909–1921. doi: 10.1111/j.1365-2486.2004.00861.x.
- Sun, S., Lei, H. and Chang, S. X. (2019) 'Drought differentially affects autotrophic and heterotrophic soil respiration rates and their temperature sensitivity', *Biology and Fertility of Soils*. doi: 10.1007/s00374-019-01347-w.
- Taneva, L. and Gonzalez-Meler, M. A. (2011) 'Distinct patterns in the diurnal and seasonal variability in four components of soil respiration in a temperate forest under free-air CO₂ enrichment', *Biogeosciences*, 8(10), pp. 3077–3092. doi: 10.5194/bg-8-3077-2011.
- Team, Rs. (2019) 'RStudio: Integrated Development for R.' Boston, MA: RStudio, Inc.
- Tomè, E. *et al.* (2016) 'Mycorrhizal contribution to soil respiration in an apple orchard', *Applied Soil Ecology*. doi: 10.1016/j.apsoil.2016.01.016.
- Trueman, R. J. and Gonzalez-Meler, M. A. (2005) 'Accelerated belowground C cycling in a managed agriforest ecosystem exposed to elevated carbon dioxide concentrations', *Global Change Biology*, 11(8), pp. 1258–1271. doi: 10.1111/j.1365-2486.2005.00984.x.
- UNFCCC (2005) *Adoption of the Paris Agreement*.
- Wei, W., Weile, C. and Shaopeng, W. (2010) 'Forest soil respiration and its heterotrophic and autotrophic components: Global patterns and responses to temperature and precipitation', *Soil Biology and Biochemistry*. doi: 10.1016/j.soilbio.2010.04.013.
- Zhang, C. *et al.* (2014) 'Effects of simulated nitrogen deposition on soil respiration components and their temperature sensitivities in a semiarid grassland', *Soil Biology and Biochemistry*, 75, pp. 113–123. doi: 10.1016/j.soilbio.2014.04.013.
- Zhao, Z. *et al.* (2017) 'Model prediction of biome-specific global soil respiration from 1960 to 2012', *Earth's Future*, 5(7), pp. 715–729. doi: 10.1002/2016EF000480.

5.8 Supplementary material

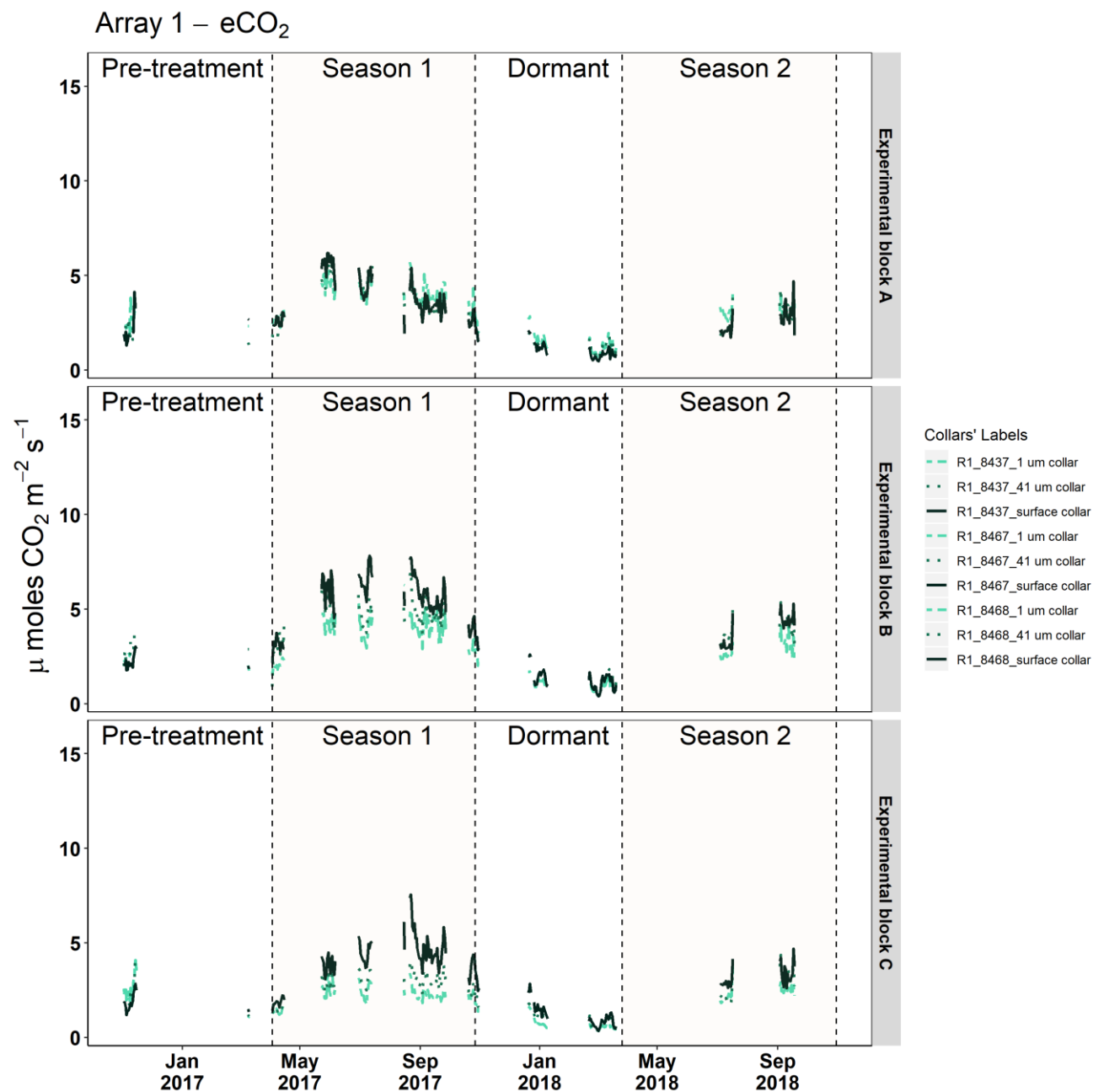


Figure S5- 1: Investigation of experimental design failures for all three experimental blocks in Array 1 (eCO₂ array) in daily averages during the first two years of eCO₂ enrichment at BIFoR FACE. Surface collars are denoted with dark green solid lines, medium collars are denoted with green dotted lines, while fine collars are denoted with light green dashed lines.

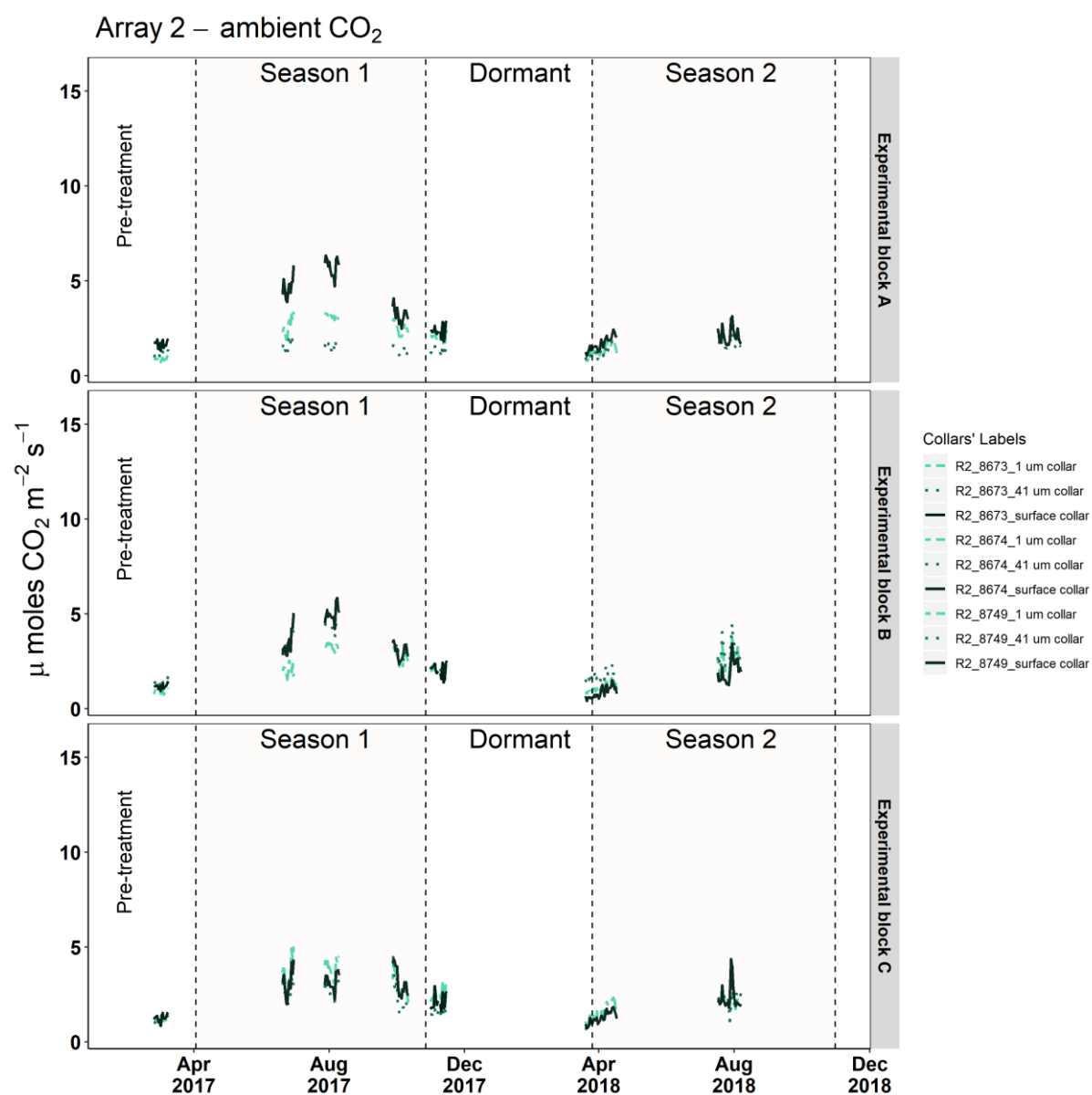


Figure S5- 2: Investigation of experimental design failures for all three experimental blocks in Array 2 (ambient array) in daily averages during the first two years of eCO₂ enrichment at BIFoR FACE. Surface collars are denoted with dark green solid lines, medium collars are denoted with green dotted lines, while fine collars are denoted with light green dashed lines.

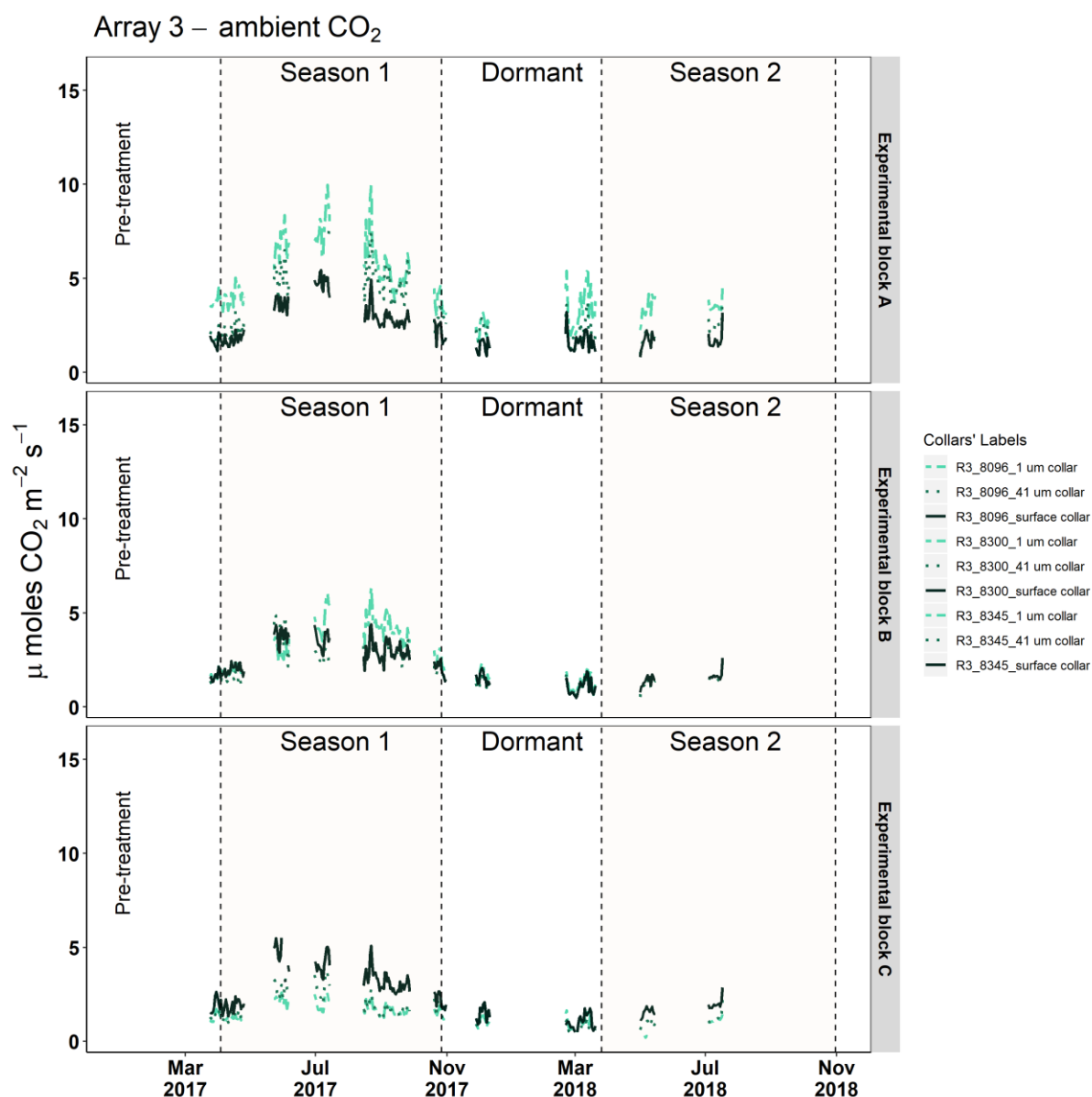


Figure S5- 3: Investigation of experimental design failures for all three experimental blocks in Array 3 (ambient array) in daily averages during the first two years of eCO₂ enrichment at BIFoR FACE. Surface collars are denoted with dark green solid lines, medium collars are denoted with green dotted lines, while fine collars are denoted with light green dashed lines.

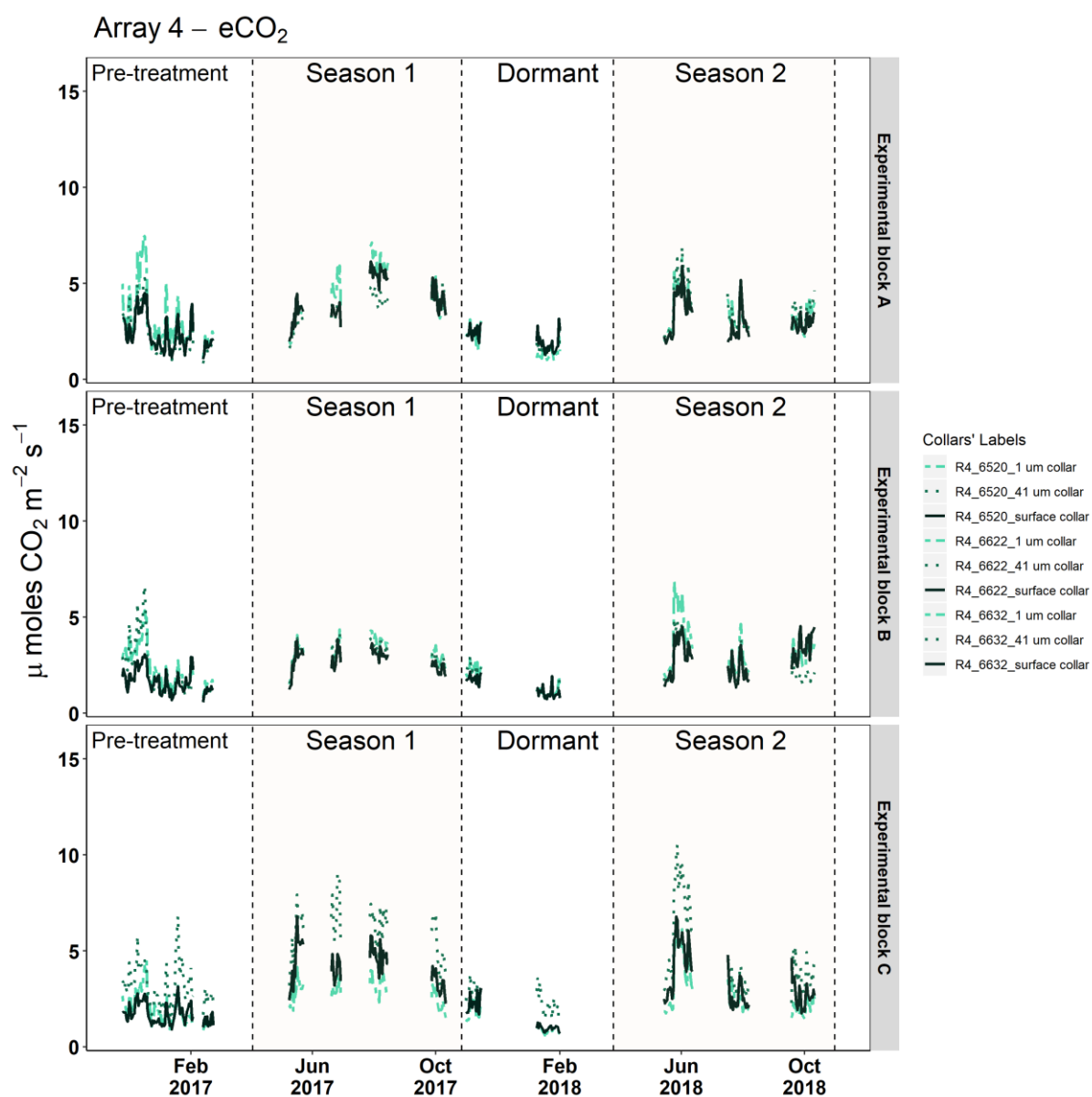


Figure S5- 4: Investigation of experimental design failures for all three experimental blocks in Array 4 (eCO₂ array) in daily averages during the first two years of eCO₂ enrichment at BIFoR FACE. Surface collars are denoted with dark green solid lines, medium collars are denoted with green dotted lines, while fine collars are denoted with light green dashed lines.

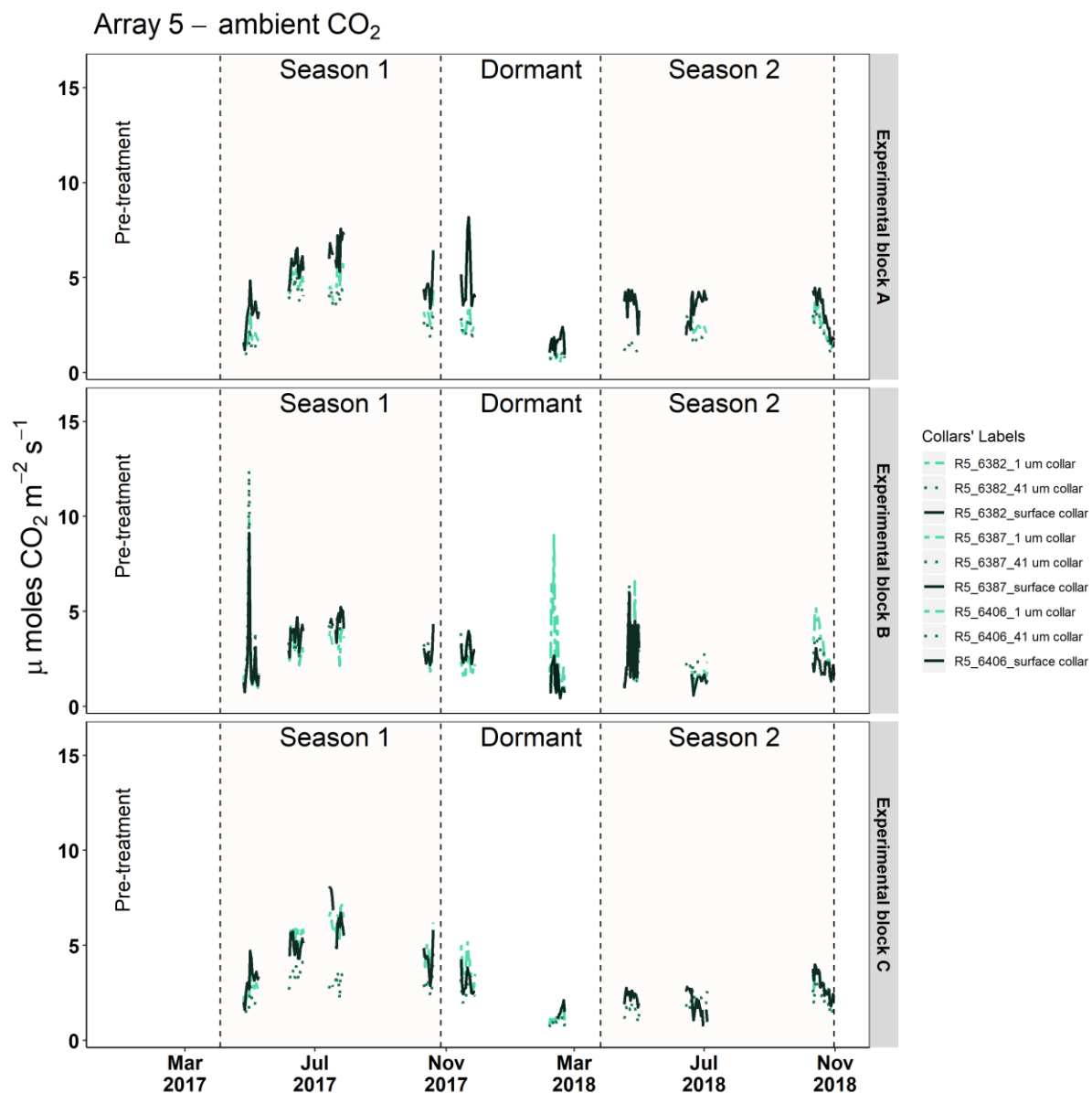


Figure S5- 5: Investigation of experimental design failures for all three experimental blocks in Array 5 (ambient array) in daily averages during the first two years of eCO₂ enrichment at BIFoR FACE. Surface collars are denoted with dark green solid lines, medium collars are denoted with green dotted lines, while fine collars are denoted with light green dashed lines.

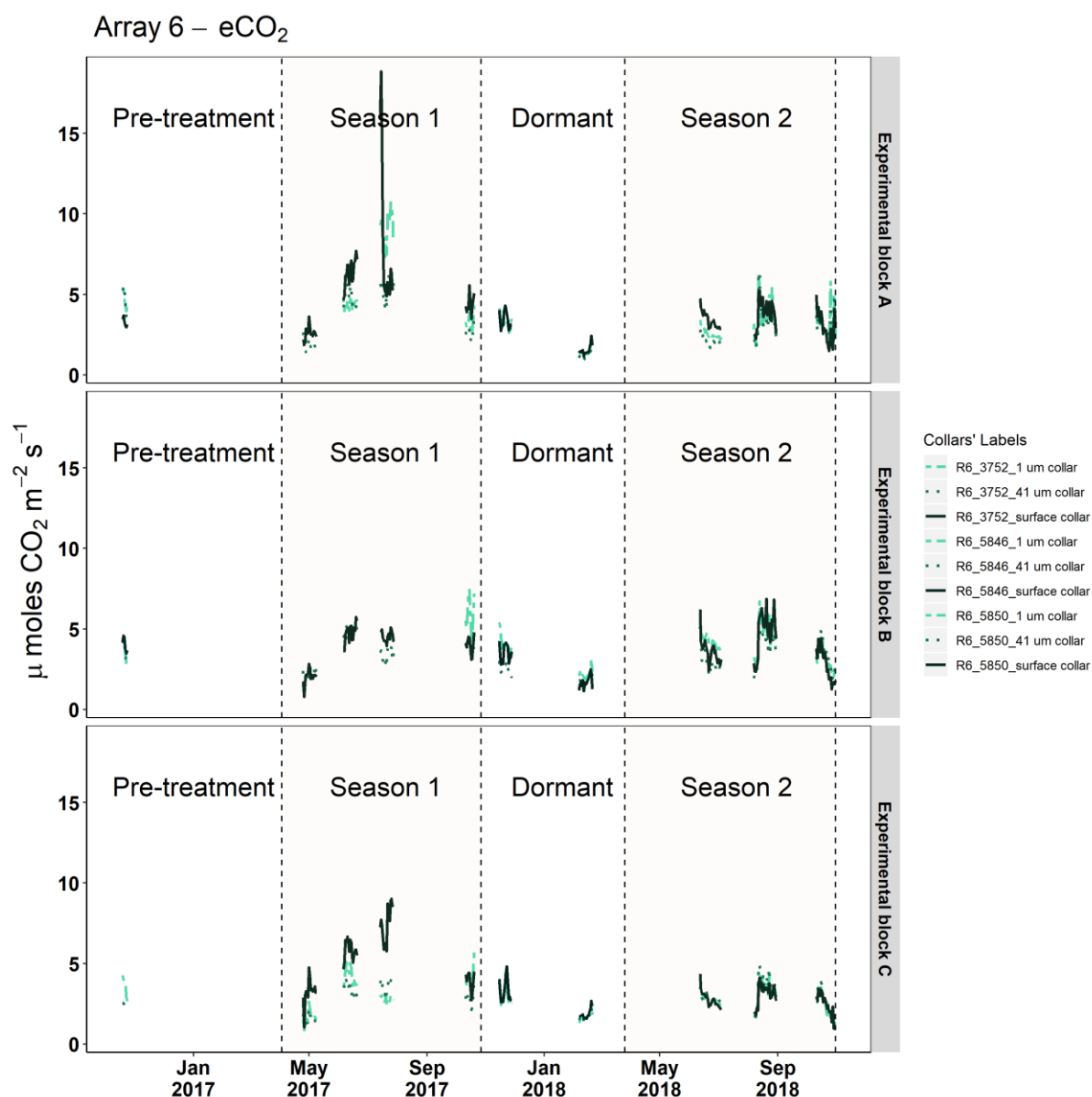


Figure S5- 6: Investigation of experimental design failures for all three experimental blocks in Array 6 (eCO₂ array) in daily averages during the first two years of eCO₂ enrichment at BIFoR FACE. Surface collars are denoted with dark green solid lines, medium collars are denoted with green dotted lines, while fine collars are denoted with light green dashed lines.

Table S5- 1: Linear equations retrieved from VWC and T correlations with R_h , R_a , R_r and R_m (daily averages) during Year 1 and 2 at BIFoR FACE.

Year 1			Year 2	
Ambient		eCO ₂	Ambient	eCO ₂
VWC				
R _h	y = 2.9 – 0.041x	y = 3.3 – 0.027x	y = 2.4 – 0.04x	y = 2 + 0.1x
R _a	y = 1.5 – 0.044x	y = 2.7 – 0.028x	y = 0.13 + 0.014x	y = 0.79 – 0.047x
R _r	y = 1.2 – 0.028x	y = 0.72 + 2.5* 10 ⁻⁵ x	y = 0.26 + 0.0068x	y = -0.0025 – 0.017x
R _m	y = 0.27 – 0.013x	y = 0.92 – 0.027x	y = 0.16 + 0.012x	y = 0.82 – 0.032x
T				
R _h	y = 0.22 + 0.18x	y = 0.83 + 0.17x	y = 1.6 + 0.033x	y = 1.6 + 0.087x
R _a	y = -0.61 + 0.13x	y = -0.87 + 0.17x	y = 0.037 + 0.021x	y = 1.1 - 0.048x
R _r	y = -0.3 + 0.098x	y = -0.12 + 0.066x	y = 0.34 + 0.000038x	y = -0.5 + 0.027x
R _m	y = -0.26 + 0.031x	y = -0.72 + 0.1x	y = -0.22 + 0.017x	y = 1.6 + 0.074x



Figure S5- 7: Experimental design failures in the root exclusion collars. Roots were penetrating the exclusion collars via the open bottom of the collar or through the meshed windows.

Chapter 6: Conclusions

The purpose of this study was to measure the soil respiration and the bioavailability of soil nutrients in a mature temperate woodland during the first two years of eCO₂ enrichment to +150 ppm above ambient conditions. This is the first time that belowground responses of soil eCO₂ fluxes and nutrient dynamics of mature temperate woodland are under high-resolution scrutiny, both temporally and spatially. Also, this is the first time soil respiration was partitioned to its respiratory sources in a forest FACE experiment. We had the opportunity to study the combined effect of eCO₂ and extreme events on belowground responses, providing a unique insight into complex interactions at an ecosystemic level. Moreover, this study provided the advantage to study the responses of the woodland under the 2050 atmospheric CO₂ scenario as a coetaneous event.

Soil respiration was higher under eCO₂ for both Year 1 and Year 2 (~21 and 36%, respectively), and the change was more prominent in Year 2. The temperature sensitivity Q_{10} was decreased by 30 and 12% for Year 1 and 2, respectively, under eCO₂. Bioavailable nitrate was decreased by 27 and 15% under eCO₂ during years 1 and 2, respectively, while there was no difference in ammonium. Moreover, phosphate had a 10% decrease during Year 1 and a 5% increase during Year 2 under eCO₂. Furthermore, there was a ~50 and 8% increase in microbial biomass carbon in the O and B horizons, respectively, whereas there was a 15% decrease in microbial biomass carbon in A horizons under eCO₂. Under eCO₂ microbial biomass nitrogen increased by 15% in the O horizon but decreased by 2 and 17 % at A and B horizons. A similar pattern was observed for microbial biomass phosphorus, with the O horizons having a 53% increase under eCO₂, while there was an 8 and 16% decrease in A and B

horizons. Lastly, both soil inorganic ammonium and nitrate decreased under eCO₂, with the decrease being intensified with depth.

Moreover, soil respiration during Year 2 was decreased by 47 and 40% under ambient and eCO₂ conditions, respectively, compared to Year 1. Contrastingly, all soil bioavailable nutrients' concentrations were higher during Year 2 under both ambient and eCO₂ conditions. Ammonium availability increased by 47 and 49% under ambient and eCO₂ conditions, respectively. Similarly, nitrate availability increased by 70 and 101% under ambient and eCO₂ conditions, respectively, during Year 2. Sequentially, phosphate availability during Year 2 increased by 100 and 133% under ambient and eCO₂ conditions, respectively.

During the first year of the experiment, although the ecosystem was still in flux, eCO₂ stimulated the total soil respiration. Both the autotrophic and heterotrophic components were stimulated under eCO₂, with the heterotrophic component having higher fluxes. Moreover, root respiration was lower in eCO₂ arrays, while hyphal respiration was higher in eCO₂ arrays.

The soil respiratory components had different sensitivities towards the abiotic factors (soil temperature and soil moisture), and eCO₂ was observed to alter those sensitivities. Thus, shifts in the relationships between soil respiratory components and abiotic factors due to eCO₂ can significantly impact the C cycle and the ecosystems' potential of sequestering C in the long-term.

Chapter 7: Future Outlook

This work highlights the importance of long-term, large-scale climatic experiments. Belowground responses can vary considerably; thus, rigorous and prolonged monitoring is required to make accurate predictions and take the correct steps for mitigation. Moreover, this work showcases that although field techniques are well established, in reality, they have multiple drawbacks and are not designed for long-term monitoring. Further work is required to focus on ensuring sufficient, cost-effective field-monitoring methods that can address a plethora of research questions at multiple temporal and spatial scales in the forest soil. Thus, it is pivotal to explore new techniques of partitioning soil respiration *in situ* in as non-destructive ways as possible. Failing to do so, a significant component of the global C cycle will remain highly uncertain.

Moreover, the eCO₂ interaction with abiotic factors and their effect on soil respiratory components remains insufficiently understood. Further work to determine individual responses is required, as well as simultaneous investigation of the respiratory components' combined responses is necessary to fully understand belowground C pools and sources and their potential shifts under eCO₂. Tackling the C budget uncertainties necessitates a deeper understanding of root, hyphal and microbial dynamics.

Furthermore, extensive work is required in the deeper soil horizons in order to be able to identify potential nutrient leaching losses through the ecosystem as well as potential shifts in microbial biomass. This will enable a more thorough understanding of soil biogeochemistry under eCO₂ to be ascertained and more effective model predictions and, thus, management strategies to be implemented.

Moreover, a more thorough investigation of the soil microbial and fungal community is required. There is still very little known about the communities' responses under eCO₂, and the scarce datasets show variable responses. The shifts in dominance of certain microbial and fungal species, the relative abundance and richness of microbial communities might have significant effects on the soil C cycle and the aboveground communities.

Another essential aspect that affects the soil cycle, and there is limited knowledge about the potential eCO₂ effect, is nutrient availability. Research is predominantly focused on nitrogen and phosphorus responses; however, availability and turnover rates of other macro-, micro-nutrients, and trace metals can significantly impact ecosystem functioning if biogeochemical cycles are observed to be decoupled under eCO₂.